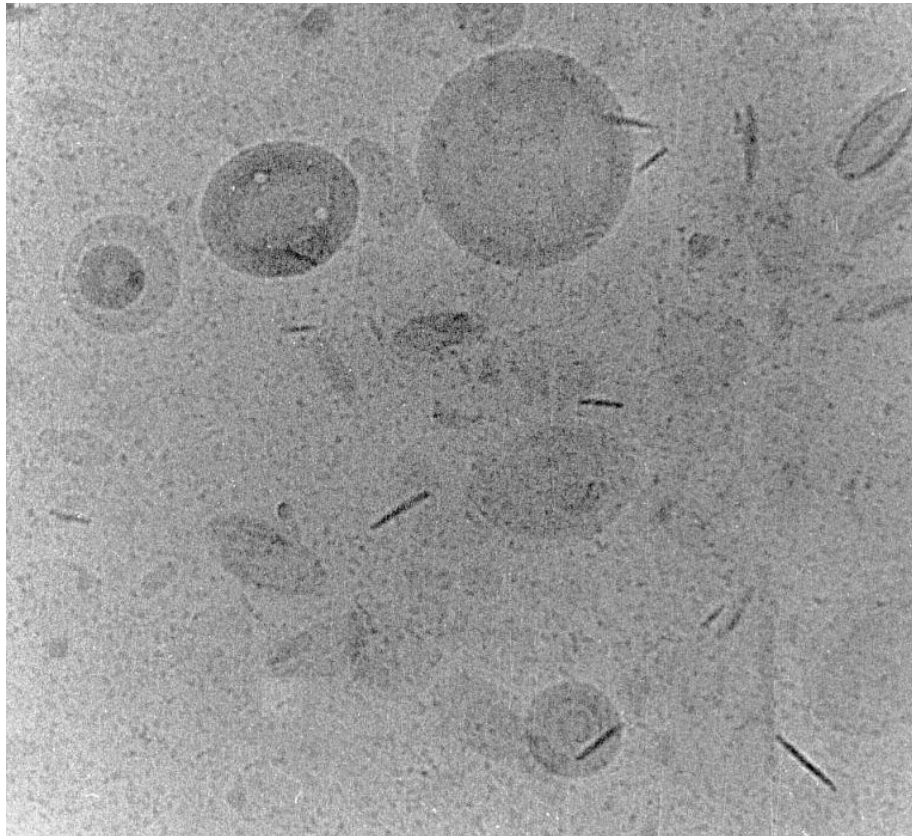


Molecular interactions between bile salts, phospholipids and cholesterol

Relevance to bile formation, cholesterol
crystallization and bile salt toxicity



Antonio Moschetta



**Molecular interactions between
bile salts, phospholipids and cholesterol**

Relevance to bile formation, cholesterol
crystallization and bile salt toxicity

Antonio Moschetta

Molecular interactions between bile salts, phospholipids and cholesterol.
Relevance to bile formation, cholesterol crystallization and bile salt toxicity
/ Antonio Moschetta

Proefschrift Universiteit Utrecht – with a summary in dutch and in italian
ISBN: 903932880-3

Cover. *front*: Cryo-electron microscopic images of bile salt-, phospholipid-
and cholesterol-micellar & vesicular structures.

Back: “il grifo” from Cathedral of Bitonto (Bari – Italy).

© A. Moschetta, Utrecht, 2001.

The printing of this thesis was supported by AstraZeneca, Beun-De Ronde,
Byk Nederland, GlaxoSmithKline, Hope Farms, Shimadzu Benelux,
Tramedico, Zambon.

Molecular interactions between bile salts, phospholipids and cholesterol

Relevance to bile formation, cholesterol
crystallization and bile salt toxicity

(with a summary in dutch and in italian)

Moleculaire interacties tussen galzouten, fosfolipiden en cholesterol.

Relevantie voor galvorming, kristallisatie van cholesterol
en galzout toxiciteit

Proefschrift ter verkrijging van de graad van doctor aan de Universiteit
Utrecht op gezag van de Rector Magnificus, Prof. Dr. W. H. Gispen
ingevolge het besluit van het College voor Promoties in het openbaar te
verdedigen op woensdag 19 december 2001 des middags te 2.45 uur

door

Antonio Moschetta

geboren op 8 juni 1973, te Bitonto (Bari, Italie)

Promotores: Prof. Dr. G.P. van Berge Henegouwen

Prof. Dr. G. Palasciano

Co-promotores: Dr. K.J. van Erpecum

Prof. Dr. P. Portincasa

Promotiecommissie: Prof. Dr. M.C. Carey

Prof. Dr. D.W. Erkelens

Prof. Dr. L.M.G. van Golde

Prof. Dr. B. de Kruijff

Dr. H.J. Verkade

CONTENTS

Chapter 1	Introduction and Aims of the thesis	1
Chapter 2	Accurate separation of vesicles, micelles and cholesterol crystals in supersaturated model bile by ultracentrifugation, ultrafiltration and dialysis <i>Biochimica et Biophysica Acta 2001; 1532:15-27.</i>	37
Chapter 3	Cholesterol crystallization in model bile: effects of bile salt and phospholipid species composition <i>Journal of Lipid Research 2001; 42:1273-81.</i>	63
Chapter 4	Asymmetric distribution of phosphatidylcholine and sphingomyelin between micellar and vesicular phases: potential implications for canalicular bile secretion <i>Journal of Lipid Research 1999; 40:2022-33.</i>	91
Chapter 5	Incorporation of cholesterol in sphingomyelin-egg yolk phosphatidylcholine vesicles has profound effects on detergent-induced phase transitions: a time-course study by cryo-transmission electron microscopy <i>submitted.</i>	127
Chapter 6	Sphingomyelin exhibits greatly enhanced protection compared with egg yolk phosphatidylcholine against detergent bile salts <i>Journal of Lipid Research 2000; 41:916-24.</i>	149
Addendum	Hepatic bile lipid composition in patients with obstructive jaundice <i>Preliminary data</i>	177
Chapter 7	Hydrophilic bile salts enhance differential distribution of sphingomyelin and phosphatidylcholine between micellar and vesicular phases: potential implications for their effects <i>in vivo</i> <i>Journal of Hepatology 2001; 34:492-99.</i>	187
Chapter 8	Sphingomyelin offers protection against apoptosis and hyperproliferation induced by the hydrophobic bile salt deoxycholate: potential implications for colon cancer <i>Preliminary data</i>	211
Summary	<i>English, Dutch, Italian</i>	227
Acknowledgements		245
Curriculum vitae et studiorum		247

ABBREVIATIONS

ABC	ATP-binding cassette
ACAT	acyl-CoA:cholesterol acyl transferase
Ac-DEVD	pNA – acetyl-Asp-Glu-Val-Asp-p-nitroaniline
AGG	aggregated vesicles
ALT	alanine transaminase
AP	alkaline phosphatase
ASBT	apical sodium-dependent bile salt transporter
AST	aspartate transaminase
BrdU	bromodeoxyuridine
BS	bile salts
CEH	cholesterol ester hydrolase
Cryo-TEM	cryo-transmission electron microscopy
CSI	cholesterol saturation index
CYP7A	cholesterol 7 α hydroxylase
DMEM	Dulbecco's modified Eagle's minimum essential medium
ERCP	endoscopic retrograde cholangio-pancreaticography
FXR	farnesoid X receptor
γ GT	gamma-glutamyl transpeptidase
HDL	high density lipoprotein
HI	hydrophobicity index
HMG-CoA	3-hydroxy-3methylglutaryl coenzyme A
IMC	intermixed micellar-vesicular bile salt concentration
LDH	lactate dehydrogenase
LDL	low density lipoprotein
LXR	liver X receptor
MIC	mixed micelles
NPC	Nieman Pick type C disease
PC	phosphatidylcholine
PC-TP	phosphatidylcholine transfer protein
PE	phosphatidylethanolamine
PS	phosphatidylserine
QLS	quasi-elastic light scattering spectroscopy
Rh	hydrodynamic radius
SM	sphingomyelin
SREBP	sterol regulatory element binding proteins
SR-B1	scavenger receptor B1
SUV	small unilamellar vesicles
TC	taurocholate
TDC	taurodeoxycholate
THDC	taurohyodeoxycholate
TLC	total lipid concentration
TUDC	tauroursodeoxycholate
VLDL	very low density lipoprotein

Chapter 1

GENERAL INTRODUCTION

Background

Bile is the primary excretory route for organic compounds with low water solubility. Cholesterol is a nonpolar lipid dietary constituent, absorbed from the small intestine, transported in blood and taken up by the liver. The hepatocyte is the major site for cholesterol synthesis and its elimination in bile. Hepatic secretion of bile salts and cholesterol into bile is the basis for the elimination of excess cholesterol from the body. First, this introduction will focus on the entero-hepatic circulation, the intrahepatic homeostasis and the detergent activity of the bile salts. Second, the cholesterol metabolism with the “reverse cholesterol transport” pathway and the intestinal absorption of the sterol will be summarized. Thereafter, the process of nascent bile formation at the level of the hepatocyte canalicular membrane will be described as well as the bile physiology within the biliary tract and the gallbladder. Finally, the key role of bile salts and phospholipids in cholesterol solubilization in bile will be discussed, together with cholesterol supersaturation and crystallization at the basis of gallstone formation.

Cholesterol

Cholesterol is a steroid nonpolar lipid that is virtually insoluble in an aqueous solution. The molecular structure of cholesterol is reported in **Figure 1**.

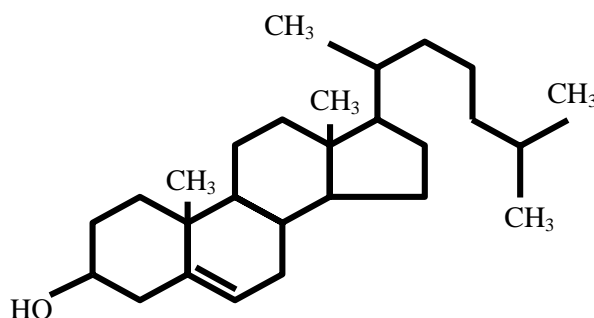


Figure 1. *The chemical structure of cholesterol (5-cholesten-3β-ol, C₂₇H₄₆O)*

The hepatocyte is the major site for the synthesis of the sterol and its elimination from the body. Cholesterol is thought to be present in the hepatocyte as metabolic active free cholesterol and in a pool of cholesterol esters. Cholesterol esters can be converted to free cholesterol by cholesterol ester hydrolase (CEH) and the reverse process is catalysed by acyl-CoA:cholesterol acyl transferase (ACAT). The synthesis of cholesterol in the hepatocytes is starting from three acetate molecules derived from oxidation of fatty acids or carbohydrate. The rate-limiting step in cholesterol neosynthesis is the reduction of 3-hydroxy-3-methylglutaryl coenzyme A (HMG-CoA) to mevalonate. The synthesis of cholesterol is also regulated by sterol regulatory element binding proteins (SREBP), which can cause upregulation of the enzymes involved in cholesterol neosynthesis (1). The secretion of cholesterol esters into blood and subsequent delivery to the tissues is mediated by very low density lipoprotein (VLDL) particles. **Figure 2** represents a scheme of cholesterol metabolism (**A**) also in relation to various risk factors (age, diet, obesity, hypertriglyceridemia and hormonal treatment) for cholesterol gallstone disease (**B**).

Phospholipids

Phosphatidylcholine, the major (>95%) phospholipid in human bile, is synthesized *de novo* in the hepatocytes, starting from diacylglycerol assembly. Then, addition of choline phosphate occurs through a direct transfer to diacylglycerol. However, an alternative pathway, the so called “methylation” pathway, can occur during hepatic phosphatidylcholine neosynthesis: newly synthesized phosphatidylethanolamine is converted to phosphatidylcholine by addition of 3 *N*-methyl groups. Most of the choline employed for phosphatidylcholine synthesis is derived from dietary sources, and choline is an essential nutrient in the human diet.

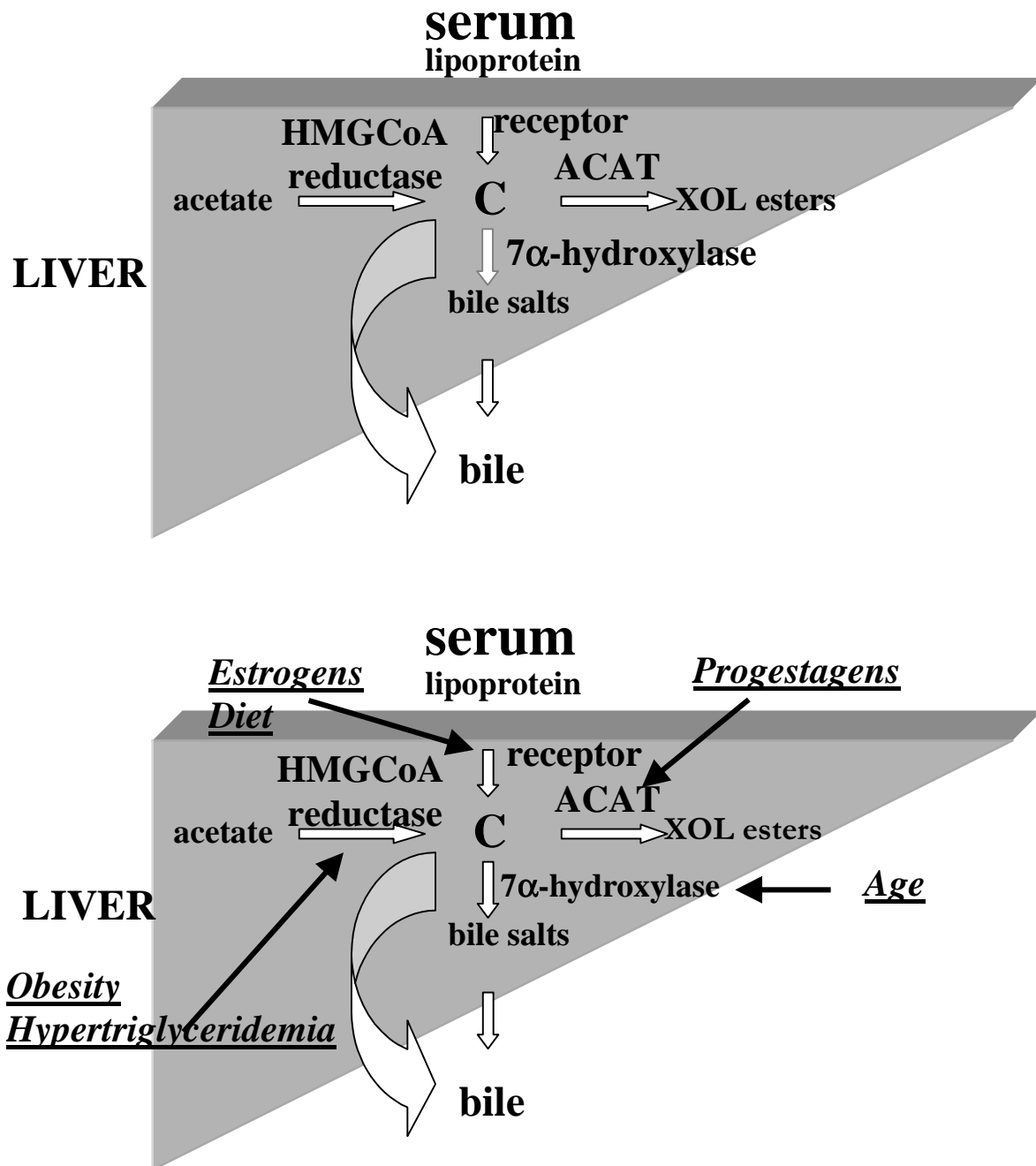


Figure 2. A schematic representation of hepatic cholesterol metabolism (A) also in relation to various risk factors for cholesterol gallstone disease (B). C= free cholesterol.

Neosynthesized phosphatidylcholine has to reach the hepatocyte canalicular membrane to be secreted into bile. How phosphatidylcholine reaches the canalicular membrane of the hepatocyte for secretion into the bile is still under debate. Three potential mechanisms may be involved in

this puzzling event: vesicular traffic, monomeric exchange through the action of cytosolic protein and lateral diffusion from the basolateral plasma membrane (2). Recently, a specific phosphatidylcholine transfer protein (PC-TP, a cytosolic protein that catalyzes intermembrane transfer of phosphatidylcholines *in vitro*) has been cloned: its hepatic expression as well as the genomic organization have been determined (3). The proposed functions include the supply of phosphatidylcholine required for secretion into bile and the facilitation of enzymatic reactions involving PC synthesis or breakdown (3). However, PC-TP knock-out mice show no differences in bile lipid content and composition as compared with normal mice (4). Also, the fact that PC molecules with 18:0 acyl chains at the *sn*-1 position are the main phospholipids bound to bovine PC-TP *in vivo* but do not occur in bile, is against a role for PC-TP in intracellular transport of bile-destined PC (5).

Bile salts

The entero-hepatic circulation

Bile salts are anionic detergents synthesized from cholesterol representing an important pathway for cholesterol catabolism. The circulating bile salt pool comprises primary and secondary bile salts. Primary bile salts (cholate and chenodeoxycholate) are synthesized *de novo* from cholesterol while secondary bile salts (deoxycholate and lithocholate) are produced in the colon by bacterial 7α -dehydroxylation. The process of hepatic bile salt secretion, expulsion in the gastrointestinal tract, reabsorption in the intestine and hepatic reuptake from sinusoidal blood is called the “entero-hepatic circulation” (**Figure 3**).

Most bile salts are amidated in the liver with glycine or taurine. Amidated bile salts are then secreted into bile (see “*lipid secretion into*

bile”) and after a period of storage in the gallbladder expelled to the duodenum.

Enterohepatic circulation of bile salts

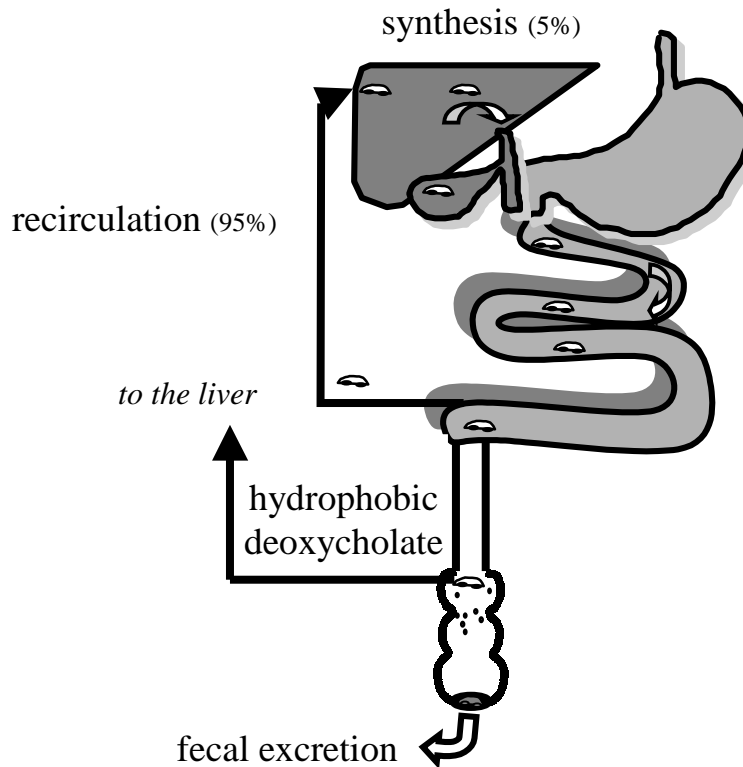


Figure 3. *The entero-hepatic circulation of bile salts. Bile salts secreted from the liver into bile, are expelled from the gallbladder into the digestive tract following meal ingestion. Most of the bile salts are reabsorbed in the ileum via a sodium-dependent transport, ASBT (see text). A small fraction of bile salts escapes ileal reabsorption, reaches the colon where they are deconjugated by anaerobic bacteria to secondary hydrophobic bile salts (deoxycholate and lithocholate). These secondary bile salts are partly reabsorbed by passive diffusion and reach the liver, where they become part of the bile salt pool. ~95% of bile salts secreted from the liver are coming from the entero-hepatic circulation and ~5% from the neosynthesis from cholesterol molecules.*

Normally, 95 to 99% of bile salts expelled into the intestine are reabsorbed in the ileum. The first step of this active process is mediated

by ileal apical sodium-dependent bile salt transporter (ASBT) (6;7). Recently, it has been shown that ASBT plays an important role in increasing bile salt pool size (8). ASBT is upregulated in case of large amounts of bile salts in the ileal lumen and downregulated in case of low amounts of ileal bile salts.

A small fraction of small intestinal bile salts escapes ileal absorption and reaches the colon, where bile salts are deconjugated by anaerobic bacteria. The resulting secondary bile salts, deoxycholate (DC, from 7α -dehydroxylation of cholate) and lithocholate (LC, from 7α -dehydroxylation of chenodeoxycholate) are partly absorbed by passive diffusion, return to the liver and are reamidated. DC is therefore part of bile salt pool and LC is first sulfated and glucuronidated in the hepatocyte before being secreted in bile.

Bile salt homeostasis

Two major pathways are described in the bile salt synthesis process: the classic “neutral” pathway employing the microsomal cholesterol 7α hydroxylase (CYP7A), which induces hydroxylation of cholesterol at the 7α position and the “alternative” pathway employing the mitochondrial cholesterol 27 hydroxylase, which induces 27-hydroxylation (9). The transgenic CYP7A knockout mice support the relevance of the “alternative” bile salt synthesis pathway since at maturity, they synthesize primary bile salts in sufficient quantities to survive and digest normally (10). Oxysterol 7α -hydroxylase is required for bile salt biosynthesis via the alternative pathway. Sterol- 12α -hydroxylase is the rate-controlling enzyme determining the ratio of the two primary bile salts (cholate to chenodeoxycholate), thus regulating the hydrophobicity of the bile salt pool (11). Recent studies have investigated the role of the

orphan nuclear receptors LXR (liver X receptor) and FXR (farnesoid X receptor) on stimulating or inhibiting bile salt synthesis, resp.

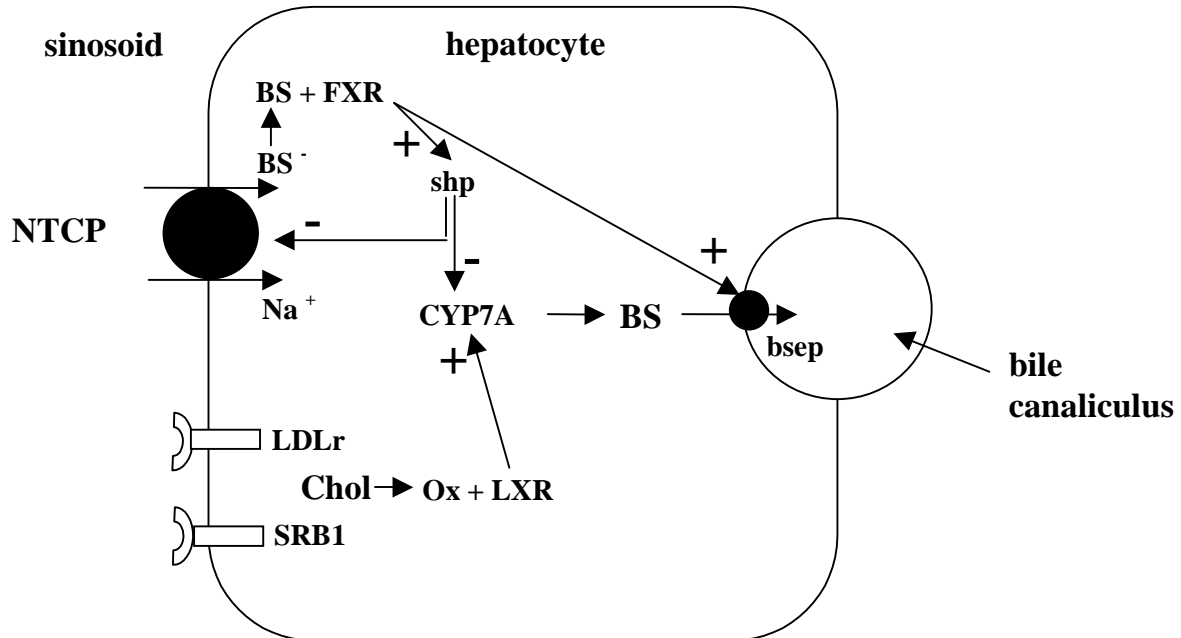


Figure 4. Bile salt homeostasis as adapted from Moseley (19). Bile salts are taken up from sinusoidal blood by NTCP. In order to modulate the intracellular bile salt concentration, bile salt-activated FXR induces shp-mediated downregulation of NTCP (which results in decreased bile salt uptake) and upregulation of bsep (an ATP-dependent transport protein which mediates bile salt transport across the hepatocyte canalicular membrane (18)). Also, FXR-induced activation of shp suppresses CYP7A activity (decreased bile salt synthesis). On the other hand, cholesterol taken up from sinusoidal blood by LDL receptors (LDLr) and scavenger receptors (SRB1) is oxidated to oxysterols (Ox). Oxysterol-induced LXR activation promotes neosynthesis of bile salts from cholesterol by upregulating CYP7A.

Oxysterols, formed by the oxidation of cholesterol in the liver, activate LXR which has been shown to upregulate the mRNA transcription of cholesterol 7 α -hydroxylase (**Figure 4**), thus stimulating the classic bile salt synthesis pathway (12). On the other hand, FXR represses the mRNA transcription of cholesterol 7 α -hydroxylase (**Figure 4**), thus inducing downregulation of bile salt synthesis (13). This process is

important in maintaining hepatic bile salt homeostasis. In fact, bile salts are downregulating the mRNA transcription of cholesterol 7 α -hydroxylase, via FXR-mediated activation of the inhibitory nuclear liver-enriched orphan receptor shp (small heterodimer partner) (14;15). Also, it has been recently shown that bile salts are able to induce a downregulation of the sinusoidal sodium/bile salt cotransporter mRNA levels (NTCP, the main uptake system for bile salts at the hepatocyte sinusoidal membrane (16)) by FXR-mediated activation of shp (17). Last, the bile salt export pump (an ATP-dependent transport protein which mediates bile salt transport across the hepatocyte canalicular membrane (18)) appears to be upregulated by high intracellular bile salt levels (19). Intracellular bile salt homeostasis is shown schematically in **Figure 4**.

In line with these findings, FXR $-/-$ mice have decreased mRNA levels of bsep and increased mRNA levels of cholesterol 7 α -hydroxylase (20). On dietary challenge with cholate, FXR $-/-$ mice develop severe hepatotoxicity reflecting the inability of these mice to deal with bile salt overload. These findings indicate that FXR plays a critical role in protecting the liver against pathological levels of bile salts and is a major regulator of bile salt homeostasis (21).

Detergent properties of bile salts

Bile salts may present as “good” or “bad” guys (22). The good aspect is their effect in intestinal lipid absorption, bile formation and cholesterol solubilization. The “bad” aspect is the bile salt-induced extracellular and intracellular toxicity.

Extracellular toxicity

Bile salts are amphiphilic compounds that act as detergents above their critical micellar concentration. The cytotoxic effect of bile salts has been

shown for hepatocytes (23), erythrocytes (24-26) and mucosa of various organs, including stomach (27), intestine (28) and gallbladder (29;30). The damaging effects of bile salts depend on their degree of hydrophobicity (31) and on the cell membrane composition (32).

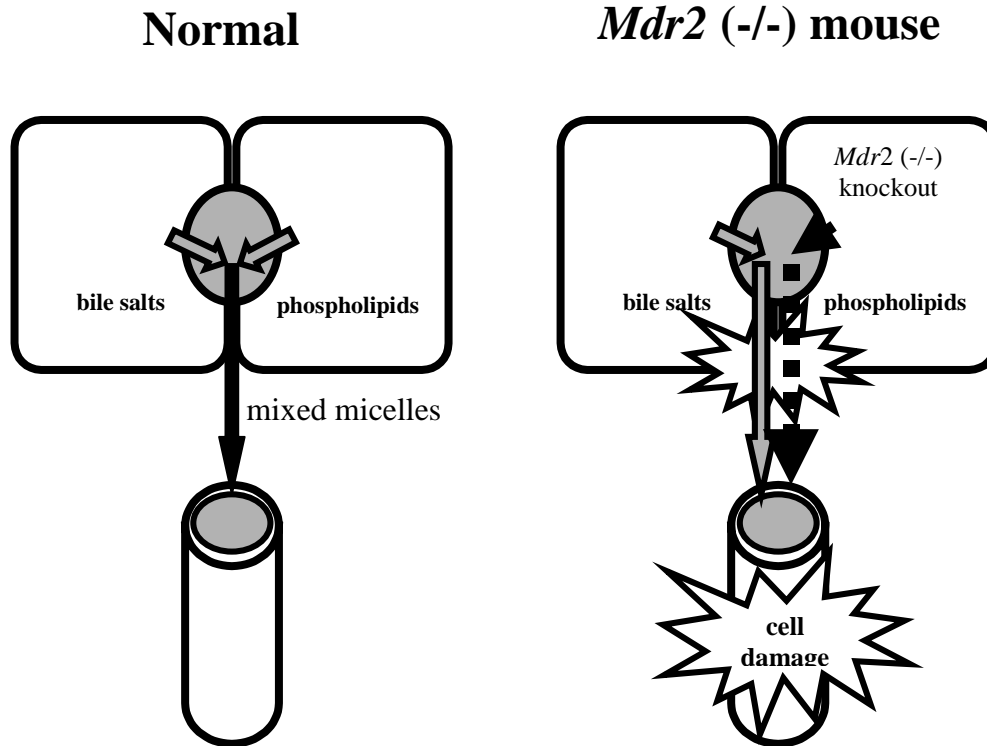


Figure 5. Protection of phospholipids against bile salt-induced cell damage. In normal conditions, phospholipids incorporated in bile salt mixed micelles within the canalicular lumen protect against bile salt cytotoxicity. On the other hand, in absence of phospholipids in bile (like in mice with homozygous disruption of the *mdr-2* gene), bile salts are inducing hepatocytic as well as cholangiocytic damage.

At physiological concentrations, in bile in the gallbladder and bile ducts and within the intestinal lumen, bile salts are associated with phospholipids and cholesterol in mixed micellar structures. However, significant amounts of bile salts are also present under these conditions as monomers and as "simple" micelles (i.e. without incorporated phospholipids). There is some evidence that this so called "intermixed

micellar-vesicular bile salt concentration" (IMC: bile salt monomers + simple micelles) (33), may be responsible for the potentially damaging effects on membrane bilayers (34;35).

At the concentrations occurring in hepatic and gallbladder biles, bile salts could theoretically damage the apical membrane of the hepatocytes and of the cells lining the biliary tract. The absence of such a damaging effect *in vivo* suggests the existence of cytoprotective mechanisms either at the level of the cell membrane or within biliary micelles. Increased concentrations of cholesterol and phospholipids (in particular sphingomyelin) in the hepatocyte canalicular membrane appear to protect against cytotoxic effects of the bile salts within the canalicular lumen (36-38). On the other hand, in *in vitro* studies, inclusion of egg yolk phosphatidylcholine (PC) within bile salt micelles protects in a concentration-dependent manner against bile salt-induced cytotoxicity (39). In line with these findings, mice with homozygous disruption of the *mdr2* gene exhibit severe bile salt-induced hepatocyte damage *in vivo*: since *mdr2* encoded P-glycoprotein -which normally functions as a "flippase" transporting PC molecules from the inner to the outer leaflet of the hepatocytic canalicular membrane- is absent, there is virtually no PC protecting against bile salt-induced hepatotoxicity in bile of these mice (**Figure 5** (40)).

Intracellular toxicity

Intracellular toxicity caused by conjugated bile salt occurs in the intact cell only when a transporter is present in the cell membrane that permits conjugated bile salts to enter the cell. Bile salt intracellular toxicity has been investigated extensively for hepatocytes (41) and cholangiocytes (42). In the hepatocyte of healthy people, bile salt uptake is followed by rapid elimination. When the elimination is impaired, bile salts accumulate intracellularly, leading to mitochondrial damage and

ultimately to apoptosis and necrosis (43;44). Unconjugated bile salts, being hydrophobic and membrane permeable, are highly cytotoxic to isolated cells *in vitro*, since they can readily accumulate to intracellular toxic levels. Cytotoxicity attributable to unconjugated bile salts *in vivo* (like secondary hydrophobic DC) is of importance for the pathogenesis of colon cancer. In this respect, it should be noted that high-fat diet promotes bile salt accumulation in feces, where enteric bacteria metabolize them to produce secondary bile salts, principally deoxycholate and lithocholate (45). Epidemiological and experimental studies have indicated a consistent correlation between increased risk of colon cancer and elevated levels of fecal bile salts in Western populations that consume high-fat diets (46;47). Consistent with this, studies on animal models of colon carcinogenesis have demonstrated that the secondary hydrophobic bile salt deoxycholate (DC) acts as tumor promoter, inducing hyperproliferation (48;49) and increasing the number of tumors elicited by complete carcinogens (50). Also, DC has been proven to be involved not only in the stimulation of DNA synthesis, but also in DNA degradation. Indeed, it has been shown that DC is also able to induce apoptosis in some adenoma and carcinoma cell lines (51).

Cholesterol metabolism

The molecular mechanisms regulating the amount of dietary cholesterol retained in the body as well as the elimination of cholesterol from the body are of extreme importance, since excess cholesterol accumulation in the body is associated with two of the major diseases of Western countries; atherosclerosis and gallstone disease.

Hepatic cholesterol uptake and “reverse cholesterol transport”

Selective LDL related- and LDL receptors are involved in the hepatocyte sinusoidal membrane uptake of esterified cholesterol from chylomicrons

and low-density lipoproteins. After transfer to the lysosomes, LDL is degraded with release of free cholesterol (52). In patients with Nieman Pick type C disease (NPC) this process is blocked; as a result, there is an accumulation of cholesterol in lysosomes, suggesting that the protein encoded by the gene mutated in NPC disease is probably involved in cholesterol intracellular trafficking (53;54).

HDL (high density lipoprotein) particles are thought to be the main source for cholesterol secreted into bile, possibly by transfer within the bilayer from the sinusoidal to the canalicular side (55).

HDL cholesterol, which originates in peripheral tissues, returns to the liver through the so called “reverse cholesterol transport pathway” (Figure 6).

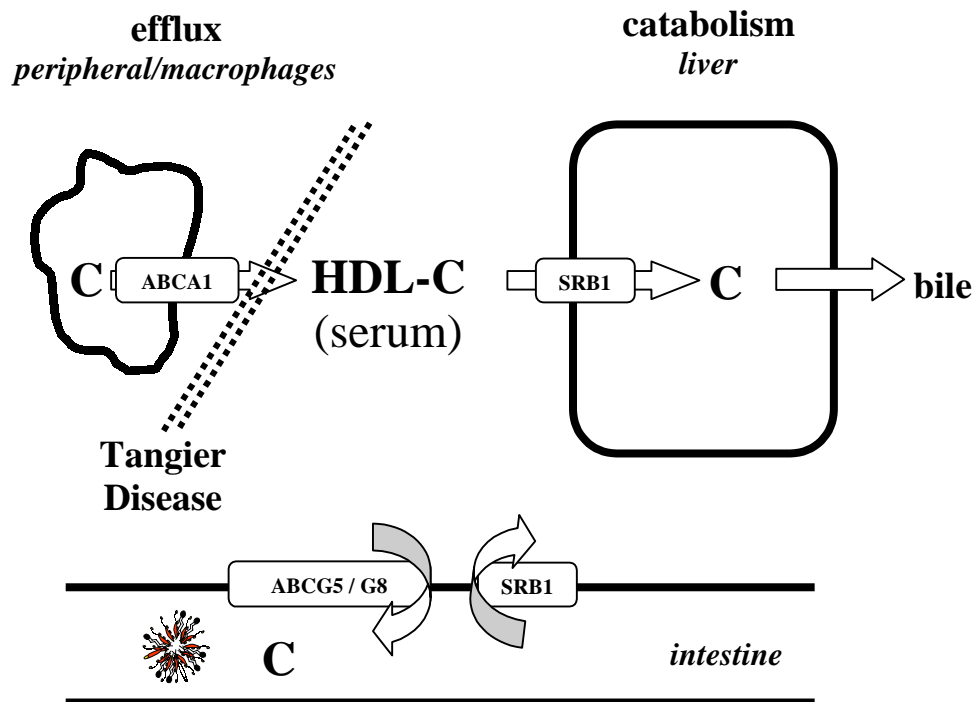


Figure 6. The “reverse cholesterol transport” pathway. ABCA1-controlled cholesterol cellular efflux to HDL, hepatic HDL cholesterol reuptake (SRB1) and intestinal dietary and biliary cholesterol absorption (SRB1, ABCG5/G8). ABCA1 is the protein mutated in Tangier Disease. C=cholesterol

This process is thought to play an essential role in the prevention of atherosclerosis. Recently, a new scavenger receptor (SR-B1) has been identified on the hepatocyte sinusoidal membrane, which binds HDL particles by a process of “docking” (no internalization of the HDL particle) (56). A protein strongly associated to this pathway is ABCA1, the protein mutated in Tangier Disease (a rare autosomal recessive disorder characterized by low circulating levels of HDL and the appearance of cholesterol-engorged macrophages and reticuloendothelial cells (57)). ABCA1 is a cellular ATP-binding cassette (ABC) transporter which influences the cellular efflux of free cholesterol and phospholipids to apolipoprotein A-I in the HDL particles from the peripheral cells. ABCA1 may also play a key role in intestinal cholesterol absorption (see further).

Intestinal cholesterol absorption

The diffusion of cholesterol from lipid rich-phases of the intestinal contents to the intestinal epithelium needs an aqueous interface and is dependent on the solubilisation of dietary and biliary cholesterol by bile salts. PC is necessary for micellar cholesterol solubilization together with bile salts in bile (58). On the other hand, incorporation of PC in bile salt-cholesterol mixed micelles suppresses cholesterol uptake by intestinal cells *in vitro* (59-61). Also, it has been shown that PC hydrolysis by phospholipase A₂ inhibits the micellar PC-induced suppression of cholesterol absorption *in vitro* (62). In contrast, the *mdr-2* knockout mouse, which lacks PC molecules in bile, displays decreased intestinal cholesterol absorption (63).

Also, the intestine displays a high rate of cholesterol biosynthesis which -under certain conditions- may even exceed synthesis in the liver (64). Intestinal mucosa is also involved in cholesterol esterification (65) and synthesis of various apolipoproteins (66). Furthermore, the enterocytes

are a site for release of chylomicrons, nascent high density lipoprotein and an intestinal form of low density lipoprotein (67;68). Animal studies have shown that jejunum and ileum combined account for 7% whole body LDL (low density lipoprotein) clearance (69), and it has been shown by immunohistochemistry that LDL receptors are present throughout the rat intestine (70). Intestinal HMG-CoA reductase and LDL receptor-mediated uptake of cholesterol are coordinately regulated in response to diminished or increased fluxes of dietary cholesterol into the intestinal mucosa, so that mucosal cholesterol concentrations remain constant (71). Also, a recent study has shown that a scavenger receptor class B type 1 (SRB1) in the intestinal brush border membrane may facilitate the uptake of intestinal cholesterol from either bile salt micelles or phospholipid vesicles (72). This receptor can also function as a port for several additional classes of lipids, including cholesteryl esters, triacylglycerols, and phospholipids. In liver and steroidogenic tissues, the physiological ligand of this receptor is high-density lipoprotein. Indeed, Hauser et al. (72) have shown that binding of high-density lipoprotein and apolipoprotein A-I to SRB1 inhibits uptake of cholesterol by the brush border membrane from lipid donor particles. This finding supports the conclusion that SRB1 influences intestinal cholesterol uptake. Recent studies have also shown that LXRs (liver X receptor) prevent overaccumulation of sterols in the intestine and macrophages (73). In the small intestine, increased dietary and/or biliary cholesterol activates LXR-induced upregulation of at least three ABC transporters, ABCA1, ABCG5 and ABCG8 (74). In the enterocyte, these transporters are hypothesized to increase cholesterol efflux into the intestinal lumen and thereby decrease net intestinal sterol absorption. Consistent with these findings, patients with sitosterolemia (a rare autosomic recessive disease with hyperabsorption of cholesterol and non-cholesterol sterols) have mutations in the ABCG5 and ABCG8 genes (75;76).

The role of ABCA1 in intestinal cholesterol absorption has recently been studied in ABCA1 *-/-* mice, which have a phenotype similar to that of human Tangier Disease (77;78). Controversial data are present in the literature. McNeish *et al* (77) reported an increase of dietary cholesterol absorption in ABCA1 knockout mice. It has therefore suggested that ABCA1 may also facilitate resecretion of cholesterol into the intestinal lumen (79). On the other hand, Drobnik *et al.* (80) with the aid of a dual stable isotope technique, concluded that there was a significant reduction (about 11%) in intestinal cholesterol absorption in the *Abca1 -/-* as compared with the wild-type mice.

Canalicular bile formation

Hepatocyte canalicular membrane

The hepatocyte plasma membrane is functionally divided into a canalicular (or apical) region adjacent to the lumen of the bile canaliculus and a sinusoidal (or basolateral) region in close contact with sinusoidal blood. Although the canalicular region comprises only 10-15% of the total plasma membrane, it plays a crucial role in the process of nascent bile formation and biliary secretion of bile salts, phospholipids and cholesterol.

Both phosphatidylcholine and sphingomyelin are the major phospholipids of the canalicular membrane outer leaflet (38;81). In contrast, phosphatidylcholine is the exclusive (>95%) phospholipid in bile. Also, acyl chain compositions of phosphatidylcholines in the canalicular membrane and in bile are different: whereas phosphatidylcholine composition in the membrane is relatively hydrophobic (mainly 16:0-18:2 PC, 16:0-20:4 PC, 18:0-20:4 PC and 18:0-18:2 PC), relatively hydrophilic phosphatidylcholines (16:0-18:2 PC and 16:0-20:4 PC) are found in bile (82). A similar phenomenon appears to occur for sphingomyelins, since canalicular membrane

sphingomyelins contain mainly long (>20 C-atoms) saturated acyl chains amidated to the sphingosine backbone, whereas the trace amounts of sphingomyelin in bile contain mainly 16:0 acyl chains (83).

Sphingomyelin is located predominantly in the external hemileaflet of the canalicular membrane (84). In most eukariotic cells, plasma membrane cholesterol is located mostly on the inner hemileaflet of the plasma membrane. However, cholesterol has a high affinity for sphingomyelin (85-87) and is thought to be preferentially located together with this phospholipid -and with specific GPI-anchored proteins involved in transmembrane signalling- in laterally separated domains ("rafts") that are detergent-resistant with low fluidity (**Figure 7**).

Lipid secretion into bile

A schematic model for canalicular bile secretion is shown in **Figure 7**.

In recent years, there has been considerable progress in understanding lipid transport mechanisms over the canalicular membrane: *mdr* (multi drug resistance) 2 P-glycoprotein functions as a "flippase" translocating phosphatidylcholine molecules from the inner to the outer leaflet of the canalicular membrane (40) and the bile salt export pump (bsep), an ATP-dependent transport protein, mediates bile salt transport across the membrane (18).

The relationship between bile salt and lipid secretion is curvilinear; the secretion of both phospholipids and cholesterol plateaus at high bile salt secretion rates (88). However, the phospholipid secretion rate is always higher than that of cholesterol. The quantity of the bile salt-induced biliary lipid secretion is positively related to the hydrophobicity of the bile salt species secreted (89).

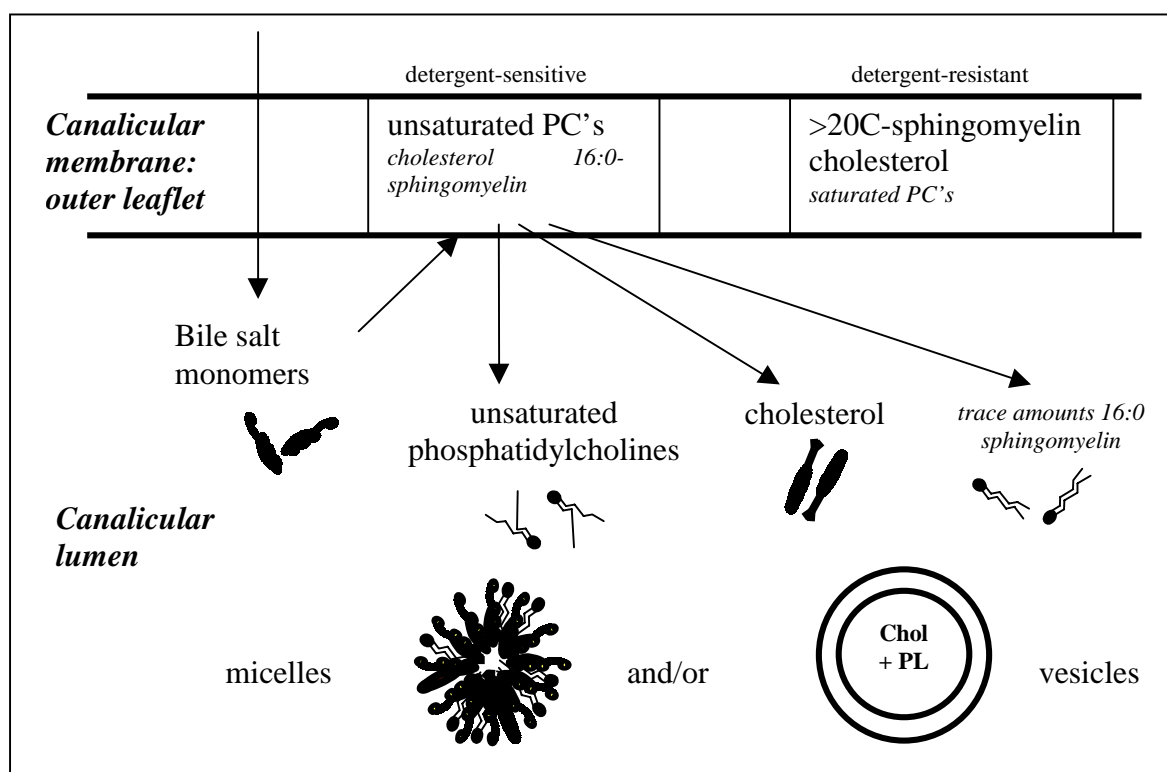


Figure 7. Canalicular bile formation. The outer leaflet of the hepatocyte canalicular membrane may contain detergent-sensitive domains with bile-destined phosphatidylcholine species, that have unsaturated acyl chains at the sn-2 position, together with small amounts of 16:0 sphingomyelin and cholesterol. In contrast, laterally separated domains of sphingomyelin with long (≥ 20 C atoms) saturated acyl chains, together with disaturated phosphatidylcholine species and cholesterol are detergent-resistant.

Secretion of "flipped" phosphatidylcholine from the outer leaflet into the canalicular lumen might happen in two ways: formation of vesicles from the external hemileaflet of the canalicular membrane or solubilization of phosphatidylcholine molecules by bile salts micelles. With the aid of ultrarapid cryofixation and electron microscopic imaging, Crawford et al. could visualize significant amounts of unilamellar vesicles within the canalicular lumen, consistent with a vesicular mode of lipid secretion (90). Nevertheless, both experimental data and theoretical considerations indicate that detergent bile salts, after their secretion into the canalicular

lumen, should micellize directly considerable amounts of lipid from the membrane (91;92).

Also, cholesterol secretion can occur in the absence of phospholipid secretion, based on experiments with *mdr2* deficient mice: in this model, the presence of a hydrophobic bile salt pool (induced by infusion of the hydrophobic bile salt deoxycholate) is sufficient for the extraction of cholesterol from the canalicular membrane in apparent absence of vesicles, since PC is not secreted under these circumstances (92).

From cholesterol solubilization to cholesterol crystallization

Cholesterol is poorly soluble in an aqueous environment, and is solubilized in bile in mixed micelles by bile salts (BS) and phospholipids (PL). Phosphatidylcholine is the major phospholipid in bile (>95% of total: mainly 16:0 acyl chains at the *sn*-1 position and mainly unsaturated (18:2>18:1>20:4) acyl chains at the *sn*-2 position (93)). In case of cholesterol supersaturation, the excess sterol may be contained in vesicles together with phospholipids (94;95) or precipitated as solid crystals. The landmark studies of Wang & Carey (96) have revealed the importance of the relative amounts of bile salts *vs* phospholipids in the system for crystallization behavior. In case of excess bile salts (PL/(BS+PL) ratios $\sim \leq 0.2$), crystals precipitate at fast rates, and both various intermediate anhydrous cholesterol crystals (needles, arcs, tubules, spirals) and mature rhomboid cholesterol monohydrate crystals can be detected by microscopy. In case of higher amounts of phospholipids, crystal precipitation proceeds at slower rates (with predominant formation of mature cholesterol monohydrate crystals), and large amounts of cholesterol are solubilized in vesicles together with phospholipids. In case of excess phospholipids (high PL/(BS+PL) ratios), solid cholesterol crystals do not occur, and cholesterol is mainly solubilized in vesicular phases. Based on these data, the equilibrium

cholesterol-bile salt-phospholipid ternary phase diagram (**Figure 8** (96;97)) is assumed to contain a one-phase zone (only micelles), a left two-phase (micelles and cholesterol crystals-containing) zone, a central three-phase (micelles, vesicles and cholesterol crystals-containing) zone and a right two-phase (micelles and vesicles-containing) zone.

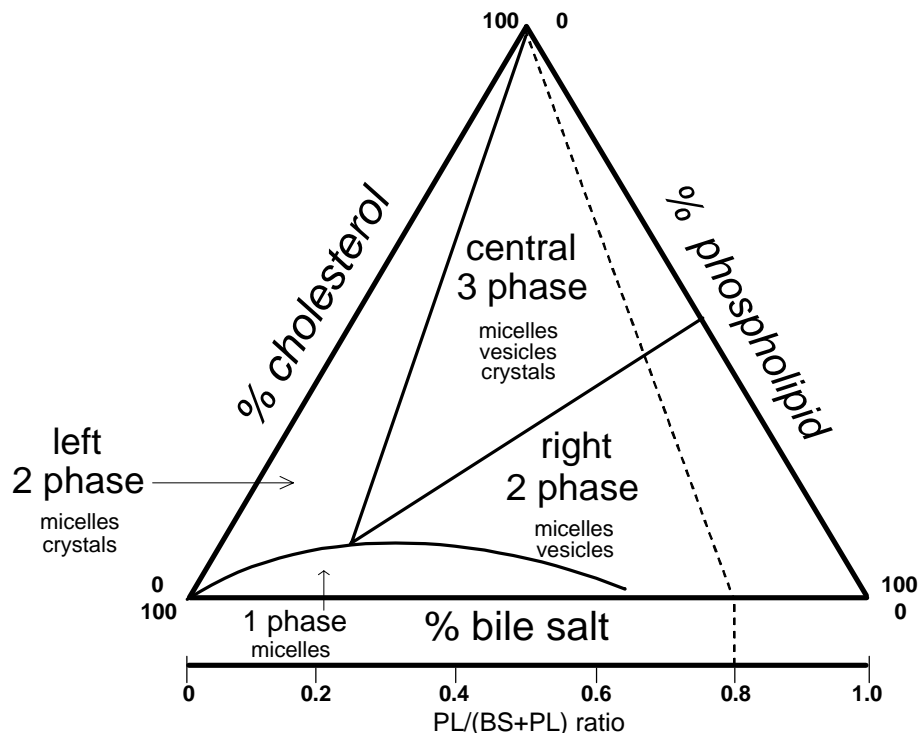


Figure 8. The ternary equilibrium cholesterol-bile salt-phospholipid phase diagram (96). The components are expressed in mol percent. Depicted are a one-phase (micellar) zone at the bottom, a left two-phase zone (containing micelles and crystals), a central three-phase zone (containing micelles, vesicles and crystals) and a right two-phase zone (containing micelles and vesicles). On the basal axis is also depicted an axis which takes into account the $PL/(BS+PL)$ ratios. Interrupted line indicates identical $PL/(BS+PL)$ ratios for all model biles plotting on the line (in this case $PL/(BS+PL)$ ratio = 0.8)

In case of disaturated phospholipids and/or hydrophilic bile salts, the right two-phase (vesicles and micelles-containing) zone is greatly expanded to the left at the expense of the crystals-containing (central three-phase and left two-phase) zones (**Figure 9** (96;97)).

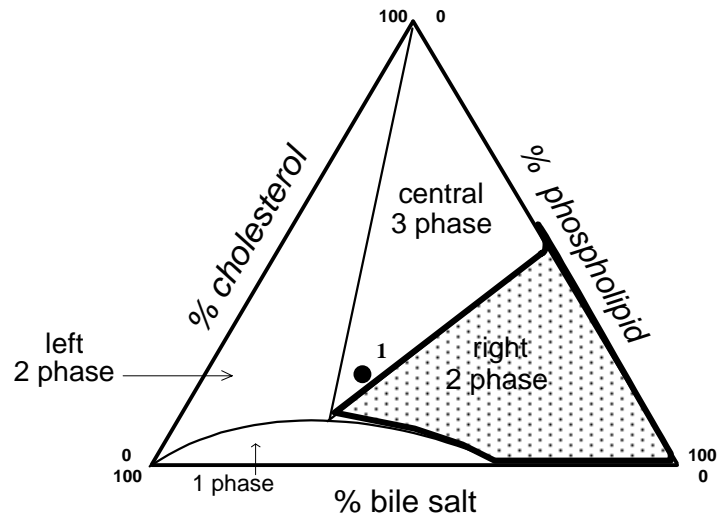
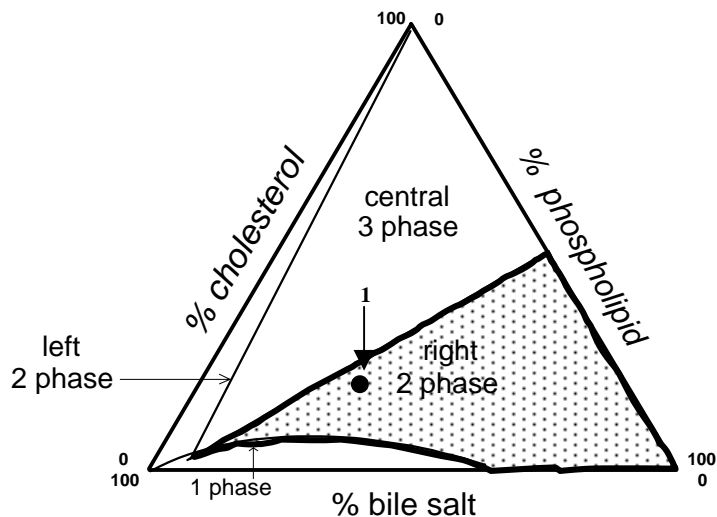
A - Hydrophobic bile salts / unsaturated phospholipids**B - Hydrophilic bile salts / saturated phospholipids**

Figure 9. (A) The ternary equilibrium cholesterol-bile salt-phospholipid phase diagram, see legend figure 7 (96). (B) In case of di-saturated phospholipids and/or hydrophilic bile salts, the right two-phase (vesicles and micelles-containing) zone is greatly expanded to the left at the expense of the crystals-containing (central three-phase and left two-phase) zones (96;97).

● = bile 1 plotting in the three-phase (crystals-containing) zone in case of hydrophobic bile salts or unsaturated phospholipids (A), but in the right-two phase zone (without crystals) in case of hydrophilic bile salts or saturated phospholipids (B), despite unchanged molar % bile salts, phospholipids and cholesterol.

Therefore, a cholesterol-supersaturated bile of (patho)physiological significance (e.g. bile 1 in Fig. 9) may plot in the three-phase (crystals-containing) zone in case of hydrophobic bile salts or unsaturated phospholipids, but in the right-two phase zone (without crystals) in case of hydrophilic bile salts or saturated phospholipids, despite unchanged molar % bile salts, phospholipids and cholesterol. As a result, hydrophobic bile salts and saturated phospholipids might theoretically prevent cholesterol crystallization and gallstone formation.

Cholesterol crystals and gallstone formation

Cholesterol gallstones are composed mainly of cholesterol and can be defined by a weight fraction of cholesterol that is greater than 70% cholesterol (98). The remainder of the cholesterol gallstone is a mixture of biliary glycoproteins, calcium salts and bile pigments (99). Cholesterol gallstones are organic concretions that represent agglomerates of monohydrate cholesterol crystals (**Figure 10**), usually oriented with the long axes radiating outward from the center of the stone and held together by an organic matrix of glycoproteins (100).

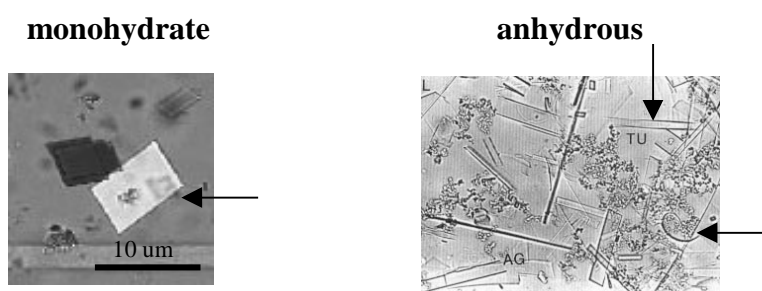


Figure 10. Crystalline structures of monohydrate and anhydrous cholesterol. Arrows indicate a plate-like monohydrate cholesterol crystal (left panel) and arc-shaped or tubule-like anhydrous cholesterol crystals (right panel).

In nature, cholesterol can exist in two different crystalline forms, anhydrous and monohydrate (**Figure 10**), both of which have been visualized in human bile of cholesterol gallstone patients (101). The structures of those crystals have been described by Craven (monohydrate crystals (102)) and by Shieh et al (anhydrous crystals (103)).

The process of cholesterol crystal formation in human or model bile has been the object of various studies. Rearrangements of cholesterol-containing lipid particles (micelles and vesicles) occur before nucleation and crystallization. Within the gallbladder, bile is concentrated due to the water absorption (total lipid conc. from 2.4 to 7.3 g/dL, hepatic vs gallbladder bile, resp. (104)) and micellar cholesterol carrying capacity increases, as shown by the increase in the one-phase zone (only micelles) of the equilibrium ternary phase diagram (96). Also, during bile concentration in the gallbladder, there is an increase in vesicular cholesterol/phospholipid ratios, with vesicular instability as a result. Vesicles aggregate and fuse (thus initiating the process of cholesterol nucleation and precipitation) in supersaturated bile when vesicular cholesterol/phospholipid ratio reaches values above 1 (105-107). Rhomboidal plates can be seen emerging from aggregated vesicles by phase-contrast microscopy (107).

Support for the “vesicular” pathway of cholesterol crystallization is coming from the observation that nucleation-promoting proteins disrupt vesicles (108) and accelerate vesicular aggregation (105). Also, proteins that prolong crystal nucleation time, like apolipoprotein A-I, prevent vesicle fusion (109). A cryo transmission electron microscopy (cryo-TEM) study supports the role of small unilamellar vesicles as key players in cholesterol nucleation (110). Recently, with the aid of video-enhanced light microscopy combined with time-lapse cryo-TEM, Konikoff et al. (111) have visualized the microstructural evolution of lipid aggregates in nucleating model and human biles. This study pointed to the role of

vesicular (uni- and multi-lamellar) aggregates in the nucleation process. Nevertheless, mixed micelles could also play a role in crystal formation (“micellar” pathway). First, mixed micelles coexisting with cholesterol-enriched vesicles may also be supersaturated (112). Second, in bile salt-cholesterol model systems, cholesterol crystals may form in absence of phospholipids, and cholesterol crystals have been suggested to derive from the micellar phase *in vivo* (113). Also, some native biles of cholesterol gallstone patients plot in the left-two (micelles plus crystals-containing) zone of the equilibrium ternary phase diagram and present the crystallization sequence of the left-two phase zone (arc-shaped crystals transformed via helices and tubules into plate-like monohydrate cholesterol crystals without formation of vesicles (114)). Finally, with the aid of an accurate technique for isolation of micellar and vesicular cholesterol carriers, it has been shown that some gallbladder biles of cholesterol gallstone patients did not contain vesicles (115).

Also, in a recent report, patients with intrahepatic cholesterol stones were found to have only small amounts of biliary phospholipids, due to a mutation in the MDR3 gene (116). One may speculate that these patients do not have sufficient vesicular cholesterol solubilizing capacity (and possibly biles plotting in the left-two phase zone of the ternary phase diagram). As a result, fast crystallization from supersaturated micelles might occur immediately after biliary lipid secretion, with hepatic gallstones as a result. These findings point to the important (but still often ignored) role that genetic defects may play in human cholesterol gallstone formation (117).

Aims of the thesis

The present work investigates the distribution of cholesterol and various phospholipids between biliary lipid carriers and the “good” and “bad” sides of bile salts.

The following questions will be addressed in this thesis:

- What are the problems with the techniques for separating micelles and vesicles? Is it possible to have an accurate isolation of biliary lipid carriers? (*chapter 2*)
- What is the influence of bile salt and phospholipid species on cholesterol crystallization? (*chapter 3*)
- Are in model systems sphingomyelin and phosphatidylcholine (the phospholipids involved in bile formation) distributing differently between vesicular and micellar phases representing canalicular membrane and bile lipids? (*chapter 4*)
- Is cholesterol influencing vesicle → micelle transitions of sphingomyelin-phosphatidylcholine containing bilayers induced by detergent bile salts? What are the intermediate lipid structures? (*chapter 5*)
- Is there a protective effect for sphingomyelin against bile salt-induced cytotoxicity? (*chapter 6*)
- Are there any lipid changes in bile of patients with obstructive jaundice especially with regard to phospholipid classes? (*addendum to chapter 6*)
- Are various hydrophobic/hydrophilic bile salts influencing the distribution of sphingomyelin and phosphatidylcholine between micellar and vesicular phases? (*chapter 7*)
- Is the diet constituent sphingomyelin protecting against bile salt-induced intracellular cytotoxicity with potential implications for colon cancer? (*preliminary data in chapter 8*).

References

1. Brown MS, Goldstein JL. Sterol regulatory element binding proteins (SREBPs): controllers of lipid synthesis and cellular uptake. *Nutr Rev* 1998; 56:S1-S3.
2. Schroeder F, Jefferson JR, Kier AB, Knittel J, Scallen TJ, Wood WG et al. Membrane cholesterol dynamics: cholesterol domains and kinetic pools. *Proc Soc Exp Biol Med* 1991; 196:235-252.
3. Cohen DE, Green RM, Wu MK, Beier DR. Cloning, tissue-specific expression, gene structure and chromosomal localization of human phosphatidylcholine transfer protein. *Biochim Biophys Acta* 1999; 1447:265-270.
4. van Helvoort A, de Brouwer A, Ottenhoff R, Brouwers JF, Wijnholds J, Beijnen JH et al. Mice without phosphatidylcholine transfer protein have no defects in the secretion of phosphatidylcholine into bile or into lung airspaces. *Proc Natl Acad Sci U S A* 1999; 96:11501-11506.
5. Geijtenbeek TB, Westerman J, Heerma W, Wirtz KW. Phosphatidylcholine transfer protein from bovine liver contains highly unsaturated phosphatidylcholine species. *FEBS Lett* 1996; 391:333-335.
6. Kramer W, Nicol SB, Girbig F, Gutjahr U, Kowalewski S, Fasold H. Characterization and chemical modification of the Na(+)-dependent bile-acid transport system in brush-border membrane vesicles from rabbit ileum. *Biochim Biophys Acta* 1992; 1111:93-102.
7. Shneider BL, Dawson PA, Christie DM, Hardikar W, Wong MH, Suchy FJ. Cloning and molecular characterization of the ontogeny of a rat ileal sodium-dependent bile acid transporter. *J Clin Invest* 1995; 95:745-754.
8. Xu G, Shneider BL, Shefer S, Nguyen LB, Batta AK, Tint GS et al. Ileal bile acid transport regulates bile acid pool, synthesis, and plasma cholesterol levels differently in cholesterol-fed rats and rabbits. *J Lipid Res* 2000; 41:298-304.
9. Björkhem I. Mechanisms of bile acid biosynthesis in mammalian liver. In: Danielsson H, Sjövall J, editors. *Sterols and Bile Acids (New Comprehensive Biochemistry)*. Amsterdam: Elsevier, 1985: 231-278.
10. Ishibashi S, Schwarz M, Frykman PK, Herz J, Russell DW. Disruption of cholesterol 7 α -hydroxylase gene in mice: 1. Postnatal lethality reversed by bile acid and vitamin supplementation. *J Biol Chem* 1996; 271:18017-18023.
11. Pandak WM, Bohdan P, Franklund C, Mallonee DH, Eggertsen G, Björkhem I et al. Expression of sterol 12 α -hydroxylase alters bile acid pool composition in primary rat hepatocytes and in vivo. *Gastroenterology* 2001; 120:1801-1809.
12. Parks DJ, Blanchard SG, Bledsoe RK, Chandra G, Consler TG, Kliewer SA et al. Bile acids: natural ligands for an orphan nuclear receptor. *Science* 1999; 284:1365-1368.

13. Makishima M, Okamoto AY, Repa JJ, Tu H, Learned RM, Luk A et al. Identification of a nuclear receptor for bile acids. *Science* 1999; 284:1362-1365.
14. Goodwin B, Jones SA, Price RR, Watson MA, McKee DD, Moore LB et al. A regulatory cascade of the nuclear receptors FXR, SHP-1, and LXR-1 represses bile acid biosynthesis. *Mol Cell* 2000; 6:517-526.
15. Lu TT, Makishima M, Repa JJ, Schoonjans K, Kerr TA, Auwerx J et al. Molecular basis for feedback regulation of bile acid synthesis by nuclear receptors. *Mol Cell* 2000; 6:507-515.
16. Meier PJ. Molecular mechanisms of hepatic bile salt transport from sinusoidal blood into bile. *Am J Physiol* 1995; 269:G801-G812.
17. Denson LA, Sturm E, Echevarria W, Zimmerman TL, Makishima M, Mangelsdorf DJ et al. The orphan nuclear receptor, shp, mediates bile acid-induced inhibition of the rat bile acid transporter, ntcp. *Gastroenterology* 2001; 121:140-147.
18. Gerloff T, Stieger B, Hagenbuch B, Madon J, Landmann L, Roth J et al. The sister of P-glycoprotein represents the canalicular bile salt export pump of mammalian liver. *J Biol Chem* 1998; 273:10046-10050.
19. Moseley RH. Bile-ology 101. *Gastroenterology* 2001; 121(1):218-220.
20. Sinal CJ, Tohkin M, Miyata M, Ward JM, Lambert G, Gonzalez FJ. Targeted disruption of the nuclear receptor FXR/BAR impairs bile acid and lipid homeostasis. *Cell* 2000; 102:731-744.
21. Arrese M, Karpen SJ. New horizons in the regulation of bile acid and lipid homeostasis: critical role of the nuclear receptor FXR as an intracellular bile acid sensor. *Gut* 2001; 49:465-466.
22. Hofmann AF. Bile Acids: The Good, the Bad, and the Ugly. *News Physiol Sci* 1999; 14:24-29.
23. Barnwell SG, Lowe PJ, Coleman R. Effect of taurochenodeoxycholate or tauroursodeoxycholate upon biliary output of phospholipids and plasma-membrane enzymes, and the extent of cell damage, in isolated perfused rat livers. *Biochem J* 1983; 216:107-111.
24. Heuman DM, Pandak WM, Hylemon PB, Vlahcevic ZR. Conjugates of ursodeoxycholate protect against cytotoxicity of more hydrophobic bile salts: in vitro studies in rat hepatocytes and human erythrocytes. *Hepatology* 1991; 14:920-926.
25. Coleman R, Iqbal S., Godfrey PP, Billington D. Membranes and bile formation. Composition of several mammalian biles and their membrane-damaging properties. *Biochem J* 1979; 178:201-208.
26. Lowe PJ, Coleman R. Membrane fluidity and bile salt damage. *Biochim Biophys Acta* 1981; 640:55-65.

27. Davenport H.W. Destruction of the gastric mucosal barrier by detergent and urea. *Gastroenterology* 1968; 54:175-181.
28. Chadwick V.S., Gaginella T.S., Carlson G.L., Debognie J.C., Phillips S.F., Hoffmann A. Effect of molecular structure on bile acid-induced alterations in absorptive function, permeability, and morphology in the perfused rabbit colon. *J Lab Clin Med* 1979; 94:661-674.
29. Ostrow JD. Absorption by the gallbladder of bile salts, sulfobromophthalein and iodipamide. *J Lab Clin Med* 1969; 74:482-494.
30. Ostrow JD. Absorption of bile pigments by the gallbladder. *J Clin Invest* 1967; 46:2035-2052.
31. Coleman R. Bile salts and biliary lipids. *Biochem Soc Trans* 1987; 15:68S-80S.
32. Coleman R, Lowe PJ, Billington D. Membrane lipid composition and susceptibility to bile salt damage. *Biochim Biophys Acta* 1980; 599:294-300.
33. Donovan JM, Timofeyeva N, Carey MC. Influence of total lipid concentration, bile salt:lecithin ratio, and cholesterol content on inter-mixed micellar/vesicular (non-lecithin-associated) bile salt concentrations in model bile. *J Lipid Res* 1991; 32:1501-1512.
34. Donovan JM, Jackson AA, Carey MC. Molecular species composition of inter-mixed micellar/vesicular bile salt concentrations in model bile: dependence upon hydrophilic-hydrophobic balance. *J Lipid Res* 1993; 34:1131-1140.
35. Angelico M, Mogavero L, Baiocchi L, Nistri A, Gandin C. Dissolution of human cholesterol gallstones in bile salt/lecithin mixtures: effect of bile salt hydrophobicity and various pHs. *Scand J Gastroenterol* 1995; 30:1178-1185.
36. Amigo L, Mendoza H., Zanlungo S., Miquel JF, Rigotti A, Gonzalez S et al. Enrichment of canalicular membrane with cholesterol and sphingomyelin prevents bile salt-induced hepatic damage. *J Lipid Res* 1999; 40:533-542.
37. Schachter D. The hepatocyte plasma membrane: organization and differentiation. In: Arias IM, Jakoby WB, Popper H, Schachter D, Shafritz DA, editors. *The Liver: Biology and Pathobiology*. New York: Raven Press, Ltd., 1988: 131-140.
38. Kremmer T, Wisher MH, Evans WH. The lipid composition of plasma membrane subfractions originating from the three major functional domains of the rat hepatocyte cell surface. *Biochim Biophys Acta* 1976; 455:655-664.
39. Velardi A.L.M., Groen AK, Oude Elferink RP, van der Meer R, Palasciano G, Tytgat GN. Cell type-dependent effect of phospholipid and cholesterol on bile salt cytotoxicity. *Gastroenterology* 1991; 101:457-464.
40. Smit JJ, Schinkel AH, Oude Elferink RPJ, Groen AK, Wagenaar E, van Deemter L et al. Homozygous disruption of the murine mdr2 P-glycoprotein

gene leads to a complete absence of phospholipid from bile and to liver disease. *Cell* 1993; 75:451-462.

41. Sodeman T, Bronk SF, Roberts PJ, Miyoshi H, Gores GJ. Bile salts mediate hepatocyte apoptosis by increasing cell surface trafficking of Fas. *Am J Physiol Gastrointest Liver Physiol* 2000; 278:G992-G999.
42. Alpini G, Glaser SS, Ueno Y, Rodgers R, Phinizy JL, Francis H et al. Bile acid feeding induces cholangiocyte proliferation and secretion: evidence for bile acid-regulated ductal secretion. *Gastroenterology* 1999; 116:179-186.
43. Roberts LR, Kurosawa H, Bronk SF, Fesmier PJ, Agellon LB, Leung WY et al. Cathepsin B contributes to bile salt-induced apoptosis of rat hepatocytes. *Gastroenterology* 1997; 113:1714-1726.
44. Rodrigues CM, Fan G, Ma X, Kren BT, Steer CJ. A novel role for ursodeoxycholic acid in inhibiting apoptosis by modulating mitochondrial membrane perturbation. *J Clin Invest* 1998; 101:2790-2799.
45. Hill MJ, Drasar BS, Hawksworth G, Aries V, Crowther JS, Williams RE. Bacteria and aetiology of cancer of large bowel. *Lancet* 1971; 1:95-100.
46. Armstrong B, Doll R. Environmental factors and cancer incidence and mortality in different countries, with special reference to dietary practices. *Int J Cancer* 1975; 15:617-631.
47. Weisburger JH, Wynder EL, Horn CL. Nutritional factors and etiologic mechanisms in the causation of gastrointestinal cancers. *Cancer* 1982; 50:2541-2549.
48. Bartram HP, Scheppach W, Schmid H, Hofmann A, Dusel G, Richter F et al. Proliferation of human colonic mucosa as an intermediate biomarker of carcinogenesis: effects of butyrate, deoxycholate, calcium, ammonia, and pH. *Cancer Res* 1993; 53:3283-3288.
49. Bartram HP, Kasper K, Dusel G, Liebscher E, Gostner A, Loges C et al. Effects of calcium and deoxycholic acid on human colonic cell proliferation in vitro. *Ann Nutr Metab* 1997; 41:315-323.
50. Reddy BS, Watanabe K, Weisburger JH, Wynder EL. Promoting effect of bile acids in colon carcinogenesis in germ-free and conventional F344 rats. *Cancer Res* 1977; 37:3238-3242.
51. Hague A, Elder DJ, Hicks DJ, Paraskeva C. Apoptosis in colorectal tumour cells: induction by the short chain fatty acids butyrate, propionate and acetate and by the bile salt deoxycholate. *Int J Cancer* 1995; 60:400-406.
52. Hussain MM. Structural, biochemical and signaling properties of the low-density lipoprotein receptor gene family. *Front Biosci* 2001; 6:D417-D428.
53. Millat G, Marcais C, Tomasetto C, Chikh K, Fensom AH, Harzer K et al. Niemann-Pick C1 disease: correlations between NPC1 mutations, levels of NPC1 protein, and phenotypes emphasize the functional significance of the

- putative sterol-sensing domain and of the cysteine-rich luminal loop. *Am J Hum Genet* 2001; 68:1373-1385.
54. Millard EE, Srivastava K, Traub LM, Schaffer JE, Ory DS. Niemann-pick type C1 (NPC1) overexpression alters cellular cholesterol homeostasis. *J Biol Chem* 2000; 275:38445-38451.
 55. Robins SJ, Fasulo JM. High density lipoproteins, but not other lipoproteins, provide a vehicle for sterol transport to bile. *J Clin Invest* 1997; 99:380-384.
 56. Acton S, Rigotti A, Landschulz KT, Xu S, Hobbs HH, Krieger M. Identification of scavenger receptor SR-BI as a high density lipoprotein receptor. *Science* 1996; 271:518-520.
 57. Young SG, Fielding CJ. The ABCs of cholesterol efflux. *Nat Genet* 1999; 22:316-318.
 58. Carey MC, Small DM. The physical chemistry of cholesterol solubility in bile. Relationship to gallstone formation and dissolution in man. *J Clin Invest* 1978; 61:998-1026.
 59. Rampone AJ, Long LW. The effect of phosphatidylcholine and lysophosphatidylcholine on the absorption and mucosal metabolism of oleic acid and cholesterol in vitro. *Biochim Biophys Acta* 1977; 486:500-510.
 60. Thomson AB, Cleland L. Intestinal cholesterol uptake from phospholipid vesicles and from simple and mixed micelles. *Lipids* 1981; 16:881-887.
 61. Reynier MO, Lafont H, Crotte C, Sauve P, Gerolami A. Intestinal cholesterol uptake: comparison between mixed micelles containing lecithin or lysolecithin. *Lipids* 1985; 20:145-150.
 62. Homan R, Hamelehle KL. Phospholipase A2 relieves phosphatidylcholine inhibition of micellar cholesterol absorption and transport by human intestinal cell line Caco-2. *J Lipid Res* 1998; 39:1197-1209.
 63. Voshol PJ, Havinga R, Wolters H, Ottenhoff R, Princen HM, Oude Elferink RP et al. Reduced plasma cholesterol and increased fecal sterol loss in multidrug resistance gene 2 P-glycoprotein-deficient mice. *Gastroenterology* 1998; 114:1024-1034.
 64. Field FJ, Kam NT, Mathur SN. Regulation of cholesterol metabolism in the intestine. *Gastroenterology* 1990; 99:539-551.
 65. Helgerud P, Saarem K, Norum KR. Acyl-CoA:cholesterol acyltransferase in human small intestine: its activity and some properties of the enzymic reaction. *J Lipid Res* 1981; 22:271-277.
 66. Rachmilewitz D, Albers JJ, Saunders DR, Fainaru M. Apoprotein synthesis by human duodenojejunal mucosa. *Gastroenterology* 1978; 75:677-682.
 67. Green PH, Tall AR, Glickman RM. Rat intestine secretes discoid high density lipoprotein. *J Clin Invest* 1978; 61:528-534.

68. Ockner RK, Hughes FB, Isselbacher KJ. Very low density lipoproteins in intestinal lymph: role in triglyceride and cholesterol transport during fat absorption. *J Clin Invest* 1969; 48:2367-2373.
69. Spady DK, Bilheimer DW, Dietschy JM. Rates of receptor-dependent and -independent low density lipoprotein uptake in the hamster. *Proc Natl Acad Sci U S A* 1983; 80:3499-3503.
70. Fong LG, Bonney E, Kosek JC, Cooper AD. Immunohistochemical localization of low density lipoprotein receptors in adrenal gland, liver, and intestine. *J Clin Invest* 1989; 84:847-856.
71. Nguyen LB, Shefer S, Salen G, Tint GS, Ruiz F, Bullock J. Mechanisms for cholesterol homeostasis in rat jejunal mucosa: effects of cholesterol, sitosterol, and lovastatin. *J Lipid Res* 2001; 42:195-200.
72. Hauser H, Dyer JH, Nandy A, Vega MA, Werder M, Bieliauskaite E et al. Identification of a receptor mediating absorption of dietary cholesterol in the intestine. *Biochemistry* 1998; 37:17843-17850.
73. Repa JJ, Turley SD, Lobaccaro JA, Medina J, Li L, Lustig K et al. Regulation of absorption and ABC1-mediated efflux of cholesterol by RXR heterodimers. *Science* 2000; 289:1524-1529.
74. Lu TT, Repa JJ, Mangelsdorf DJ. Orphan nuclear receptors as eLiXiRs and FiXeRs of sterol metabolism. *J Biol Chem* 2001; *in press*.
75. Berge KE, Tian H, Graf GA, Yu L, Grishin NV, Schultz J et al. Accumulation of dietary cholesterol in sitosterolemia caused by mutations in adjacent ABC transporters. *Science* 2000; 290:1771-1775.
76. Lee MH, Lu K, Hazard S, Yu H, Shulenin S, Hidaka H et al. Identification of a gene, ABCG5, important in the regulation of dietary cholesterol absorption. *Nat Genet* 2001; 27:79-83.
77. McNeish J, Aiello RJ, Guyot D, Turi T, Gabel C, Aldinger C et al. High density lipoprotein deficiency and foam cell accumulation in mice with targeted disruption of ATP-binding cassette transporter-1. *Proc Natl Acad Sci U S A* 2000; 97:4245-4250.
78. Orso E, Broccardo C, Kaminski WE, Bottcher A, Liebisch G, Drobnik W et al. Transport of lipids from golgi to plasma membrane is defective in tangier disease patients and Abc1-deficient mice. *Nat Genet* 2000; 24:192-196.
79. Oram JF, Lawn RM. ABCA1. The gatekeeper for eliminating excess tissue cholesterol. *J Lipid Res* 2001; 42:1173-1179.
80. Drobnik W, Lindenthal B, Lieser B, Ritter M, Christiansen WT, Liebisch G et al. ATP-binding cassette transporter A1 (ABCA1) affects total body sterol metabolism. *Gastroenterology* 2001; 120:1203-1211.

81. Higgins JA, Evans WH. Transverse organization of phospholipids across the bilayer of plasma membrane subfractions of rat hepatocytes. *Biochem J* 1978; 174:563-567.
82. Nibbering CP, Groen AK, Ottenhoff R, Brouwers JFHM, Van Berge-Henegouwen GP, Van Erpecum KJ. Regulation of biliary cholesterol secretion is independent of hepatocyte canalicular membrane lipid composition: a study in the diosgenin-fed rat model. *J Hepatol* 2001; 35:164-169.
83. Nibbering CP, Carey MC. Sphingomyelins of rat liver: biliary enrichment with molecular species containing 16:0 fatty acids as compared to canalicular-enriched plasma membranes. *J Membr Biol* 1999; 167:165-171.
84. Fielding CJ, Fielding PE. Molecular physiology of reverse cholesterol transport. *J Lipid Res* 1995; 36:211-228.
85. Lund-Katz S, Laboda HM, McLean LR, Phillips MC. Influence of molecular packing and phospholipid type on rates of cholesterol exchange. *Biochemistry* 1988; 27:3416-3423.
86. Bar LK, Barenholz Y, Thompson TE. Dependence on phospholipid composition of the fraction of cholesterol undergoing spontaneous exchange between small unilamellar vesicles. *Biochemistry* 1987; 26:5460-5465.
87. Mattjus P, Bittman R, Vilcheze C, Slotte JP. Lateral domain formation in cholesterol/phospholipid monolayers as affected by the sterol side chain conformation. *Biochim Biophys Acta* 1995; 1240:237-247.
88. Barnwell SG, Tuchweber B, Yousef IM. Biliary lipid secretion in the rat during infusion of increasing doses of unconjugated bile acids. *Biochim Biophys Acta* 1987; 922:221-233.
89. Verkade HJ, Vonk RJ, Kuipers F. New insights into the mechanism of bile acid-induced biliary lipid secretion. *Hepatology* 1995; 21:1174-1189.
90. Crawford JM, Mockel GM, Crawford AR, Hagen SJ, Hatch VC, Barnes S et al. Imaging biliary lipid secretion in the rat: ultrastructural evidence for vesiculation of the hepatocyte canalicular membrane. *J Lipid Res* 1995; 36:2147-2163.
91. Oude Elferink RPJ, Tytgat GNJ, Groen AK. The role of *mdr2* P-glycoprotein in hepatobiliary lipid transport. *FASEB J* 1997; 11:19-28.
92. Oude Elferink RPJ, Ottenhoff R, van Wijland M, Frijters CM, van Nieuwkerk C, Groen AK. Uncoupling of biliary phospholipid and cholesterol secretion in mice with reduced expression of *mdr2* P-glycoprotein. *J Lipid Res* 1996; 37:1065-1075.
93. Hay DW, Cahalane MJ, Timofeyeva N, Carey MC. Molecular species of lecithins in human gallbladder bile. *J Lipid Res* 1993; 34:759-768.

94. Mazer NA, Carey MC. Quasielastic light scattering studies of aqueous biliary lipid systems. Cholesterol solubilization and precipitation in model bile solutions. *Biochemistry* 1983; 22:426-442.
95. Sömjen GJ, Gilat T. A non-micellar mode of cholesterol transport in human bile. *FEBS Lett* 1983; 156:265-268.
96. Wang DQH, Carey MC. Complete mapping of crystallization pathways during cholesterol precipitation from model bile: influence of physical-chemical variables of pathophysiologic relevance and identification of a stable liquid crystalline state in cold, dilute and hydrophilic bile salt-containing systems. *J Lipid Res* 1996; 37:606-630.
97. Van Erpecum KJ, Carey MC. Influence of bile salts on molecular interactions between sphingomyelin and cholesterol: relevance to bile formation and stability. *Biochim Biophys Acta* 1997; 1345:269-282.
98. Bills PM, Lewis D. A structural study of gallstones. *Gut* 1975; 16:630-637.
99. Nakayama F. Quantitative microanalysis of gallstones. *J Lab Clin Med* 1968; 72(4):602-611.
100. Abe A, Tsuchiya Y, Sugiura N, Saisho H, Nishimura K, Takeo K. Ultrastructure of cholesterol gallstones as observed by electron microscopy after freeze-fracturing. *Tissue Cell* 1997; 29:191-197.
101. Portincasa P, Van Erpecum KJ, Jansen A, Renooij W, Gadellaa M, VanBerge-Henegouwen GP. Behaviour of various cholesterol crystals in bile from patients with gallstones. *Hepatology* 1996; 23:738-748.
102. Craven BM. Crystal structure of cholesterol monohydrate. *Nature* 1976; 260:727-729.
103. Shieh HS, Hoard LG, Nordman CE. Crystal structure of anhydrous cholesterol. *Nature* 1977; 267:287-289.
104. Eckhardt ER, Van Erpecum KJ, de Smet MB, Go PM, Berge-Henegouwen GP, Renooij W. Lipid solubilization in human gallbladder versus hepatic biles. *J Hepatol* 1999; 31:1020-1025.
105. Afdhal NH, Niu N, Nunes DP, Bansil R, Cao XX, Gantz D et al. Mucin-vesicle interactions in model bile: evidence for vesicle aggregation and fusion before cholesterol crystal formation. *Hepatology* 1995; 22:856-865.
106. Halpern Z, Dudley MA, Lynn MP, Nader JM, Breuer AC, Holzbach RT. Vesicle aggregation in model systems of supersaturated bile: relation to crystal nucleation and lipid composition of the vesicular phase. *J Lipid Res* 1986; 27:295-306.
107. Halpern Z, Dudley MA, Kibe A, Lynn MP, Breuer AC, Holzbach RT. Rapid vesicle formation and aggregation in abnormal human biles. A time-lapse video enhanced contrast microscopy study. *Gastroenterology* 1986; 90:875-885.

108. de Bruijn MA, Goldhoorn BG, Zijlstra AI, Tytgat GN, Groen AK. Interaction of cholesterol-crystallization-promoting proteins with vesicles. *Biochem J* 1995; 305:93-96.
109. Tao S, Tazuma S, Kajiyama G. Apolipoprotein A-I stabilizes phospholipid lamellae and thus prolongs nucleation time in model bile systems: an ultrastructural study. *Biochim Biophys Acta* 1993; 1166:25-30.
110. Gantz DL, Wang DQH, Carey MC, Small DM. Cryoelectron microscopy of a nucleating model bile in vitreous ice: formation of primordial vesicles. *Biophys J* 1999; 76:1436-1451.
111. Konikoff FM, Danino D, Weihs D, Rubin M, Talmon Y. Microstructural evolution of lipid aggregates in nucleating model and human biles visualized by cryogenic transmission electron microscopy. *Hepatology* 2000; 31:261-268.
112. Donovan JM, Jackson AA. Accurate separation of biliary lipid aggregates requires the correct intermixed micellar/intervesicular bile salt concentration. *Hepatology* 1998; 27:641-648.
113. Ahrendt SA, Fox-Talbot K, Kaufman HS, Lillemoie KD, Pitt HA. Cholesterol nucleates rapidly from mixed micelles in the prairie dog. *Biochim Biophys Acta* 1994; 1211:7-13.
114. Wang DQH, Carey MC. Characterization of crystallization pathways during cholesterol precipitation from human gallbladder biles: Identical pathways to corresponding model biles with three predominating sequences. *J Lipid Res* 1996; 37:2539-2549.
115. Eckhardt ERM, van de Heijning BJM, Van Erpecum KJ, Renooij W, VanBerge-Henegouwen GP. Quantitation of cholesterol-carrying particles in human gallbladder bile. *J Lipid Res* 1998; 39:594-603.
116. Rosmorduc O, Hermelin B, Poupon R. MDR3 gene defect in adults with symptomatic intrahepatic and gallbladder cholesterol cholelithiasis. *Gastroenterology* 2001; 120:1459-1467.
117. Khanuja B, Cheah YC, Hunt M, Nishina PM, Wang DQ, Chen HW et al. Lith1, a major gene affecting cholesterol gallstone formation among inbred strains of mice. *Proc Natl Acad Sci USA* 1995; 92:7729-7733.

chapter 2

ACCURATE SEPARATION OF VESICLES, MICELLES AND CHOLESTEROL CRYSTALS IN SUPERSATURATED MODEL BILES BY ULTRACENTRIFUGATION, ULTRAFILTRATION AND DIALYSIS

Antonio Moschetta*, Erik R.M. Eckhardt*, Martin B.M. de Smet,
Willem Renooij, Gerard P. vanBerge Henegouwen, Karel J. van
Erpecum.

Biochimica et Biophysica Acta

-Molecular and cell biology of lipids- 2001; 1532:15-27.

* *Authors who equally contributed to the work*

Abstract

Gel filtration with bile salts at intermixed micellar/vesicular concentrations (IMC) in the eluant has been proposed to isolate vesicles and micelles from supersaturated model biles, but the presence of vesicular aggregates makes this method unreliable. We have now validated a new method for isolation of various phases. First, aggregated vesicles and -if present- cholesterol crystals are pelleted by short ultracentrifugation. Cholesterol contained in crystals and vesicular aggregates can be quantitated from the difference of cholesterol contents in the pellets before and after bile salt-induced solubilization of the vesicular aggregates. Micelles are then isolated by ultrafiltration of the supernatant through a highly selective 300 kDa filter and unilamellar vesicles by dialysis against buffer containing bile salts at IMC values. Lipids contained in unilamellar vesicles are also estimated by subtraction of lipid contents in filtered micelles from lipid contents in (unilamellar vesicles+micelles containing) supernatant (“subtraction method”). “Ultrafiltration-dialysis” and “subtraction” methods yielded identical lipid solubilization in unilamellar vesicles and identical vesicular cholesterol/phospholipid ratios. In contrast, gel filtration yielded much more lipids in micelles and less in unilamellar vesicles, with much higher vesicular cholesterol/phospholipid ratios. When vesicles obtained by dialysis were analyzed by gel filtration, vesicular cholesterol/phospholipid ratios increased strongly, despite correct IMC values for bile salts in the eluant. Subsequent extraction of column material showed significant amounts of lipids. In conclusion, gel filtration may underestimate vesicular lipids and overestimate vesicular cholesterol/phospholipid ratios, supposedly because of lipids remaining attached to the column. Combined ultracentrifugation-ultrafiltration-dialysis should be considered state-of-the-art methodology for quantification of cholesterol carriers in model biles.

INTRODUCTION

Precipitation of cholesterol crystals from supersaturated bile is a prerequisite for gallstone formation (1). The sterol molecule is poorly soluble in an aqueous environment, and is solubilized in bile in mixed micelles together with bile salts and phospholipids (mainly phosphatidylcholine). In case of cholesterol supersaturation, the sterol may also be solubilized in vesicles together with phospholipids (2-5). Crystals may precipitate from cholesterol-enriched vesicles after their

aggregation and fusion (6-8). Accurate quantification of vesicular and micellar phases is important in order to increase insight in the process of crystallization and gallstone formation.

Apart from extent of cholesterol supersaturation and total lipid concentration, the relative amount of bile salts vs phospholipids is also an important factor in cholesterol crystallization. In case of excess bile salts (phospholipid/(bile salt+phospholipid) ratios $\sim \leq 0.2$), crystals precipitate at fast rates, and both various intermediate anhydrous cholesterol crystals (needles, arcs, tubules, spirals) and mature rhomboid cholesterol monohydrate crystals can be detected by microscopy. In case of higher amounts of phospholipids, crystal precipitation proceeds at slower rates (with predominant formation of mature cholesterol monohydrate crystals), and large amounts of cholesterol are solubilized in vesicles together with phospholipids. In case of excess phospholipids (high phospholipid/(bile salt+phospholipid) ratios), solid cholesterol crystals do not occur, and cholesterol is mainly solubilized in vesicular phases. Based on these data, the equilibrium cholesterol-bile salt-phospholipid ternary phase diagram (Fig. 1: (9)) is assumed to contain a one-phase zone (only micelles), a left two-phase (micelles and cholesterol crystals-containing) zone, a central three-phase (micelles, vesicles and cholesterol crystals-containing) zone and a right two-phase (micelles and vesicles-containing) zone.

Apart from mixed micelles, bile contains non-phospholipid associated bile salts, either as monomers or -above their critical micellar concentration- associated in simple micelles. The monomeric plus simple micellar bile salt concentration is referred to as “intermixed micellar/vesicular concentration”, usually abbreviated as “IMC” (10). The fact that vesicles and mixed micelles are in a delicate dynamic balance with bile salt monomers and simple micelles makes accurate isolation and purification technically difficult. Most isolation procedures,

like gel filtration and density gradient ultracentrifugation, inevitably cause dilution of the sample, which may change the IMC and hence the distribution of lipids between vesicles and micelles. Recently, a centrifugal ultrafiltration procedure was developed to rapidly measure IMC values in model bile (11). Subsequent gel filtration of bile using an eluant containing bile salts in concentrations and composition identical to the IMC of the original model bile should theoretically allow separation and isolation of vesicles and mixed micelles without artifactual perturbation of the lipid distribution pseudoequilibrium (11;12). This is the method of choice when human biles are analyzed (13), which usually contain only small amounts of mostly unilamellar vesicles. In contrast, supersaturated model biles with often large amounts of aggregated vesicles cannot generally be analyzed properly by this procedure, as recently discussed by Donovan (14). Aggregated vesicles are too large to enter the gel properly and may be lost during the procedure.

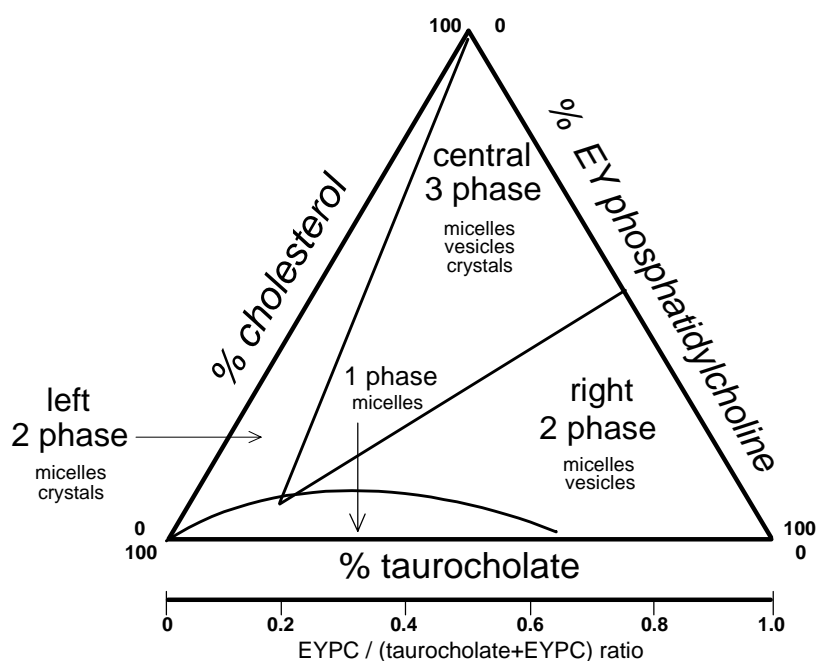


Figure 1: Equilibrium taurocholate-EYPC-cholesterol ternary phase diagram (9). The components are expressed in mol percent. Depicted are

a one-phase (micellar) zone at the bottom, a left two-phase zone (containing micelles and crystals), a central three-phase zone (containing micelles, vesicles and crystals) and a right two-phase zone (containing micelles and vesicles). On the basal axis, phospholipid/(bile salt + phospholipid) ratios are shown.

In the present study we tested a new approach with the aid of ultracentrifugation and ultrafiltration/dialysis of the supernatant to isolate mixed micelles, vesicles and -if present- cholesterol crystals from supersaturated model biles.

MATERIALS AND METHODS

Materials

Taurocholate was obtained from Sigma Chemical Co. (St. Louis, MO, USA) and yielded a single spot upon thin-layer chromatography (butanol-acetic acid-water, 10:1:1 vol/vol/vol, application of 200 µg bile salt). Cholesterol (Sigma) was $\geq 98\%$ pure by reverse-phase HPLC (isopropanol - acetonitrile 1:1, vol/vol, detection at 210 nm). Phosphatidylcholine from egg yolk (EYPC; Sigma) yielded a single spot upon thin-layer chromatography (chloroform-methanol-water 65:25:4, vol/vol/vol, application of 200 µg lipid). As shown by reverse-phase HPLC, EYPC contained mainly 16:0 acyl chains at the *sn*-1 position and mainly unsaturated (18:1>18:2>20:4) acyl chains at the *sn*-2 position, similar to phosphatidylcholine in human bile (15). All other chemicals and solvents were of ACS or reagent grade quality.

Ultrafilters with a Mwco of 10 and 300 kDa were purchased from Sartorius (Göttingen, Germany: Centrisart I). SpectraPor[®] dialysis devices containing membranes with a Mwco of 300 kDa were obtained from Spectrum Laboratories (Laguna Hills, CA, USA: SpectraPor). Sephacryl S400 gel filtration material was purchased from Pharmacia LKB Biotechnology AB (Uppsala, Sweden). The enzymatic cholesterol

assay kit was obtained from Boehringer (Mannheim, Germany) and the enzymatic phospholipid kit from Sopar Biochem (Brussels, Belgium). 3α -Hydroxysteroid dehydrogenase for the enzymatic measurement of bile salt concentrations (16) and a colorimetric chloride-kit were purchased from Sigma. The reverse-phase C18 HPLC column was from Supelco (Supelcosil LC-18-DB, Supelco, Bellefonte, PA, USA).

Preparation of model biles

Lipid mixtures containing variable proportions of cholesterol, phospholipids (both from stock solutions in chloroform) and taurocholate (from stock solutions in methanol) were vortex-mixed and dried at 45°C under a mild stream of nitrogen, and subsequently lyophilized during 24 hrs, before being dissolved in aqueous 150 mM NaCl plus 3mM NaN_3 . Tubes were sealed with Teflon-lined screw caps under a blanket of nitrogen to prevent lipid oxidation and vortex-mixed for 5 min. followed by incubation at 37°C in the dark. All solutions were warmed up to 45°C for 10 min. before use. The final mol percentages of cholesterol, phospholipids and bile salts did not differ more than 1% from intended mol percentages. Also, model systems always plotted in the intended zones of the taurocholate-phosphatidylcholine-cholesterol ternary phase diagram (9), as inferred from microscopic examinations.

Lipid measurement

Cholesterol and phospholipid concentrations were determined with enzymatic assays (17;18). Bile salt concentrations were measured with the 3α -hydroxysteroid dehydrogenase method (16). Cholesterol saturation index (CSI) was calculated according to Carey's critical tables (19).

Quasi - elastic light scattering spectroscopy (QLS)

QLS was performed with a Malvern 4700c spectrometer (Malvern Ltd., Malvern, UK) equipped with an argon laser (Uniphase Corp., San Jose, CA, USA) at a wavelength of 488 nm. In optical clear solutions such as 300 kDa filtrates, the power of the laser was tuned to 50 mW. Data are given as hydrodynamic radius (Rh) and are means of at least 3 measurements.

IMC measurement

Apart from mixed (i.e. phospholipid-bile salt) micelles, model bile systems also contain non-phospholipid associated bile salts, either as monomers or -above their critical micellar concentration- associated in "simple" micelles. The monomeric plus simple micellar bile salt concentration is referred to as “intermixed micellar/vesicular (non phospholipid-associated) bile salt concentration”, usually abbreviated as “IMC” (10). We determined IMC in various model systems, using the rapid centrifugal ultrafiltration technique (10 kDa Centriscart ultrafilter) with correction for Gibbs-Donnan effects (11;12;20;21)

Quantification of aggregated vesicles and cholesterol crystals

In case of model biles plotting in the right two-phase (vesicles and micelles containing) zone (see Fig. 1), aggregated vesicles were pelleted by ultracentrifugation during 30 min. at 50,000 *g* and 37°C in a TLS 55 rotor (Beckman, Palo Alto, CA) (22). After removal of the entire supernatant, the pellet was washed with 150 mM NaCl plus 3 mM NaN₃, containing taurocholate at intermixed micellar/vesicular concentrations, and after repeated ultracentrifugation resuspended in 1.5 mL isopropanol. IMC values measured in non-centrifuged model biles were identical to IMC values in the corresponding supernatants. We did not find a bile salt gradient in the supernatant after centrifugation, indicating that the short

centrifugation procedure did not cause an inhomogeneous distribution of micelles or unilamellar vesicles in the tube. Furthermore, centrifugation did not influence the content of mixed micelles in the model bile, since lipid contents in micelles obtained by ultrafiltration of supernatant through the 300 kDa Mwco filter (see below) were identical to lipid concentrations in ultrafiltrates of corresponding whole model biles.

In case of coexistent cholesterol crystals and aggregated vesicles (three-phase (micelles, vesicles and crystals-containing) zone: see Fig. 1), centrifugation of an additional bile sample was also performed 10 min. after addition of deoxycholate in quantities sufficient to desaturate the model system (final CSI <1). After such incubation, light microscopy and stability of turbidity measurements (405 nm OD (23)) revealed that all vesicular aggregates had been completely micellized. Experiments with isolated cholesterol crystals showed that solubilization of the cholesterol crystals did not occur during the short incubation with deoxycholate. Therefore, cholesterol crystal mass equals cholesterol content in the pellet after addition of deoxycholate, and cholesterol content in vesicular aggregates can be calculated from the difference of cholesterol contents between the pellets without and with added deoxycholate (23).

Quantification of small unilamellar vesicles and micelles by various methods

Ultrafiltration and dialysis: After centrifugation, micelles in the supernatant were isolated by filtration through a Sartorius Centrisart[®] ultrafiltration device containing a membrane with a Mwco of 300 kDa (average pore radius 23 nm). The membrane was first rinsed with 2 mL saline containing taurocholate at IMC values by centrifugation at 500 g during 5 min. to remove glycerol remnants. Remaining saline was carefully removed with a syringe and thereafter, by drying under N₂ at

37°C. The membrane-containing inner tube was then placed membrane-down on the surface of 1 mL supernatant and allowed to sink by gravity until 100 µL of filtrate was produced, which usually took one hour.

The 300 kDa filters were completely permeable to simple and mixed bile salt/phospholipid micelles (tested with mixed micelles at 37°C, at total lipid concentrations of 2.5, 5 and 10 g/dL and at phospholipid/(bile salt+phospholipid) ratios of 0.3, 0.4, 0.5 and 0.55, either without or with cholesterol: with taurocholate or taurodeoxycholate or tauroursodeoxycholate as bile salt), but were completely impermeable to small unilamellar or aggregated vesicles, as confirmed by quasielastic light scattering spectroscopy of the filtrate. A further indication for the complete permeability of the 300 kDa membrane for mixed micelles was the absence of Gibbs-Donnan effects over the membrane, as can be concluded from the identical chloride concentrations in filtrant and filtrate (10;11).

Small unilamellar vesicles were isolated from the supernatant with the aid of a SpectraPor dialysis device (Mwco of the membrane: 300 kDa) by dialysis during 16 hrs. against 3 times 20 mL 0.15 M NaCl containing bile salts at IMC values. After dialysis during 16 hrs of sonicated small unilamellar vesicles (EYPC:cholesterol 1:1; 1.0 mM phospholipid, Rh by quasielastic light scattering spectroscopy 44 nm), no vesicles (by QLS) or lipids could be detected in the dialysate, indicating complete impermeability of the filter for small unilamellar vesicles. When the procedure was applied to unsaturated mixed micellar solutions (total lipid conc. 2.5, 5 or 10 g/dL; EYPC/(taurocholate+EYPC) ratios 0.3, 0.4 or 0.5; 6 mol% cholesterol), no cholesterol or phospholipids could be detected in the dialysant after the 16 hours of dialysis, indicating that all mixed micelles had passed the membrane.

Also, when the supernatant of supersaturated dilute model bile (2.4 g/dL; EYPC/(taurocholate+EYPC) ratio =0.3; 10.7 mol% cholesterol) was

dialysed against 0.15 M NaCl containing taurocholate at IMC values, no Gibbs-Donnan effects could be appreciated over the dialysis membrane, indicating that mixed micelles were not selectively retained by the membrane (10;11). The dialysant was also analyzed after completion of dialysis by gel filtration using 0.15 M NaCl containing taurocholate at IMC values as eluant. Since only vesicles could be detected by this procedure, mixed micelles had apparently been completely removed from the dialysant.

Lipids contained in small unilamellar vesicles were also quantified indirectly by subtracting cholesterol and phospholipid concentrations measured in the 300 KDa (only micelles-containing) filtrate from the lipid concentrations measured in the (micelles + small unilamellar vesicles containing) supernatant (“Subtraction” method).

Gel filtration: a LKB-Pharmacia column (gel bed 30 cm, internal diameter 1.5 cm), equipped with a thermostated water jacket, was packed with Sephacryl S400. Before each model bile fractionation, the column was first equilibrated at 30 mL/hr with two column volumes of Tris-buffered saline (10 mM Tris, 150 mM NaCl, 3 mM NaN₃, pH 7.5) containing taurocholate at IMC values as previously measured in that model system. Thereafter, 1-4 mL of supernatant from previously centrifuged model bile was fractionated on the column at a flow rate of 12 mL/hr. The eluate was collected in 40 fractions of 1 mL and cholesterol, phospholipid and bile salt concentrations were determined in each fraction.

Statistical analysis

Values are expressed as means \pm SEM. Differences between groups were tested for statistical significance by analysis of variance with the aid of NCSS software (Kaysville, Utah, USA). When ANOVA detected a significant difference, results were further compared for contrasts using

Fisher’s least significant difference test as post-hoc test. Statistical significance was defined as a two-tailed probability of less than 0.05.

RESULTS

Comparison between various methods for phase separation

The sum of lipids in the individual fractions (pellet, filtrate and dialyzed supernatant) was equal (~ 98%) to amounts of lipids in corresponding total model bile.

Lipid concentrations in fractions after gel filtration also indicated acceptable recovery (> 80%). Lipid distribution into small unilamellar vesicles and micelles as determined by combined dialysis and ultrafiltration was virtually identical to data obtained in the same supernatant with the “subtraction” method (see “methods”). In contrast, gel filtration yielded consistently more lipids in mixed micelles and less in small unilamellar vesicles than the “subtraction” method (Fig. 2 A-D). Cholesterol/phospholipid ratios in vesicles obtained by dialysis of the supernatant were much lower than cholesterol/phospholipid ratios in vesicles obtained by gel filtration of the same supernatant. When vesicles obtained by dialysis were subsequently analyzed with gel filtration, the cholesterol/phospholipid ratios in these vesicles increased significantly (from 0.99 ± 0.10 to 1.98 ± 0.56 : identical to vesicular cholesterol/phospholipid ratios by gel filtration of the supernatant, $P < 0.05$). This increase could not be ascribed to the presence of mixed micelles in the dialyzed sample, because these were not detectable with gel filtration (Figure 3).

Figure 4 shows the results of three additional gel filtration experiments performed with vesicles obtained by dialysis, together with (between brackets) their initial cholesterol/phospholipid ratios. There was a clear increase of vesicular cholesterol/phospholipid ratios after gel filtration procedure. Lipid extraction of the top 2 mL Sephacryl column material

(24) and measurement of phospholipids and cholesterol in the extract indicated that appreciable amounts of lipids remained attached to the column material (phosphatidylcholine $0.07 \mu\text{mol} / \text{mL}$ column material: cholesterol $0.04 \mu\text{mol} / \text{mL}$ column material).

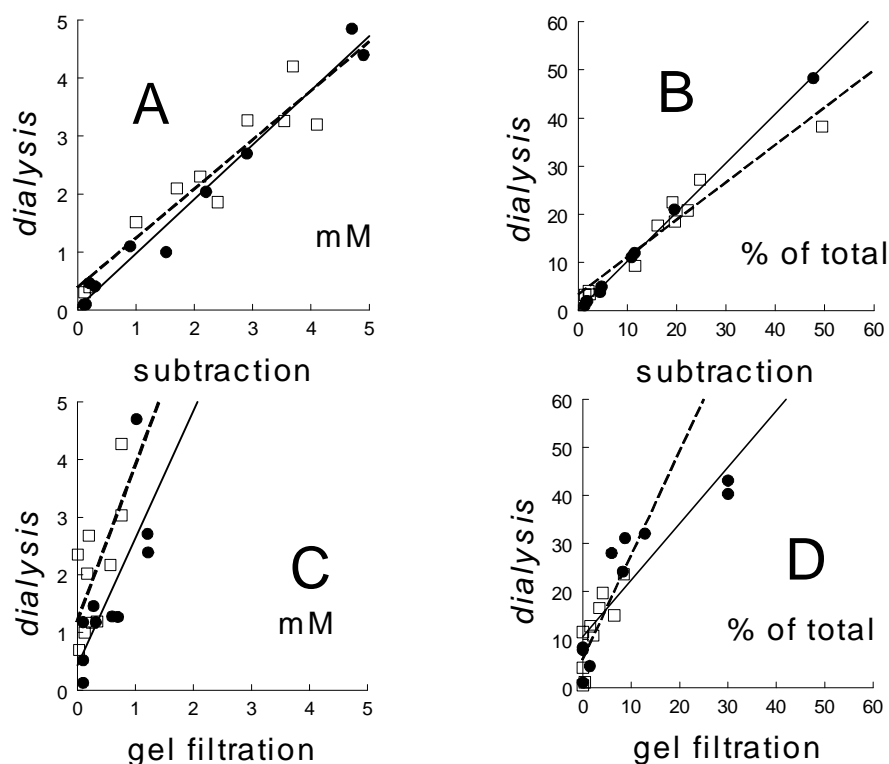


Figure 2: **A and B)** Relationship between results obtained by “subtraction” and dialysis” methods for cholesterol (●) and phospholipid (□) distribution into small unilamellar vesicles in supernatant from model billes with various compositions. **C and D)** Relationship between results obtained by “gel filtration” and “dialysis” methods for cholesterol (●) and phospholipids (□) distribution into small unilamellar vesicles in supernatant. Whereas “dialysis” and “subtraction” methods yield highly similar results, considerably lower lipid distribution into small unilamellar vesicles is found with gel filtration. Reciprocal results are found for micellar lipid solubilization (not shown). (A and C expressed in mM, B and D expressed as % of total; continuous and interrupted lines indicate correlation by linear regression analysis for cholesterol resp. phospholipids).

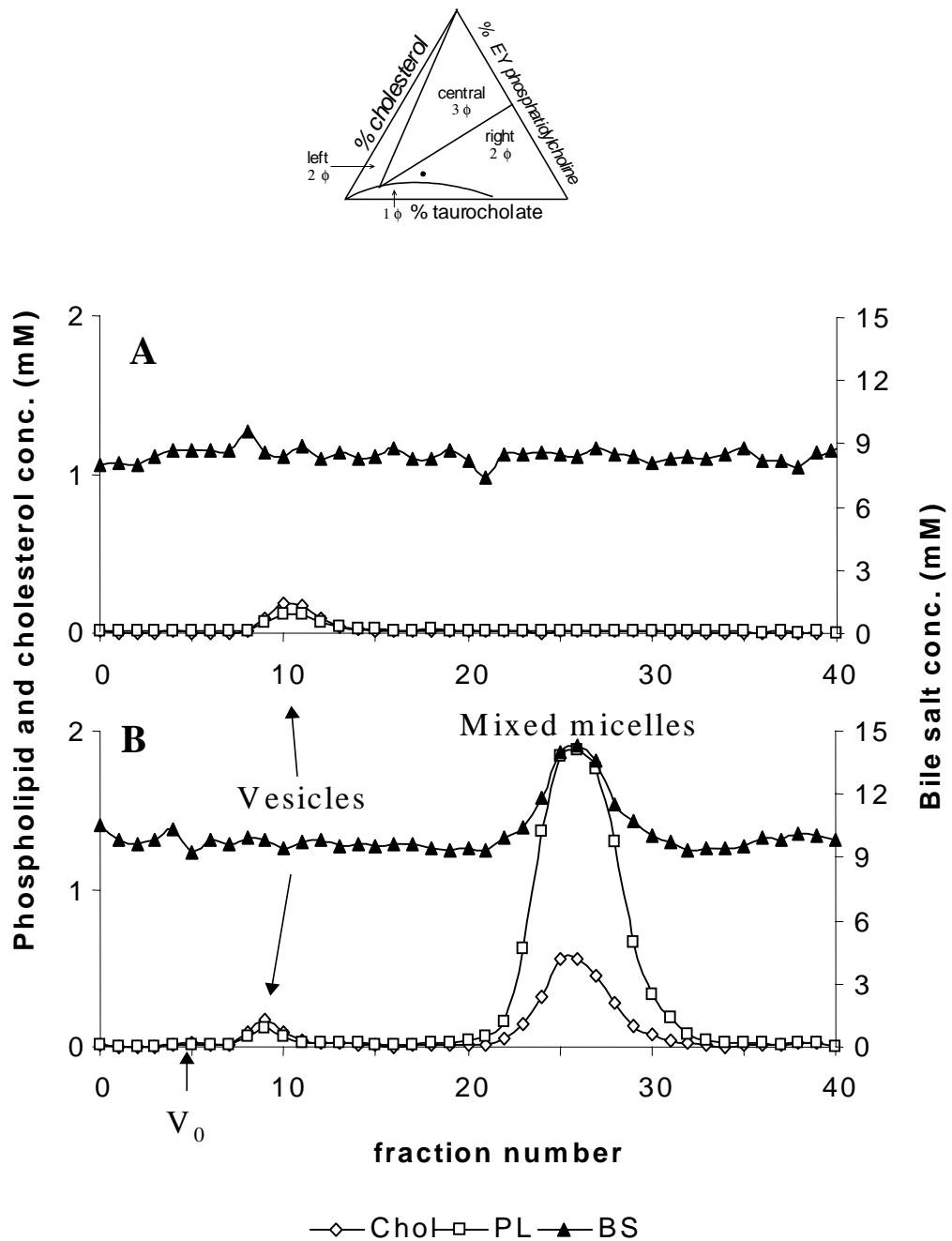


Figure 3: **A)** Gel filtration of the residual vesicle suspension after dialysis during 16 hrs of model bile (2.4 g/dL; (EYPC/(taurocholate+EYPC) =0.3; 10.7% cholesterol; CSI 1.7; aggregated vesicles previously removed by centrifugation) against 3 x 20 volumes of 0.15 M NaCl containing taurocholate at intermixed micellar/vesicular concentrations. All mixed micelles have been washed out by dialysis. **B)** Gel filtration of the corresponding non-dialyzed supernatant. Inset: equilibrium taurocholate-EYphosphatidylcholine-cholesterol ternary phase diagram (9). Dot indicates model bile plotting in right two-phase zone.

Table 1. Cholesterol/phospholipid ratios in vesicular and micellar phases isolated by combined ultrafiltration/dialysis method and by gel filtration method .

Model bile	Cholesterol/phospholipid ratio		
	SUV (gel filtration)	SUV (dialysis)	MIC
2.4 g / dL	1.64 ± 0.09	0.99 ± 0.10	0.27 ± 0.04 (1.02)
7.3 g / dL	1.97 ± 0.26	0.96 ± 0.21	0.30 ± 0.03 (0.97)

Model biles were prepared with the following composition: EYPC/(taurocholate+EYPC) ratio 0.3; 10.7 % cholesterol; CSI 1.7 (2.4 g/dL) or 1.4 (7.3 g/dL) and were incubated during 14 days before analysis. For micelles, CSI is given between brackets.

SUV, small unilamellar vesicles; MIC, mixed micelles.

Influence of total lipid concentration on lipid distribution into various phases

Upon centrifugation, aggregated vesicles were pelleted down to the bottom of the tube in the case of dilute model biles (2.4 g/dL), but were found in a zone on top of the fluid phase in case of concentrated model bile (total lipid concentration 7.3 g/dL), probably resulting from different densities of supernatants of dilute and concentrated model biles (1.0137 ± 0.0019 g/mL vs. 1.0226 ± 0.0013 g/mL; $P < 0.02$). After two weeks incubation, considerable quantities of lipids (approximately 30% of cholesterol and 5-10% of EYPC) were solubilized in vesicular aggregates, both in dilute and concentrated model biles.

Amounts of cholesterol and EYPC contained in unilamellar vesicles were two-fold higher in dilute than in concentrated model biles, with reciprocal differences in mixed micellar lipid solubilization (Figure 5). Although results obtained by gel filtration were similar in a qualitative way, more lipids were solubilized in mixed micelles and less in vesicles, with higher vesicular cholesterol/phospholipid ratios (Figure 5, Table 1).

Isolation of various phases in model biles that contain cholesterol crystals

Results reported above were all obtained from model biles that did not contain cholesterol crystals (i.e. plotting in the right two-phase (vesicles and micelles containing) zone). In case of model biles plotting in the central three-phase (micelles, vesicles and cholesterol crystals containing) zone, cholesterol in crystals and in vesicular aggregates can be quantitated from the difference of cholesterol contents in the pellet before and after bile salt-induced solubilization of the vesicular aggregates (see “Methods”). Figure 6 shows lipid distribution and cholesterol/phospholipid ratios in various phases obtained by combined ultracentrifugation-ultrafiltration-dialysis methodology under these circumstances after 1 and 14 days incubation.

After 14 days incubation, there was a strong decrease of cholesterol content in vesicles and micelles, coinciding with a strong increase of cholesterol crystal mass. There were only small changes of phospholipid content in various phases during this time period. As a result, vesicular cholesterol/phospholipid ratios, that were above 1 on day 1, decreased to values ~ 1 on day 14. Micellar CSI values ~ 1 and vesicular cholesterol/phospholipid ratios ~ 1 on day 14 indicate thermodynamic equilibrium after this incubation period.

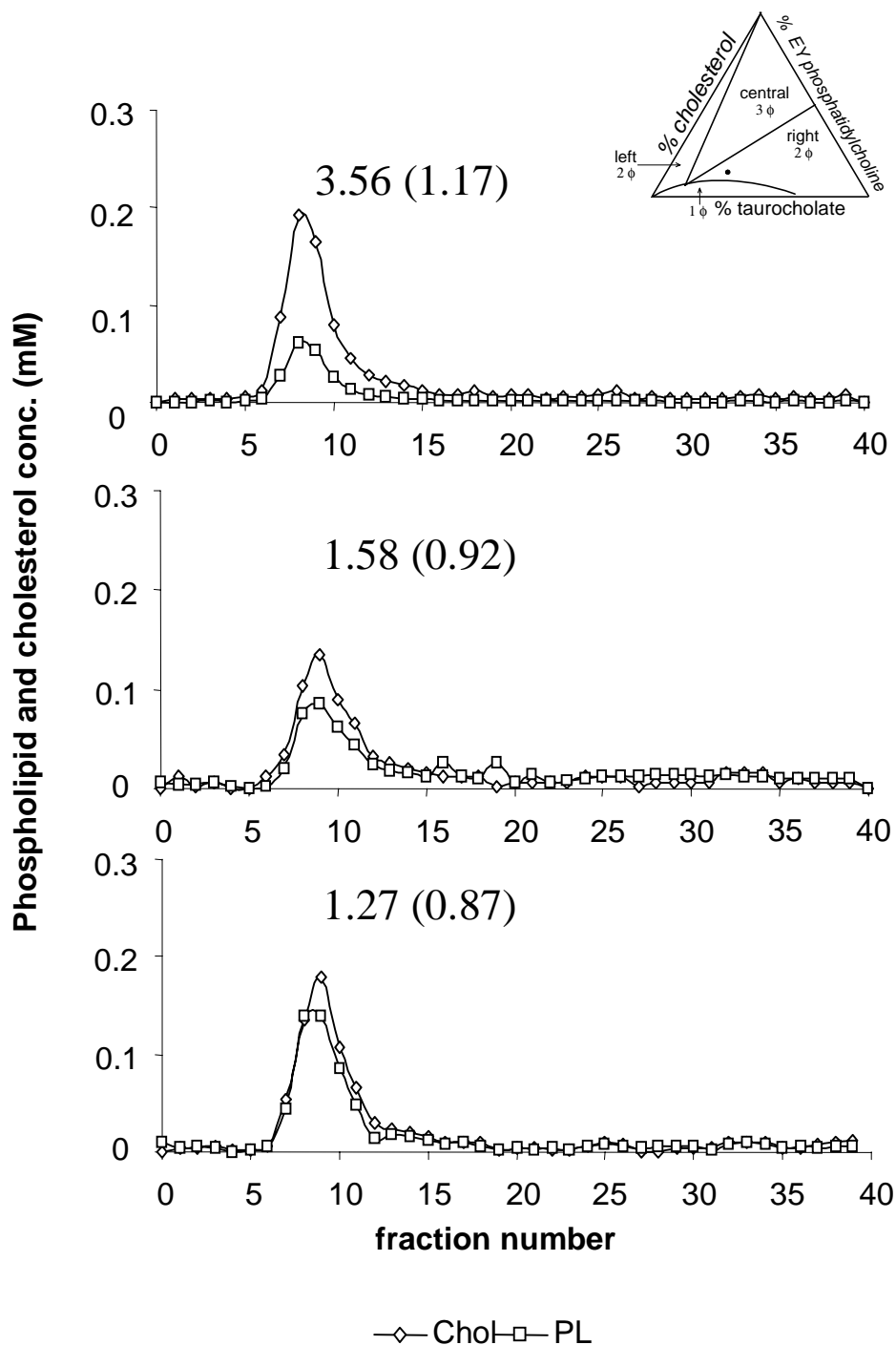


Figure 4: Gel filtration of dialyzed vesicles with an eluant containing taurocholate at intermixed micellar/vesicular concentrations after 1 (A), 10 (B) or 40 (C) days incubation. Model bile composition is identical to Figure 3. The vesicular cholesterol/phospholipid ratios decrease with time. Vesicular cholesterol/phospholipid ratios in the original dialysant before gel filtration (indicated between brackets) are much lower than in the same vesicles after gel filtration, which can not be explained by the presence in the filtrant of residual phospholipid-rich mixed micelles, because these are not detectable by gel filtration. *Inset:* equilibrium taurocholate-EYphosphatidylcholine-cholesterol ternary phase diagram (9). Dot indicates model bile plotting in right two-phase zone.

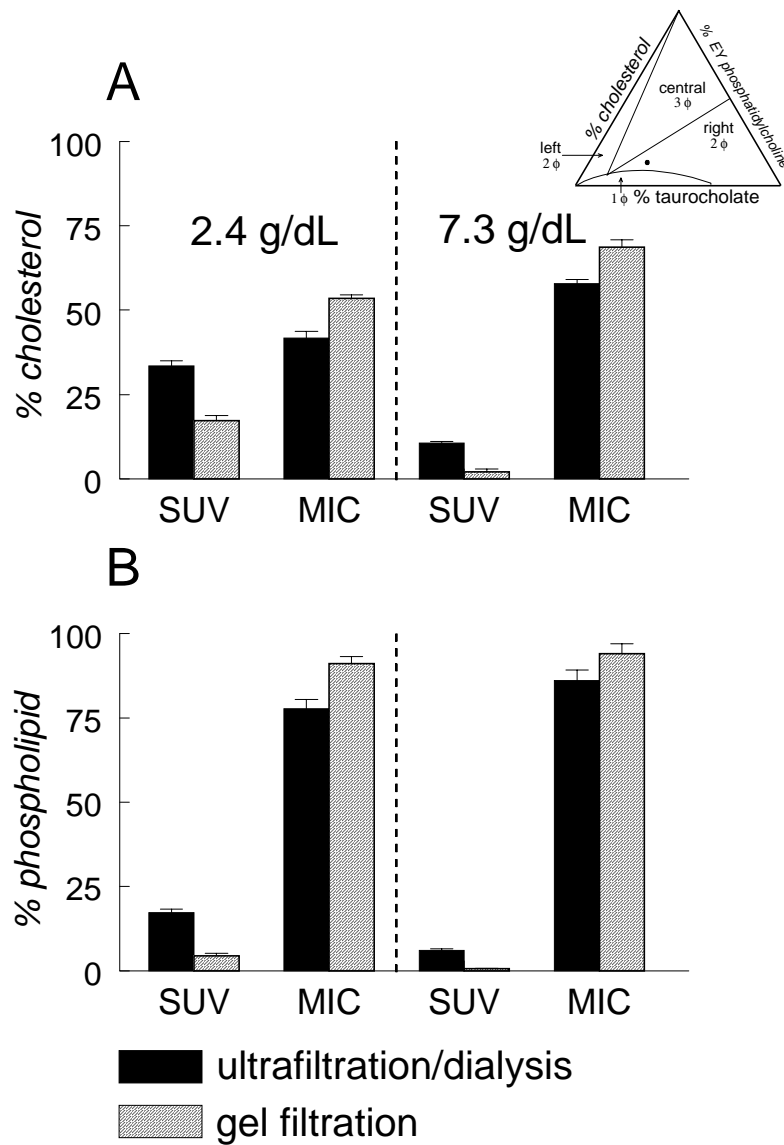


Figure 5: Distribution of cholesterol (A) and EYPC (B) between small unilamellar vesicles (SUV) and mixed micelles (MIC) in dilute (2.4 g/dL) and concentrated (7.3 g/dL) model bile (14 days incubation at 37°C: EYPC/(taurocholate+EYPC) = 0.3; 10.7 % cholesterol; CSI = 1.7 and 1.4 in diluted and concentrated bile). Lipid distribution in small unilamellar vesicles was significantly higher with combined ultracentrifugation / ultrafiltration / dialysis method compared to gel filtration method. Reciprocal results were obtained for micellar lipid solubilization. With both methods, the amounts of lipids contained in small unilamellar vesicles were significantly higher in the dilute bile. Inset: equilibrium taurocholate-EYphosphatidylcholine-cholesterol ternary phase diagram (9). Dot indicates model bile plotting in the right two-phase zone.

DISCUSSION

Understanding cholesterol solubilization in model bile requires accurate isolation of cholesterol-containing lipid particles. Although gel filtration with bile salts at IMC values in the eluant is suitable for human bile, which generally contains only small amounts of mostly unilamellar vesicles (13), this method may be problematic in case of supersaturated model biles which often contain large amounts of aggregated vesicles that may not enter the column properly (14). In the present study, we first pelleted aggregated vesicles by ultracentrifugation, and obtained micelles and small unilamellar vesicles by ultrafiltration resp. dialysis of the supernatant.

The short centrifugation procedure did not significantly affect IMC values, nor did it cause a bile salt gradient, which may occur during prolonged ultracentrifugation as a result of precipitation of mixed micelles (25). The concentration of mixed micellar lipids obtained by ultrafiltration through the 300 kDa filter was also not affected by centrifugation. These observations suggest that no net vesicle \leftrightarrow micelle transitions occur during centrifugal precipitation of aggregated vesicles.

The hydrodynamic radius of mixed micelles, in native bile 1 - 6.7 nm (26), should allow them to freely pass the 23 nm pores of the 300 kDa Mwco. Unilamellar vesicles should be retained completely since their hydrodynamic radius in bile is ≥ 35 nm (2;3). A filter with a similar cut-off has recently been used for removal of vesicles from human gallbladder bile (27). The 300 kDa Mwco filter used in the present study was indeed entirely permeable for a wide range of mixed micelles at a wide range of phospholipid/(bile salt + phospholipid) ratios and lipid concentrations, factors known to influence micellar sizes (28).

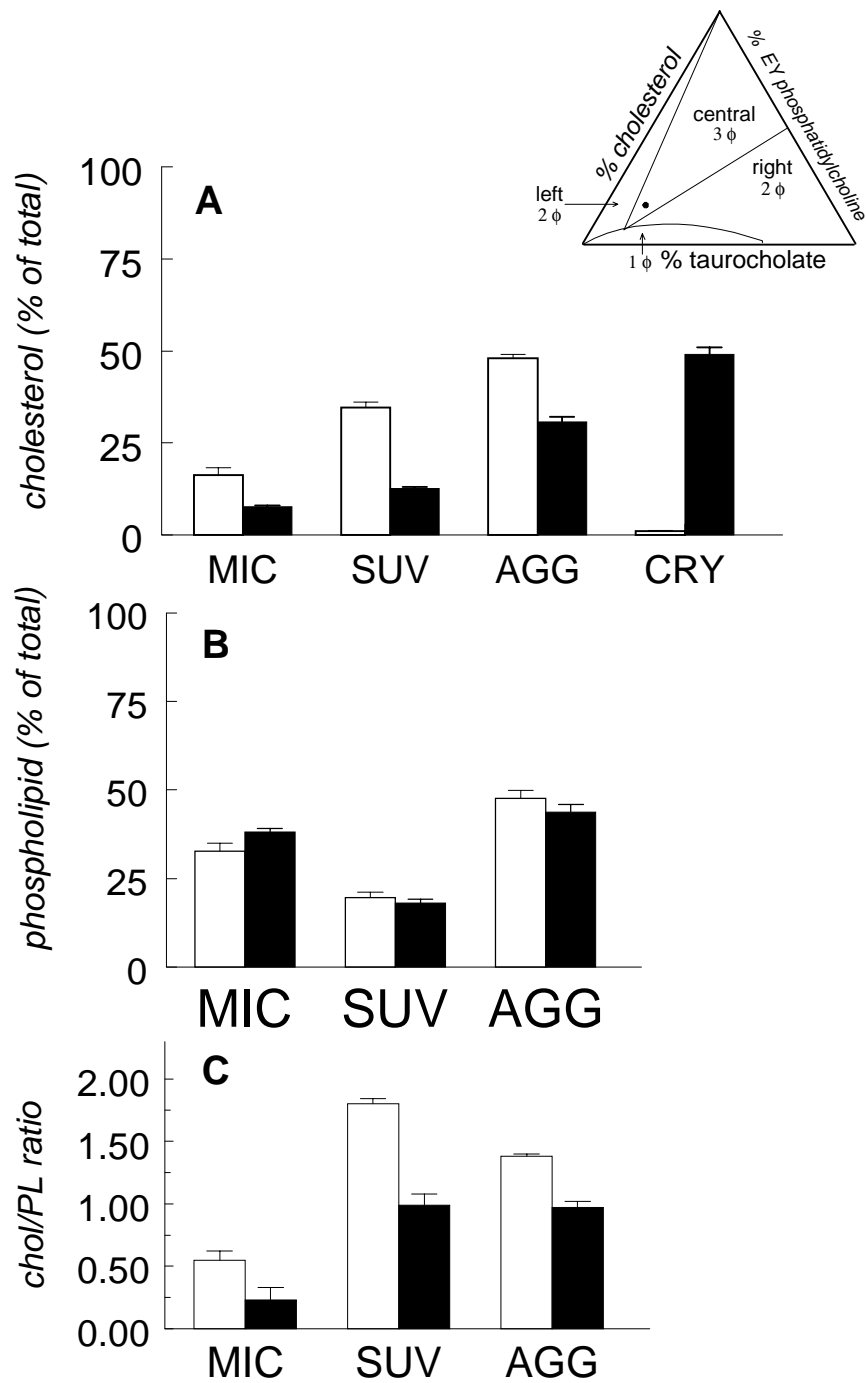


Figure 6: Distribution of cholesterol (A) and phospholipid (B) into various phases in supersaturated model bile composed with EYPC and TC, plotting in the central three-phase zone (total lipid conc. = 3.6 g/dL, PL/(BS+PL) ratio = 0.2, 20 mol% cholesterol, 37°C). Various phases were isolated after 1 day (open bars) and 14 days (closed bars) incubation at 37°C. There is a decrease of cholesterol content of micelles and vesicles after 14 days, coinciding with an increased crystal mass and decreased chol/PL ratios (C). MIC, micelles; SUV, small unilamellar vesicles; AGG, aggregated vesicles; CRY, cholesterol crystal mass.

Inset: equilibrium taurocholate-EYphosphatidylcholine-cholesterol ternary phase diagram (9). Dot indicates model bile plotting in three-phase zone.

Additional evidence for complete permeability was provided by the absence of Gibbs-Donnan effects (an indicator for asymmetric distribution of non-filterable ions). QLS measurements confirmed that filtrates of supersaturated model biles never contained vesicles. Furthermore, in supersaturated biles near or at equilibrium, the filtrate should have a cholesterol saturation index around 1, as in the present study (Table 1).

Unilamellar vesicles were isolated from centrifuged model bile by dialysis through a membrane with a similar cut-off (300 kDa) as used during ultrafiltration. This membrane was completely impermeable to small unilamellar vesicles, whereas mixed micelles were completely washed out (Figure 3).

With gel filtration more lipid was contained in mixed micelles, and less in unilamellar vesicles (Figures 2 and 5), with much higher vesicular cholesterol/phospholipid ratios compared to ultrafiltration/dialysis (Table 1). These differences could be due to interactions between biliary lipid particles and the matrix in case of gel filtration. The matrix surface to which the sample is exposed during analysis is several orders of magnitude smaller in case of ultrafiltration and dialysis. A standard protocol for gel filtration of phospholipid liposomes requires thorough equilibration of the gel filtration column material with large volumes of phospholipid dispersions prior to analysis of the sample to saturate the matrix and avoid possible interactions of the sample with the matrix (29). In the case of bile, however, this is impossible, since detergent bile salts in the eluant would dissolve phospholipids attached to the matrix in a previously equilibrated column. Interactions of phospholipids with the matrix could have a profound impact on the delicate pseudoequilibrium

in (model) bile systems. We provide some evidence for such interactions during gel filtration. First, we observed that gel filtration of dialyzed unilamellar vesicles strongly increased their cholesterol/phospholipid ratios. This was not caused by micellization of part of these vesicles, since mixed micelles could not be detected during gel filtration (Figure 3). Furthermore, vesicular cholesterol/phospholipid ratios after gel filtration of the supernatant or gel filtration of vesicles obtained by dialysis were identical. Secondly, we could detect considerable amounts of phosphatidylcholine and cholesterol attached to gel filtration material. Therefore, the vesicular cholesterol/phospholipid ratio observed after gel filtration may be unreliable, which is of major concern as an increase of this parameter has been strongly associated with cholesterol crystallization (6;7). Since vesicular cholesterol/phospholipid ratios consistently increased during gel filtration, affinity of phospholipid may be higher than affinity of cholesterol for the column material.

Concentration of bile in the gallbladder is an important factor for cholesterol crystallization (30). In the present study, we compared lipid solubilization in dilute and concentrated model biles with identical mol% lipids. We found that in dilute model biles, more lipids are contained within unilamellar vesicles and less in mixed micelles, in agreement with previous data (6;25) (Figure 5). Although gel filtration and combined ultracentrifugation / ultrafiltration / dialysis yielded similar results in a qualitative sense, again amounts of lipid contained in small unilamellar vesicles were lower and vesicular cholesterol/phospholipid ratios higher with gel filtration.

We employed in the present study mainly model biles plotting in the right (micelles + vesicles containing) two-phase zone of the equilibrium ternary phase diagram (9). Nevertheless, as shown in Figure 6, the procedure of centrifugation with ultrafiltration/dialysis of the supernatant

can be easily adapted to solid crystals-containing model biles by quantitating aggregated vesicles and crystals in the pellet separately.

In summary, we have shown that ultracentrifugation can be used to isolate aggregated vesicles and -if present- cholesterol crystals from model biles without disturbing the delicate balance between vesicular and micellar phases. We further demonstrate that ultrafiltration can be used to accurately isolate mixed micelles in a rapid and simple procedure. Unilamellar vesicles can be isolated by dialysis against a solution containing bile salts at IMC values. This methodology should be considered the procedure of choice for the separation of these phases from supersaturated model biles.

References

1. Holan KR, Holzbach RT, Hermann RE, Cooperman AM, Claffey WY. Nucleation time: a key factor in the pathogenesis of cholesterol gallstone disease. *Gastroenterology* 1979; 77:611-617.
2. Mazer NA, Carey MC. Quasielastic light scattering studies of aqueous biliary lipid systems. Cholesterol solubilization and precipitation in model bile solutions. *Biochemistry* 1983; 22:426-442.
3. Sömjen GJ, Gilat T. A non-micellar mode of cholesterol transport in human bile. *FEBS Lett* 1983; 156:265-268.
4. Schriever CE, Jüngst D. Association between cholesterol-phospholipid vesicles and cholesterol crystals in human gallbladder bile. *Hepatology* 1989; 9:541-546.
5. Lee SP, Park HZ, Madani H, Kaler EW. Partial characterization of a nonmicellar system of cholesterol solubilization in bile. *Am J Physiol* 1987; 252:G374-G383.
6. Halpern Z, Dudley MA, Lynn MP, Nader JM, Breuer AC, Holzbach RT. Vesicle aggregation in model systems of superaturated bile: relation to crystal nucleation and lipid composition of the vesicular phase. *J Lipid Res* 1986; 27:295-306.
7. Halpern Z, Dudley MA, Kibe A, Lynn MP, Breuer AC, Holzbach RT. Rapid vesicle formation and aggregation in abnormal human biles. A time-lapse video enhanced contrast microscopy study. *Gastroenterology* 1986; 90:875-885.
8. van de Heijning BJM, Stolk MFJ, Van Erpecum KJ, Renooij W, Berge-Henegouwen GPv. The effects of bile salt hydrophobicity on model bile vesicle morphology. *Biochim Biophys Acta* 1994; 1212:203-210.

9. Wang DQH, Carey MC. Complete mapping of crystallization pathways during cholesterol precipitation from model bile: influence of physical-chemical variables of pathophysiologic relevance and identification of a stable liquid crystalline state in cold, dilute and hydrophilic bile salt-containing systems. *J Lipid Res* 1996; 37:606-630.
10. Donovan JM, Timofeyeva N, Carey MC. Influence of total lipid concentration, bile salt:lecithin ratio, and cholesterol content on inter-mixed micellar/vesicular (non-lecithin-associated) bile salt concentrations in model bile. *J Lipid Res* 1991; 32:1501-1512.
11. Donovan JM, Jackson AA. Rapid determination by centrifugal ultrafiltration of inter-mixed micellar/vesicular (non-lecithin-associated) bile salt concentrations in model bile: influence of Donnan equilibrium effects. *J Lipid Res* 1993; 34:1121-1129.
12. Donovan JM, Jackson AA, Carey MC. Molecular species composition of inter-mixed micellar/vesicular bile salt concentrations in model bile: dependence upon hydrophilic-hydrophobic balance. *J Lipid Res* 1993; 34:1131-1140.
13. Eckhardt ERM, van de Heijning BJM, Van Erpecum KJ, Renooij W, VanBerge-Henegouwen GP. Quantitation of cholesterol-carrying particles in human gallbladder bile. *J Lipid Res* 1998; 39:594-603.
14. Donovan JM, Jackson AA. Accurate separation of biliary lipid aggregates requires the correct intermixed micellar/intervesicular bile salt concentration. *Hepatology* 1998; 27:641-648.
15. Hay DW, Cahalane MJ, Timofeyeva N, Carey MC. Molecular species of lecithins in human gallbladder bile. *J Lipid Res* 1993; 34:759-768.
16. Turley SD, Dietschy JM. Reevaluation of the 3 α -hydroxysteroid dehydrogenase assay for total bile acids in bile. *J Lipid Res* 1978; 19:924-928.
17. Fromm H, Hamin P, Klein H, Kupke I. Use of a simple enzymatic assay for cholesterol analysis in human bile. *J Lipid Res* 1980; 21:259-261.
18. Takayama M, Itoh S, Nagasaki T, Tanimizu I. A new enzymatic method for determination of serum choline-containing phospholipids. *Clin Chim Acta* 1977; 79:93-98.
19. Carey MC. Critical tables for calculating the cholesterol saturation of native bile. *J Lipid Res* 1978; 19:945-965.
20. Eckhardt ERM, Moschetta A, Renooij W, Goerdal SS, Van Berge-Henegouwen GP, van Erpecum K.J. Asymmetric distribution of phosphatidylcholine and sphingomyelin between micellar and vesicular phases: potential implication for canalicular bile formation. *J Lipid Res* 1999; 40:2022-2033.
21. Moschetta A, Van Berge-Henegouwen GP, Portincasa P, Palasciano G, Groen AK, Van Erpecum KJ. Sphingomyelin exhibits greatly enhanced protection

- compared with egg yolk phosphatidylcholine against detergent bile salts. *J Lipid Res* 2000; 41:916-924.
22. Schroeder RJ, London E, Brown DA. Interactions between saturated acyl chains confer detergent resistance on lipids and glycosylphosphatidylinositol (GPI)-anchored proteins: GPI- anchored proteins in liposomes and cells show similar behavior. *Proc Natl Acad Sci U S A* 1994; 91:12130-12134.
 23. Somjen GJ, Ringel Y, Konikoff FM, Rosenberg R, Gilat T. A new method for the rapid measurement of cholesterol crystallization in model bile using a spectrophotometric microplate reader. *J Lipid Res* 1997; 38:1048-1052.
 24. Bligh EG, Dyer WJ. A rapid method of total lipid extraction and purification. *Can J Biochem Physiol* 1959; 37:911-917.
 25. Kibe A, Dudley MA, Halpern Z, Lynn MP, Breuer AC, Holzbach RT. Factors affecting cholesterol monohydrate crystal nucleation time in model systems of supersaturated bile. *J Lipid Res* 1985; 26:1102-1111.
 26. Mazer NA, Schurtenberg P, Carey MC, Preisig R, Weigand K, Kanzig W. Quasi-elastic light scattering studies of native hepatic bile from the dog: comparison with aggregative behavior of model biliary lipid systems. *Biochemistry* 1984; 23:1994-2005.
 27. Kiyosawa R, Chijiwa K, Hirota I, Nakayama F. Possible factors affecting the cholesterol nucleation time in human bile: a filtration study. *J Gastroenterol Hepatol* 1992; 7:142-147.
 28. Mazer NA, Benedek GB, Carey MC. Quasielastic light-scattering studies of aqueous biliary lipid systems. Mixed micelle formation in bile salt-lecithin solutions. *Biochemistry* 1980; 19:601-615.
 29. Reynolds JA, Nozaki Y, Tanford C. Gel-exclusion chromatography on S1000 Sephacryl: application to phospholipid vesicles. *Anal Biochem* 1983; 130:471-474.
 30. Van Erpecum KJ, Van Berge-Henegouwen GP, Stoelwinder B, Schmidt YM, Willekens FL. Bile concentration is a key factor for nucleation of cholesterol crystals and cholesterol saturation index in gallbladder bile of gallstone patients. *Hepatology* 1990; 11:1-6.

chapter 3

**CHOLESTEROL CRYSTALLIZATION IN MODEL BILES:
EFFECTS OF BILE SALT AND PHOSPHOLIPID SPECIES
COMPOSITION.**

Antonio Moschetta, Gerard P. vanBerge-Henegouwen, Piero Portincasa,
Giuseppe Palasciano and Karel J. van Erpecum.

Journal of Lipid Research 2001; 42:1273-81.

ABSTRACT

Cholesterol in human bile is solubilized in micelles by (relatively hydrophobic) bile salts and phosphatidylcholine (unsaturated acyl chains at *sn*-2 position). Hydrophilic tauroursodeoxycholate, dipalmitoyl phosphatidylcholine and sphingomyelin all decrease cholesterol crystals-containing zones in the equilibrium ternary phase diagram (K. J. van Erpecum and M.C. Carey. *Biochim. Biophys. Acta* 1997;1345:269-282) and thus could be valuable in gallstone prevention. We have now compared crystallization in cholesterol-supersaturated model systems (3.6 g/dL, 37°C) composed with various bile salts as well as egg yolk phosphatidylcholine (unsaturated acyl chains at *sn*-2 position), dipalmitoyl phosphatidylcholine or sphingomyelin throughout the phase diagram. At low phospholipid contents (left two-phase -micelles+crystals-containing- zone), tauroursodeoxycholate, dipalmitoyl phosphatidylcholine and sphingomyelin all enhanced crystallization. At pathophysiologically relevant intermediate phospholipid contents (central three-phase -micelles+vesicles+crystals-containing- zone), tauroursodeoxycholate inhibited, but dipalmitoyl phosphatidylcholine and sphingomyelin enhanced crystallization. Also, during 10 days incubation, there was a strong decrease of vesicular cholesterol contents and vesicular cholesterol/phospholipid ratios (~1 on day 10), coinciding with a strong increase of crystal mass. At high phospholipid contents (right two-phase -micelles+vesicles-containing- zone), vesicles were always unsaturated and crystallization did not occur. Strategies aiming to increase amounts of hydrophilic bile salts may be preferable to increasing saturated phospholipids in bile, since the latter may enhance crystallization.

INTRODUCTION

Precipitation of cholesterol crystals from supersaturated bile is a prerequisite for gallstone formation (1). The sterol is poorly soluble in an aqueous environment, and is solubilized in bile in mixed micelles by bile salts (BS) and phospholipids (PL). Phosphatidylcholine is the major phospholipid in bile (>95% of total: mainly 16:0 acyl chains at the *sn*-1 position and mainly unsaturated (18:2>18:1>20:4) acyl chains at the *sn*-2 position (2)). In case of cholesterol supersaturation, the excess sterol may be contained in vesicles together with phospholipids (3,4) or precipitated as solid crystals.

The studies of Wang & Carey (5) have revealed the importance of the relative amounts of bile salts *vs* phospholipids in the system for crystallization behavior. In case of excess bile salts (PL/(BS+PL) ratios $\sim \leq 0.2$), crystals precipitate at fast rates, and both various intermediate anhydrous cholesterol crystals (needles, arcs, tubules, spirals) and mature rhomboid cholesterol monohydrate crystals can be detected by microscopy. In case of higher amounts of phospholipids, crystal precipitation proceeds at slower rates (with predominant formation of mature cholesterol monohydrate crystals), and large amounts of cholesterol are solubilized in vesicles together with phospholipids. In case of excess phospholipids (high PL/(BS+PL) ratios), solid cholesterol crystals do not occur, and cholesterol is mainly solubilized in vesicular phases. Based on these data, the equilibrium cholesterol-bile salt-phospholipid ternary phase diagram (Fig. 1: (5,6)) is assumed to contain a one-phase zone (only micelles), a left two-phase (micelles and cholesterol crystals-containing) zone, a central three-phase (micelles, vesicles and cholesterol crystals-containing) zone and a right two-phase (micelles and vesicles-containing) zone. The phase diagram describes occurrence of cholesterol crystals, micelles and vesicles at equilibrium conditions, but accurate quantification of these phases has been hampered by methodological problems. Micelles and vesicles may be separated with the aid of gel filtration with bile salts at intermixed micellar/vesicular concentrations in the eluant buffer in order to avoid artifactual shifts of lipids between phases (7-9). However, gel filtration is only suitable in case of highly diluted and slightly supersaturated model systems: in more concentrated or supersaturated model systems, large amounts of vesicular aggregates occur that do not completely pass the column (10). We recently developed and validated a method for accurate separation of various phases under these circumstances (11). Aggregated vesicles are first precipitated by short ultracentrifugation, and micelles or

small unilamellar vesicles are subsequently isolated from the supernatant with the aid of highly selective ultrafilters and dialysis, taking into account the intermixed micellar/vesicular bile salt concentration.

In the present study, we have systematically determined distribution of lipids into various phases throughout the ternary phase diagram. The hydrophilic bile salt ursodeoxycholate is frequently used in clinical practice to dissolve cholesterol gallstones, and dietary modulation of biliary phospholipid composition has been suggested to prevent gallstone formation (12-15). We therefore also evaluated effects of bile salt species and phospholipid class composition on crystallization.

MATERIALS AND METHODS

Materials

Taurocholate (TC), taurodeoxycholate (TDC) and tauroursodeoxycholate (TUDC) were obtained from Sigma Chemical Co. (St. Louis, MO, USA) and yielded a single spot upon thin-layer chromatography (butanol-acetic acid-water, 10:1:1 vol/vol/vol, application of 200 μg bile salt). Cholesterol (Sigma) was $\geq 98\%$ pure by reverse-phase HPLC (isopropanol-acetonitrile 1:1, vol/vol, detection at 210 nm). Phosphatidylcholine from egg yolk (EYPC; Sigma), dipalmitoyl phosphatidylcholine (DPPC; Sigma) and sphingomyelin from egg yolk (EYSM; Avanti Polar-Lipids Inc., Alabaster, AL, USA) yielded a single spot upon thin-layer chromatography (chloroform-methanol-water 65:25:4, vol/vol/vol, application of 200 μg lipid). Acyl chain compositions as determined by gas-liquid chromatography (16) were virtually identical to previously published data (6) and showed a preponderance of 16:0 acyl chains for egg yolk SM, similar to trace SM in bile (17). As shown by reverse-phase HPLC, EYPC contained mainly 16:0 acyl chains at the *sn*-1 position and mainly unsaturated (18:1>18:2>20:4) acyl chains at the *sn*-2 position, similar to PC in

human bile (2). All other chemicals and solvents were of ACS or reagent grade quality.

Ultrafilters with a Mwco of 10 and 300 kDa were purchased from Sartorius (Göttingen, Germany: Centrisart I), and dialysis membranes with a Mwco of 300 kDa from Spectrum Laboratories (Laguna Hills, CA, USA: SpectraPor). The enzymatic cholesterol assay kit was obtained from Boehringer (Mannheim, Germany) and the enzymatic phospholipid kit from Sopar Biochem (Brussels, Belgium). 3 α -Hydroxysteroid dehydrogenase for the enzymatic measurement of bile salt concentrations (18) and a colorimetric chloride-kit were purchased from Sigma. The reverse-phase C18 HPLC column was from Supelco (Supelcosil LC-18-DB, Supelco, Bellefonte, PA, USA).

Preparation of model biles

Lipid mixtures containing variable proportions of cholesterol, phospholipids (both from stock solutions in chloroform) and bile salts (from stock solutions in methanol) were vortex-mixed and dried at 45°C under a mild stream of nitrogen, and subsequently lyophilized during 24 hrs, before being dissolved in aqueous 150 mM NaCl plus 3mM NaN₃. Tubes were sealed with Teflon-lined screw caps under a blanket of nitrogen to prevent lipid oxidation and vortex-mixed for 5 min. followed by incubation at 37°C in the dark. All solutions were warmed up to 45°C for 10 min. before use. The final mol percentages of cholesterol, phospholipids and bile salts did not differ more than 1% from the intended mol percentages. Also, model systems always plotted in the intended zones of the appropriate phase diagrams (5,6), as inferred from microscopic examination.

Lipid measurement

Phospholipid concentrations in model systems were assayed by determining inorganic phosphate (19). Cholesterol concentrations were determined with an enzymatic assay (20), and bile salts with the 3α -hydroxysteroid dehydrogenase method (18).

IMC measurement

Apart from mixed (i.e. phospholipid-bile salt) micelles, model bile systems also contain non-phospholipid associated bile salts, either as monomers or -above their critical micellar concentration- associated in “simple” micelles. The monomeric plus simple micellar bile salt concentration is referred to as “intermixed micellar/vesicular (non phospholipid-associated) bile salt concentration”, usually abbreviated as “IMC” (9). We determined IMC in various model systems, using the rapid centrifugal ultrafiltration technique with correction for Gibbs-Donnan effects (7-11,21).

Isolation of various lipid phases

Cholesterol crystals and aggregated vesicles: After 10 and 40 days (in some cases also after 1 day) incubation at 37°C, various phases were isolated from cholesterol-supersaturated model systems as described (11). In brief, detergent-resistant aggregated vesicles were precipitated by ultracentrifugation during 30 min. at 50000 g and at 37°C in a TLS 55 rotor (Beckman, Palo Alto, CA, USA) (22). In case of coexistent cholesterol crystals and aggregated vesicles (three-phase (micelles, vesicles and crystals-containing) zone: see Fig. 1), centrifugation of an additional bile sample was also performed 10 min. after addition of deoxycholate in quantities sufficient to desaturate the model system (final CSI <1). After such incubation, light microscopy and stability of turbidity measurements (405 nm OD (23)) revealed that all vesicular

aggregates had been completely micellized. Experiments with isolated cholesterol crystals showed that solubilization of the cholesterol crystals did not occur during the short incubation with deoxycholate. Therefore, cholesterol crystal mass equals cholesterol content in the pellet after addition of deoxycholate, and cholesterol content in vesicular aggregates can be calculated from the difference of cholesterol contents between the pellets without and with added deoxycholate (23). IMC values measured in non-centrifuged model biles were identical to IMC values in the corresponding supernatants. We did not find a bile salt gradient in the supernatant after centrifugation, indicating that the short centrifugation procedure did not cause an inhomogeneous distribution of micelles or unilamellar vesicles in the tube. Furthermore, centrifugation did not influence the content of mixed micelles in the model bile, since lipid contents in micelles obtained by ultrafiltration of supernatant through the 300 kDa Mwco filter (see below) were identical to lipid concentrations in ultrafiltrates of corresponding whole model biles.

As model systems plotting in the left-two phase zone (see Fig. 1) contain only micelles and cholesterol crystals at thermodynamic equilibrium, cholesterol crystals were precipitated in this case by ultracentrifugation, without added deoxycholate. Although studies by quasielastic light scattering spectroscopy (5) have suggested that small unilamellar vesicles may occur transiently in supersaturated model systems in the left two-phase zone before equilibrium is reached, amounts of cholesterol in these vesicles are expected to be minor compared to cholesterol crystal mass. Recovery of cholesterol and phospholipid in various phases was always 95-100%.

Micelles and small unilamellar vesicles: Micelles were isolated from the supernatant by ultrafiltration with a highly selective 300 kDa ultrafilter. Small unilamellar vesicles were obtained by dialysis (500 μ L sample, 16 hours, 37°C) in a SpectraPor[®] dialysis device with a molecular weight

cut-off of 300 kDa, against three times 20 volumes of aqueous 0.15 M NaCl plus 3 mM NaN₃ containing the relevant bile salt at concentrations identical to the IMC of the various original model system in order to avoid artifactual shifts of lipids between vesicles and micelles (11,21). The ultrafilters and dialysis membranes were completely impermeable to small unilamellar or aggregated vesicles but completely permeable to simple and mixed micelles (tested with a wide range of micellar compositions (11), including TDC-, TC-, TUDC-containing mixed micelles at 37°C, at a total lipid concentration of 3.6 g/dL and at PL/(BS+PL) ratios of 0.2-0.55, either without or with cholesterol; with SM or PC as phospholipid). Recovery of cholesterol and phospholipids in various phases was always 95-100%.

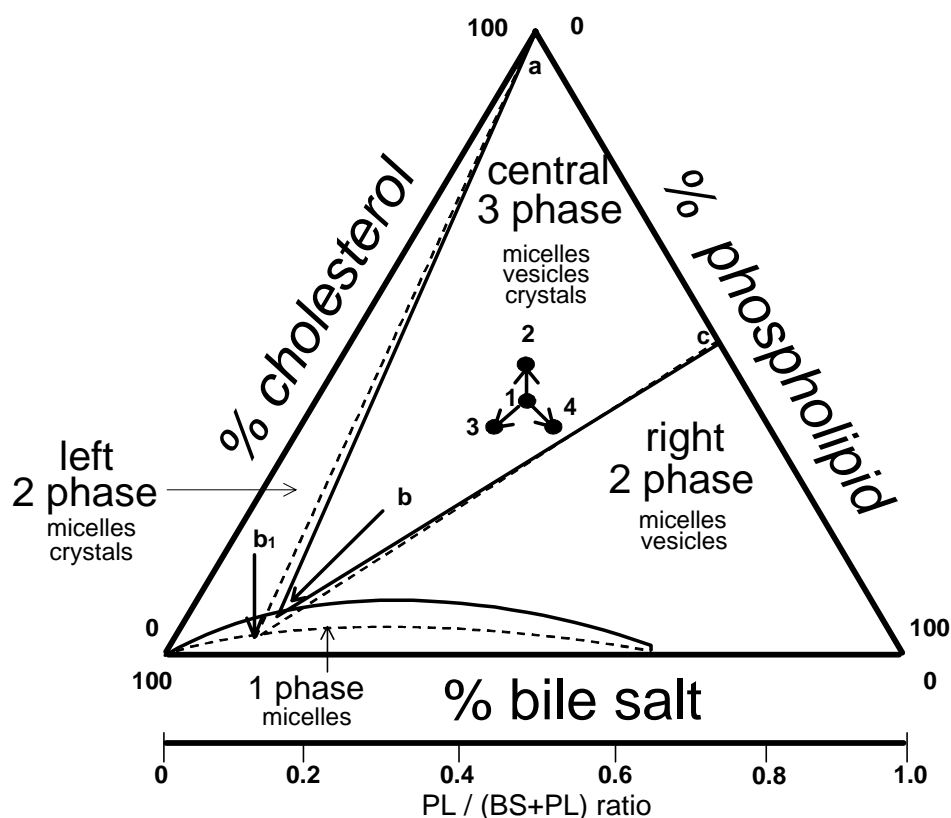


Figure 1: Equilibrium taurocholate-EYPC-cholesterol ternary phase diagram (5). The components are expressed in mol percent. Depicted are a one-phase (micellar) zone at the bottom, a left two-phase zone (containing micelles and crystals), a central three-phase zone (containing micelles, vesicles and crystals) and a right two-phase zone

(containing micelles and vesicles). The apices of the central three-phase zone are represented by a, b and c. Positions in the three-phase zone of 4 different model biles are represented by 1-4 (see text). Interrupted line indicates reduced one-phase micellar zone and left-ward expansion of the right two-phase zone in case of hydrophilic bile salts (5) or saturated phospholipids (6).

Quantitation of cholesterol crystals by microscopy

Numbers of various cholesterol crystal shapes (intermediate anhydrous crystals such as arcs, needles, tubules and spirals: mature rhomboid monohydrate crystals) were determined by daily examinations during 10 days with the aid of a polarizing microscope and KOVA[®] plastic slides (Hycor Biomedical inc., Garden Grove, California, USA) with 10 standardized examination chambers. Each chamber contains one large grid (3 x 3 mm; volume: 0.9 μ L), divided in 81 small grids (size: 0.33 mm x 0.33 mm). 7 μ L from a 10x diluted sample was placed on a KOVA[®] slide and crystal numbers were counted in 9 consecutive small grids at 100x magnification. In model biles plotting in the left two-phase zone, sizes of cholesterol monohydrate crystals were highly variable and data for small ($\leq 10\mu$ m diameter) and larger monohydrate crystals are given separately. Daily examinations of crystal numbers and mass during 10 days were performed 2-3 times, and representative curves are shown.

Statistical analysis

Data for lipid distribution into various phases are expressed as means \pm SEM of 4-5 experiments. Differences between groups were tested for statistical significance by analysis of variance (ANOVA) with the aid of NCSS software (Kaysville, Utah, USA). When ANOVA detected a significant difference, results were further compared for contrasts using Fisher's least significant difference test as post-hoc test. Statistical significance is defined as a two-tailed probability of less than 0.05.

RESULTS

Three-phase (micelles, vesicles and cholesterol crystals – containing) zone

Influence of phospholipid class: Figures 2 and 3 show lipid distribution into various phases after 1, 10 and 40 days incubation of SM- or EYPC-containing supersaturated model systems plotting in the three-phase zone (TC as bile salt in all cases: see insets Figs 2 and 3). In SM-containing systems, ~90 % of all phospholipid was contained in vesicular aggregates (Fig. 2B). By contrast, in EYPC-containing systems with the same relative composition, large amounts of phospholipids also distributed into micelles and small unilamellar vesicles (Fig. 3B). Amounts of cholesterol contained in micelles or small unilamellar vesicles were also significantly larger in EYPC- than in SM-containing systems (Figs 2A and 3A). After 10 days incubation, there was a strong decrease of cholesterol content in aggregated or small unilamellar vesicles and -less pronounced- in micelles as compared with one day incubation, coinciding with a strong increase of cholesterol crystal mass (Figs 2A and 3A). There were only small changes of phospholipid content in various phases during this time period (Figs 2B and 3B). As a result, vesicular chol/PL ratios, that were above 1 on day 1 (particularly in small unilamellar vesicles) decreased to values ~1 at day 10 (Figs 2C and 3C). Also, chol/PL ratios in micelles (that were slightly supersaturated on day 1), decreased (micellar CSI ~1 on day 10). There were no significant changes after longer (40 days) incubation (Figs 2 and 3). Results in DPPC-containing systems (not shown) and SM-containing systems of the same relative composition were identical throughout the study period.

Although with daily examination during the first 10 days, numbers of cholesterol monohydrate crystals were larger in EYPC- than in SM- or

DPPC-containing systems (Fig. 4A), crystals were much larger in SM- or DPPC-containing systems. Cholesterol crystal mass was also larger in SM- or DPPC-containing systems both during the 10-day study period (Fig. 4B) and after 40 days incubation (Figs 2A and 3A).

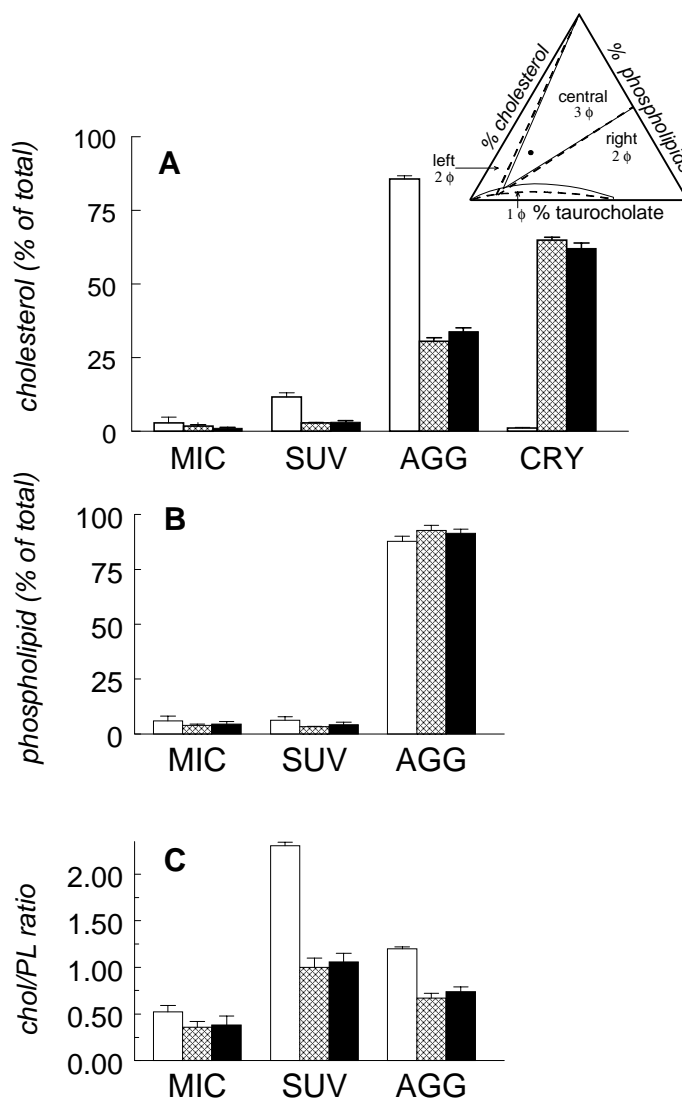


Figure 2: Distribution of cholesterol (A) and phospholipid (B) into various phases in supersaturated model bile composed with SM and TC, plotting in the central three-phase zone (total lipid conc. = 3.6 g/dL, PL/(BS+PL) ratio = 0.2, 24.8 mol% cholesterol, 37°C). Various phases were isolated after 1 day (open bars), 10 days (hatched bars) and 40 days (closed bars) incubation. There is a decrease of cholesterol and (less pronounced) phospholipid content in micelles and vesicles after 10 days, coinciding with an increased crystal mass and decreased chol/PL

ratios (C). MIC, micelles; SUV, small unilamellar vesicles; AGG, aggregated vesicles; CRY, cholesterol crystal mass.

Inset: equilibrium bile salt-phospholipid-cholesterol ternary phase diagram. Continuous line: phase diagram for EYPC (5). Interrupted line: decreased one-phase micellar zone and extension of right two-phase zone in case of DPPC or SM as phospholipid (6). Dot indicates model bile plotting in three-phase zone.

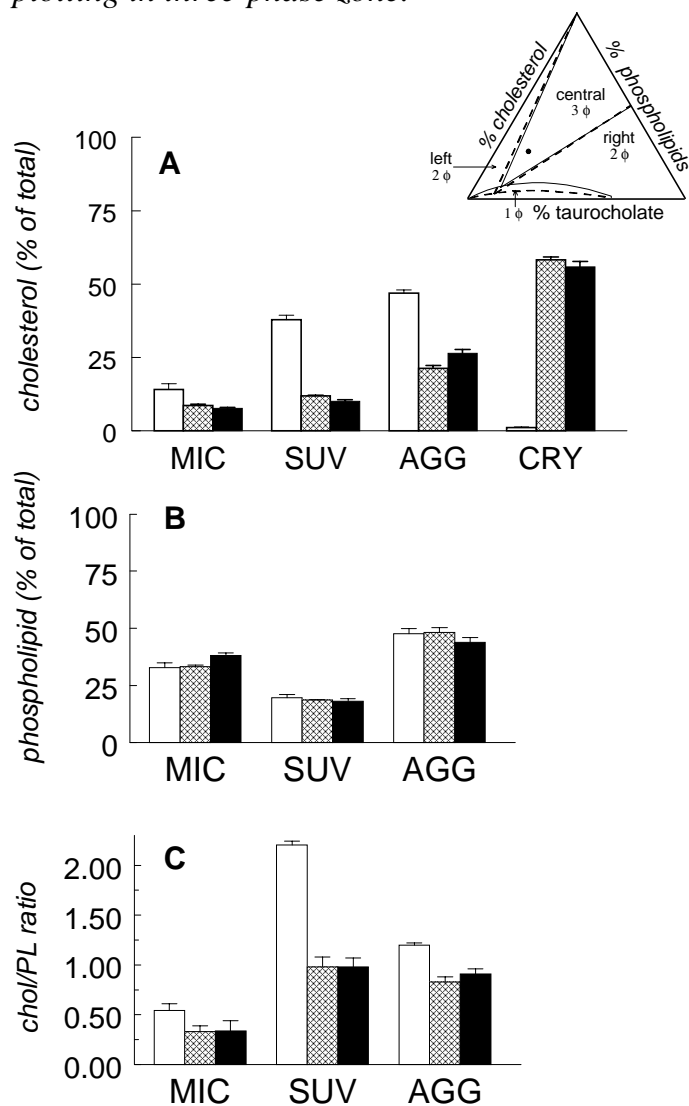


Figure 3: Distribution of cholesterol (A) and phospholipid (B) into various phases in supersaturated model bile composed with EYPC and TC, plotting in the central three-phase zone (same relative lipid composition as in Fig. 2). Various phases were isolated after 1 day (open bars), 10 days (hatched bars) and 40 days (closed bars) incubation at 37°C. There is a decrease of cholesterol content of micelles and vesicles after 10 days, coinciding with an increased crystal mass and decreased chol/PL ratios (C). MIC, micelles; SUV, small unilamellar vesicles; AGG, aggregated vesicles; CRY, cholesterol crystal mass.

Inset: equilibrium bile salt-phospholipid-cholesterol ternary phase diagram. Continuous line: phase diagram for EYPC (5). Interrupted line: decreased one-phase micellar zone and extension of right two-phase zone in case of DPPC or SM as phospholipid (6). Dot indicates model bile plotting in three-phase zone.

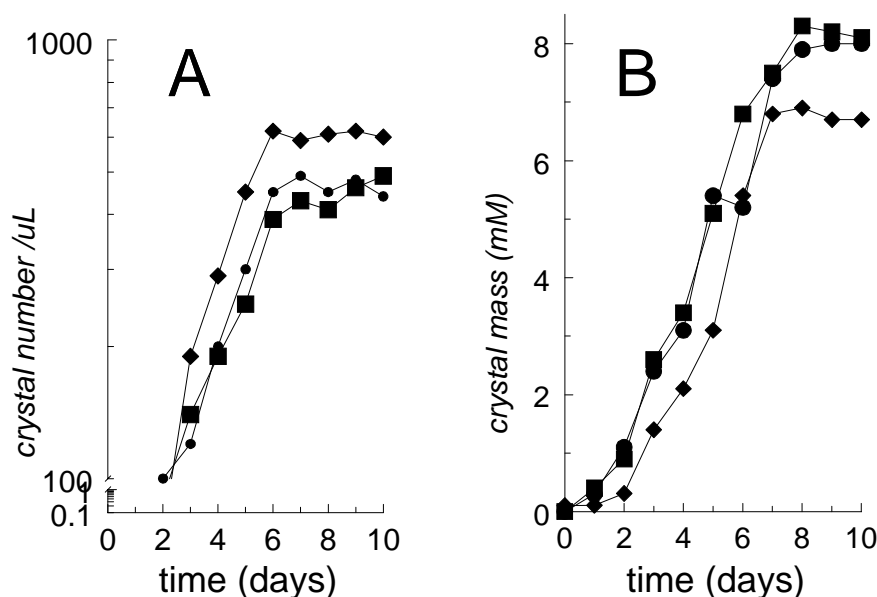


Figure 4: Numbers of cholesterol monohydrate crystals (A) and crystal mass (B) during 10 days incubation in supersaturated model systems containing EYPC, SM or DPPC and plotting in the central three-phase zone (TC as bile salt in all cases: for relative lipid composition see Figs 2 and 3). Although crystal numbers are larger in case of EYPC, crystal mass is higher in case of SM or DPPC, related to greater crystal sizes. (◆) EYPC; (●) SM; (■) DPPC. Please note logarithmic scale for 4A.

Influence of bile salt species: Figure 5 shows lipid distribution into various phases after 10 days incubation of supersaturated model systems composed with TDC, TC or TUDC and plotting in the three-phase zone (EYPC as phospholipid in all cases: inset Fig. 5). There were increased amounts of phospholipids and cholesterol contained in aggregated and small unilamellar vesicles in case of more hydrophilic bile salts, whereas solubilization in micelles was decreased. Micellar CSI as well as chol/PL ratios in small unilamellar or aggregated vesicles (Fig. 5C) were ~ 1 in all

cases. Results were essentially the same after 40 days incubation (not shown). With daily examination during the first 10 days, numbers of (mainly cholesterol monohydrate) crystals were much larger in case of more hydrophobic bile salts (TDC>TC>TUDC: Fig. 6A). Cholesterol crystal mass was also significantly higher in case of more hydrophobic bile salts (Fig. 6B: TDC>TC>TUDC).

We also examined effects of increasing contents of one of the three lipids by 5 mol %, keeping ratio between the other two lipids constant (model biles 1-4 in Fig. 1). Despite changed relative lipid composition, all model biles plotted in the central three-phase zone of the appropriate phase diagram (5). As predicted by the “Phase Rule” (24), after 40 days incubation, micelles are of one invariant composition, represented by the micellar apex of the three phase-zone (for TC-containing systems: PL/(BS+PL) ratio of 0.148, i.e. point b in Fig. 1). Location of the micellar apex depends on hydrophobicity of the bile salts incorporated in the system, with a leftward shift in case of TUDC-containing systems (point b₁ in Fig. 1: PL/(BS+PL) ratio of 0.127) and a rightward shift in case of TDC-containing systems (PL/(BS+PL) ratio of 0.169). In all model systems, micellar CSI of 1 and chol/PL ratios of ~1 in (unilamellar and aggregated) vesicles (represented by point c in Fig.1) indicate thermodynamic equilibrium after the prolonged (40-day) incubation.

Right two-phase (micelles and vesicles– containing) zone

Influence of phospholipid class: We examined lipid distribution into various phases after 10 days incubation of EYPC-, SM- or DPPC-containing systems plotting in the right-two phase zone (TC as bile salt in all cases: total lipid conc.=3.6 g/dL, PL/(BS+PL) ratio = 0.4, 15 mol% cholesterol, 37°C). In SM- or DPPC-containing systems, 95% of cholesterol was contained in vesicular aggregates. In contrast, in EYPC-

containing model biles of the same relative composition, considerable amounts of cholesterol were also contained in micelles (~20%) and small unilamellar vesicles (~15%).

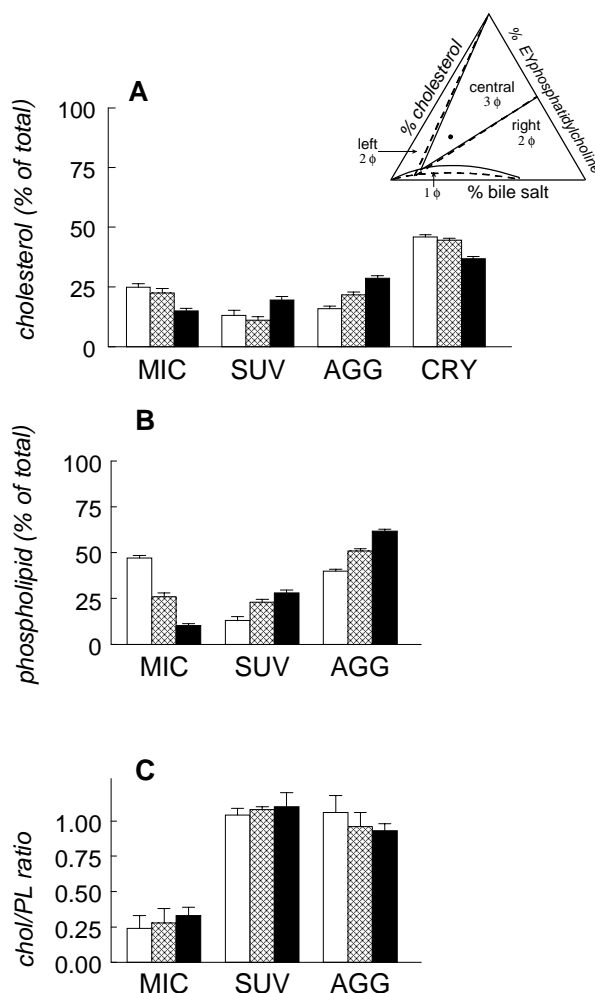


Figure 5: Distribution of cholesterol (A) and phospholipid (B) into various phases in supersaturated model biles containing TDC or TC or TUDC and plotting in the central three-phase zone (EYPC as phospholipid in all cases: total lipid conc = 3.6 g/dL, PL/(BS+PL) ratio = 0.3, 25 mol% cholesterol, 37°C). Various phases were isolated after 10 days incubation. Distribution of phospholipids and cholesterol into vesicles is increased in case of hydrophilic bile salts (TDC<TC<TUDC), with a reciprocal decrease in micelles. Crystal mass is significantly lower in case of hydrophilic bile salts (TDC>TC>TUDC). Chol/PL ratios in small unilamellar and aggregated vesicles are ~1 in all cases (C). Open bars, TDC; hatched bars, TC; closed bars, TUDC. MIC, micelles; SUV, small unilamellar vesicles; AGG, aggregated vesicles; CRY, cholesterol crystal mass.

Inset: equilibrium bile salt-phospholipid-cholesterol ternary phase diagram. Continuous line: phase diagram for hydrophobic bile salts. Interrupted line: decreased one-phase micellar zone and extension of right two-phase zone in case of hydrophilic bile salts (5). Dot indicates model bile plotting in three-phase zone.

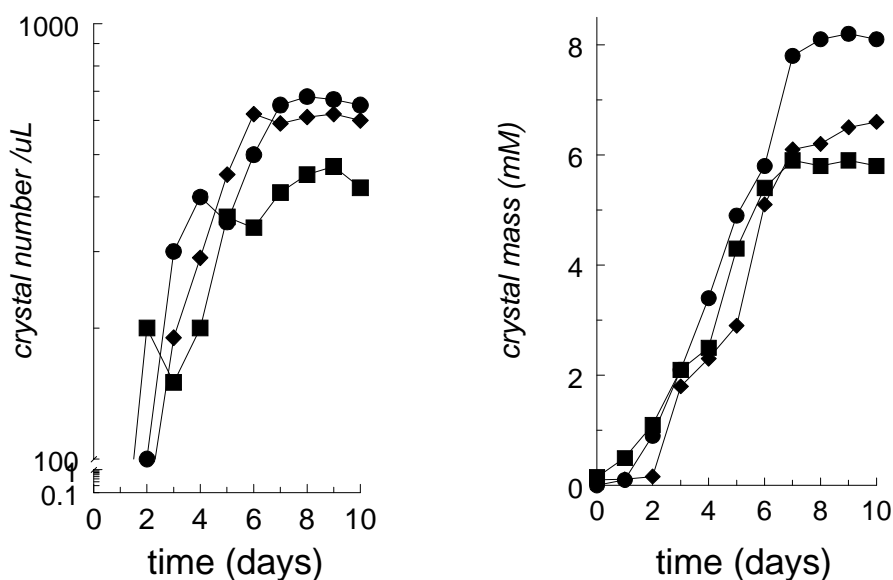


Figure 6: Numbers of cholesterol monohydrate crystals (A) and crystal mass (B) during 10 days incubation in supersaturated model systems containing TDC, TC or TUDC and plotting in the central three-phase zone (EYPC as phospholipid in all cases: for relative lipid composition see Fig. 5). Crystal numbers and mass are larger in case of more hydrophobic bile salts (TDC>TC>TUDC).

(●) TDC; (◆) TC; (■) TUDC. Please note logarithmic scale for 6A

There was also a preferential ($\geq 50\%$) distribution of phospholipids into aggregated vesicles in case of SM- or DPPC-containing model systems, with lower amounts in micelles ($\sim 30\%$) and small unilamellar vesicles ($\sim 20\%$). In case of EYPC-containing systems, distribution of phospholipids into aggregated vesicles was lower ($\sim 40\%$), with larger amounts in micelles or small unilamellar vesicles ($\sim 35\%$ and $\sim 25\%$ resp.) compared to SM- or DPPC-containing systems. Chol/PL ratios in aggregated and small unilamellar vesicles were far below 1 in all cases. Results were essentially the same after 40 days incubation.

Influence of bile salt species: We also determined lipid distribution into various phases after 10 days incubation of supersaturated model biles containing TDC, TC or TUDC and plotting in the right-two phase zone (EYPC as phospholipid in all cases: total lipid conc. 3.6 g/dL, PL/BS+PL) ratio 0.5, 17 mol% cholesterol, 37°C). Distribution of cholesterol and phospholipids into aggregated vesicles increased in the rank order: TDC<TC<TUDC-containing systems, with reciprocal decreases of micellar solubilization. Chol/PL ratios in small unilamellar or aggregated vesicles were far below 1 in all cases. Results were essentially the same after 40 days incubation.

Left two-phase (micelles + vesicles– containing) zone

In model systems plotting in the left-two phase zone, vesicles could not be detected. With daily examination during the first 10 days, cholesterol crystal mass as well as numbers of small cholesterol monohydrate crystals were always higher in SM- or DPPC-containing systems than in EYPC-containing systems (Fig. 7). Anhydrous crystal forms occurred more frequently in EYPC-containing systems.

In contrast to results in the three-phase zone, cholesterol crystal masses and numbers of cholesterol monohydrate crystals were higher in case of more hydrophilic bile salts (TDC<TC<TUDC, Fig. 8). Reciprocal effects were found for cholesterol solubilization in micelles (TDC>TC>TUDC). Anhydrous crystal forms occurred more frequently in case of hydrophobic bile salts.

DISCUSSION

Biliary cholesterol supersaturation has traditionally been considered as the major factor determining precipitation of cholesterol crystals and

gallstone formation. The studies of Wang and Carey (5) have revealed the importance of relative amounts of bile salts vs phospholipids in the system for the crystallization process. In case of excess bile salts, precipitation of –intermediate anhydrous and mature monohydrate-cholesterol crystals occurs at fast rates. At higher phospholipid contents, cholesterol-phospholipid vesicles are formed, with the result that precipitation of cholesterol crystals is diminished (three-phase zone), or even completely prevented (right two-phase zone). We have evaluated in the present study lipid distribution into various phases throughout the phase diagram.

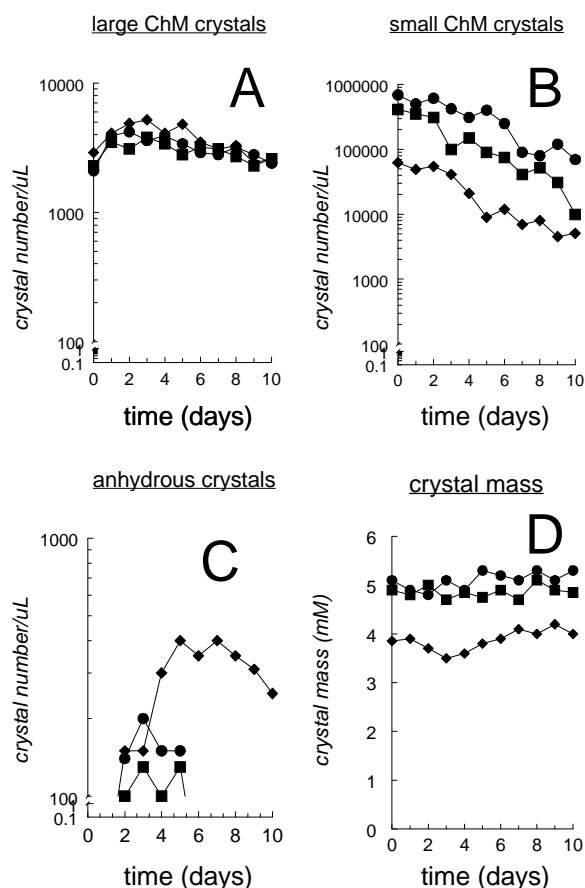


Figure 7: Numbers of large cholesterol monohydrate (ChM) crystals (A), small cholesterol monohydrate crystals (B), anhydrous cholesterol crystals (arcs, needles, tubules, spirals; C) and crystal mass (D) during 10 days incubation in supersaturated model systems containing EYPC, SM or DPPC and plotting in the left two-phase zone (TC as bile salt in

all cases: total lipid conc = 3.6 g/dL, PL/(BS+PL) ratio = 0.02, 10 mol% cholesterol, 37°C). Crystal mass is larger in case of SM or DPPC than for EYPC throughout the observation period.

(◆) EYPC; (●) SM; (■) DPPC. Please note logarithmic scale for 7A, B, C.

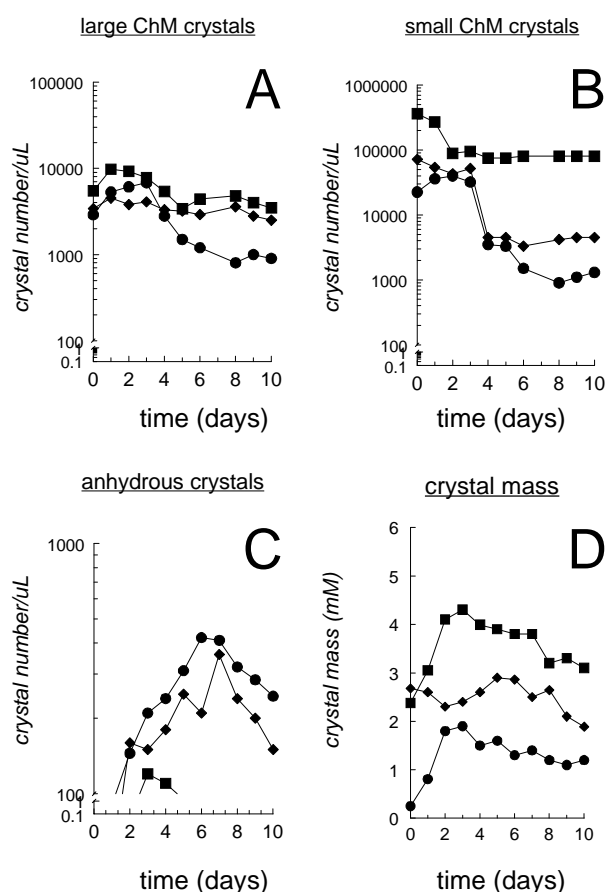


Figure 8. Numbers of large cholesterol monohydrate (ChM) crystals (A), small cholesterol monohydrate crystals (B), anhydrous cholesterol crystals (arcs, needles, tubules, spirals; C) and crystal mass (D) during 10 days incubation in supersaturated model systems containing TDC, TC or TUDC and plotting in the left two-phase zone (EYPC as phospholipid in all cases: total lipid conc = 3.6 g/dL, PL/(BS+PL) ratio = 0.04, 8 mol% cholesterol, 37°C). Crystal mass is larger in case of more hydrophilic bile salts throughout the observation period.

(●) TDC; (◆) TC; (■) TUDC. Please note logarithmic scale for 8A, B, C.

We also determined in supersaturated three-phase model systems that contained cholesterol, EYPC, SM or DPPC, and TC, lipid distribution into various phases as a function of time (after 1, 10 and 40 days incubation: Figs 2-3). After one day, small unilamellar and aggregated vesicles were supersaturated (chol/PL ratios >1). During prolonged incubation, and coinciding with progressive cholesterol crystallization, vesicular cholesterol contents and chol/PL ratios decreased, approaching equilibrium (chol/PL ratio ~ 1) on day 10.

Data obtained by video enhanced contrast microscopy have suggested that precipitation of cholesterol crystals occurs from aggregated vesicular phases (25). In the present study, magnitude of shifts of cholesterol between various phases (large increase of crystal mass; large decrease of cholesterol contained in aggregated vesicles: particularly in case of SM: Fig. 2) also provide indirect evidence for crystal precipitation from vesicular aggregates. In the right two phase-zone, chol/PL ratios in (unilamellar and aggregated) vesicles were always below 1, thus explaining absence of cholesterol crystallization.

We also examined effects of varying phospholipid class. In model systems plotting in the left two-phase or central three-phase (crystal-containing) zones, speed and extent of crystallization was enhanced in case of DPPC or SM as compared with EYPC. In contrast, previous studies (12-14) have indicated that disaturated PC species inhibit crystallization, and PC species with unsaturated acyl chains at the *sn*-2 position promote crystallization progressively at increasing unsaturation. We have previously developed the equilibrium ternary phase diagram for cholesterol, taurocholate and SM- or DPPC-containing systems (6). Compared to EYPC-containing systems under the same conditions (5), the right two-phase (vesicles and micelles-containing) zone is greatly expanded to the left at the expense of the crystals-containing (central three-phase and left two-phase) zones. In previous studies (12-14),

position in the phase diagram was probably changed from the central three-phase zone to the right two-phase zone in case of more saturated PC species, thus explaining suppressed crystallization. However, with careful attention (as in the present study) that model systems -with identical relative lipid composition- are composed so that they all plot in the central three-phase zone of the appropriate ternary phase diagram (5,6), more saturated phospholipids apparently promote crystallization. Dietary modification toward more saturated biliary phospholipids has been proposed to prevent gallstone formation in humans (15). Nevertheless, effects of dietary modification are expected to be relatively small, and insufficient to induce a change from central three-phase toward right two-phase zone position. Indeed, no changes in biliary cholesterol crystallization or lipid solubilization could be induced by such a dietary modification in humans (15).

More hydrophilic bile salts such as TUDC reduced crystallization in model biles plotting in the central three phase-zone, in agreement with previous data (26). In contrast, in model biles plotting in the left two-phase zone, crystallization was enhanced at increasing bile salt hydrophilicity, in the rank order: TDC<TC<TUDC. Apparently, solubilization of cholesterol in vesicular phases (i.e. position in the central three-phase zone) is a prerequisite for reduced crystallization by TUDC. Enhanced crystallization in TUDC-containing model biles that do not contain vesicles (i.e. plot in the left two-phase zone) can easily be explained by the decreased micellar cholesterol solubility in case of more hydrophilic bile salts (5). Although most cholesterol-supersaturated human biles are assumed to plot in the central three phase-zone, some may be located in the left two-phase zone, based on crystallization sequences (27) and absence of vesicular phases (28,29). These data would suggest potential adverse effects of ursodeoxycholate therapy (frequently used in clinical practice to dissolve cholesterol gallstones) at

the local level in bile. However, the major effects of ursodeoxycholate in humans are a decrease of intestinal cholesterol absorption (30) and a lower biliary cholesterol secretion, with the result that bile becomes unsaturated. Indeed, we found that cholesterol crystals decreased in size or even disappeared during prolonged *ex vivo* incubation of gallbladder biles obtained from gallstone patients treated with ursodeoxycholate (31).

Different effects of bile salt hydrophilicity *vs* phospholipid acyl chain saturation on crystallization behavior in the three phase-zone (i.e. inhibition *vs* promotion) may relate to different effects on micellar cholesterol solubilization. Whereas TUDC decreases solubilization of the sterol to a relatively minor degree (5), there is a 70% reduction of micellar solubility limits for SM- or DPPC-containing systems as compared to EYPC-containing system (6). Apparently, such strongly reduced micellar solubilization cannot be compensated for by enhanced vesicular solubilization. One should also realize, that our data on lipid distribution with various phospholipid classes (Figs 2-4) cannot be compared in a quantitative way with data obtained by modulation of bile salt species (Figs 5,6) since lipid composition could not be completely identical due to limitations of the phase diagram (5,6).

The present study increases insight in physical-chemical interactions between bile salts, phospholipids and cholesterol and in the process of crystallization. Nevertheless, several limitations apply to the (patho)physiological relevance of our findings. Obviously, residence time of bile in the gallbladder and bile ducts *in vivo* is much shorter than our prolonged *in vitro* model bile incubation times. Also, composition of our model systems was far from physiological: proteins were absent, only one bile salt was incorporated instead of a mixture of various bile salts, and there is virtually no sphingomyelin in human bile. Furthermore, although large amounts of aggregated vesicles form within

a few hours of *ex vivo* incubation of human biles, as observed by video-enhanced microscopy (25), vesicle aggregation may be particularly extensive in model biles (10). These aggregated vesicles preclude accurate separation of vesicular and micellar phases with the aid of gel filtration (10). We therefore included an initial ultracentrifugation step in our protocol. We obtained in our three-phase model biles at equilibrium, vesicular cholesterol/phospholipid ratios of ~1 and micellar CSI-values of ~1, as expected from theoretical considerations (24). Nevertheless, we cannot definitely exclude that our multistep protocol could induce some artifactual shifts between various lipid phases.

In summary, we found enhanced lipid distribution into vesicular phases, and reciprocal decreases of micellar lipid solubilization in case of more hydrophilic bile salts or more saturated phospholipids. Whereas egg yolk phosphatidylcholine decreases crystallization compared to sphingomyelin or dipalmitoyl phosphatidylcholine in all crystal-containing zones, formation of vesicular phases is a prerequisite for inhibition of crystallization by the hydrophilic bile salt tauroursodeoxycholate.

References

1. Holan, K. R., R. T. Holzbach, R. E. Hermann, A. M. Cooperman, and W. Y. Claffey. 1979. Nucleation time: a key factor in the pathogenesis of cholesterol gallstone disease. *Gastroenterology*. 77: 611-617.
2. Hay, D. W., M. J. Cahalane, N. Timofeyeva, and M. C. Carey. 1993. Molecular species of lecithins in human gallbladder bile. *J.Lipid Res.* 34: 759-768.
3. Mazer, N. A. and M. C. Carey. 1983. Quasielastic light scattering studies of aqueous biliary lipid systems. Cholesterol solubilization and precipitation in model bile solutions. *Biochemistry*. 22: 426-442.
4. Sömjen, G. J. and T. Gilat. 1983. A non-micellar mode of cholesterol transport in human bile. *FEBS Lett.* 156: 265-268.
5. Wang, D. Q. H. and M. C. Carey. 1996. Complete mapping of crystallization pathways during cholesterol precipitation from model bile: influence of physical-chemical variables of pathophysiologic relevance and identification of a stable

- liquid crystalline state in cold, dilute and hydrophilic bile salt-containing systems. *J.Lipid Res.* 37: 606-630.
6. van Erpecum, K. J. and M. C. Carey. 1997. Influence of bile salts on molecular interactions between sphingomyelin and cholesterol: relevance to bile formation and stability. *Biochim.Biophys.Acta.* 1345: 269-282.
 7. Donovan, J. M. and A. A. Jackson. 1993. Rapid determination by centrifugal ultrafiltration of inter-mixed micellar/vesicular (non-lecithin-associated) bile salt concentrations in model bile: influence of Donnan equilibrium effects. *J.Lipid Res.* 34: 1121-1129.
 8. Donovan, J. M., A. A. Jackson, and M. C. Carey. 1993. Molecular species composition of inter-mixed micellar/vesicular bile salt concentrations in model bile: dependence upon hydrophilic-hydrophobic balance. *J.Lipid Res.* 34: 1131-1140.
 9. Donovan, J. M., N. Timofeyeva, and M. C. Carey. 1991. Influence of total lipid concentration, bile salt:lecithin ratio, and cholesterol content on inter-mixed micellar/vesicular (non-lecithin-associated) bile salt concentrations in model bile. *J.Lipid Res.* 32: 1501-1512.
 10. Donovan, J. M. and A. A. Jackson. 1998. Accurate separation of biliary lipid aggregates requires the correct intermixed micellar/intervesicular bile salt concentration. *Hepatology.* 27: 641-648.
 11. Eckhardt, E. R. M., A. Moschetta, W. Renooij, S. S. Goerdayal, G. P. van Berge-Henegouwen, and van Erpecum K.J. 1999. Asymmetric distribution of phosphatidylcholine and sphingomyelin between micellar and vesicular phases: potential implication for canalicular bile formation. *J.Lipid Res.* 40: 2022-2033.
 12. Nishioka, T., S. Tazuma, G. Yamashita, and G. Kajiyama. 1998. Quantitative assessment of comparative potencies of cholesterol-crystal-promoting factors: relation to mechanistic characterization. *Biochem.J.* 332: 343-350.
 13. Ringel, Y., G. J. Sömjen, F. M. Konikoff, R. Rosenberg, and T. Gilat. 1998. Increased saturation of the fatty acids in the sn-2 position of phospholipids reduces cholesterol crystallization in model biles. *Biochim.Biophys.Acta.* 1390: 293-300.
 14. Halpern, Z., M. Moshkowitz, H. Laufer, Y. Peled, and T. Gilat. 1993. Effect of phospholipids and their molecular species on cholesterol solubility and nucleation in human and model biles. *Gut.* 34: 110-115.
 15. Pakula, R., F. M. Konikoff, M. Rubin, Y. Ringel, Y. Peled, A. Tietz, and T. Gilat. 1996. The effects of dietary phospholipids enriched with phosphatidylethanolamine on bile and red cell membrane lipids in humans. *Lipids.* 31: 295-303.
 16. Hakomori, S. 1983. Chemistry of Glycosphingolipids, *In Handbook of Lipid Research.* Hanahan, D. J. editor. Plenum Press, New York, 37-39.

17. Nibbering, C. P. and M. C. Carey. 1999. Sphingomyelins of rat liver: biliary enrichment with molecular species containing 16:0 fatty acids as compared to canalicular-enriched plasma membranes. *J.Membr.Biol.* 167: 165-171.
18. Turley, S. D. and J. M. Dietschy. 1978. Reevaluation of the 3α -hydroxysteroid dehydrogenase assay for total bile acids in bile. *J.Lipid Res.* 19: 924-928.
19. Rouser, G., S. Fleischer, and A. Yamamoto. 1970. Two dimensional thin layer chromatographic separation of polar lipids and determination of phospholipids by phosphorus analysis of spots. *Lipids.* 5: 494-496.
20. Fromm, H., P. Hamin, H. Klein, and I. Kupke. 1980. Use of a simple enzymatic assay for cholesterol analysis in human bile. *J.Lipid Res.* 21: 259-261.
21. Moschetta, A., G. P. vanBerge-Henegouwen, P. Portincasa, G. Palasciano, A. K. Groen, and K. J. van Erpecum. 2000. Sphingomyelin exhibits greatly enhanced protection compared with egg yolk phosphatidylcholine against detergent bile salts. *J.Lipid Res.* 41: 916-924.
22. Schroeder, R. J., E. London, and D. A. Brown. 1994. Interactions between saturated acyl chains confer detergent resistance on lipids and glycosylphosphatidylinositol (GPI)-anchored proteins: GPI- anchored proteins in liposomes and cells show similar behavior. *Proc.Natl.Acad.Sci.U.S.A.* 91: 12130-12134.
23. Sömjen, G. J., Y. Ringel, F. M. Konikoff, R. Rosenberg, and T. Gilat. 1997. A new method for the rapid measurement of cholesterol crystallization in model biles using a spectrophotometric microplate reader. *J.Lipid Res.* 38: 1048-1052.
24. Carey, M. C. 1988. Lipid solubilisation in bile, *In Bile acids in health and disease.* Northfield, T. C., R. P. Jazrawi and P. Zentler-Munro, editors. Kluwer Acad Publ., London, 61-82.
25. Halpern, Z., M. A. Dudley, A. Kibe, M. P. Lynn, A. C. Breuer, and R. T. Holzbach. 1986. Rapid vesicle formation and aggregation in abnormal human biles. A time-lapse video enhanced contrast microscopy study. *Gastroenterology.* 90: 875-885.
26. Nishioka, T., S. Tazuma, G. Yamashita, and G. Kajiyama. 1999. Partial replacement of bile salts causes marked changes of cholesterol crystallization in supersaturated model bile systems. *Biochem.J.* 340: 445-451.
27. Wang, D. Q. H. and M. C. Carey. 1996. Characterization of crystallization pathways during cholesterol precipitation from human gallbladder biles: Identical pathways to corresponding model biles with three predominating sequences. *J.Lipid Res.* 37: 2539-2549.
28. Eckhardt, E. R. M., B. J. M. van de Heijning, K. J. van Erpecum, W. Renooij, and G. P. vanBerge-Henegouwen. 1998. Quantitation of cholesterol-carrying particles in human gallbladder bile. *J.Lipid Res.* 39: 594-603.

29. Eckhardt, E. R., K. J. van Erpecum, M. B. de Smet, P. M. Go, G. P. vanBerge-Henegouwen, and W. Renooij. 1999. Lipid solubilization in human gallbladder versus hepatic biles. *J.Hepatol.* 31: 1020-1025.
30. Tint, G. S., G. Salen, and S. Shefer. 1986. Effect of ursodeoxycholic acid and chenodeoxycholic acid on cholesterol and bile acid metabolism. *Gastroenterology.* 91: 1007-1018.
31. van Erpecum, K. J., P. Portincasa, E. R. M. Eckhardt, P. M. N. Y. H. Go, G. P. vanBerge-Henegouwen, and A. K. Groen. 1996. Ursodeoxycholic acid reduces protein levels and nucleation-promoting activity in human gallbladder bile. *Gastroenterology.* 110: 1225-1237.

chapter 4

**ASYMMETRIC DISTRIBUTION OF PHOSPHATIDYLCHOLINE
AND SPHINGOMYELIN BETWEEN MICELLAR AND
VESICULAR PHASES: POTENTIAL IMPLICATIONS FOR
CANALICULAR BILE FORMATION**

Erik R.M. Eckhardt, Antonio Moschetta, Willem Renooij, Soenita S.
Goerdalay, Gerard P. van Berge-Henegouwen, Karel J. van Erpecum.

Journal of Lipid Research 1999; 40:2022-2033.

Abstract

Both phosphatidylcholine (PC) and sphingomyelin (SM) are the major phospholipids in the outer leaflet of the hepatocyte canalicular membrane. Yet, the phospholipids secreted into bile consist principally (>95%) of PC. In order to understand the physical-chemical basis for preferential biliary PC secretion, we compared interactions with bile salts (taurocholate) and cholesterol of egg yolk (EY)SM (mainly 16:0 acyl chains, similar to trace SM in bile), buttermilk (BM)SM (mainly saturated long (>20 C-atoms) acyl chains, similar to canalicular membrane SM) and egg yolk (EY)PC (mainly unsaturated acyl chains at *sn*-2 position, similar to bile PC). Main gel to liquid-crystalline transition temperatures were 33.6°C for BMSM and 36.6°C for EYSM. There were no significant effects of varying phospholipid species on micellar sizes or intermixed-micellar/vesicular bile salt concentrations in taurocholate-phospholipid mixtures (3 g/dL, 37°C, PL/BS+PL=0.2 or 0.4). Various phases were separated from model systems containing both EYPC and (EY or BM)SM, taurocholate and variable amounts of cholesterol, by ultracentrifugation with ultrafiltration and dialysis of the supernatant. At increasing cholesterol content, there was preferential distribution of lipids and enrichment with SM containing long saturated acyl chains in the detergent-insoluble pelletable fraction consisting of aggregated vesicles. In contrast, both micelles and small unilamellar vesicles in the supernatant were progressively enriched in PC. Although SM-containing vesicles without cholesterol were very sensitive to micellar solubilization upon taurocholate addition, incorporation of the sterol rendered SM-containing vesicles highly resistant against the detergent effects of the bile salt. These findings may have important implications for canalicular bile formation.

INTRODUCTION

The hepatocyte plasma membrane is functionally divided into a canalicular (or apical) region adjacent to the lumen of the bile canaliculus and a sinusoidal (or basolateral) region in close contact with sinusoidal blood (1). Although the canalicular region comprises only 10-15% of the total plasma membrane, it plays a crucial role in the process of nascent bile formation and biliary secretion of bile salts, phosphatidylcholine (PC) and cholesterol.

In recent years, there has been considerable progress in understanding

transport mechanisms of these lipids over the canalicular membrane: *mdr* (multi drug resistance) 2 P-glycoprotein functions as a "flippase" translocating PC molecules from the inner to the outer leaflet of the canalicular membrane (2) and the so-called "Sister P-glycoprotein" appears to mediate bile salt transport (3). Nevertheless, only limited data are available on the events occurring during nascent canalicular bile formation and the physical-chemical mechanisms involved. With the aid of ultrarapid cryofixation and electron microscopic imaging, Crawford could visualize significant amounts of unilamellar vesicles within the canalicular lumen, consistent with a vesicular mode of cholesterol and PC secretion (4). Nevertheless, these findings do not exclude the possibility that detergent bile salts, after their secretion into the canalicular lumen, could micellize considerable amounts of cholesterol and PC from the outer leaflet of the canalicular membrane.

Another matter of debate is why PC is the predominant phospholipid in bile: both sphingomyelin (SM) and PC are the major structural phospholipids in the outer leaflet of the hepatocyte canalicular membrane (in an average ratio of 0.7) (1,5), but PC is the major ($\approx 95\%$) phospholipid species in bile (6). It has been well known since long, that biliary PC contains mainly 16:0 acyl chains at the *sn*-1 position and predominantly unsaturated (18:2>18:1>20:4) acyl chains at the *sn*-2 position (7). Recent data by Nibbering and Carey (8) indicate that the trace amounts of SM in rat bile contain mainly 16:0 acyl chains, whereas canalicular membrane SM contains predominantly long (>20 C-atoms) saturated acyl chains amide-linked to the sphingosine moiety. Similar predominance of SM with long saturated acyl chains has previously been reported for hepatocyte plasma membrane (9). Contents of SM and cholesterol are higher in the canalicular than in the sinusoidal membrane (1,10), with decreased fluidity and increased resistance against detergent

effects of bile salts as a result. Extensive physical-chemical and cell-biological studies indicate that cholesterol has a higher affinity for natural SM than for PC (11-17) and may be tightly bound in laterally segregated SM domains in the hepatocyte canalicular membrane (14,18). The present study aims to increase insight in the process of canalicular bile formation by means of studying interactions of bile salts with SM and PC -with or without cholesterol- in a number of complementary *in vitro* systems. We used PC from egg yolk (mainly 16:0 acyl chains at the *sn*-1 position, and mainly unsaturated acyl chains at the *sn*-2 position, similar to PC in bile (7)), SM from egg yolk (mainly 16:0 acyl chains, similar to trace SM in bile (8)) and SM from buttermilk (mainly long saturated acyl chains, similar to SM in the canalicular membrane (8,9)).

MATERIAL AND METHODS

Materials

Taurocholate was obtained from Sigma Chemical Co. (St. Louis, MO, USA) and yielded a single spot upon thin-layer chromatography (butanol-acetic acid-water, 10:1:1 vol/vol/vol, application of 200 µg bile salt). Cholesterol (Sigma) was $\geq 98\%$ pure by reverse-phase HPLC (isopropanol - acetonitril 1:1, vol/vol, detection at 210 nm). Phosphatidylcholine from egg-yolk (EYPC; Sigma), sphingomyelin from egg-yolk (EYSM; Avanti Polar-Lipids Inc., Alabaster, AL, USA), and sphingomyelin from buttermilk (BMSM; Matreya Inc., Pleasant Gap, PA, USA) all yielded a single spot on thin-layer chromatography (chloroform-methanol-water 65:25:4, vol/vol/vol, application of 200 µg lipid). Methylated fatty acids (16:0, 18:0, 18:1, 18:2, 20:0, 21:0, 22:0, 23:0, 24:0, 24:1, 25:0), used as standards for gas-liquid chromatography, were purchased from Sigma. Acyl chain compositions as determined by gas-liquid chromatography (19) were virtually identical to previously

published data (20) and showed mainly saturated long (≥ 20 C-atoms) acyl chains for BMSM, similar to acyl chain composition of SM in hepatocytic plasma membranes (8,9), and a preponderance of 16:0 acyl chains for EYSM. As shown by reverse-phase HPLC, EYPC contained mainly 16:0 acyl chains at the *sn*-1 position and mainly unsaturated (18:1>18:2>20:4) acyl chains at the *sn*-2 position (21), similar to phosphatidylcholine in human bile (7). All other chemicals and solvents were of ACS or reagent grade quality.

Ultrafilters with a molecular weight cut-off of 10 kDa and 300 kDa were purchased from Sartorius (Göttingen, Germany: Centrisart I), dialysis membranes with a molecular weight cut-off of 300 kDa from Spectrum Laboratories (Laguna Hills, CA, USA: SpectraPor). Sephacryl S400 gel filtration material was from Pharmacia LKB Biotechnology AB (Uppsala, Sweden). The enzymatic cholesterol assay kit was obtained from Boehringer (Mannheim, Germany), and the enzymatic phospholipid kit from Sopar Biochem (Brussels, Belgium). 3α -Hydroxysteroid dehydrogenase for the enzymatic measurement of bile salt concentrations (22) and a colorimetric chloride-kit were purchased from Sigma. The reverse-phase C18 HPLC column was from Supelco (Supelcosil LC-18-DB, Supelco, Bellefonte, PA, USA).

Preparation of model systems

Lipid mixtures containing variable proportions of cholesterol, phospholipids (both from stock solutions in chloroform), or taurocholate (from stock solutions in methanol) were vortex-mixed and dried at 45°C under a mild stream of nitrogen and subsequently lyophilized during 24 hrs, before being dissolved in aqueous 0.15 M NaCl plus 3 mM NaN₃. Tubes were sealed with Teflon-lined screw caps under a blanket of nitrogen to prevent lipid oxidation and vortex-mixed for 5 min followed

by incubation at 37°C in the dark. The final mol percentages cholesterol, phospholipid and bile salt did not differ more than 2.5% from the intended mol percentages.

Differential Scanning Calorimetry

BMSM or EYSM (10 mg), from stock solutions in chloroform, were dried at 45°C under a mild stream of nitrogen and dissolved in 1 mL H₂O followed by 5 cycles of freeze-thawing. Main gel to liquid-crystalline phase transition temperatures (melting temperatures: T_m) were measured with a Perkin-Elmer DSC-4 differential scanning calorimeter (Perkin-Elmer, Norwalk, CT, USA), at a scan rate of 5°C / min.

Quasielastic light-scattering (QLS) spectroscopy

QLS measurements of micelles in mixtures of taurocholate and phospholipids were performed on a home-built apparatus, the details of which were published elsewhere (23). Measurements were performed with the argon laser tuned to 514.5 nm at a scattering angle of 90°. Vesicular sizes were measured with a Malvern 4700c QLS spectrometer (Malvern Ltd., Malvern, UK), equipped with an argon laser (Uniphase Corp., San Jose, CA, USA) at a wavelength of 488 nm. All samples were maintained at a constant temperature of 37°C by means of a Peltier thermostatic block or a water bath. To remove dust, tubes were first centrifuged for 10 min. at 10000 x g. Data are given as hydrodynamic radius (R_h : means of at least 3 measurements).

Lipid analysis

Phospholipid concentrations in model systems were assayed by determining inorganic phosphate according to Rouser (24), but in serial fractions from gel-filtration experiments with an enzymatic assay.

Cholesterol concentrations were determined with an enzymatic assay or by reverse-phase HPLC (acetonitril–isopropanol 1:1, vol/vol, detection at 210 nm), and bile salts with the 3 α -hydroxysteroid dehydrogenase method (22) or by HPLC (25). In systems containing both EYPC and SM, the phospholipids were extracted according to Bligh and Dyer (26), separated by thin-layer chromatography (chloroform-methanol-acetic acid-water 50:25:8:2, vol/vol/vol/vol), and quantified by determination of phosphorus contents of separated phospholipid spots. In order to determine the fatty-acid profiles of sphingomyelin, 1 μ mol sphingomyelin was hydrolyzed in 1 mL nitrogen-flushed HCl-methanol-H₂O (8.3:80.6:11.1, vol/vol/vol, 16hrs, 70°C) (19). The methylated fatty acids were extracted three times with 1 mL hexane; the pooled hexane phase was washed with 3 mL H₂O, dried over Na₂SO₄, and concentrated under nitrogen. The fatty-acid methyl-esters were dissolved in 30 μ L hexane, 2 μ L of which were injected in a GC14-A gas-chromatograph (Shimadzu, Kyoto, Japan), equipped with a bonded FSOT capillary column (length 30m, \varnothing 0.32 mm).

IMC measurement

Apart from mixed (i.e. phospholipid–bile salt) micelles, model bile systems also contain non phospholipid–associated bile salts, either as monomers or, above their critical micellar concentration, associated in small simple micelles. The monomeric plus simple micellar bile salt concentration is referred to as “intermixed micellar/vesicular (non phospholipid-associated) bile salt concentration”, usually abbreviated as "IMC" (27). We determined the IMC in micellar model systems with relatively low or relatively high amounts of either EYSM, BMSM or EYPC as phospholipid and taurocholate as bile salt ((PL / (PL + bile salt) ratio = 0.2 and 0.4; total lipid concentration 3 g / dL, 37°C). The effect of

incorporating small (3 mol %) amounts of cholesterol on the IMC in these systems was also explored.

A 10 kDa Centriscart ultrafilter was rinsed with H₂O and centrifuged for 5 min at 500 g in order to remove glycerol remnants from the membrane. The water was removed carefully from both sides of the membrane with a syringe. The filter was preincubated at 37°C during 30 min. before usage. A 2 mL aliquot of model system was put into the filter device (in duplicate) and centrifuged at 500 g for 5 min. in a pre-warmed (37°C) centrifuge. The filtrate was carefully collected with a syringe. Filtration was repeatedly performed, adjusting centrifugal speed so as to obtain constant filtrate volumes of approximately 50 µL. Bile salt and chloride concentrations reached stable values in the third filtrate. Slightly lower concentrations in the first and second filtrates resulted from small amounts of water remaining in the membrane after rinsing the ultrafilter (28). We considered the third filtrate to represent the simple micellar + monomeric fraction, and therefore decided to use the third filtrate for measurement of the IMC (the first two filtrates were added each time to the filtrant) (28,29). No phospholipids were detectable in the filtrates (detection limit of the assay: 0.048 mM), indicating that no mixed micelles had passed through the filter. During ultrafiltration, Gibbs-Donnan effects occur as a result of uneven distribution across the membrane of non-filterable particles with a highly negative charge (in particular mixed micelles), thus leading to an overestimation of the concentrations of negatively charged monomeric and simple micellar bile salts in the filtrate (27,28). We corrected the concentrations of bile salts measured in the filtrate for Gibbs-Donnan effects by multiplying the bile salt concentration in the filtrate with the ratio of chloride concentrations in filtrant and filtrate (27-29).

Separation of vesicular and micellar phases

Two independent procedures were used to separate vesicular and micellar phases: ultrafiltration of the whole system or ultracentrifugation with subsequent ultrafiltration and dialysis of the supernatant. With the first procedure (ultrafiltration), micellar phases were isolated from model systems containing both EYPC and SM as phospholipid, taurocholate and various amounts of cholesterol (10 mM EYPC, 6.6 mM EYSM or BMSM, 16.6 mM taurocholate, and 1.6, 3.2 or 6.4 mM cholesterol: cholesterol / phospholipid ratios 0.1, 0.2 or 0.4). These model systems all plot in the right two-phase zone of the equilibrium ternary phase diagram (20,30) and contain micelles and vesicles of various compositions. We used one additional model system (57mM taurocholate, 19mM EYPC, 19mM EYSM, 46mM cholesterol) plotting in the middle three-phase (micelles, vesicles and solid cholesterol crystals containing) zone of the equilibrium ternary phase diagram (20,30). According to the phase rule, all three phases of this system should have one, invariant composition at equilibrium (31). The ultrafilter had a molecular weight cut-off of 300 kDa, and had previously been rinsed with aqueous 0.15 M NaCl plus 3 mM NaN₃, containing taurocholate at concentrations identical to the IMC of the original model systems, in order to avoid artifactual shifts of lipids between vesicles and micelles (27-29). These filters were completely permeable not only to simple micelles but also to mixed taurocholate / phospholipid micelles (tested with mixed micelles at 37°C, at total lipid concentrations of 2, 5 and 10 g/dL and at PL/(BS+PL) ratios of 0.55, 0.5, 0.4 and 0.3, either without or with small amounts (0.25 mol%) cholesterol: either SM, EYPC or both SM and EYPC (SM/PC ratio 0.37) as the phospholipid), but were completely impermeable to small unilamellar or aggregated vesicles. The membrane-containing inner tube of the filter device (placed membrane-down on top of 2 mL of model

system) was allowed to sink slowly into the filtrant by gravity, thus producing approximately 200 μL micelle-containing filtrate within 2 hrs. In order to purify the vesicles, 200 μL of the remaining filtrant then was diluted 10 times with aqueous 0.15 M NaCl / 3 mM NaN_3 containing taurocholate according to the IMC (in order to avoid artefactual shifts of lipids between various phases), followed by ultrafiltration until approximately 90% of the volume was contained within the filtrate. This procedure was repeated twice in order to wash out the remaining mixed micelles.

With the second procedure, aggregated vesicles in 2 mL of model system were precipitated by ultracentrifugation during 30 minutes at 50.000 g and 37°C in a TLS 55 rotor (Beckman, Palo Alto, CA, USA) (32). The pellet was resuspended in a final volume of 2 mL isopropanol. A Tyndall effect was generally visible in the supernatant, consistent with the presence of small unilamellar vesicles, as confirmed with quasi-elastic light scattering spectroscopy. Micelles were isolated from the supernatant by ultrafiltration with the aid of the 300 kDa filter described above (identical micellar compositions had been obtained by ultrafiltration of the corresponding whole model system, indicating that the short ultracentrifugation procedure did not induce artefactual shifts between phases). Small unilamellar vesicles were isolated from the supernatant by dialysis (500 μL sample, 16h, 37°C) in a SpectraPor® dialysis device with a molecular weight cut-off of 300 kDa, against two times 20 volumes of aqueous 0.15 M NaCl plus 3 mM NaN_3 containing taurocholate at concentrations identical to the IMC of the original model system. The dialysis membrane was completely permeable for the same micelles used to validate the 300 kDa ultrafilter (see above), but not for small unilamellar vesicles or for aggregated vesicles. Recovery of cholesterol and phospholipids in separated micellar, unilamellar and

aggregated vesicular phases was 95-100 % of lipids in the corresponding whole model system.

In some experiments, small unilamellar vesicles were also separated from micelles in model systems by gel filtration of the supernatant on a Sephacryl S400 column (gel bed 30 cm, diameter 1.5 cm, flow-rate 0.5 ml/min, 1 mL fractions), equilibrated with aqueous 0.15 M NaCl plus 3 mM NaN₃ containing taurocholate at concentrations identical to the IMC of the original model system (27-29). Combined dialysis and ultrafiltration yielded the same amounts of vesicles and micelles as gel filtration, but is less time-consuming, requires smaller amounts of aqueous bile salt solution, and does not lead to dilution of the sample. Therefore, combined dialysis and ultrafiltration was considered to be the preferable method to isolate micelles and small unilamellar vesicles from the model system.

Preparation of small unilamellar vesicles

Small unilamellar vesicles were prepared by sonication. Lipids, from stock-solutions in chloroform, were vortex-mixed, dried under a mild stream of nitrogen and subsequently lyophilized during 24 hrs. The lipid film was dissolved in nitrogen-flushed aqueous 0.15 M NaCl plus 3 mM NaN₃, and thereafter, the suspensions were probe-sonicated during 30 min. at 50°C (above the main transition temperatures of the phospholipids). After sonication, the suspension was centrifuged during 30 min. at 50000 x g at 40°C, in order to remove potential remaining vesicular aggregates and titanium particles. The resulting small unilamellar vesicles were stored at temperatures above 40°C, and used within 24 hrs. Small unilamellar vesicles were prepared with 100% EYPC, 100% (EY or BM)SM, 80% EYPC / 20% (EY or BM)SM, or 60% EYPC / 40% (EY or BM)SM as the phospholipid. Final

phospholipid concentrations were 4 mM. Vesicles were either prepared without or with cholesterol (cholesterol / phospholipid ratio 0, 0.2 or 0.4).

Interactions of small unilamellar vesicles with bile salts

Interactions of small unilamellar vesicles with taurocholate were examined by measuring optical density at 405 nm every min. during 80 minutes at 37°C, in a thermostated Benchmark microplate reader (BioRad, Hercules, CA, USA). The solutions were stirred for 2 seconds prior to each measurement. A decrease of the OD 405 after addition of taurocholate is compatible with micellization of the vesicles, whereas an increase can be attributed to growth, fusion or aggregation of the vesicles (33). Absorbance measured in control vesicles without taurocholate always remained stable during the experiment. In the case of cholesterol-containing vesicles, after the experiment the mixtures were observed by polarizing light microscopy, in order to examine whether liquid or solid cholesterol crystals had formed.

In additional experiments, we added taurocholate to sonicated EYPC, BMSM and cholesterol containing vesicles (final composition of the system: 16 mM taurocholate, 10 mM EYPC, 6.6 mM BMSM and 6.4 mM cholesterol) and determined SM/PC ratios in micelles (obtained by ultrafiltration) at 10 min, 1 hr, 4 hrs and 12 hrs, in order to obtain further information on extent of asymmetric phospholipid distribution as a function of time.

Statistical analysis

Values are expressed as mean \pm SEM. Differences between groups were tested for statistical significance by analysis of variance with the aid of SPSS software, version 7.5. When ANOVA detected a significant difference, results were further compared for contrasts using Fisher's

least significant difference test as post-hoc test. Statistical significance was defined as a two-tailed probability of less than 0.05.

RESULTS

Main gel to liquid crystalline phase transition temperatures of BMSM and EYSM

Main gel to liquid crystalline phase transition temperatures as determined by differential scanning calorimetry were 33.6°C for hydrated BMSM (maximum $\Delta H/\text{sec}$ at 29°C) and 36.6°C for hydrated EYSM (maximum $\Delta H/\text{sec}$ at 33°C).

Micellar sizes and intermixed micellar/vesicular bile salt concentrations of taurocholate–phospholipid systems.

The hydrodynamic radius (R_h) of taurocholate–phospholipid mixed micelles (3 g/dL, 37°C) was 2.1 ± 0.1 nm at low phospholipid content (PL / (PL + BS) ratio = 0.2) but increased to 2.9 ± 0.1 nm at higher phospholipid content (PL / (PL + BS) ratio = 0.4). There were no significant differences in sizes between EYPC-, EYSM- or BMSM-containing mixed micelles at these ratios. Intermixed micellar/vesicular (i.e. monomeric + simple micellar) bile salt concentrations (IMC) of the same systems also strongly depended on phospholipid content: the IMC was 17.5 ± 0.3 mM at PL / (PL + BS) ratio 0.2, but 8.4 ± 0.3 mM at PL / (PL + BS) ratio 0.4 (37°C, 3 g/dL). Again, there were no significant differences between systems containing EYPC, EYSM or BMSM as the phospholipid. Inclusion of small amounts (3 mol %) of cholesterol in the system led to turbidity due to formation of vesicles in EYSM- or BMSM-containing systems, whereas systems containing EYPC remained clear under these circumstances. However, the IMC did not change by inclusion of the sterol in EYSM-, BMSM-, or EYPC-containing systems.

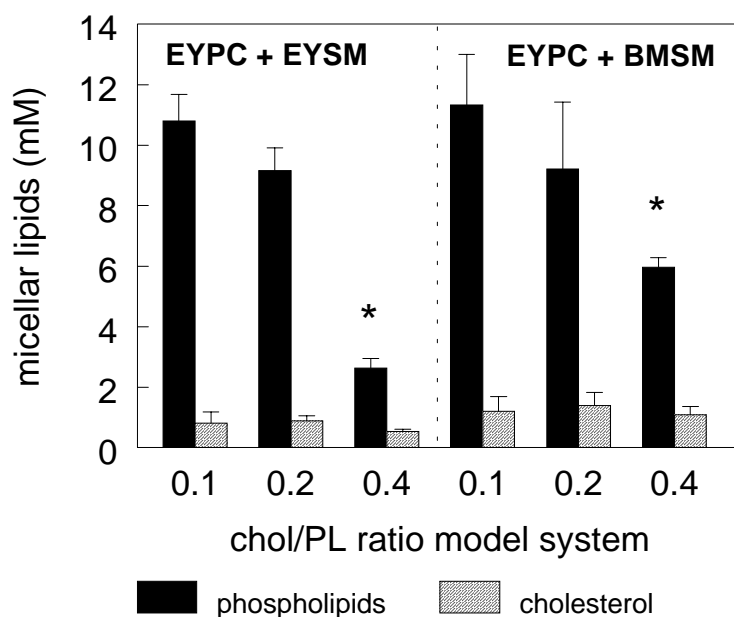


Figure 1: Micellar solubilization of phospholipids (solid bars) and cholesterol (hatched bars) as determined by ultrafiltration of model systems after 2 weeks incubation at 37°C (16.6 mM taurocholate, 10 mM EYPC, 6.6 mM EYSM or BMSM, 1.6, 3.2 or 6.4 mM cholesterol, cholesterol/phospholipid ratios 0.1, 0.2 and 0.4). The amount of phospholipid solubilized in micelles decreased significantly at higher cholesterol content of the systems, whereas the amount of cholesterol solubilized in micelles did not change at varying cholesterol contents. There were no significant differences between EYSM- and BMSM-containing systems. An asterisk (*) indicates significant difference from chol/PL ratios 0.1 and 0.2.

Distribution of cholesterol and phospholipid between micellar and vesicular phases

Model systems composed with taurocholate, both EYPC and sphingomyelin as phospholipid, and variable amounts of cholesterol (16.6 mM taurocholate / 10 mM EYPC / 6.6 mM EYSM or BMSM / 1.6, 3.2 or 6.4 mM cholesterol, see also "Materials and Methods") were studied after 2 weeks of incubation at 37°C. These systems were highly turbid and microscopic examination revealed the presence of large

amounts of aggregated vesicles. Solid cholesterol crystals, however, were not observed. In a first series of experiments, micelles were isolated from model systems by ultrafiltration. As shown in Figure 1, with increasing cholesterol content of the model systems, micellar phospholipid solubilization decreased strongly, whereas micellar cholesterol solubilization remained constant. The decrease of micellar phospholipid occurred both in EYSM- and BMSM-containing systems.

In subsequent experiments, various cholesterol-containing phases were separated by ultracentrifugation followed by ultrafiltration and dialysis of the supernatant (see "Materials and Methods" section). After precipitation of aggregated vesicles by ultracentrifugation, the supernatant displayed a typical Tyndall effect, indicating the presence of small unilamellar vesicles. Indeed, quasielastic light scattering spectroscopy of the supernatant revealed the presence of particles with a hydrodynamic radius of 43 ± 12 nm, consistent with small unilamellar vesicles.

As shown in Figure 2A-B, at increasing cholesterol content of the system, the excess cholesterol was mainly distributed into the detergent-insoluble pelletable fraction consisting of aggregated vesicles. Distribution of cholesterol into small unilamellar vesicles and in mixed micelles decreased. Although the total amount of phospholipids was kept constant in the system, distribution of phospholipids into aggregated vesicles increased at higher cholesterol contents, whereas the amount of phospholipids in small unilamellar vesicles and mixed micelles decreased (Figure 2C-D). Whereas the cholesterol/phospholipid ratios in micelles and small unilamellar vesicles increased only slightly at higher cholesterol content of the system, there was a strong increase of cholesterol/phospholipid ratio in aggregated vesicles (Figure 2E, F). The effects of cholesterol tended to be more pronounced in systems

containing EYSM (Figure 2A, C, E) than in systems composed with BMSM (Figure 2B, D, F).

Distribution of sphingomyelin and egg yolk phosphatidylcholine between vesicles and micelles

Figure 3 shows the distribution of SM and EYPC into vesicles (small unilamellar and aggregated combined) and micelles quantified after separation of the phases by means of ultrafiltration (see “Materials and Methods”). Micellar enrichment with PC and vesicular enrichment with SM is evident, particularly at high cholesterol contents of the system. A similar pattern of phospholipid distribution was observed when various phases were separated by ultracentrifugation with subsequent dialysis and ultrafiltration of the supernatant. Apart from data on phospholipid solubilization in micelles, this procedure also yielded separate information on phospholipid distribution into small unilamellar and into large aggregated vesicles (Figure 4). SM was highly enriched in aggregated vesicles. In contrast, PC preferentially distributed into micelles and into small unilamellar vesicles, particularly at high cholesterol contents of the system. Asymmetric distribution of phospholipids tended to be more pronounced in EYSM containing systems (Figure 4A) than in BMSM containing systems (Figure 4B), but significance was not reached.

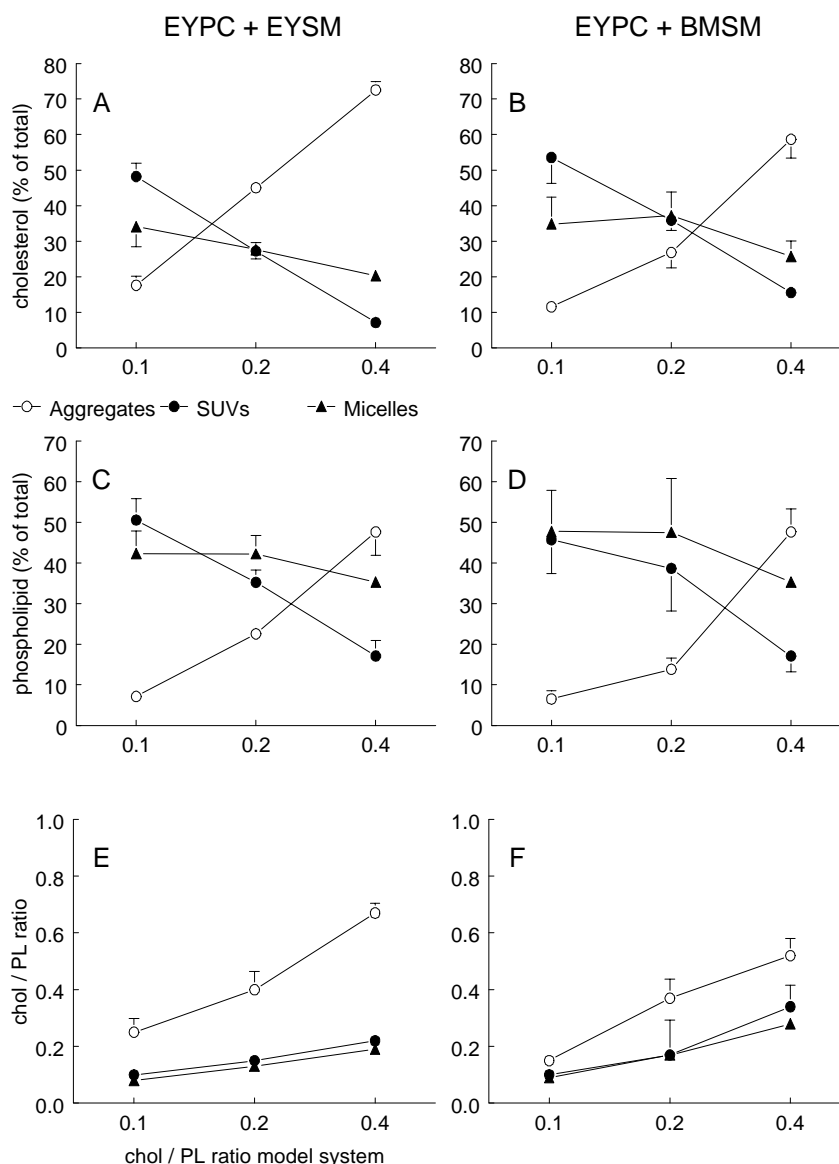


Figure 2: Solubilization of cholesterol and phospholipids in aggregated vesicles (open circles), unilamellar vesicles (closed circles), and mixed micelles (triangles) in model systems after 1 week incubation at 37°C. Lipid composition of the model systems was the same as in Figure 1. The phases were separated by ultracentrifugation and subsequent ultrafiltration and dialysis of the supernatant (see “Materials and Methods”). Figure 2A and B show cholesterol solubilization, 2C and D phospholipid solubilization and 2E and F cholesterol/phospholipid ratios. Figures 2A, C, E apply to EYSM-containing systems and Figures 2B, D, F to BMSM-containing systems. At increasing cholesterol contents of the system, solubilization of cholesterol and phospholipids in aggregated vesicles increased strongly, whereas solubilization of these lipids in small unilamellar vesicles decreased strongly (significant differences between all chol/PL ratios). The amount of mixed micellar cholesterol and phospholipid also tended to decrease at increasing

cholesterol content in the system. Cholesterol/phospholipid ratios increased significantly at increasing cholesterol contents in the system, particularly in aggregated vesicles. There was no significant influence of SM-type on lipid solubilization in the various phases, although effects of cholesterol inclusion tended to be more pronounced in case of EYSM.

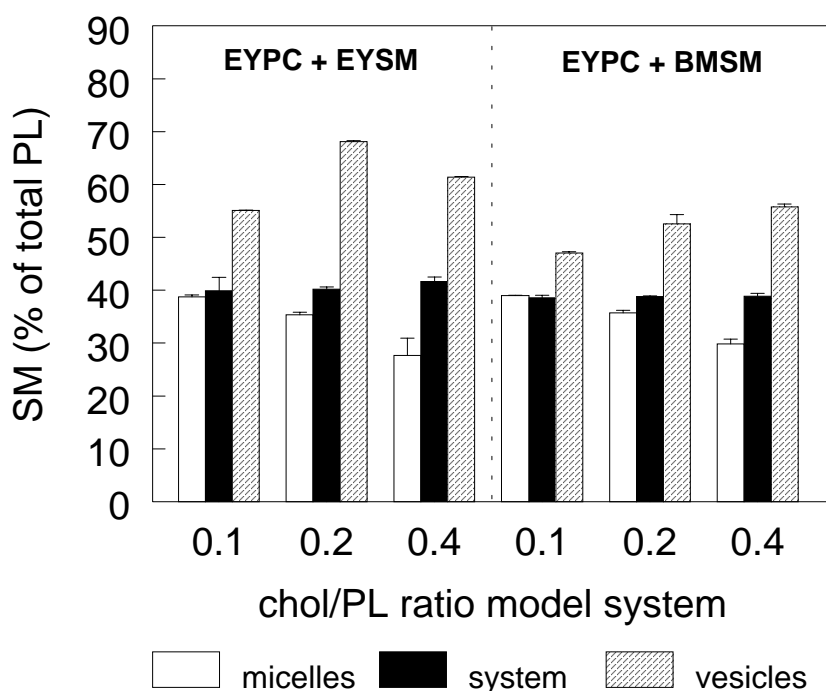


Figure 3: Distribution of SM and PC between vesicles and micelles, as determined by ultrafiltration of model systems after 2 weeks incubation at 37°C. Lipid composition of the model systems was the same as in Figure 1. Micellar SM solubilization decreased, and vesicular SM solubilization increased at increasing cholesterol content of the system (differences significant between all chol/PL ratios). Reciprocal results were obtained for PC solubilization.

As shown in Figure 5, in systems composed with BMSM, there was a preferential distribution of SM with long (> 21 C-atoms) saturated acyl chains into aggregated vesicles, and a preferential distribution of SM with shorter or unsaturated acyl chains in micelles or small unilamellar vesicles, provided that the systems also contained cholesterol. No such

asymmetric distribution occurred in systems composed with EYSM, which can be explained by the small amounts of long acyl chains in EYSM.

The model systems that we used above all plotted in the right two-phase zone of the equilibrium ternary phase diagram (20,30) and contained micelles and vesicles of various compositions. In addition, we determined composition and SM/PC ratio of micelles from a model system (57 mM taurocholate, 19 mM EYPC, 19 mM EYSM, 46 mM cholesterol), plotting in the middle three-phase (micelles, vesicles and solid cholesterol crystals containing) zone of the ternary phase diagram (20,30), after 50 days incubation at 37°C. According to the phase rule, all micelles in this three-phase system should have the same, invariant composition at thermodynamic equilibrium (31). Microscopical examination of the model system revealed aggregated vesicles and solid cholesterol crystals. Composition of micelles (obtained by ultrafiltration of the supernatant) was 41 mM (77 mol %) taurocholate, 11 mM (21 mol %) phospholipids and 1.2 mM (2 mol %) cholesterol and micellar SM/PC ratio was 0.33 (versus 1.0 in the whole system).

We also determined micellar SM/PC ratios at various time points after addition of taurocholate to sonicated EYPC, BMSM and cholesterol containing vesicles (final composition of the system : 16.6 mM taurocholate, 10 mM EYPC, 6.6 mM BMSM, 6.4 mM cholesterol). Micellar SM/PC ratio at 10 min. after addition of taurocholate was 0.67 (identical to the SM/PC ratio of 0.66 in the whole system) but decreased to 0.61 after 1 hr, 0.55 after 4 hrs and 0.41 after 12 hrs.

Resistance of phospholipid vesicles against detergent bile salts

As shown in Figure 6A, vesicles without cholesterol and containing EYPC as the sole phospholipid tended to be rather resistant against the

detergent effects of taurocholate, as indicated by the slow decrease of absorption values during the time period studied (conditions: vesicular phospholipid 4 mM final concentration: addition of taurocholate at 5 mM final concentration, 37°C).

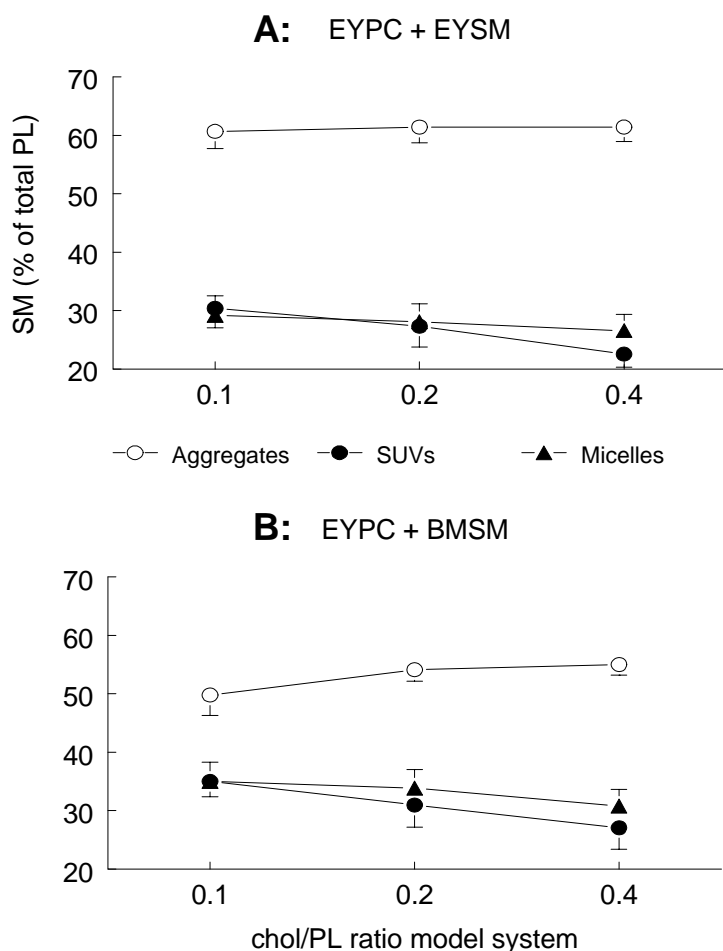


Figure 4: Distribution of SM and PC between aggregated vesicles (open circles), small unilamellar vesicles (closed circles) and micelles (triangles), as determined by ultracentrifugation (see “Materials and Methods”) of model systems after 1 week incubation at 37°C. Lipid composition of the model systems was the same as in Figure 1. SM solubilization in micelles and small unilamellar vesicles decreased and SM solubilization in aggregated vesicles increased significantly at increasing cholesterol content of the system (significant differences between all chol/PL ratios). Reciprocal results were obtained for PC solubilization. There was no significant influence of SM-type on the distribution of phospholipids between the various phases, although effects of cholesterol inclusion tended to be more pronounced in the case of EYSM.

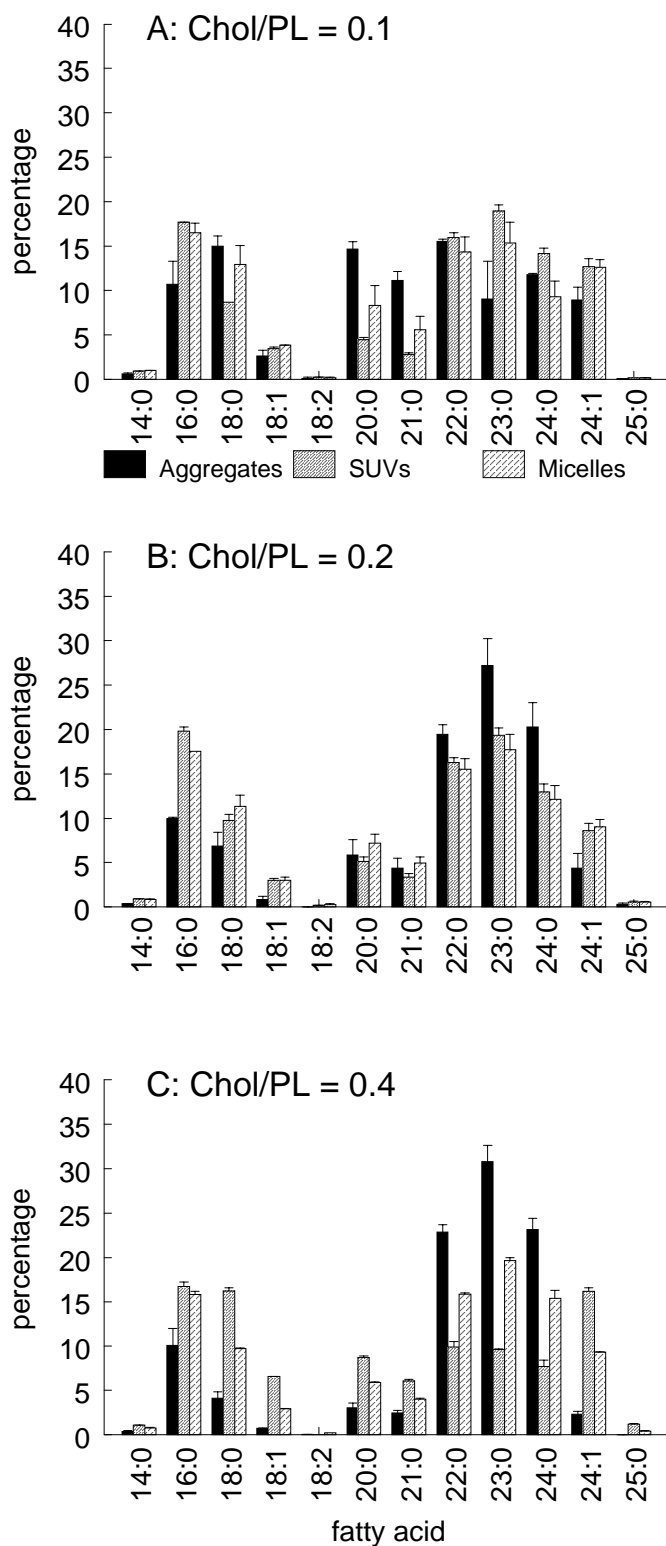


Figure 5: Distribution of SM species between aggregated vesicles, small unilamellar vesicles and micelles in model systems after incubation at 37°C (16 mM taurocholate, 10 mM EYPC, 6.6 mM BMSM, 1.6, 3.2 or 6.4 mM cholesterol, cholesterol/phospholipid ratios 0.1, 0.2 or 0.4). At

high cholesterol content, there is a preferential distribution of SM with long (> 21 C-atoms) saturated acyl chains into aggregated vesicles and a preferential distribution of SM with shorter or unsaturated acyl chains in micelles and small unilamellar vesicles (significant effects for % long and % saturated acyl chains: ANOVA).

In contrast, vesicles without cholesterol and containing (EY or BM)SM as the sole phospholipid were extremely sensitive, with a virtual instantaneous drop of absorbance to 0 upon addition of taurocholate. Also, partial replacement of vesicular EYPC by EYSM or BMSM (vesicular EYPC/SM ratios 80/20 or 60/40), without inclusion of cholesterol, led to significant vesicular destabilization, as evidenced by absorbance values upon addition of taurocholate. The vesicular destabilization depended on the amount of EYPC replaced by SM and was strongest in case of partial replacement by EYSM (Figure 6A). Essentially the same results were obtained upon addition of taurocholate at 4, 6 and 7 mM final concentrations (results not shown).

As shown in Figure 6B, incorporation of cholesterol in SM-containing EYPC vesicles prevented the destabilizing effect of SM (conditions: vesicular phospholipid 4 mM final concentration; vesicular EYPC/SM 80/20 or 60/40; vesicular cholesterol/phospholipid ratio 0.4; addition of taurocholate at 5 mM final concentration; 37°C): Absorbances by spectrophotometry of these cholesterol-enriched vesicles were stable in case of EYPC as the sole vesicular phospholipid but increased in the case of incorporation of SM in the vesicles. The extent of increase depended on the amount of EYPC replaced by SM and was strongest in case of replacement by EYSM. Microscopical examination revealed formation of aggregated vesicles under the latter circumstances, whereas solid cholesterol crystals were absent.

As shown in Figure 6C, the increase in absorption observed in the case of SM-containing vesicles was proportional to their cholesterol content

(vesicular phospholipid 4mM final concentration, vesicular EYPC/SM ratio 60/40; vesicular cholesterol/phospholipid ratio 0.2 and 0.4, addition of taurocholate at a final concentration of 5 mM, 37°C). The increase of absorption was stronger in case of EYSM- than BMSM-containing vesicles.

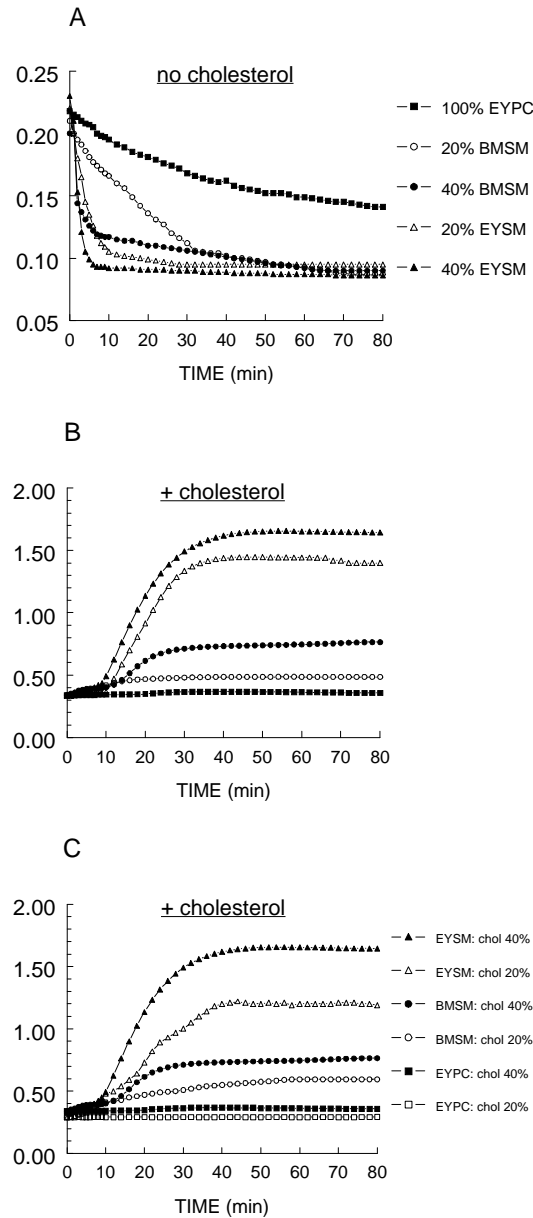


Figure 6: Effects of taurocholate (final conc. 5 mM) on vesicles (final phospholipid conc. 4 mM) with or without cholesterol (37°C). (A) Vesicles without cholesterol and with variable phospholipid composition. Vesicles are composed with 100% EYPC or with 20% or 40% of the EYPC replaced by either EYSM or BMSM. In the absence of cholesterol, vesicles are progressively destabilized at increasing SM contents (EYSM>BMSM). (B)

Vesicles composed with fixed amounts of cholesterol and with variable phospholipid composition. Incorporation of cholesterol (chol/PL ratio = 0.4) prevents the destabilizing effects of SM. Absorption values now even increase upon addition of taurocholate, depending on SM content (EYSM>BMSM) consistent with aggregation or fusion of vesicles (33). (C) Vesicles composed with variable amounts of cholesterol and with variable phospholipid composition. The increase of absorption in case of cholesterol-containing vesicles is also proportional to their cholesterol content and stronger in case of partial replacement with EYSM than with BMSM. Vesicles are composed with 100% EYPC, or 40% of EYPC replaced with EYSM or BMSM. Variable amounts (20% or 40%) of cholesterol are also incorporated in the vesicles. Symbols for (A) also apply to (B).

The hydrodynamic radius (Rh) as determined by quasielastic light scattering spectroscopy of the small unilamellar vesicles composed with 100% EYPC and without cholesterol was 50 ± 1.65 nm. Vesicles with only SM as phospholipid were smaller, with a Rh of 38.0 ± 2.1 nm (EYSM) and 34.2 ± 1.9 nm (BMSM). Partial replacement of EYPC with SM also led to slightly decreased vesicle sizes (43.5 ± 1.23 nm in case of 40% EYSM, 43.9 ± 0.97 nm in case of 40% BMSM). Vesicle sizes increased slightly with inclusion of cholesterol (67.2 ± 0.9 nm, 49.6 ± 1.6 nm and 49.6 ± 2.6 nm for 100% EYPC, EYSM and BMSM respectively; 62.1 ± 1.3 nm and 63.2 ± 1.9 nm in case of partial replacement of EYPC with 40% EYSM and 40% BMSM respectively, all at cholesterol/phospholipid ratio 0.4).

DISCUSSION

The major finding of the present study was the asymmetric distribution of PC and SM between vesicular and micellar phases, provided that the system also contained cholesterol. Similar results have been reported after incubation with bile salts of isolated vesicular hepatocyte canalicular membrane subfractions (34,35) or erythrocytes (36).

In most experiments, we have exploited the approach of Schroeder et al.

(32) to pellet detergent insoluble material with the aid of ultracentrifugation. These authors aptly state that “although it is likely that any sedimentable lipids are not solubilized, the inability to sediment does not guarantee solubilization”. Nevertheless, they considered “for convenience the pelletable material as insoluble and material that remains in the supernatant as soluble” (32) . We found evidence that the supernatant was not homogeneous but contained small unilamellar vesicles in addition to mixed micelles. We further separated these phases with the aid of ultrafiltration and dialysis, or gel filtration techniques, taking into account the intermixed micellar/vesicular bile salt concentration (IMC), in order to avoid artifactual shifts between phases (27-29). In the supernatant, both mixed micelles and small unilamellar vesicles proved to be enriched in PC. In contrast, the pelletable fraction - consisting of aggregated vesicles- was enriched in SM.

The 300 kDa ultrafilter that we used was completely permeable for mixed micelles of a wide range of compositions but completely impermeable for vesicles. We also found strong micellar depletion of SM in a model system plotting in the middle (micelles, vesicles and solid cholesterol crystal containing) three-phase zone of the ternary phase diagram (20,30), after 50 days incubation (assumed thermodynamic equilibrium). According to the phase rule (31), at thermodynamic equilibrium, micelles in this system should be of one, invariant composition. Therefore, these findings definitely exclude preferential passage of phosphatidylcholine-enriched micelles through the ultrafilter as the explanation of micellar SM depletion.

We also determined micellar SM/PC ratios as a function of time after addition of taurocholate to sonicated SM, EYPC and cholesterol containing vesicles. The fact that micellar SM depletion was not present immediately after taurocholate addition but occurred at later stages,

excludes artifacts during preparation of the model systems as the explanation of our findings.

The present data on asymmetric distribution of (EY)PC and (EY or BM)SM between micellar and vesicular phases are in agreement with equilibrium ternary phase diagrams of (EY or BM)SM, taurocholate and cholesterol (37°C, 3g/dL) (20): compared to EYPC-containing systems under the same conditions (30), one-phase micellar zones are strongly reduced in SM-containing systems, and there is a marked expansion of the right two-phase (micelles + vesicles-containing) zone (20). The fact that ternary phase diagrams for systems composed with (disaturated) dipalmitoyl (DP)PC (T_m 41 °C) are identical to phase diagrams of SM-containing systems (20) points to the importance of acyl chain composition and/or physical state of the phospholipid. Also, after separation of micellar and vesicular phases from analogous EYPC-containing model systems with the aid of gel filtration, PC species with unsaturated acyl chains distribute preferentially into micelles, whereas vesicles are enriched in disaturated PC species, supposedly due to packing constraints with more efficient packing of disaturated PC species in vesicles (37). Similarly, differences in packing constraints in small unilamellar vs aggregated vesicles (38) may explain their different phospholipid composition.

Another factor of potential relevance may be the much higher gel to liquid crystalline phase transition temperature (T_m) for SM compared to EYPC: whereas EYPC has a T_m below 0 °C (39), we found T_m of hydrated EYSM to be 36.6 °C, similar to previous data (39). The slightly lower T_m (33.6 °C) for hydrated BMSM (not studied before) is not unexpected, since in general, T_m decreases with increasing chain length (39). Pure phospholipids exist in a solid, ordered gel phase below a melting temperature (T_m) that is characteristic of each lipid, and in a

liquid disordered (also called "liquid crystalline") phase above T_m . In contrast, in the presence of cholesterol, lipids with a high T_m in the pure state (e.g. disaturated PC species and sphingomyelins) may form a so-called "liquid-ordered" phase around T_m (40-42). This liquid-ordered phase has properties intermediate between the gel and liquid-crystalline phases: Like the gel phase, the liquid-ordered phase is characterized by tight acyl-chain packing and relatively extended acyl chains. On the other hand, like lipids in the liquid-crystalline phase, lipids in the liquid-ordered phase exhibit relatively rapid lateral mobility within the bilayer. Recent data indicate that in bilayers containing more than one phospholipid, in the presence of cholesterol, phase separation of the phospholipids with the higher T_m (such as SM) into cholesterol-rich liquid-ordered domains occurs, and that such a phase separation is a prerequisite for detergent-resistance (41,42). We propose that SM in cholesterol-rich liquid ordered domains is relatively resistant to the micellizing effects of detergent bile salts, thus explaining asymmetric PC and SM distribution as found in the present study.

There is some evidence that monomeric and simple micellar rather than mixed micellar (i.e. phospholipid-associated) bile salts exert the detergent effect on membrane bilayers (43). However, we did not find an effect of varying phospholipid species on intermixed micellar/vesicular (IMC: i.e. simple micellar + monomeric) bile salt concentrations or micellar sizes. In agreement with previous data, micellar sizes were larger (44) and IMC values were lower (27) at increasing phospholipid contents. The absence of any change in IMC values when vesicles were formed by inclusion of cholesterol in the system is in agreement with a previous report of Donovan et al. (27). These findings suggest that enhanced resistance to bile salt dissolution for cholesterol-enriched membranes as reported in this and previous studies (45) is due to intrinsic

properties of the membranes rather than to alterations of the IMC (43).

The pivotal role of cholesterol is also dramatically illustrated by the incubation experiments shown in Figure 6. In agreement with previous data (46), in the absence of cholesterol, vesicles composed with SM were highly sensitive to detergent bile salts. Incorporation of cholesterol restored membrane resistance against detergent bile salts and even led in some cases to vesicle aggregation (33). Vesicles without cholesterol were only slightly smaller than vesicles with cholesterol. Nevertheless, we cannot definitely exclude the possibility that reduced interactions between phospholipid molecules, due to increased curvature strain (16,17,47,48) could explain decreased stability of the vesicles without cholesterol.

In the present study, effects of cholesterol inclusion on vesicle aggregation or asymmetric distribution of PC and SM tended to be more pronounced in EYSM- than in BMSM- containing systems, possibly related to different acyl chain composition and/or to subtle differences in physical state due to different T_m of EYSM and BMSM. We (20) and others (15) have found in vesicle-transfer experiments evidence for a higher affinity of cholesterol for EYSM than for SM that contains long-chain fatty acids such as BMSM.

Pathophysiological correlations

The findings in the present study may be relevant for epithelial cells in general, which contain large amounts of glycosphingolipids in the apical membrane (49). We were particularly interested to increase insight in some puzzling events occurring at the canalicular membrane during nascent bile formation. Since the hepatocyte –another highly polarized cell- is enriched at the canalicular side in cholesterol and SM with long saturated acyl chains (1,8-10), our data on BMSM with similar acyl chain

composition appear to be most relevant. The fact that PC is the major phospholipid secreted into bile, with only trace amounts of SM (6), despite the presence of large quantities of both phospholipids in the outer leaflet of the canalicular membrane (1,5) may relate to a high lateral pressure due to translocation of PC molecules by *mdr2* P-glycoprotein (2). No such protein is known to be present for SM. The present study indicates that the physical-chemical state of phospholipids in the canalicular membrane could also contribute to preferential PC secretion. The high cholesterol content of SM domains that are laterally segregated –perhaps in conjunction with disaturated PC species- might impede bile salt-dependent biliary secretion of SM. Furthermore, recent data by Nibbering and Carey (8) indicate that trace SM in bile contains mainly 16:0 acyl chains, despite the predominance of long acyl chains in canalicular membrane SM (8,9). Using ultracentrifugation, we found a strong preferential distribution of SM with long acyl chains in the “pelletable insoluble fraction” (according to the terminology of Schroeder (32)) and a preferential distribution of 16:0 SM in the “soluble supernatant”, which proved to contain mixed micelles and small unilamellar vesicles. By using electron microscopic techniques, Crawford has demonstrated the presence of significant amounts of such small unilamellar vesicles within the canalicular lumen, consistent with a vesicular mode of cholesterol and phospholipid secretion (4). Nevertheless, the finding that infusion of the hydrophobic bile salt taurodeoxycholate restores cholesterol secretion in the *mdr2* “knockout” mice to normal levels (50) would suggest a micellar mode of cholesterol secretion since PC is still virtually absent in this situation. When one considers our present data, there is a distinct possibility that vesicular and micellar modes of lipid secretion could coexist during nascent bile formation. As recently discussed by Oude Elferink (51,52), the non-linear

relationship between phospholipid and cholesterol secretion as recently found in mice with various expression of the *mdr2* gene is consistent with a micellar (or alternatively combined micellar + vesicular) but not with a pure vesicular mechanism of biliary lipid secretion.

Lastly, the inhibiting effects of cholesterol within the membrane on the amounts of phospholipids solubilized in micelles (Figure 1), would lead to the hypothesis that cholesterol in the canalicular membrane could exert a modulating role in regulation of biliary lipid secretion. For example, biliary secretion of NBD-sphingomyelin infused in isolated livers of *mdr2* “knockout” mice is strongly decreased compared to *mdr2* (+/+) mice, although SM should be the predominant phospholipid on the outer leaflet of the canalicular membrane in the absence of PC translocating activity in *mdr* “knockout” mice (Frijters, C., Groen, A.K., Oude Elferink, R.J., personal communication). This puzzling finding would be easily understood if one assumes inhibiting effects on biliary phospholipid secretion of an increased cholesterol content in the outer leaflet.

In conclusion, our data reveal preferential distribution of lipids and enrichment of SM with long saturated acyl chains in vesicular aggregates at increasing cholesterol content. In contrast, there is preferential distribution of PC into mixed micelles and small unilamellar vesicles under these circumstances. These findings may be relevant for canalicular bile formation.

References

1. Schachter, D. 1988. The hepatocyte plasma membrane: organization and differentiation, *In* The Liver: Biology and Pathobiology. I.M. Arias, W.B. Jakoby, H. Popper, D. Schachter, and D.A. Shafritz, editors. Raven Press, Ltd., New York, NY. 131-140.
2. Smit, J.J., A.H. Schinkel, R.P.J. Oude Elferink, A.K. Groen, E. Wagenaar, L. van Deemter, C.A. Mol, R. Ottenhoff, N.M. van der Lugt, and M.A. van Roon. 1993. Homozygous disruption of the murine *mdr2* P-glycoprotein gene leads to a complete absence of phospholipid from bile and to liver disease. *Cell*. **75**: 451-462.
3. Gerloff, T., B. Stieger, B. Hagenbuch, J. Madon, L. Landmann, J. Roth, A.F. Hofmann, and P.J. Meier. 1998. The sister of P-glycoprotein represents the canalicular bile salt export pump of mammalian liver. *J.Biol.Chem.* **273**: 10046-10050.
4. Crawford, J.M., G.M. Mockel, A.R. Crawford, S.J. Hagen, V.C. Hatch, S. Barnes, J.J. Godleski, and M.C. Carey. 1995. Imaging biliary lipid secretion in the rat: ultrastructural evidence for vesiculation of the hepatocyte canalicular membrane. *J.Lipid Res.* **36**: 2147-2163.
5. Higgins, J.A. and W.H. Evans. 1978. Transverse organization of phospholipids across the bilayer of plasma membrane subfractions of rat hepatocytes. *Biochem.J.* **174**: 563-567.
6. Alvaro, D., A. Cantafora, A.F. Attili, C.S. Ginanni, C. De Luca, G. Minervini, A. Di Biase, and M. Angelico. 1986. Relationships between bile salts hydrophilicity and phospholipid composition in bile of various animal species. *Comp.Biochem.Physiol.[B.]*. **83**: 551-554.
7. Hay, D.W., M.J. Cahalane, N. Timofeyeva, and M.C. Carey. 1993. Molecular species of lecithins in human gallbladder bile. *J.Lipid Res.* **34**: 759-768.
8. Nibbering, C.P. and M.C. Carey. 1999. Sphingomyelins of rat liver: biliary enrichment with molecular species containing 16:0 fatty acids as compared to canalicular-enriched plasma membranes. *J.Membr.Biol.* **167**: 165-171.
9. van Hoesven, R.P., P. Emmelot, J.H. Krol, and E.P.M. Oomen-Meulemans. 1975. Studies on plasma membranes. XXII. Fatty acid profiles of lipid classes in plasma membranes of rat and mouse livers and hepatomas. *Biochim.Biophys.Acta.* **380**: 1-11.
10. Kremmer, T., M.H. Wisher, and W.H. Evans. 1976. The lipid composition of plasma membrane subfractions originating from the three major functional domains of the rat hepatocyte cell surface. *Biochim.Biophys.Acta.* **455**: 655-664.
11. Lund-Katz, S., H.M. Laboda, L.R. McLean, and M.C. Phillips. 1988. Influence of molecular packing and phospholipid type on rates of cholesterol exchange.

- Biochemistry*. **27**: 3416-3423.
12. Lange, Y., J.S. D'Alessandro, and D.M. Small. 1979. The affinity of cholesterol for phosphatidylcholine and sphingomyelin. *Biochim.Biophys.Acta*. **556**: 388-398.
 13. Slotte, J.P. 1992. Enzyme-catalyzed oxidation of cholesterol in mixed phospholipid monolayers reveals the stoichiometry at which free cholesterol clusters disappear. *Biochemistry*. **31**: 5472-5477.
 14. Demel, R.A., J.W.C.M. Jansen, P.W.M. Van Dijke, and L.L.M. Van Deenen. 1977. The preferential interaction of cholesterol with different classes of phospholipids. *Biochim.Biophys.Acta*. **465**: 1-10.
 15. Bar, L.K., Y. Barenholz, and T.E. Thompson. 1987. Dependence on phospholipid composition of the fraction of cholesterol undergoing spontaneous exchange between small unilamellar vesicles. *Biochemistry*. **26**: 5460-5465.
 16. Yeagle, P.L. and J.E. Young. 1986. Factors contributing to the distribution of cholesterol among phospholipid vesicles. *J.Biol.Chem*. **261**: 8175-8181.
 17. Fugler, L., S. Clejan, and R. Bittman. 1985. Movement of cholesterol between vesicles prepared with different phospholipids or sizes. *J.Biol.Chem*. **260**: 4098-4102.
 18. Mattjus, P., R. Bittman, C. Vilcheze, and J.P. Slotte. 1995. Lateral domain formation in cholesterol/phospholipid monolayers as affected by the sterol side chain conformation. *Biochim.Biophys.Acta*. **1240**: 237-247.
 19. Hakomori, S. 1983. Chemistry of Glycosphingolipids, *In Handbook of Lipid Research*. D.J. Hanahan, editor. Plenum Press, New York, 37-39.
 20. van Erpecum, K.J. and M.C. Carey. 1997. Influence of bile salts on molecular interactions between sphingomyelin and cholesterol: relevance to bile formation and stability. *Biochim.Biophys.Acta*. **1345**: 269-282.
 21. Renooij, W., P.J. van Gaal, K.J. van Erpecum, B.J.M. van de Heijning, and G.P. vanBerge-Henegouwen. 1996. Quantifying vesicle/mixed micelle partitioning of phosphatidylcholine in model bile by using radiolabeled phosphatidylcholine species. *J.Lab.Clin.Med*. **128**: 561-567.
 22. Turley, S.D. and J.M. Dietschy. 1978. Reevaluation of the 3 α -hydroxysteroid dehydrogenase assay for total bile acids in bile. *J.Lipid Res*. **19**: 924-928.
 23. Cohen, D.E., M. Angelico, and M.C. Carey. 1989. Quasielastic light scattering evidence for vesicular secretion of biliary lipids. *Am.J.Physiol*. **257**: G1-G8.
 24. Rouser, G., S. Fleischer, and A. Yamamoto. 1970. Two dimensional thin layer chromatographic separation of polar lipids and determination of phospholipids by phosphorus analysis of spots. *Lipids*. **5**: 494-496.
 25. Rossi, S.S., J.L. Converse, and A.F. Hofmann. 1987. High pressure liquid chromatographic analysis of conjugated bile acids in human bile: simultaneous

- resolution of sulfated and unsulfated lithocholyl amidates and the common conjugated bile acids. *J.Lipid Res.* **28**: 589-595.
26. Bligh, E.G. and W.J. Dyer. 1959. A rapid method of total lipid extraction and purification. *Can.J.Biochem.Physiol.* **37**: 911-917.
 27. Donovan, J.M., N. Timofeyeva, and M.C. Carey. 1991. Influence of total lipid concentration, bile salt:lecithin ratio, and cholesterol content on inter-mixed micellar/vesicular (non-lecithin-associated) bile salt concentrations in model bile. *J.Lipid Res.* **32**: 1501-1512.
 28. Donovan, J.M. and A.A. Jackson. 1993. Rapid determination by centrifugal ultrafiltration of inter-mixed micellar/vesicular (non-lecithin-associated) bile salt concentrations in model bile: influence of Donnan equilibrium effects. *J.Lipid Res.* **34**: 1121-1129.
 29. Eckhardt, E.R.M., B.J.M. van de Heijning, K.J. van Erpecum, W. Renooij, and G.P. vanBerge-Henegouwen. 1998. Quantitation of cholesterol-carrying particles in human gallbladder bile. *J.Lipid Res.* **39**: 594-603.
 30. Wang, D.Q.H. and M.C. Carey. 1996. Complete mapping of crystallization pathways during cholesterol precipitation from model bile: influence of physical-chemical variables of pathophysiologic relevance and identification of a stable liquid crystalline state in cold, dilute and hydrophilic bile salt-containing systems. *J.Lipid Res.* **37**: 606-630.
 31. Carey, M.C. 1988. Lipid solubilisation in bile, *In Bile acids in health and disease.* T.C. Northfield, R.P. Jazrawi, and P. Zentler-Munro, editors. Kluwer Acad Publ., London, 61-82.
 32. Schroeder, R.J., E. London, and D.A. Brown. 1994. Interactions between saturated acyl chains confer detergent resistance on lipids and glycosylphosphatidylinositol (GPI)-anchored proteins: GPI- anchored proteins in liposomes and cells show similar behavior. *Proc.Natl.Acad.Sci.U.S.A.* **91**: 12130-12134.
 33. Luk, A.S., E.W. Kaler, and S.P. Lee. 1997. Structural mechanisms of bile salt-induced growth of small unilamellar cholesterol-lecithin vesicles. *Biochemistry.* **36**: 5633-5644.
 34. Yousef, I.M. and M.M. Fisher. 1976. In vitro effect of free bile acids on the bile canalicular membrane phospholipids in the rat. *Can.J.Biochem.* **54**: 1040-1046.
 35. Gerloff, T., P.J. Meier, and B. Stieger. 1998. Taurocholate induces preferential release of phosphatidylcholine from rat liver canalicular vesicles. *Liver.* **18**: 306-312.
 36. Billington, D., R. Coleman, and Y.A. Lusak. 1977. Topographical dissection of sheep erythrocyte membrane phospholipids by taurocholate and glycocholate. *Biochim.Biophys.Acta.* **466**: 526-530.
 37. Cohen, D.E. and M.C. Carey. 1991. Acyl chain unsaturation modulates

- distribution of lecithin molecular species between mixed micelles and vesicles in model bile. Implications for particle structure and metastable cholesterol solubilities. *J.Lipid Res.* **32**: 1291-1302.
38. Epand, R.M. 1998. Lipid polymorphism and protein-lipid interactions. *Biochim.Biophys.Acta.* **1376**: 353-368.
 39. Koynova, R. and M. Caffrey. 1995. Phases and phase transitions of the sphingolipids. *Biochim.Biophys.Acta.* **1255**: 213-236.
 40. Xiang, T.X. and B.D. Anderson. 1998. Phase structures of binary lipid bilayers as revealed by permeability of small molecules. *Biochim.Biophys.Acta.* **1370**: 64-76.
 41. Ahmed, S.N., D.A. Brown, and E. London. 1997. On the origin of Sphingolipid/Cholesterol-rich detergent-insoluble cell membranes: physiological concentrations of cholesterol and sphingolipid induce formation of a detergent-insoluble, liquid-ordered lipid phase in model membranes. *Biochemistry.* **36**: 10944-10953.
 42. Schroeder, R.J., S.N. Ahmed, Y. Zhu, E. London, and D.A. Brown. 1998. Cholesterol and sphingolipid enhance the triton X-100 insolubility of glycosylphosphatidylinositol-anchored proteins by promoting the formation of detergent-insoluble ordered membrane domains. *J.Biol.Chem.* **273**: 1150-1157.
 43. Donovan, J.M., A.A. Jackson, and M.C. Carey. 1993. Molecular species composition of inter-mixed micellar/vesicular bile salt concentrations in model bile: dependence upon hydrophilic-hydrophobic balance. *J.Lipid Res.* **34**: 1131-1140.
 44. Mazer, N.A., G.B. Benedek, and M.C. Carey. 1980. Quasielastic light-scattering studies of aqueous biliary lipid systems. Mixed micelle formation in bile salt-lecithin solutions. *Biochemistry.* **19**: 601-615.
 45. Cohen, D.E., M. Angelico, and M.C. Carey. 1990. Structural alterations in lecithin-cholesterol vesicles following interactions with monomeric and micellar bile salts: physical-chemical basis for subselection of biliary lecithin species and aggregative states of biliary lipids during bile formation. *J.Lipid Res.* **31**: 55-70.
 46. Schubert, R. and K.-H. Schmidt. 1988. Structural changes in vesicle membranes and mixed micelles of various lipid compositions after binding of different bile salts. *Biochemistry.* **27**: 8787-8794.
 47. McLean, L.R. and M.C. Phillips. 1984. Cholesterol transfer from small and large unilamellar vesicles. *Biochim.Biophys.Acta.* **776**: 21-26.
 48. Phillips, M.C., W.J. Johnson, and G.H. Rothblat. 1987. Mechanisms and consequences of cellular cholesterol exchange and transfer. *Biochim.Biophys.Acta.* **906**: 223-276.
 49. Simons, K. and G. van Meer. 1988. Lipid sorting in epithelial cells. *Biochemistry.* **27**: 6197-6202.

50. Oude Elferink, R.P.J., R. Ottenhoff, M. van Wijland, C.M. Frijters, C. van Nieuwkerk, and A.K. Groen. 1996. Uncoupling of biliary phospholipid and cholesterol secretion in mice with reduced expression of mdr2 P-glycoprotein. *J.Lipid Res.* **37**: 1065-1075.
51. Oude Elferink, R.P.J., G.N.J. Tytgat, and A.K. Groen. 1997. The role of mdr2 P-glycoprotein in hepatobiliary lipid transport. *FASEB J.* **11**: 19-28.
52. Smith, A.J., J.M. de Vree, R. Ottenhoff, R.P. Oude Elferink, A.H. Schinkel, and P. Borst. 1998. Hepatocyte-specific expression of the human MDR3 P-glycoprotein gene restores the biliary phosphatidylcholine excretion absent in Mdr2 (-/-) mice. *Hepatology.* **28**: 530-536.

chapter 5

**INCORPORATION OF CHOLESTEROL IN SPHINGOMYELIN-
EGG YOLK PHOSPHATIDYLCHOLINE VESICLES HAS
PROFOUND EFFECTS ON DETERGENT-INDUCED PHASE
TRANSITIONS:
A TIME-COURSE STUDY BY CRYO-TRANSMISSION
ELECTRON MICROSCOPY**

Antonio Moschetta, Peter M. Frederik, Piero Portincasa,
Gerard P. vanBerge-Henegouwen, Karel J. van Erpecum.

submitted

Abstract

Vesicle \leftrightarrow micelle transitions are important phenomena during bile formation and intestinal lipid processing. The hepatocyte canalicular membrane outer leaflet contains appreciable amounts of phosphatidylcholine (PC) and sphingomyelin (SM), and both phospholipids are found in the human diet. We therefore studied detergent-induced phase transitions in SM-PC vesicles. Methods: Phase transitions were evaluated by spectrophotometry and cryo-transmission electron microscopy (cryo-TEM) after addition of taurocholate (3-7 mM) to SM-PC vesicles (4 mM phospholipid, SM/PC 40%/60%, without or with 1.6 mM cholesterol). Results: After addition of excess (5-7 mM) taurocholate, SM-PC vesicles were more sensitive to micellization than PC vesicles. As shown by sequential cryo-TEM, addition of equimolar (4 mM) taurocholate to SM-PC vesicles induced formation of open vesicles, then (at the absorbance peak) multilamellar and fused vesicular structures coinciding with thread-like micelles, and finally transformation into a uniform picture with long thread-like micelles. Incorporation of cholesterol in the SM/PC bilayer changed initial vesicular shape from spherical into ellipsoid and profoundly increased detergent resistance. Disk-like micelles and multilamellar vesicles, and then extremely large vesicular structures were observed by sequential cryo-TEM under these circumstances, with persistently increased absorbance values by spectrophotometry. These findings may be relevant for bile formation and intestinal lipid processing.

Introduction

Micelle \leftrightarrow vesicle phase transitions have been studied extensively during the past decades for various reasons. For example, to incorporate membrane proteins into phospholipid vesicles, in general, mixed micelles containing surfactant, phospholipid and the protein of choice are first constructed, and functional insertion of the protein within the bilayer of the vesicles is subsequently obtained by inducing micelle \rightarrow vesicle transitions through removal of the surfactant. Also, several phase transitions occur during the process of bile secretion. Nascent bile within the canaliculus is generally believed to contain cholesterol-phospholipid vesicles (1). Upon progressive bile concentration in the bile ducts and in

the gallbladder, these vesicles are largely transformed into mixed bile salt-phospholipid-cholesterol micelles. During this process, cholesterol crystal formation (an essential step in gallstone formation) may occur in case of cholesterol supersaturated bile, possibly after aggregation of small unilamellar vesicles (2). Alternatively, primordial and multilamellar vesicles have been visualized by cryo transmission electron microscopy during the crystallization process (3-5).

After a meal, the gallbladder empties, and dilution of bile upon entering the intestine induces micelle → vesicle phase transitions. Enzymes within the intestinal lumen such as phospholipase A₂ may then induce the reverse process again with formation of open vesicles, bilayer fragments and micelles (6). The intermediate structures formed during vesicle → micelle transition, and the vesicles and micelles themselves, are thought to be important for optimal activities of various digestive enzymes, and for intestinal absorption of various lipids. Vesicle ↔ micelle transitions have therefore been studied in some detail by turbidity measurements (7;8), nuclear magnetic resonance (8;9) and cryo-transmission electron microscopy (10;11).

These studies were generally performed with phosphatidylcholine as the phospholipid (often with phosphatidylcholine from egg yolk, which contains 16:0 acyl chains at the *sn*-1 position and mainly unsaturated (18:1>18:2>20:4) acyl chains at the *sn*-2 position). Although phosphatidylcholine is the exclusive (>95%) phospholipid in human bile (with an acyl chain composition similar to egg yolk phosphatidylcholine (12)), considerable amounts of saturated phosphatidylcholines and sphingomyelins may occur in human food (13). Preliminary data in the mouse suggest that dietary sphingomyelins may reduce markedly intestinal cholesterol absorption (14). It should also be taken into account, that both phosphatidylcholine and sphingomyelin are the major

phospholipids of the hepatocyte canalicular membrane outer leaflet (15). Cholesterol has a high affinity for sphingomyelin (16-18) and is thought to be preferentially located together with this phospholipid in detergent-resistant rafts (19). We therefore studied effects of including sphingomyelin within egg yolk phosphatylcholine containing-vesicles (with and without cholesterol) on vesicle → micelle phase transitions by means of spectrophotometry and by sequential state-of-the-art cryo-transmission electron microscopy. Whereas previous electron microscopy studies were often prone to artefacts such as evaporation, advances in technology now avoid these caveats with the aid of temperature- and humidity-controlled conditions (37°C, 100% humidity, see “Methods”).

MATERIALS AND METHODS

Materials

Taurocholate was obtained from Sigma Chemical Co. (St. Louis, MO, USA) and yielded a single spot upon thin-layer chromatography (butanol-acetic acid-water, 10:1:1 vol/vol/vol, application of 200 µg bile salt). Cholesterol (Sigma) was ≥ 98% pure by reverse-phase HPLC (isopropanol - acetonitril 1:1, vol/vol, detection at 210 nm). Phosphatidylcholine from egg-yolk (EYPC; Sigma), and sphingomyelin from egg-yolk (EYSM; Avanti Polar-Lipids Inc., Alabaster, AL, USA) yielded a single spot on thin-layer chromatography (chloroform-methanol-water 65:25:4, vol/vol/vol, application of 200 µg lipid). Acyl chain compositions as determined by gas-liquid chromatography (20) showed a preponderance of 16:0 acyl chains for EYSM. As shown by reverse-phase HPLC, EYPC contained mainly 16:0 acyl chains at the *sn*-1 position and mainly unsaturated (18:1>18:2>20:4) acyl chains at the *sn*-2 position, similar to phosphatidylcholine in human bile (12). All other chemicals and solvents were of ACS or reagent grade quality.

The enzymatic cholesterol assay kit was obtained from Boehringer (Mannheim, Germany), 3 α -hydroxysteroid dehydrogenase for the enzymatic measurement of bile salt concentrations (21) from Sigma. The reverse-phase C18 HPLC column was from Supelco (Supelcosil LC-18-DB, Supelco, Bellefonte, PA, USA).

Preparation of model systems

Lipid mixtures containing variable proportions of cholesterol, phospholipids (both from stock solutions in chloroform), or taurocholate (from stock solutions in methanol) were vortex-mixed and dried at 45°C under a mild stream of nitrogen and subsequently lyophilized during 24 hrs, before being dissolved in aqueous 0.15 M NaCl plus 3 mM NaN₃. Tubes were sealed with teflon-lined screw caps under a blanket of nitrogen to prevent lipid oxidation and vortex-mixed for 5 min followed by incubation at 37°C in the dark. The final mol percentages cholesterol, phospholipid and bile salt did not differ more than 1% from the intended mol percentages.

Lipid analysis

Phospholipid concentrations in model systems were assayed by determining inorganic phosphate according to Rouser (22). Cholesterol concentrations were determined with an enzymatic assay (23), and bile salts with the 3 α -hydroxysteroid dehydrogenase method (21).

Preparation of small unilamellar vesicles

Small unilamellar vesicles were prepared by sonication. Lipids, from stock-solutions in chloroform, were vortex-mixed, dried under a mild stream of nitrogen and subsequently lyophilized during 24 hrs. The lipid film was dissolved in nitrogen-flushed aqueous 0.15 M NaCl plus 3 mM

NaN₃, and thereafter, the suspensions were probe-sonicated during 30 min. at 50°C (above the main transition temperatures of the phospholipids). After sonication, the suspension was centrifuged during 30 min. at 50000 x g at 40°C, in order to remove potential remaining vesicular aggregates and titanium particles. The resulting small unilamellar vesicles were stored at temperatures above 40°C, and used within 24 hrs. Small unilamellar vesicles were prepared with 100% PC, or SM 40% / PC 60% as the phospholipid. Final phospholipid concentration was 4 mM. Vesicles were either prepared without or with cholesterol (cholesterol / phospholipid ratio 0 or 0.4).

Interactions of small unilamellar vesicles with taurocholate

Interactions of small unilamellar vesicles with various taurocholate solutions (final concentrations varying between 3 and 7 mM) were followed by measuring optical density (OD) at 405 nm every min. during 80 min. at 37°C, in a thermostated Benchmark microplate reader (BioRad, Hercules, CA, USA). The solutions were stirred for 3 seconds prior to each measurement. During this period, the time course of various phase transitions was visualized by performing cryo-transmission electron microscopy at several time points during the incubation. In the case of cholesterol-containing vesicles, at the end of the incubation, the mixtures were also examined by polarizing light microscopy, in order to examine whether liquid or solid cholesterol crystals had formed.

Cryo-transmission electron microscopy (cryo-TEM): sample preparation for cryo-TEM was done in a temperature and humidity controlled chamber using a fully automated (pc-controlled) vitrification robot (Vitrobot, patent applied). This system was recently developed in collaboration with one of the authors (PMF) based on the work by Bellare et al. (24) and Frederik et al. (25). Within an environmental

chamber (temperature controlled and equipped with an ultrasonic device generating a mist to attain a relative humidity of ~100%), a specimen grid is dipped into a suspension, withdrawn and excess liquid is blotted away between two filter papers backed by foam pads. Thin films are formed between the bars of the grid, and to vitrify these thin films, the grid is ‘shot’ into melting ethane placed just outside the chamber and accessed through a shutter. Once a thin film is formed, it has a large surface to volume ratio, which makes heat and mass exchange fast processes. About dew point temperature will be attained in 0.1 sec. and further evaporation may be substantial at this point. At normal room conditions (24 °C, 40% relative humidity) a thin film may lose 50% of its water within 2 seconds and osmotic effects therefore have to be considered when not working at a 100% relative humidity (see also Hubert et al. and Frederik et al., Conference proceedings EUREM Brno 2000 and submitted). All the experiments are conducted at 37 °C with 100% relative humidity.

When the vitrification robot is set up (vial with suspension in place, filter papers mounted, all parameters set) a forceps with grid is loaded from outside and melting ethane is prepared and for the rest the preparation/vitrification process runs automatically under PC command to end with a grid in melting ethane. The grids with vitrified thin films were analysed in a CM-12 transmission microscope (Philips, Eindhoven, The Netherlands) at -170°C using a Gatan-626 cryo-specimen holder and cryo-transfer system (Gatan, Warrendale, PA/ USA). The vitrified films were studied at 120 kV with a pressure lower than 0.2×10^{-3} Pa., and at standard low-dose conditions, micrographs were taken.

RESULTS

Resistance of phospholipid vesicles against detergent bile salts in the absence of cholesterol

As shown in Figure 1A-C, vesicles without cholesterol and containing PC as the sole phospholipid tended to be rather resistant against the detergent effects of taurocholate, as indicated by the relatively slow decrease of absorption values during the time period studied (conditions: vesicular phospholipid 4 mM final concentration, addition of taurocholate at 7-5 mM final concentration, 37°C). Partial replacement of vesicular PC by SM, without inclusion of cholesterol, led to significant vesicular destabilization, as evidenced by low absorption values upon addition of taurocholate. Figures 1D-E show the results obtained upon incubation of the same vesicle population with progressively decreasing concentrations of taurocholate. At taurocholate concentration of 4 mM (Fig. 1D) added to PC-containing vesicles, a small increase of the absorbance can be observed. In case of SM-PC vesicles, there is a large but reversible increase of absorbance after addition of 4 mM taurocholate. After addition of taurocholate at a concentration of 3 mM (Fig. 1E), increased absorbance appears not to be reversible during the experiment, especially in case of SM-PC vesicles.

In Figure 2, the time-course of SM-PC vesicle → micelle transitions after addition of equimolar (4 mM) taurocholate is visualized by sequential cryo-transmission electron microscopy (TEM). Initial vesicles before addition of the detergent are spherical (Fig. 2A: time point a in Fig. 1D). During the uphill part of the absorbance curve (time point b in Fig. 1D), multiple open vesicles coexist with globular micelles. Maximal vesicular sizes have increased from 60 nm to 100 nm diameter (Fig. 2B). At the absorbance peak (time point c in Fig. 1D), globular micelles,

multilamellar and fused vesicular structures are present. Vesicles have further increased in size. Also, at this time point, some thread-like micelles have formed (Fig 2C). During the downhill part of the absorbance curve (time point d in Fig 1D: results not shown) and at the end of the experiment (time point e in Fig 1D), an uniform picture of long thread-like micelles is present (Fig 2D). In contrast, cryo-TEM after addition of excess (7 mM) taurocholate to SM-PC vesicles revealed globular micelles at the end of the experiment (time point a in Fig. 1A: results not shown).

Resistance of cholesterol-containing phospholipid vesicles against detergent bile salts

As shown in Figure 3A, incorporation of cholesterol in SM-PC vesicles prevents the destabilizing effect of SM (conditions: vesicular phospholipid 4 mM final concentration; vesicular SM/PC 40%/60%; vesicular cholesterol/phospholipid ratio 0.4; addition of taurocholate at 7 mM final concentration; 37°C). Absorbances of these cholesterol-enriched vesicles were stable in case of PC as the sole vesicular phospholipid, but increased markedly in the case of incorporation of SM in the vesicles. The same happened with incubation at lower taurocholate concentrations (6 mM, 5mM, 4mM and 3 mM; figures 2B, 2C, 2D and 2E, resp.).

Figure 1

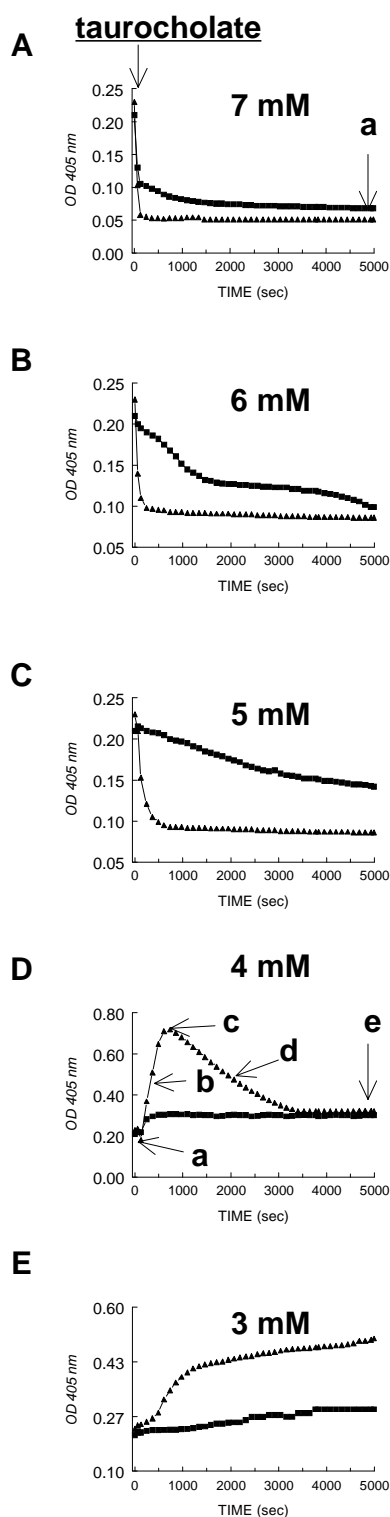


Figure 1: Effects of taurocholate on sonicated small unilamellar vesicles without cholesterol, composed with 100% PC or with 40% of PC replaced by SM (final phospholipid conc. 4 mM, 37°C). As shown by the decrease of absorbance values (OD 405nm), in case of excess taurocholate, vesicles exhibit enhance sensitivity to detergent when SM is also included in the bilayer. (final taurocholate conc. 7mM, 6mM and

5mM, **A**, **B** and **C**, resp.). At lower taurocholate concentrations (4 mM in **D**; 3 mM in **E**) an increase of the absorbance values can be observed. ■ = EYPC; ▲ = EYSM.

Figure 2

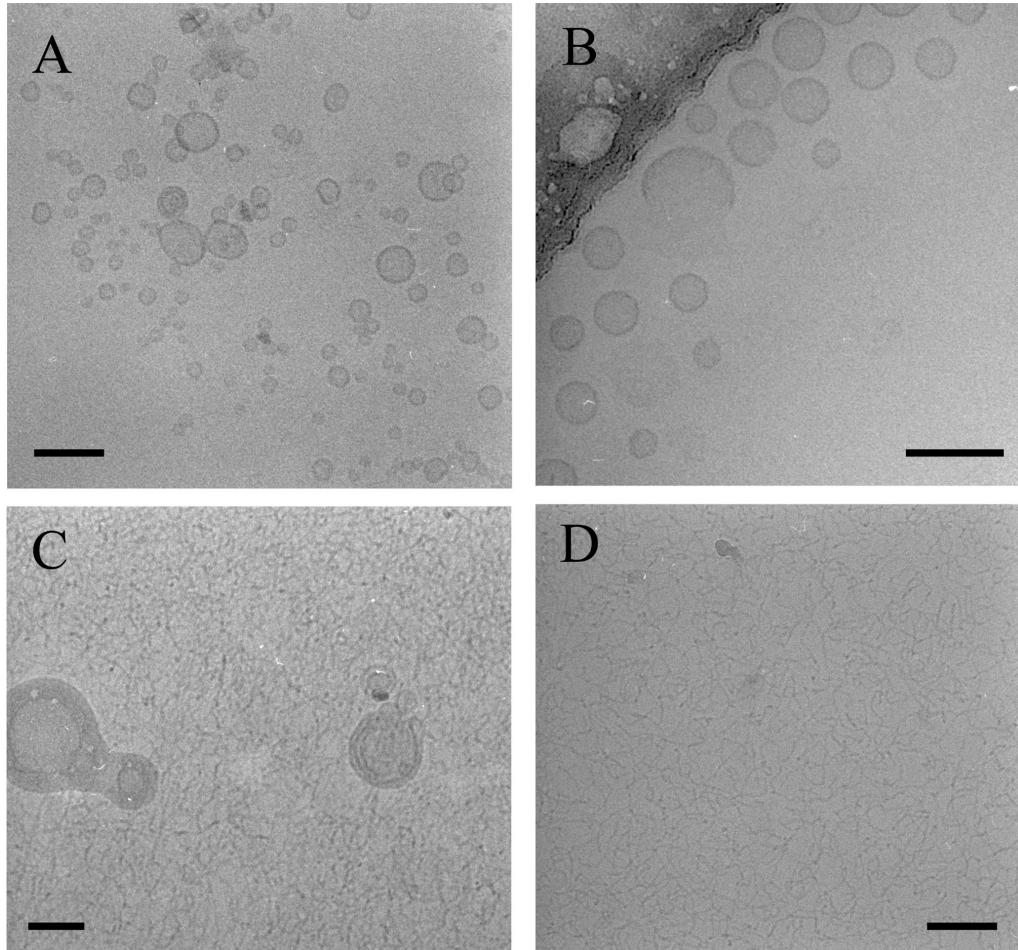


Figure 2: Cryo-transmission electron microscopic images after addition of equimolar taurocholate (4 mM final conc.) to sonicated small unilamellar vesicles composed with 40% SM and 60% PC without cholesterol (final phospholipid conc. 4 mM, preparation at 37°C, 100% relative humidity). **A:** Sphere-like vesicles (max size ~ 60 nm) at initiation of the experiment (time point a in Fig. 1D). **B:** during the uphill part of the absorbance curve (time point b in Fig. 1D), there are some open vesicles (max size ~ 100 nm). **C:** at the absorbance peak (time point c in Fig. 1D), multilamellar and fused vesicles (max size < 290 nm), globular and thread-like micelles are present. **D:** at the end of experiment, there are large numbers of “thread”-like micelles (time point e in Fig. 1D).

Bar represents 100 nm.

In Figure 4, the time-course of phase transitions after addition of 4 mM taurocholate to cholesterol-containing SM-PC vesicles is followed by sequential cryo-TEM. As shown in Figure 4A, initial vesicles often appear ellipsoid (time point a in Fig. 3D). During the uphill part of the absorbance curve (time point b in Fig. 3D), large numbers of multilamellar vesicles are observed, together with disk-like micelles (Fig. 4B). At the end of the experiments (time point c in Fig. 3D), extremely large vesicular structures are present, precluding adequate visualization by electron microscopy. Concomitant light microscopy revealed numerous aggregated and fused large vesicular structures.

DISCUSSION

The present study points to a key role of cholesterol in formation of pathophysiologically relevant phosphatidylcholine plus sphingomyelin-containing bilayers and in modulating interactions between those vesicles and detergent bile salts. We have obtained a time-course of bile salt-induced phase transitions with the aid of state-of-the-art cryo-TEM. By vitrification from 37°C with 100% relative humidity, osmotic and temperature-induced artefacts are prevented, thus allowing observation of lipid-rich structures close to their original state: at the moment of vitrification by ultra-rapid cooling (10^{-5} sec.), the vapour pressure reduces, all supramolecular motions are arrested, thereby preserving microstructures and avoiding any artifacts related to crystallization of water and other compounds (24;25).

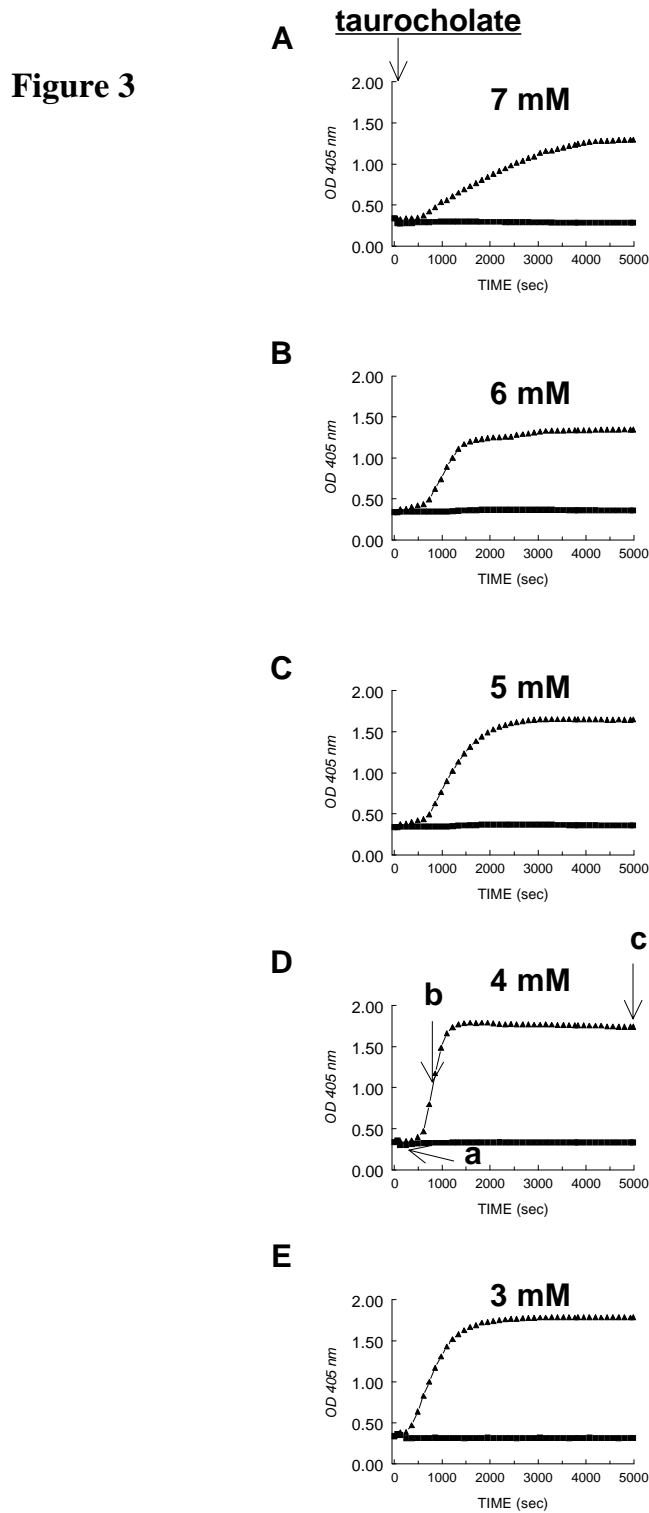


Figure 3: Effects of taurocholate on sonicated small unilamellar vesicles composed with fixed amounts of cholesterol (chol/PL ratio = 0.4) and with 100% PC or with 40% of PC replaced by SM (final phospholipid conc. 4 mM, 37°C). Incorporation of cholesterol prevents the destabilizing effects of SM (taurocholate final conc. 7 mM in A; 6 mM in B; 5 mM in C; 4 mM in D; 3 mM in E).

■ = EYPC; ▲ = EYSM.

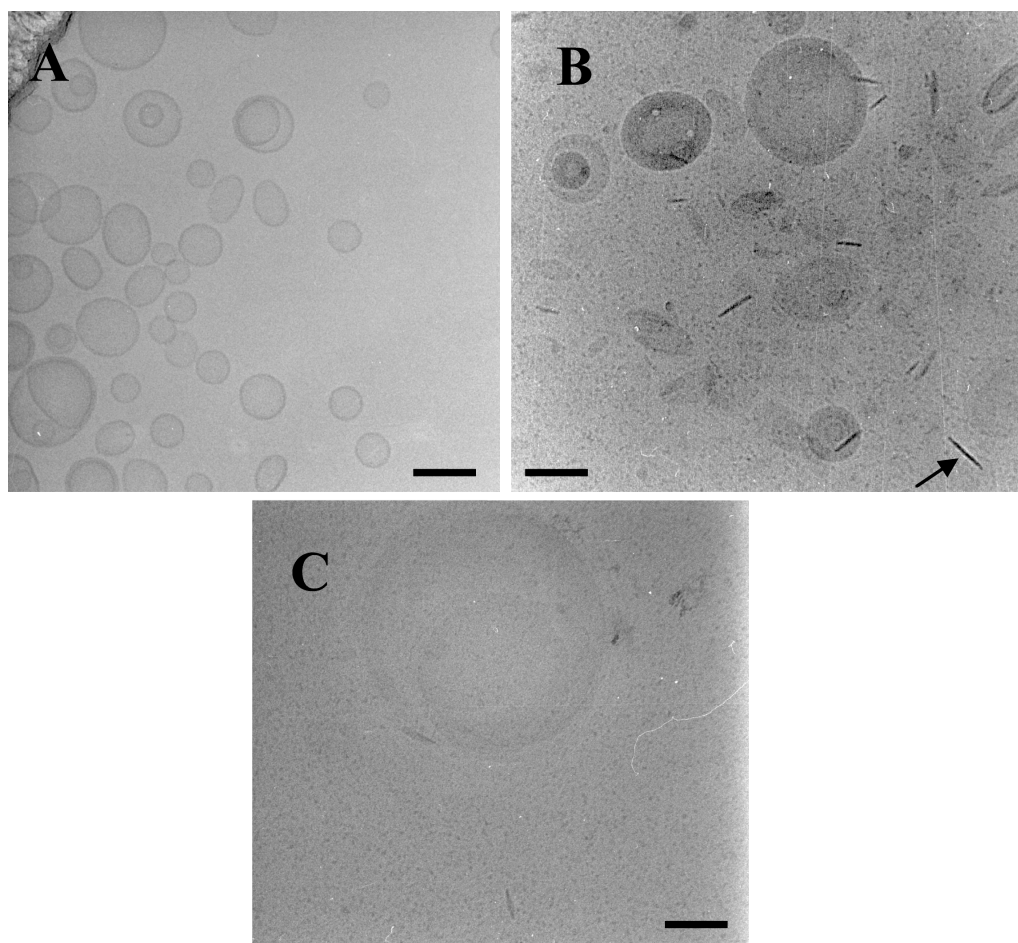
Figure 4

Figure 4: Cryo-transmission electron microscopy images after addition of taurocholate (4 mM final conc.) to sonicated small unilamellar SM-PC vesicles (final phospholipid conc. 4 mM, SM/PC ratio 40/60, chol/phospholipid ratio 0.4, 37°C, 100% humidity). **A:** Some vesicles have an ellipsoid shape at the initiation of the experiment (time point a in Fig. 3D). **B:** During the uphill part of the absorbance curve (time point b in Fig. 3D), large numbers of multilamellar vesicles are observed, together with disk-like micelles (arrows). **C:** At the end of the experiment (time point c in Fig. 3D), extremely large vesicular structures are present.

Bar represents 100 nm.

Previous studies have examined in detail phase transitions induced by addition of detergent to egg yolk phosphatidylcholine-containing vesicles or by dilution of micellar solutions, with formation of long cylindrical

micelles as intermediate structures (10;11;26;27). In the present study, we have focused on phase transitions of SM-EYPC vesicles –with or without cholesterol incorporated in the bilayer- after addition of various amounts of taurocholate. In the absence of cholesterol, and after addition of excess taurocholate (final taurocholate/phospholipid ratio >1), SM-containing vesicles exhibited increased sensitivity to the detergent, compared to vesicles composed exclusively with EYPC, as shown by spectrophotometry (Fig. 1A-C). These data are in line with previous reports (28-30). At equimolar taurocholate-phospholipid ratios, there was a strong but transient increase of absorbance values. Sequential cryo-transmission electron microscopy revealed in the early stages after addition of the detergent open vesicles, then (coinciding with the absorbance peak) multilamellar and fused vesicles and finally (coinciding with low absorption values) an uniform picture of thread-like micelles. Open vesicular structures that we visualized in the early stages after addition of the detergent have been described before (6) and may indicate initiation of transition toward micellar phases. Upon addition of low amounts of taurocholate (taurocholate/phospholipid ratio <1), increased absorbance values were not reversible during the experiment. After addition of excess taurocholate (taurocholate/phospholipid ratio >1), the resulting bile salt-phospholipid mixtures plot in the one-phase zone (only micelles) of the equilibrium ternary phase diagram (31;32) and vesicle → micelle transitions progress at extremely fast rates, thus precluding visualization of intermediate structures. In contrast, after addition of equimolar amounts of taurocholate (taurocholate/phospholipid ratio $=1$), resulting model systems plot near or at the border of the one-phase (micellar) zone and the right two-phase (micelles and vesicles-containing) zone (31;32), and vesicle → micelle transitions progress at slow rates, thus allowing visualization of intermediate structures.

Incorporation of cholesterol in the vesicular bilayer had profound effects on detergent-induced phase transitions. In the absence of the sterol, and in the earliest stages, spherical vesicles were visualized, but in presence of the sterol the vesicles often had an ellipsoid shape (Fig. 2A and 4A). The changes in bilayer two-dimensional conformation observed in presence of cholesterol may be due interactions between aliphatic chains of two sterol molecules (one in each monolayer) in cholesterol-sphingomyelin microdomains (33), thus inducing a local decrease in bilayer curvature. Interestingly, Crawford et al. (1;34) with the aid of electron microscopy could visualize in the bile canaliculi mostly ellipsoid non-spherical unilamellar vesicles, which probably contained cholesterol and phospholipid. It has been postulated that the non-spherical shapes of vesicles with decreased curvatures at the lateral sides may have relevance for interactions of cholesterol with detergent bile salts and subsequent solubilization in mixed micelles (34).

Sphingomyelin-phosphatidylcholine vesicles with cholesterol incorporated in the bilayers were highly resistant against detergent-induced micellar solubilization. Intermediate multilamellar vesicles, disk-like micelles and –at the end of the experiments- large vesicular aggregates were formed upon addition of the detergent. SM exhibits a much higher gel to liquid crystalline phase transition temperature (T_m) than EYPC: whereas EYPC has a T_m below 0 °C (35), we previously found T_m of hydrated EYSM to be 36.6 °C (30). Pure phospholipids exist in a solid, ordered gel phase below a melting temperature (T_m) that is characteristic of each lipid, and in a liquid disordered (also called "liquid crystalline") phase above T_m . Note that the T_m of EYSM is close to the incubation temperature in our experiments including preparation for cryo-EM. For this lipid species it is particularly essential to attain 100% humidity (as in the present study) during cryo-preparation to prevent a

temperature drop (“dew-point” effect) below T_m , which is known to change the shape of vesicles. The phase behaviour around T_m is influenced by presence of cholesterol: lipids with a high T_m in the pure state (e.g. disaturated PC species and sphingomyelins) may form a so called “liquid-ordered” phase around T_m (36-38). This liquid-ordered phase has properties intermediate between the gel and liquid-crystalline phases: Like in the gel phase, tight acyl-chain packing and relatively extended acyl chains characterize the liquid-ordered phase. On the other hand, like lipids in the liquid-crystalline phase, lipids in the liquid-ordered phase exhibit relatively rapid lateral mobility within the bilayer. Recent data indicate that in bilayers containing more than one phospholipid, in the presence of cholesterol, phase separation of the phospholipids with the higher T_m (such as SM) into cholesterol-rich liquid-ordered domains occurs, and that such a phase separation is a prerequisite for detergent-resistance (37;38). We propose that, when present together with cholesterol in liquid ordered domains, SM becomes relatively resistant to the micellizing effects of detergent bile salts.

In conclusion, we have shown that incorporation of sphingomyelin in egg yolk phosphatidylcholine vesicles enhances vesicle → micelle phase transitions, with formation of intermediate open, multilamellar and fused vesicular structures. When cholesterol is also included in the bilayer, sphingomyelin-egg yolk phosphatidylcholine vesicles appear resistant against bile salt-induced micellar solubilization. Instead, multilamellar and large aggregated vesicles are formed. These findings may have implications for canalicular bile formation and intestinal lipid solubilization.

References

1. Crawford JM, Mockel GM, Crawford AR, Hagen SJ, Hatch VC, Barnes S et al. Imaging biliary lipid secretion in the rat: ultrastructural evidence for vesiculation of the hepatocyte canalicular membrane. *J Lipid Res* 1995; 36:2147-2163.
2. Halpern Z, Dudley MA, Kibe A, Lynn MP, Breuer AC, Holzbach RT. Rapid vesicle formation and aggregation in abnormal human bile. A time-lapse video enhanced contrast microscopy study. *Gastroenterology* 1986; 90:875-885.
3. Kaplun A, Talmon Y, Konikoff FM, Rubin M, Eitan A, Tadmor M et al. Direct visualization of lipid aggregates in native human bile by light- and cryo-transmission electron-microscopy. *FEBS Lett* 1994; 340:78-82.
4. Konikoff FM, Danino D, Weihs D, Rubin M, Talmon Y. Microstructural evolution of lipid aggregates in nucleating model and human bile visualized by cryogenic transmission electron microscopy. *Hepatology* 2000; 31:261-268.
5. Gantz DL, Wang DQ, Carey MC, Small DM. Cryoelectron microscopy of a nucleating model bile in vitreous ice: formation of primordial vesicles. *Biophys J* 1999; 76:1436-1451.
6. Callisen TH, Talmon Y. Direct imaging by cryo-TEM shows membrane break-up by phospholipase A2 enzymatic activity. *Biochemistry* 1998; 37:10987-10993.
7. Almog S, Kushnir T, Nir S, Lichtenberg D. Kinetic and structural aspects of reconstitution of phosphatidylcholine vesicles by dilution of phosphatidylcholine-sodium cholate mixed micelles. *Biochemistry* 1986; 25:2597-2605.
8. Lichtenberg D, Zilberman Y, Greenzaid P, Zamir S. Structural and kinetic studies on the solubilization of lecithin by sodium deoxycholate. *Biochemistry* 1979; 18:3517-3525.
9. Almog S, Litman BJ, Wimley W, Cohen J, Wachtel EJ, Barenholz Y et al. States of aggregation and phase transformations in mixtures of phosphatidylcholine and octyl glucoside. *Biochemistry* 1990; 29:4582-4592.
10. Walter A, Vinson PK, Kaplun A, Talmon Y, Vlahcevic ZR. Intermediate structures in the cholate-phosphatidylcholine vesicle-micelle transition. *Biophys J* 1991; 60:1315-1325.
11. Vinson PK, Talmon Y, Walter A. Vesicle-micelle transition of phosphatidylcholine and octyl glucoside elucidated by cryo-transmission electron microscopy. *Biophys J* 1989; 56:669-681.
12. Hay DW, Cahalane MJ, Timofeyeva N, Carey MC. Molecular species of lecithins in human gallbladder bile. *J Lipid Res* 1993; 34:759-768.

13. Parodi PW. Cows' milk fat components as potential anticarcinogenic agents. *J Nutr* 1997; 127:1055-1060.
14. Eckhardt ERM, Wang DQH, Donovan JM, Carey MC. Dietary sphingomyelin (SM) significantly inhibits intestinal cholesterol absorption by lowering thermodynamic activity (TA) of Ch in bile salt mixed micellar solution. *Gastroenterology* 2001; 120:A-679.
15. Kremmer T, Wisner MH, Evans WH. The lipid composition of plasma membrane subfractions originating from the three major functional domains of the rat hepatocyte cell surface. *Biochim Biophys Acta* 1976; 455:655-664.
16. Lund-Katz S, Laboda HM, McLean LR, Phillips MC. Influence of molecular packing and phospholipid type on rates of cholesterol exchange. *Biochemistry* 1988; 27:3416-3423.
17. Bar LK, Barenholz Y, Thompson TE. Dependence on phospholipid composition of the fraction of cholesterol undergoing spontaneous exchange between small unilamellar vesicles. *Biochemistry* 1987; 26:5460-5465.
18. Mattjus P, Bittman R, Vilcheze C, Slotte JP. Lateral domain formation in cholesterol/phospholipid monolayers as affected by the sterol side chain conformation. *Biochim Biophys Acta* 1995; 1240:237-247.
19. Schroeder RJ, London E, Brown DA. Interactions between saturated acyl chains confer detergent resistance on lipids and glycosylphosphatidylinositol (GPI)-anchored proteins: GPI- anchored proteins in liposomes and cells show similar behavior. *Proc Natl Acad Sci U S A* 1994; 91:12130-12134.
20. Hakomori S. Chemistry of Glycosphingolipids. In: Hanahan DJ, editor. *Handbook of Lipid Research*. New York: Plenum Press, 1983: 37-39.
21. Turley SD, Dietschy JM. Reevaluation of the 3 α -hydroxysteroid dehydrogenase assay for total bile acids in bile. *J Lipid Res* 1978; 19:924-928.
22. Rouser G, Fleischer S, Yamamoto A. Two dimensional thin layer chromatographic separation of polar lipids and determination of phospholipids by phosphorus analysis of spots. *Lipids* 1970; 5:494-496.
23. Fromm H, Hamin P, Klein H, Kupke I. Use of a simple enzymatic assay for cholesterol analysis in human bile. *J Lipid Res* 1980; 21:259-261.
24. Bellare JR, Davis HT, Scriven LE, Talmon Y. Controlled environment vitrification system: an improved sample preparation technique. *J Electron Microscop Tech* 1988; 10:87-111.
25. Frederik PM, Stuart MC, Bomans PH, Busing WM, Burger KN, Verkleij AJ. Perspective and limitations of cryo-electron microscopy. From model systems to biological specimens. *J Microsc* 1991; 161:253-262.
26. Long MA, Kaler EW, Lee SP. Structural characterization of the micelle-vesicle transition in lecithin-bile salt solutions. *Biophys J* 1994; 67:1733-1742.

27. Cohen DE, Thurston GM, Chamberlin RA, Benedek GB, Carey MC. Laser light scattering evidence for a common wormlike growth structure of mixed micelles in bile salt- and straight-chain detergent-phosphatidylcholine aqueous systems: relevance to the micellar structure of bile. *Biochemistry* 1998; 37:14798-14814.
28. Schubert R, Schmidt K-H. Structural changes in vesicle membranes and mixed micelles of various lipid compositions after binding of different bile salts. *Biochemistry* 1988; 27:8787-8794.
29. Moschetta A, vanBerge-Henegouwen GP, Portincasa P, Palasciano G, Groen AK, van Erpecum KJ. Sphingomyelin exhibits greatly enhanced protection compared with egg yolk phosphatidylcholine against detergent bile salts. *J Lipid Res* 2000; 41:916-924.
30. Eckhardt ERM, Moschetta A, Renooij W, Goerdal SS, vanBerge-Henegouwen GP, van Erpecum K.J. Asymmetric distribution of phosphatidylcholine and sphingomyelin between micellar and vesicular phases: potential implication for canalicular bile formation. *J Lipid Res* 1999; 40:2022-2033.
31. Wang DQH, Carey MC. Complete mapping of crystallization pathways during cholesterol precipitation from model bile: influence of physical-chemical variables of pathophysiologic relevance and identification of a stable liquid crystalline state in cold, dilute and hydrophilic bile salt-containing systems. *J Lipid Res* 1996; 37:606-630.
32. Van Erpecum KJ, Carey MC. Influence of bile salts on molecular interactions between sphingomyelin and cholesterol: relevance to bile formation and stability. *Biochim Biophys Acta* 1997; 1345:269-282.
33. Sankaram MB, Thompson TE. Cholesterol-induced fluid-phase immiscibility in membranes. *Proc Natl Acad Sci USA* 1991; 88:8686-8690.
34. Crawford AR, Smith AJ, Hatch VC, Oude Elferink RPJ, Borst P, Crawford JM. Hepatic secretion of phospholipid vesicles in the mouse critically depends on *mdr2* or *MDR3* P-glycoprotein expression. Visualization by electron microscopy. *J Clin Invest* 1997; 100:2562-2567.
35. Koynova R, Caffrey M. Phases and phase transitions of the sphingolipids. *Biochim Biophys Acta* 1995; 1255:213-236.
36. Xiang TX, Anderson BD. Phase structures of binary lipid bilayers as revealed by permeability of small molecules. *Biochim Biophys Acta* 1998; 1370:64-76.
37. Ahmed SN, Brown DA, London E. On the origin of Sphingolipid/Cholesterol-rich detergent-insoluble cell membranes: physiological concentrations of cholesterol and sphingolipid induce formation of a detergent-insoluble, liquid-ordered lipid phase in model membranes. *Biochemistry* 1997; 36:10944-10953.

38. Schroeder RJ, Ahmed SN, Zhu Y, London E, Brown DA. Cholesterol and sphingolipid enhance the triton X-100 insolubility of glycosylphosphatidylinositol-anchored proteins by promoting the formation of detergent-insoluble ordered membrane domains. *J Biol Chem* 1998; 273:1150-1157.

chapter 6

**SPHINGOMYELIN EXHIBITS GREATLY ENHANCED
PROTECTION COMPARED WITH EGG YOLK
PHOSPHATIDYLCHOLINE AGAINST DETERGENT BILE SALTS**

Antonio Moschetta, Gerard P. vanBerge Henegouwen, Piero Portincasa,

Giuseppe Palasciano, Albert K. Groen, Karel J. van Erpecum.

Journal of Lipid Research 2000;41:916-924.

Abstract

Inclusion of phosphatidylcholine within bile salt micelles protects against bile salt-induced cytotoxicity. In addition to phosphatidylcholine, bile may contain significant amounts of sphingomyelin, particularly under cholestatic conditions. We compared protective effects of egg yolk phosphatidylcholine (similar to phosphatidylcholine in bile), egg yolk sphingomyelin (mainly 16:0 acyl chains) and dipalmitoyl phosphatidylcholine against taurocholate in complementary *in vitro* studies. Upon addition of taurocholate-containing micelles to sonicated egg yolk phosphatidylcholine vesicles, subsequent micellization of the vesicular bilayer proved to be retarded when phospholipids had also been included in these micelles in the rank order: egg yolk phosphatidylcholine < dipalmitoyl phosphatidylcholine < sphingomyelin. Hemolysis of erythrocytes and LDH release by CaCo-2 cells after addition of taurocholate micelles were strongly reduced by including small amounts of sphingomyelin or dipalmitoyl phosphatidylcholine in these micelles ($PL/(PL+BS) \geq 0.1$), whereas egg yolk phosphatidylcholine provided less protection. Amounts of non-phospholipid-associated bile salts (thought to be responsible for cytotoxicity) in egg yolk phosphatidylcholine-containing micelles were significantly higher than in corresponding sphingomyelin- or dipalmitoyl phosphatidylcholine-containing micelles (tested at PL/(PL+BS) ratios 0.1, 0.15 and 0.2). LDH release upon incubation of CaCo-2 cells with taurocholate simple micelles at these so-called "intermixed micellar-vesicular" concentrations was identical to LDH release upon incubation with corresponding taurocholate-phospholipid mixed micelles. In conclusion, we found greatly enhanced protective effects of sphingomyelin and dipalmitoyl phosphatidylcholine compared to egg yolk phosphatidylcholine against bile salt-induced cytotoxicity, related to different amounts of non-phospholipid-associated bile salts. These findings may be relevant for protection against bile salt-induced cytotoxicity *in vivo*.

INTRODUCTION

Bile salts are amphiphilic compounds that act as detergents above their critical micellar concentration. The cytotoxic effect of bile salts has been shown for hepatocytes (1,2), erythrocytes (2-4) and mucosa of various organs, including stomach (5), intestine (6) and gallbladder (7,8). The

damaging effects of bile salts depend on their degree of hydrophobicity (9) and on the cell membrane composition (10). At physiological concentrations, in bile in the gallbladder and bile ducts and within the intestinal lumen, bile salts are associated with phospholipids and cholesterol in mixed micellar structures. However, significant amounts of bile salts are also present under these conditions as monomers and as "simple" micelles (i.e. without incorporated phospholipids). There is some evidence that this so called "intermixed micellar-vesicular bile salt concentration" (IMC: bile salt monomers + simple micelles) (11), may be responsible for the potentially damaging effects on membrane bilayers (12,13). At the concentrations occurring in hepatic and gallbladder biles, bile salts could theoretically damage the apical membrane of the hepatocytes and of the cells lining the biliary tract. The absence of such a damaging effect *in vivo* suggests the existence of cytoprotective mechanisms either at the level of the cell membrane or within biliary micelles. Increased concentrations of cholesterol and phospholipids (in particular sphingomyelin) in the hepatocyte canalicular membrane appear to protect against cytotoxic effects of the bile salts within the canalicular lumen (14-16). On the other hand, in *in vitro* studies, inclusion of egg yolk phosphatidylcholine (PC) within bile salt micelles protects in a concentration-dependent manner against bile salt-induced cytotoxicity (17). In line with these findings, mice with homozygous disruption of the *mdr2* gene exhibit severe bile salt-induced hepatocyte damage *in vivo*: since *mdr2* encoded P-glycoprotein -which normally functions as a "flippase" transporting PC molecules from the inner to the outer leaflet of the hepatocytic canalicular membrane- is absent, there is virtually no PC protecting against bile salt-induced hepatotoxicity in bile of these mice (18).

Both PC and sphingomyelin (SM) are the major phospholipids of the canalicular membrane outer leaflet (16,19). Although PC is the major phospholipid species in *gallbladder* bile, with minor amounts of SM (20), larger quantities of SM could be present in nascent bile *within the canalicular lumen*, particularly under pathological conditions such as cholestasis. When, in the rat model, cholestasis is induced by bile salt infusion, there is a considerable increase of SM content, from 3% to $\leq 30\%$ of total phospholipids in bile (21). Also, an alkaline sphingomyelinase recently detected in human bile (22) could contribute to the virtual absence of SM in *gallbladder* bile under non-cholestatic conditions because of reabsorption by the bile duct epithelial cells of the hydrolytic product ceramide, which is more hydrophobic than SM (23). This hypothesis is supported by the fact that sheep, which secrete significant amounts of SM in their biles (20), exhibit no biliary sphingomyelinase activity (22).

In the present study we examined the protective effects of various phospholipids against detergent taurocholate in a number of complementary *in vitro* studies. We compared the effects of PC from egg yolk (EYPC, mainly 16:0 acyl chains at the *sn*-1 position and mainly unsaturated (18:1>18:2>20:4) acyl chains at the *sn*-2 position, similar to PC in human bile (24)), SM from egg yolk (EYSM, mainly 16:0 acyl chains, similar to SM in bile (25)) and dipalmitoyl PC (DPPC, similar structure and gel-to-liquid crystalline transition temperature (26) as SM).

MATERIAL AND METHODS

Materials

Taurocholate was obtained from Sigma Chemical Co. (St. Louis, MO, USA) and yielded a single spot upon thin-layer chromatography (butanol-acetic

acid-water, 10:1:1 vol/vol/vol, application of 200 µg bile salt). Cholesterol (Sigma) was $\geq 98\%$ pure by reverse-phase HPLC (isopropanol - acetonitrile 1:1, vol/vol, detection at 210 nm). Phosphatidylcholine from egg yolk (EYPC; Sigma), dipalmitoyl phosphatidylcholine (DPPC; Sigma) and sphingomyelin from egg yolk (EYSM; Avanti Polar-Lipids Inc., Alabaster, AL, USA) all yielded a single spot upon thin-layer chromatography (chloroform-methanol-water 65:25:4, vol/vol/vol, application of 200 µg lipid). Acyl chain compositions as determined by gas-liquid chromatography (27) were virtually identical to previously published data (23) and showed a preponderance of 16:0 acyl chains for EYSM, similar to sphingomyelin in human bile (25). As shown by reverse-phase HPLC, EYPC contained mainly 16:0 acyl chains at the *sn*-1 position and mainly unsaturated (18:1>18:2>20:4) acyl chains at the *sn*-2 position, similar to phosphatidylcholine in human bile (24). Dulbecco's modified Eagle's minimum essential medium (DMEM) was obtained from Flow Laboratories (Irvine, G.B.). All other chemicals and solvents were of ACS or reagent grade quality.

Ultrafilters with a molecular weight cut-off of 5 kDa were obtained from Sartorius (Göttingen, Germany: Centrisart I). The enzymatic cholesterol assay kit was obtained from Boehringer (Mannheim, Germany). 3 α -Hydroxysteroid dehydrogenase for the enzymatic measurement of bile salt concentrations (28) and a colorimetric chloride-kit were purchased from Sigma. The reverse-phase C18 HPLC column was from Supelco (Supelcosil LC-18-DB, Supelco, Bellefonte, PA, USA).

Preparation of lipid solutions

Lipid mixtures containing variable proportions of cholesterol, phospholipids (both from stock solutions in chloroform) and taurocholate (from stock solutions in methanol) were vortex-mixed and dried at 45°C under a mild stream of nitrogen, and subsequently lyophilized during 24 hrs, before being dissolved in aqueous 0.15 M NaCl plus 3mM NaN₃. Tubes were sealed with Teflon-lined screw caps under a blanket of nitrogen to prevent lipid oxidation and vortex-mixed for 5 min. followed by incubation at 37°C in the dark. All solutions were warmed up to 45°C for 10 min. before use. The final mol percentages of cholesterol, phospholipids and bile salts did not differ more than 1% from the intended mol percentages.

Lipid analysis

Phospholipid concentrations in solutions were assayed by determining inorganic phosphate according to Rouser (29). Cholesterol concentrations were determined with an enzymatic assay (30) and bile salts with the 3 α -hydroxysteroid dehydrogenase method (28).

Preparation of small unilamellar vesicles

Small unilamellar vesicles were prepared by sonication. Lipids, from stock-solutions in chloroform, were vortex-mixed, dried under a mild stream of nitrogen, freeze-dried in liquid nitrogen and subsequently lyophilized during 24 hrs. The lipid film was dissolved in nitrogen-flushed aqueous 0.15 M NaCl plus 3 mM NaN₃ and thereafter, the suspensions were probe-sonicated during 30 min. at 45°C (above the main transition temperatures of the phospholipids). After sonication, the suspension was centrifuged during 30 min. at 50000 g at 40°C, in order to remove potential remaining vesicular

aggregates and titanium particles. The resulting small unilamellar vesicles were stored above 40°C, and used within 12 hrs. Small unilamellar vesicles were prepared with 100% EYPC or 80% EYPC / 20% EYSM or 60% EYPC / 40% EYSM as phospholipid (final phospholipid conc. 4mM). The hydrodynamic radius (Rh: at 37°C), as determined by quasielastic light scattering spectroscopy, of the small unilamellar vesicles composed with 100% EYPC was 50 ± 1.65 nm. Partial replacement of EYPC with EYSM led to slightly decreased vesicle sizes (mean \pm SEM: 43.5 ± 1.23 nm in case of 40% EYSM).

Resistance of vesicles against taurocholate or taurocholate-phospholipid mixed micelles

Interactions of sonicated small unilamellar vesicles with taurocholate were examined by measuring optical density at 405 nm every min during 30 min. at 37°C in a thermostated Benchmark microplate reader (BioRad, Hercules, CA, USA). Solutions were stirred for 2 sec. prior to each measurement. A decrease of the OD at 405 nm after addition of taurocholate is compatible with micellization of the vesicles. Absorbance measured in control vesicles without addition of taurocholate always remained stable during the experiments. We added taurocholate (final conc. 6 mM) or mixed micellar solutions containing both taurocholate (final conc. 6 mM) and either EYPC or EYSM or DPPC (PL / (PL+BS) ratio = 0.2, 37°C) to EYPC-containing vesicles (final vesicular phospholipid conc. 4 mM). Furthermore, we added taurocholate (final conc. 5 mM) to sonicated vesicles containing 100% EYPC or 80% EYPC / 20% EYSM or 60% EYPC / 40% EYSM as phospholipids (final phospholipid conc. 4 mM, 37°C).

Last, 40 μL of taurocholate simple micelles or mixed micellar solutions containing both taurocholate and either EYPC or EYSM or DPPC (PL/(PL+BS) ratio = 0.2, 180 mM taurocholate, 37°C) were added to 200 μL of supersaturated model bile (10.5 mM EYPC, 42.3 mM taurocholate, 17.5 mM cholesterol), in order to decrease cholesterol saturation of the resulting model system to unsaturated levels (see inset Fig. 3: final cholesterol saturation index 0.25 and 0.21, resp. (according to Carey's Critical Tables (31,32), which are based on EYPC-containing systems)). Because micellar cholesterol solubility in SM- or DPPC-containing systems is approximately one-third of micellar solubility in EYPC-containing system (23), all final systems were unsaturated regardless phospholipid type. Since the original model bile was composed so, that it plotted in the middle three-phase zone of the equilibrium ternary phase diagram (33) and thus contained large quantities of vesicles in addition to micelles and cholesterol monohydrate crystals, a decrease of OD at 405 nm was considered to be consistent with micellization of these vesicles.

Resistance of erythrocytes against taurocholate simple micelles and taurocholate-phospholipid mixed micelles

Fresh human erythrocytes (aliquots of 10 mL human blood from a single volunteer) were sedimented 3 times by centrifugation at 3000 rpm for 15 min.; the plasma and buffy coat were discarded and the pellet was resuspended to the original blood volume in TRIS buffer (10 mM TRIS, 130 mM NaCl and 10 mM glucose, pH 7.4). A constant temperature of 37°C was maintained during the experiment. When these erythrocytes are incubated during 15 min. with 50 mM taurocholate, hemolysis amounts to 95-100% (i.e. identical to values after 15 min. incubation in distilled water (17)). In

order to determine potential protective effects of various phospholipids against detergent bile salts, erythrocytes (0.2 mL) were added to 0.8 mL taurocholate (50 mM) or mixed micellar solutions containing both taurocholate (50 mM) and increasing amounts (5, 10, 15, 20 or 25 mM) of either EYPC or EYSM or DPPC. After incubation for 15 min., 7 mL buffer was added, in order to decrease the progress of hemolysis to negligible levels (2). The samples were then centrifuged for 1 min. at 10000 g and the extent of lysis was assayed in the supernatant (absorbance at 540 nm).

In order to examine potential changes of erythrocyte membrane composition due to incubation with mixed phospholipid-taurocholate micelles, after such incubation (PL / (PL+BS) ratio of added mixed micelles = 0.35: complete protection against hemolysis at this ratio), erythrocytes were washed extensively and membrane phospholipids extracted according to Reed (34), separated by thin-layer chromatography (chloroform-methanol-acetic acid-water 50:25:8:4 vol/vol/vol/vol) and separated spots quantified with the Rouser assay (29).

Finally we incubated erythrocytes with mixed micellar solutions containing taurocholate (50 mM) and small amounts (total phospholipid conc. 5 mM) of *both* EYPC and EYSM at various ratios (PC/SM ratios: 100/0, 90/10, 80/20, 70/30, 60/40, 50/50, 40/60, 30/70, 20/80, 10/90 and 0/100).

Resistance of CaCo-2 cells against taurocholate simple micelles and taurocholate-phospholipid mixed micelles

CaCo-2 cells were cultured as previously described (35) with minor modification. Briefly, CaCo-2 cells were grown in T-75 plastic flasks in DMEM supplemented with 20% fetal calf serum (Gibco, New England, N.Y., USA), 50 U/mL penicillin and 50 U/mL streptomycin (Irvine, GB).

Before confluency, the cells were split (split ratio 1:8) as follows: CaCo-2 cells were rinsed twice with Hank's balanced salt solution (Gibco, New England, N.Y., USA) and incubated during 5 min. at 37°C with 1 mL of dissociation solution (Sigma, St. Louis MO, USA), after DMEM medium supplemented with 20% fetal calf serum was added to the cell suspension. Monolayers were grown in microwell plates in DMEM, which was replaced daily with fresh medium. After 10 days, the postconfluent cultures were washed with phosphate-buffered saline (pH 7.4) and the cells were incubated with taurocholate (bile salt conc. 30 mM) or mixed micelles containing taurocholate plus EYPC or EYSM or DPPC (bile salt conc. 30mM, PL / (PL+BS) ratio = 0.05, 0.1, 0.15, 0.2, 0.25 and 0.3, 37°C, pH 7.4). After 30 min. incubation, the medium was collected and the cells were treated with 0.4% Triton X-100. Lactate dehydrogenase (LDH) activity -as a sensitive parameter of cell damage- was measured according to Mitchell et al. (36) in both medium and in Triton X-100 treated cells. Fat-free bovine serum albumine (final concentration 0.6%) was added to prevent interference of bile salts with the spectrophotometric assay of LDH activity. Enzyme activity in each single experiment was normalized as percentage of the total LDH activity (medium + Triton X-100 treated cells).

IMC measurement

Under the conditions of the experiments in this study, in systems containing taurocholate and phospholipids, taurocholate is contained not only in mixed (i.e. bile salt-phospholipid) micelles, but occurs also as non-phospholipid-associated bile salt, either as monomers or -above the critical micellar concentration- in small "simple" micelles. The monomeric plus simple micellar bile salt concentration is referred to as "intermixed micellar-

vesicular (non phospholipid-associated) bile salt concentration”, usually abbreviated as “IMC” (11). We determined IMC in micellar model systems containing either EYPC, DPPC or EYSM as phospholipids and taurocholate as bile salt (PL / (PL+BS) ratio = 0.1, 0.15 and 0.2, bile salt concentration 30 mM, 37°C), using a minor modification of the rapid centrifugal ultrafiltration technique (37).

A 5 kDa Centriscart ultrafilter was rinsed with H₂O and centrifuged for 5 min. at 500 g in order to remove glycerol remnants from the membrane. The water was removed carefully from both sides of the membrane with a syringe. The filter was preincubated at 37°C during 1 hr before usage. A 2 mL aliquot of model system was put into the filter device (in duplicate) and centrifuged at 500 g for 5 min. in a pre-warmed (37°C) centrifuge. The filtrate was carefully collected with a syringe. Filtration was repeatedly performed, adjusting centrifugal speed so as to obtain constant filtrate volumes of approximately 50 µL. Bile salt and chloride concentrations reached stable values in the third filtrate. Slightly lower concentrations in the first and second filtrates resulted from small amounts of water remaining in the membrane after rinsing the ultrafilter (37). We considered the third filtrate to represent the simple micellar + monomeric fraction, and therefore decided to use the third filtrate for measurement of the IMC (the first two filtrates were added each time to the filtrant) (37). This technique has been validated before (12,37,38). During ultrafiltration, Gibbs-Donnan effects occur as result of uneven distribution across the membrane of non-filterable particles with a highly negative charge (in particular mixed micelles), thus leading to an overestimation of the concentrations of negatively charged monomeric and simple micellar bile salts in the filtrate (11,37). We corrected the concentrations of bile salts measured in the filtrate for Gibbs-

Donnan effects by multiplying the bile salt concentration in the filtrate with the ratio of chloride concentrations in filtrant and filtrate (11,37,38).

Statistical analysis

Values are expressed as means \pm SEM. Differences between groups were tested for statistical significance by analysis of variance with the aid of NCSS software (Kaysville, Utah, USA). When ANOVA detected a significant difference, results were further compared for contrasts using Fisher's least significant difference test as post-hoc test. Statistical significance was defined as two-tailed probability of less than 0.05.

RESULTS

Interaction between phospholipid vesicles and taurocholate or taurocholate-phospholipid mixed micelles

Incubation with detergent taurocholate led to fast micellization of sonicated EYPC vesicles as indicated by decrease of absorbance values (Fig. 1). Incorporation of phospholipid in taurocholate micelles delayed micellization of the vesicular bilayer in the rank order: EYPC < DPPC < EYSM. In order to examine whether this protective effect was caused by phospholipid transfer from mixed micelles into the vesicular bilayer, we performed the following experiment: EYPC in vesicles was partially replaced by EYSM (vesicular SM/PC ratios 20/80 or 40/60).

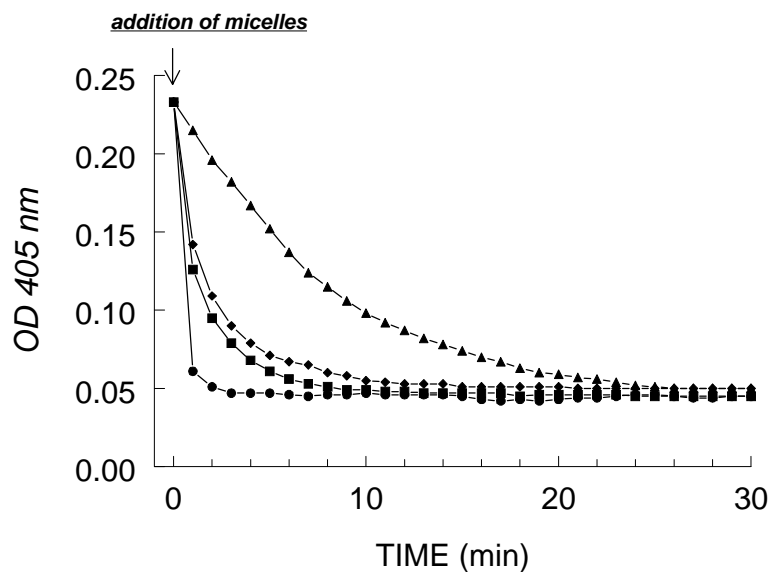


Figure 1: Effects of taurocholate (final conc. 6 mM) or taurocholate plus phospholipid-containing mixed micelles (final taurocholate conc. 6 mM, PL / (PL+BS) ratio = 0.2, 37 °C) on sonicated EYPC vesicles (final vesicular EYPC conc. 4 mM). Compared to taurocholate alone, decrease of absorption was delayed by incorporation of phospholipid in the micelles in the rank order: EYPC < DPPC < EYSM, consistent with delayed micellization of the vesicle bilayers. SEMs are contained within the symbols (n=4).

(●) taurocholate; (■) EYPC-taurocholate; (◆) DPPC-taurocholate; (▲) EYSM-taurocholate.

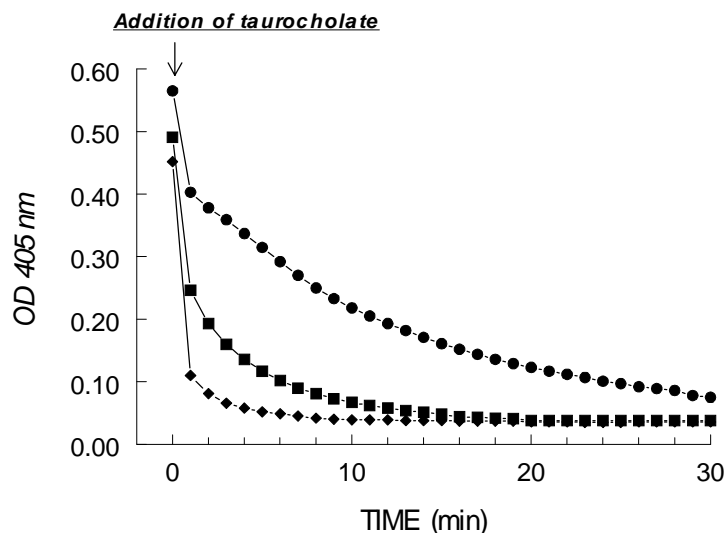


Figure 2: Effect of taurocholate (final conc. 5 mM) on vesicles (final vesicular phospholipid conc. 4 mM, 37 °C). Vesicles were composed with 100% EYPC or with 20% or 40% of the EYPC replaced by EYSM. Decrease

of absorption values was enhanced by inclusion of SM in the vesicular bilayer, depending on the amount of vesicular SM. These findings indicate faster micellization in case of SM-containing vesicles. SEMs are contained within the symbols (n=4).

(●) 100% EYPC; (■) 80% EYPC / 20% EYSM; (◆) 60% EYPC / 40% EYSM.

As shown in Fig. 2, these SM-containing vesicles exhibited increased rather than decreased sensitivity for the detergent action of taurocholate, the magnitude of this effect depending on the amount of vesicular EYPC replaced by EYSM. These results suggest that protective effects of phospholipids such as SM occur because of decreased detergent effects of mixed EYSM-taurocholate micelles compared to simple micelles or EYPC-taurocholate micelles rather than transfer of EYSM from mixed micelles into the vesicular bilayer.

Micellization of vesicles in supersaturated EYPC-containing model bile after addition of taurocholate simple micelles in quantities sufficient to decrease CSI to unsaturated levels was delayed by incorporation of phospholipid in these micelles in the rank order: EYPC < DPPC < EYSM (Fig. 3).

Effect of various phospholipids on taurocholate-induced hemolysis

When erythrocytes were incubated with 50 mM taurocholate, cytolysis amounted to 95-100% (virtually identical to values after incubation with distilled water). Whereas incorporation of EYPC in quantities ≥ 20 mM (PL / (PL+BS) ratio ≥ 0.29) in taurocholate micelles reduced cytolysis appreciably, the same protective effect occurred for taurocholate-DPPC and taurocholate-EYSM micelles already at phospholipid concentrations ≥ 5 mM (PL / (PL+BS) ratio ≥ 0.1 , Fig. 4). When the erythrocytes were incubated

with mixed micelles containing *both* EYPC and EYSM (bile salt conc. 50 mM, total phospholipid conc. 5 mM), hemolysis was progressively inhibited at increasing SM contents (Fig. 5).

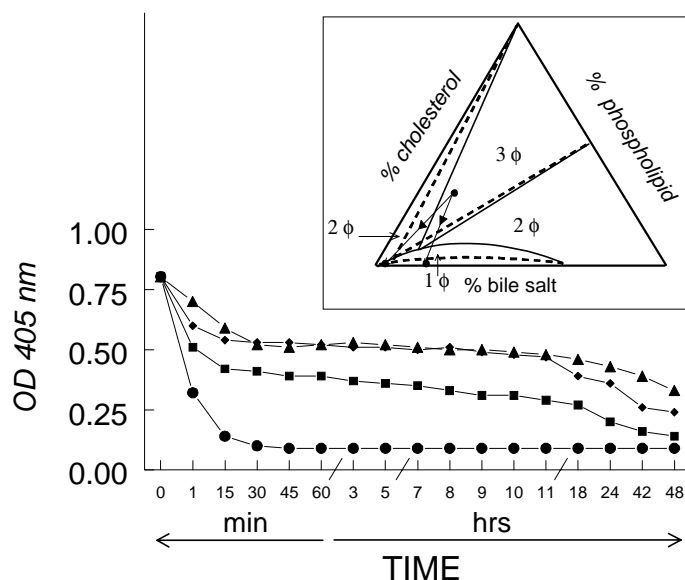


Figure 3: Effect of taurocholate simple micelles or mixed micelles containing taurocholate and either EYPC or EYSM or DPPC (PL / (PL+BS) ratio = 0.2, 37°C) on supersaturated model bile (42.3 mM taurocholate, 10.5 mM EYPC, 17.5 mM cholesterol, total lipid concentration 3.6 g/dL), plotting in the middle three-phase zone of the ternary equilibrium phase diagram (33), and containing large amounts of vesicles besides mixed micelles and cholesterol monohydrate crystals. Inclusion of phospholipids in the taurocholate micelles reduced decrease of absorption values in the rank order EYPC < DPPC < EYSM, indicating decreased micellization of vesicular bilayers. Note non-linear scale for X-axis.

(●) taurocholate; (■) EYPC-taurocholate; (◆) DPPC-taurocholate; (▲) EYSM-taurocholate.

Inset: equilibrium taurocholate-phospholipid-cholesterol ternary phase diagram for EYPC- (continuous lines (33)) as well as DPPC- or EYSM- (interrupted lines (23)) containing systems. Arrows indicate changes in relative lipid composition after addition of simple or mixed micelles. 1φ = 1-phase zone; 2φ = 2-phase zone; 3φ = 3-phase zone.

Light microscopical examination of red blood cells after incubation with each micellar solution revealed no differences in sizes or shapes compared with control erythrocytes. Moreover, no changes in phospholipid composition or SM/PC ratio in erythrocyte membranes were found after incubation with EYPC-taurocholate or EYSM-taurocholate mixed micelles: 25% of total phospholipids consisted of PE, 14% of PI-PS, 25% of SM and 36% of PC, and SM/PC ratios were 0.68, 0.65 and 0.69 for control erythrocytes, after incubation with EYPC-taurocholate micelles and EYSM-taurocholate micelles respectively. It should be noted that these data were obtained after incubation with micelles at a micellar PL / (PL+BS) ratio of 0.35, in order to ensure complete protection against hemolysis.

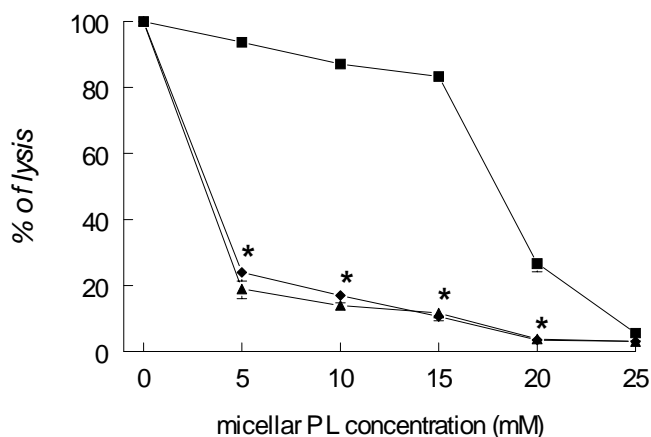


Figure 4: Effect of phospholipids on taurocholate-induced lysis of human erythrocytes. Red blood cells were incubated for 15 min. at 37°C with 50 mM taurocholate (100% lysis) or with mixed micelles containing taurocholate (50 mM) and progressive amounts of phospholipids. EYSM and DPPC had enhanced protective effects compared with EYPC.

(■) EYPC-taurocholate; (◆) DPPC-taurocholate; (▲) EYSM-taurocholate.
* $P < 0.05$ compared to EYPC-taurocholate

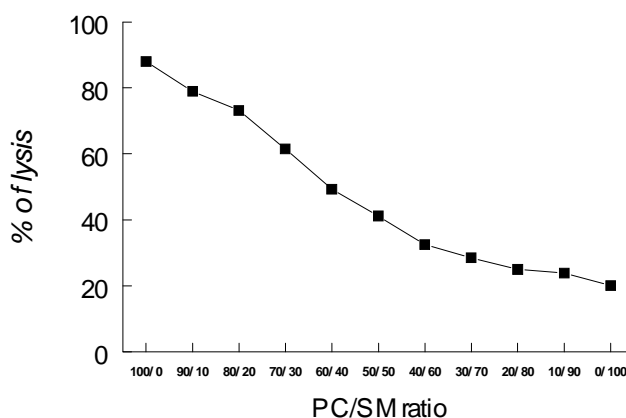


Figure 5: Effects of phospholipids on taurocholate-induced lysis of human erythrocytes. Red blood cells were incubated for 15 min. at 37°C with mixed micelles (taurocholate conc. 50 mM, total phospholipid conc. 5mM) that contained variable amounts of both EYPC and EYSM. Hemolysis was progressively inhibited at increasing SM contents.

Effect of various phospholipids on taurocholate-induced damage of CaCo-2 cells and on intermixed micellar-vesicular bile salt concentrations

As shown in Figure 6A, incorporation of increasing amounts of phospholipids (up to PL/(BS+PL) ratio 0.3) in taurocholate micelles (bile salt conc. 30 mM) progressively reduced LDH release upon incubation with CaCo-2 cells. Protective effects were significantly higher for EYSM or DPPC than EYPC. Intermixed micellar-vesicular (i.e. monomeric plus simple micellar) bile salt concentrations (IMC) in EYPC-containing micellar solutions were significantly higher than in corresponding EYSM- or DPPC-containing solutions at all ratios examined (PL/(BS+PL) ratios 0.1, 0.15 and 0.2). For all taurocholate-phospholipid systems, there was a decrease of IMC at increasing phospholipid contents (Table 1).

Since the intermixed micellar-vesicular (IMC) bile salts have been suggested to be responsible for the membrane-damaging effects (12,13), we also

incubated CaCo-2 cells with taurocholate simple micelles (i.e. without phospholipids) at concentrations identical to IMC values of Table 1. Whereas there was only minor LDH release below 15 mM bile salt concentrations, there was a steep increase of LDH release at higher concentrations (Fig. 6B). LDH release after incubation with mixed (phospholipid-containing) taurocholate micelles was virtually the same as LDH release after incubation with taurocholate simple micelles (without phospholipids) at concentrations identical to corresponding IMC values (Fig. 6C).

TABLE 1: Intermixed micellar-vesicular bile salt concentration (IMC) in systems containing taurocholate and various phospholipids.

	IMC (mM)		
PL / (PL+BS) ratio	0.1	0.15	0.2
TC + EYPC	19±0.6	17.7±0.8	14±1.1
TC + SM	14.6±0.6	12.9±0.8	10.9±0.4
TC + DPPC	13.8±0.7	12.4±0.4	11.2±0.6

Monomeric plus simple micellar bile salt concentration (IMC) measured in model systems containing constant taurocholate concentration (30 mM) plus increasing amounts of EYPC or SM or DPPC. Values are expressed as means ± SEM of three different experiments in duplicate. There was a significant difference at all PL / (PL+BS) ratios between EYPC-containing systems and SM- or DPPC-containing systems. Moreover, for all phospholipids there was a significant decrease of IMC values at increasing phospholipid contents.

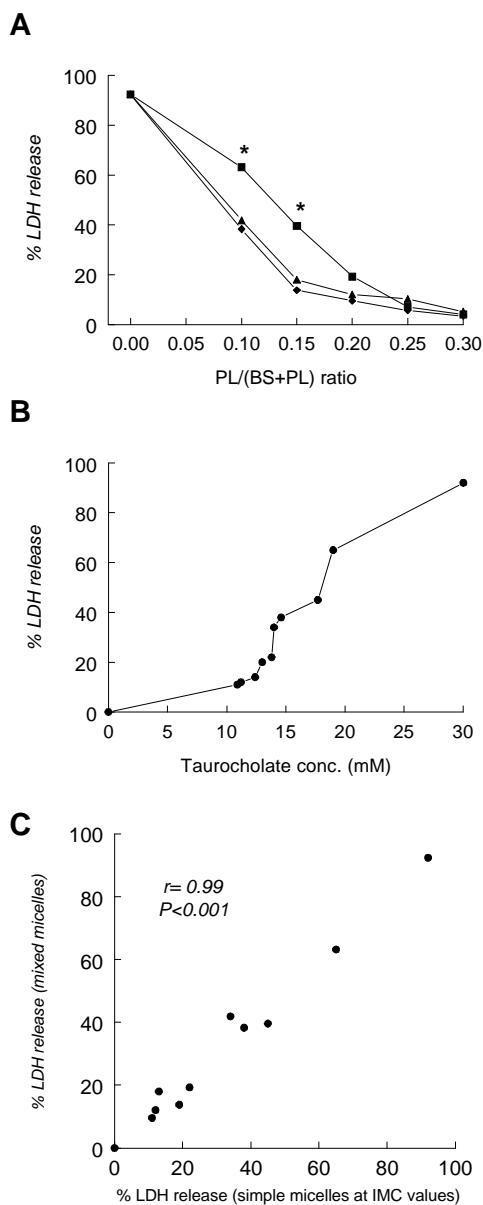


Figure 6 A): Effect of phospholipids on taurocholate-induced LDH release by CaCo-2 cells. CaCo-2 cells were incubated for 30 min. at 37°C with taurocholate simple micelles (30 mM) or mixed micelles containing taurocholate (30 mM) and progressive amounts of phospholipids. Protective effects of SM and DPPC were greater than protective effects of EYPC. (■) EYPC-taurocholate; (◆) DPPC-taurocholate; (▲) EYSM-taurocholate. * $P < 0.05$ compared to EYSM- and DPPC-taurocholate. **B):** LDH release by CaCo-2 cells upon incubation with taurocholate simple micelles at concentrations identical to IMC-values of mixed micelles used in 6A (given in Table 1). **C):** Identical LDH release upon incubation of CaCo-2 cells with taurocholate-phospholipid mixed micelles or taurocholate simple micelles at corresponding IMC concentrations.

DISCUSSION

Bile salts play a pivotal role in cholesterol and phospholipid secretion in bile and in intestinal lipid absorption. Nevertheless, in particular hydrophobic bile salts may also have adverse effects: they may damage the canalicular membrane of the hepatocyte in cholestasis, and promote formation of adenomas and cancer in the colon (39).

The main finding in the present study was that incorporation of phospholipids in taurocholate micelles protected against detergent effects of the bile salts, with a greater protection offered by EYSM or DPPC than EYPC. Similar results were obtained in a large variety of *in vitro* systems such as sonicated vesicles, supersaturated model systems, human erythrocytes and the CaCo-2 cell line. In the experiments with sonicated EYPC vesicles (Fig. 1), including phospholipids within taurocholate micelles retarded micellization. Nevertheless, at the end of the experiment, absorbance values were very low regardless whether simple or mixed (phospholipid-containing) micelles had been added. These findings are consistent with complete micellization of all vesicles and thermodynamic equilibrium reached during the experiment. These results can easily be explained since, in the absence of cholesterol, final compositions of all model systems plot in the (one-phase) micellar zone of the appropriate equilibrium phase diagrams (23,33). In contrast, in the experiments with cholesterol-supersaturated EYPC-containing model systems (Fig. 3), absorbance values at the end of the experiment were much higher after addition of phospholipid-containing mixed micelles (rank order EYPC < DPPC < EYSM) than after addition of simple taurocholate micelles, indicating persistence of significant amounts of vesicles. For all these systems, cholesterol saturation after addition of micelles was far below 1.

Therefore, all final systems were unsaturated and should have contained only micelles at equilibrium, even if one takes into account the considerably reduced micellar cholesterol solubility in SM- or DPPC-containing systems compared to EYPC-containing systems (23). The progressive decreases of absorbance after addition of phospholipid-containing micelles, as well as the high absorbance values at the end of the experiment, indicate that thermodynamic equilibrium was not reached during the experiment. The slower decrease of absorbance after addition of EYSM- (or DPPC-) containing mixed micelles than after addition of EYPC-containing mixed micelles can easily be explained by the well-known prolonged metastability of SM-containing systems (40). One should realize in interpreting results in cholesterol-supersaturated model systems displayed in Fig. 3, that decreases of turbidity are supposed to reflect a (partial) shift of lipids from vesicles to mixed micelles, but that we cannot exclude the possibility that disaggregation of large into smaller vesicular clusters or precipitation of cholesterol crystals could have contributed to decreased absorbance values under these circumstances.

In principle, protective effects could result from transfer of phospholipids from mixed micelles into the membrane bilayer or from a local effect of the phospholipids within the mixed micelles. There were no changes in phospholipid composition or SM/PC ratio of the erythrocyte membrane after incubation with EYPC- or EYSM-containing taurocholate micelles. Also, we found no changes of erythrocyte morphology after incubation with these micelles. Even small changes in phospholipid composition of the erythrocyte membrane should have had a profound impact on erythrocyte shape (41). Furthermore, incubation of sonicated EYPC vesicles with EYSM-containing taurocholate micelles resulted in delayed micellization of the vesicular

bilayer compared to incubation with taurocholate micelles. In contrast, partial replacement of vesicular EYPC by EYSM increased rather than decreased sensitivity to taurocholate, in line with previous studies (42). Taken together, these findings suggest that protective effects of including phospholipids such as EYSM within the micelles are not caused by transfer of these phospholipids from the micelles into the vesicular bilayer, but rather by a local effect at the level of the micelles.

The so called "intermixed micellar/vesicular bile salt concentration" (IMC: bile salt monomers + simple micelles (11)) has been proposed to exert the damaging effects on the membrane bilayer (12,13). Indeed, LDH release upon incubation of CaCo-2 cells with the various mixed (phospholipid-containing) taurocholate micelles was identical to LDH release upon incubation with taurocholate simple micelles at corresponding IMC values (Fig. 6C). The enhanced protective effect of incorporating EYSM or DPPC compared to EYPC within taurocholate micelles can thus be explained by the much lower intermixed micellar-vesicular bile salt concentrations found in the present study for EYSM- and DPPC-containing micelles. Similar magnitude of protective effects of including EYSM or DPPC within taurocholate micelles may relate to similarity in molecular structure and acyl chain composition of both phospholipids: whereas DPPC contains 16:0 acyl chains at both *sn*-1 and *sn*-2 positions, in case of EYSM, 16:0 is also the major acyl chain amidated to the sphingosine backbone. Also, main gel to liquid-crystalline transition temperatures are similar for DPPC and EYSM (42°C vs 37°C; (26)). EYPC offered less protection against detergent effects of taurocholate than EYSM or DPPC. EYPC has a molecular structure quite different from both other phospholipids, due the presence of cis-unsaturated

acyl chains at the *sn*-2 position. Also main gel to liquid-crystalline transition temperature is much lower ($< 0^{\circ}\text{C}$; (26)).

The differences in IMC values found in the present study suggest different micellar structure and a smaller “coexistence (mixed + simple micelles containing) region” (43) for EYSM- or DPPC-taurocholate micelles compared to EYPC-taurocholate micelles: more taurocholate molecules may be required to dissolve a molecule of EYSM or DPPC than a molecule of EYPC. As a result, in a mixed micellar solution, the proportion of taurocholate associated with phospholipid would be greater in case of EYSM or DPPC than EYPC, with reciprocal decrease of taurocholate concentration in the IMC.

Our findings may be relevant for canalicular bile formation. Upon addition of bile salts to isolated canalicular membranes (44,45) or erythrocytes (46), there is a considerable release of PC but not of SM from the membranes. In line with these *in vitro* findings, PC is the major phospholipid species in *gallbladder* bile, with minor amounts of SM (20). Nevertheless, these data do not exclude the possibility that larger amounts of SM could be present in nascent bile *within the canalicular lumen*, due to a putative cholehepatic shunt (23) after hydrolysis of SM to more hydrophobic ceramide by an alkaline sphingomyelinase recently detected in bile (22). Also, under pathological condition such as cholestasis, large amounts of SM may appear in bile (21). Under such cholestatic conditions, SM within micelles in the canalicular lumen could protect against further bile salt-induced liver injury. The protective effects of SM may also be relevant at the level of the intestinal tract. In the small intestine, intraluminal bile salts exert a negative feedback control on cholecystokinin release and gallbladder contraction (47). We have found in duodenal infusion experiments in humans that the

extent of the negative feedback control is decreased by including phospholipids in bile salt micelles that are infused, with stronger effects for DPPC or EYSM than EYPC, supposedly due to different IMC values (unpublished data).

Phospholipids may also be relevant at the level of the colon, in particular by decreasing IMC for hydrophobic bile salts such as deoxycholate, a well known promotor of colon cancer (39). It has indeed been shown recently, that rats fed a high sphingomyelin diet exhibit a significantly reduced susceptibility for colon cancer on experimental carcinogenic diet (48,49).

In conclusion, our data reveal greatly enhanced protective effects of sphingomyelin and dipalmitoyl phosphatidylcholine compared to egg yolk phosphatidylcholine against bile salt-induced cytotoxicity, which may relate to different intermixed micellar-vesicular (i.e. non-phospholipid associated) bile salt concentrations. These findings may be relevant at the level of the hepatocyte canalicular membrane and intestinal lumen.

References

1. Barnwell, S. G., P. J. Lowe, and R. Coleman. 1983. Effect of taurochenodeoxycholate or tauroursodeoxycholate upon biliary output of phospholipids and plasma-membrane enzymes, and the extent of cell damage, in isolated perfused rat livers. *Biochem. J.* **216**: 107-111.
2. Heuman, D. M., W. M. Pandak, P. B. Hylemon, and Z. R. Vlahcevic. 1991. Conjugates of ursodeoxycholate protect against cytotoxicity of more hydrophobic bile salts: in vitro studies in rat hepatocytes and human erythrocytes. *Hepatology* **14**: 920-926.
3. Coleman, R., S. Iqbal, P. P. Godfrey, and D. Billington. 1979. Membranes and bile formation. Composition of several mammalian biles and their membrane-damaging properties. *Biochem. J.* **178**: 201-208.
4. Lowe, P. J., and R. Coleman. 1981. Membrane fluidity and bile salt damage. *Biochim. Biophys. Acta* **640**: 55-65.

5. Davenport, H.W. 1968. Destruction of the gastric mucosal barrier by detergent and urea. *Gastroenterology* **54**: 175-181.
6. Chadwick, V.S., T. S. Gagarella, G. L. Carlson, J. C. Debognie, S. F. Phillips, and A. Hoffmann. 1979. Effect of molecular structure on bile acid-induced alterations in absorptive function, permeability, and morphology in the perfused rabbit colon. *J. Lab. Clin. Med.* **94**: 661-674.
7. Ostrow, J. D. 1969. Absorption by the gallbladder of bile salts, sulfobromophthalein and iodipamide. *J. Lab. Clin. Med.* **74**: 482-494.
8. Ostrow, J. D. 1967. Absorption of bile pigments by the gallbladder. *J. Clin. Invest.* **46**: 2035-2052.
9. Coleman R. 1987. Bile salts and biliary lipids. *Biochem. Soc. Trans.* **15**: 68S-80S.
10. Coleman, R., P. J. Lowe, and D. Billington. 1980. Membrane lipid composition and susceptibility to bile salt damage. *Biochim. Biophys. Acta* **599**: 294-300.
11. Donovan, J. M., N. Timofeyeva, and M. C. Carey. 1991. Influence of total lipid concentration, bile salt:lecithin ratio, and cholesterol content on inter-mixed micellar/vesicular (non-lecithin-associated) bile salt concentrations in model bile. *J. Lipid Res.* **32**: 1501-1512.
12. Donovan, J. M., A. A. Jackson, and M. C. Carey. 1993. Molecular species composition of inter-mixed micellar/vesicular bile salt concentrations in model bile: dependence upon hydrophilic-hydrophobic balance. *J. Lipid Res.* **34**: 1131-1140.
13. Narain, P. K., E. J. DeMaria, and D. M. Heuman. 1998. Lecithin protects against plasma membrane disruption by bile salts. *J. Surg. Res.* **78**: 131-136.
14. Amigo, L., H. Mendoza, S. Zanolungo, J. F. Miquel, A. Rigotti, S. Gonzalez, and F. Nervi. 1999. Enrichment of canalicular membrane with cholesterol and sphingomyelin prevents bile salt-induced hepatic damage. *J. Lipid Res.* **40**: 533-542.
15. Schachter, D. 1988: The hepatocyte plasma membrane: organization and differentiation. In *The Liver: Biology and Pathobiology*. Arias I. M., W. B. Jakoby, H. Popper, D. Schachter, and D. A. Shafritz, editors. Raven Press, Ltd., New York, NY. 131-140.
16. Kremmer, T., M. H. Wisher, and W. H. Evans. 1976. The lipid composition of plasma membrane subfractions originating from the three major functional domains of the rat hepatocyte cell surface. *Biochim. Biophys. Acta* **455**: 655-664.
17. Velardi, A.L.M., A. K. Groen, R. P. Oude Elferink, R. van der Meer, G. Palasciano, and G. N. Tytgat. 1991. Cell type-dependent effect of phospholipid and cholesterol on bile salt cytotoxicity. *Gastroenterology* **101**: 457-464.

18. Smit, J. J., A. H. Schinkel, R. P. J. Oude Elferink, A. K. Groen, E. Wagenaar, L. van Deemter, C. A. Mol, R. Ottenhoff, N. M. van der Lugt, and M. A. van Roon. 1993. Homozygous disruption of the murine *mdr2* P-glycoprotein gene leads to a complete absence of phospholipid from bile and to liver disease. *Cell* **75**: 451-462.
19. Higgins, J. A., and W. H. Evans. 1978. Transverse organization of phospholipids across the bilayer of plasma membrane subfractions of rat hepatocytes. *Biochem. J.* **174**: 563-567.
20. Alvaro, D., A. Cantafora, A. F. Attili, C. S. Ginanni, C. De Luca, G. Minervini, A. Di Biase, and M. Angelico. 1986. Relationships between bile salts hydrophilicity and phospholipid composition in bile of various animal species. *Comp. Biochem. Physiol. [B.]* **83**: 551-554.
21. Barnwell, S. G., B. Tuchweber, and I. M. Yousef. 1987. Biliary lipid secretion in the rat during infusion of increasing doses of unconjugated bile acids. *Biochim. Biophys. Acta* **922**: 221-233.
22. Duan, R. D., E. Hertvig, L. Nyberg, T. Hauge, B. Sternby, J. Lillienau, A. Farooqi, and A. Nilsson. 1996. Distribution of alkaline sphingomyelinase activity in human beings and animals. Time and species differences. *Dig. Dis. Sci.* **41**: 1801-1806.
23. van Erpecum K. J., and M. C. Carey. 1997. Influence of bile salts on molecular interactions between sphingomyelin and cholesterol: relevance to bile formation and stability. *Biochim. Biophys. Acta* **1345**: 269-282.
24. Hay, D. W., M. J. Cahalane, N. Timofeyeva, and M. C. Carey. 1993. Molecular species of lecithins in human gallbladder bile. *J. Lipid Res.* **34**: 759-768.
25. Nibbering, C. P., and M. C. Carey. 1999. Sphingomyelins of rat liver: biliary enrichment with molecular species containing 16:0 fatty acids as compared to canalicular-enriched plasma membranes. *J. Membr. Biol.* **167**: 165-171.
26. Koynova, R., and M. Caffrey. 1995. Phases and phase transitions of the sphingolipids. *Biochim. Biophys. Acta* **1255**: 213-236.
27. Hakomori, S. 1983. Chemistry of Glycosphingolipids. In *Handbook of Lipid Research*. Hanahan D. J., editor. Plenum Press, New York, NY. 37-39.
28. Turley, S. D., and J. M. Dietschy. 1978. Reevaluation of the 3α -hydroxysteroid dehydrogenase assay for total bile acids in bile. *J. Lipid Res.* **19**: 924-928.
29. Rouser, G., S. Fleischer, and A. Yamamoto. 1970. Two dimensional thin layer chromatographic separation of polar lipids and determination of phospholipids by phosphorus analysis of spots. *Lipids* **5**: 494-496.

30. Fromm, H., P. Hamin, H. Klein, and I. Kupke. 1980. Use of a simple enzymatic assay for cholesterol analysis in human bile. *J. Lipid Res.* **21**: 259-261.
31. Carey, M. C. 1978. Critical tables for calculating the cholesterol saturation of native bile. *J. Lipid Res.* **19**: 945-965.
32. Carey, M. C., and D. M. Small. 1978. The physical chemistry of cholesterol solubility in bile. Relationship to gallstone formation and dissolution in man. *J. Clin. Invest.* **61**: 998-1026.
33. Wang, D. Q. H., and M. C. Carey. 1996. Complete mapping of crystallization pathways during cholesterol precipitation from model bile: influence of physical-chemical variables of pathophysiologic relevance and identification of a stable liquid crystalline state in cold, dilute and hydrophilic bile salt-containing systems. *J. Lipid Res.* **37**: 606-630.
34. Reed, C.F., S. N. Swisher, G. V. Marinetti, and E.G. Eden. 1960. Studies of the lipids of the erythrocyte. I. Quantitative analysis of the lipids of normal human red blood cells. *J. Lab. Clin. Med.* **56**: 281-289.
35. Mohrmann, I., M. Mohrmann, J. Biber, and H. Urer. 1986. Sodium-dependent transport of Pi by an established intestinal epithelial cell line (CaCo-2). *Am. J. Physiol.* **250**: G323-G330.
36. Mitchell, D.B., K. S. Santone, and D. Acosta. 1980. Evaluation of cytotoxicity in cultured cells by enzyme leakage. *J. Tissue Cult. Methods* **6**: 113-116.
37. Donovan, J. M., and A. A. Jackson. 1993. Rapid determination by centrifugal ultrafiltration of inter-mixed micellar/vesicular (non-lecithin-associated) bile salt concentrations in model bile: influence of Donnan equilibrium effects. *J. Lipid Res.* **34**: 1121-1129.
38. Eckhardt, E. R. M., B. J. M. van de Heijning, K. J. van Erpecum, W. Renooij, and G. P. vanBerge-Henegouwen. 1998. Quantitation of cholesterol-carrying particles in human gallbladder bile. *J. Lipid Res.* **39**: 594-603.
39. Hori, T., K. Matsumoto, Y. Sakaitani, M. Sato, and M. Morotomi. 1998. Effect of dietary deoxycholic acid and cholesterol on fecal steroid concentration and its impact on the colonic crypt cell proliferation in azoxymethane-treated rats. *Cancer Lett.* **124**: 79-84.
40. Estep, T. N., W. I. Calhoun, Y. Barenholz, R. L. Biltonen, G. G. Shipley, and T. E. Thompson. 1980. Evidence for metastability in stearyl sphingomyelin bilayers. *Biochemistry* **19**: 20-24.
41. Kuypers, F. A., B. Roelofsen, W. Berendsen, J. A. Op den Kamp, and L. L. van Deenen. 1984. Shape changes in human erythrocytes induced by replacement of the

- native phosphatidylcholine with species containing various fatty acids. *J. Cell Biol.* **99**: 2260-2267.
42. Schubert, R., and K.-H. Schmidt. 1988. Structural changes in vesicle membranes and mixed micelles of various lipid compositions after binding of different bile salts. *Biochemistry* **27**: 8787-8794.
 43. Mazer, N. A., G. B. Benedek, and M. C. Carey. 1980. Quasielastic light-scattering studies of aqueous biliary lipid systems. Mixed micelle formation in bile salt-lecithin solutions. *Biochemistry* **19**: 601-615.
 44. Yousef, I. M., and M. M. Fisher. 1976. In vitro effect of free bile acids on the bile canalicular membrane phospholipids in the rat. *Can. J. Biochem.* **54**: 1040-1046.
 45. Gerloff, T., P. J. Meier, and B. Stieger. 1998. Taurocholate induces preferential release of phosphatidylcholine from rat liver canalicular vesicles. *Liver* **18**: 306-312.
 46. Billington, D., R. Coleman, and Y. A. Lusak. 1977. Topographical dissection of sheep erythrocyte membrane phospholipids by taurocholate and glycocholate. *Biochim. Biophys. Acta* **466**: 526-530.
 47. Thimister, P. W. L., W. P. M. Hopman, C. E. J. Sloots, G. Rosenbusch, A. Tangerman, H. L. Willems, C. B. H. W. Lamers, and J. B. M. J. Jansen. 1994. Effect of bile salt binding or protease inactivation on plasma cholecystokinin and gallbladder responses to bombesin. *Gastroenterology* **107**: 1627-1635.
 48. Dillehay, D. L., S. K. Webb, E. M. Schmelz, and A. H. J. Merrill. 1994. Dietary sphingomyelin inhibits 1,2-dimethylhydrazine-induced colon cancer in CF1 mice. *J. Nutr.* **124**: 615-620.
 49. Parodi, P. W. 1997. Cows' milk fat components as potential anticarcinogenic agents. *J. Nutr.* **127**: 1055-1060.

Addendum

**HEPATIC BILE LIPID COMPOSITION IN PATIENTS WITH
OBSTRUCTIVE JAUNDICE**

Antonio Moschetta^{*}, Piero Portincasa^{*}, Karel J. van Erpecum,
O. Caputi-Iambrenghi, W. Renooij, Gerard P. vanBerge-henegouwen,
Giuseppe Palasciano.

preliminary data

^{*} *Authors who equally contributed to the work*

Introduction

In vitro experiments indicate that phospholipids with saturated acyl chains such as sphingomyelin or dipalmitoyl phosphatidylcholine may offer enhanced protection against detergent bile salts compared to phospholipids that contain unsaturated acyl chains such as phosphatidylcholine from egg yolk or phospholipids that are present in human bile under normal conditions (1).

Although the outer leaflet of the hepatocyte canalicular membrane contains both phosphatidylcholine and sphingomyelin as major phospholipids (2), phosphatidylcholine (mainly unsaturated (18:2>18:1>20:4) acyl chains at *sn*-2 position) is the exclusive phospholipid in normal human bile (3). We hypothesized that under cholestatic conditions considerable amounts of sphingomyelin may occur in bile, with potential amelioration of cytotoxicity as a result. We therefore examined hepatic bile lipid composition in patients with obstructive jaundice due to bile duct stones.

Materials and Methods

Subjects

Bile was aspirated from the common bile duct during endoscopic retrograde cholangio-pancreaticography (ERCP) in seven patients with choledocholithiasis (male/female ratio 4/3, age 56±6 years, mean±SD). Only antibiotics (quinolones) and anti-inflammatory drugs were administered before ERCP. An increase in cholestatic indices (bilirubin, gamma-GT, alkaline phosphatase) was observed in all patients (**table 1**). The data reported in table 1 were obtained on the day of the ERCP. All patients presented small birifrangent monohydrate cholesterol crystals as observed at polarized light microscopy in bile immediately after aspiration. During ERCP, a cholangiography catheter was inserted proximally in the common bile duct after passing the stone and the first

mL of bile was discarded. Thereafter, hepatic bile was collected during 2-3 min (~2 mL). All bile samples were immediately extracted according to Bligh and Dyer (4). Extracts were stored at -20°C until further analysis. The protocol was approved by the hospital’s ethical committee and all patients had consented to participate in the study.

Table 1.

Liver biochemistry in 7 patients with choledocholithiasis.

Patient	ALT (U/L)	AST (U/L)	γ-GT (U/L)	Bilirubin tot (μmol/L)	AP (U/L)
A	45	61	110	20.6	283
B	50	78	109	22.4	351
C	43	59	210	27.0	296
D	60	75	159	37.6	259
E	51	82	181	39.3	314
F	55	61	131	33.2	330
G	49	59	124	33.7	381
mean±SE	50±2	68±4	146±15	31±3	316±16
Normal values	< 35	< 35	< 45	< 17	< 120

ALT: alanine transaminase; AST: aspartate transaminase; γ-GT: gamma-glutamyl transpeptidase; AP: alkaline phosphatase.

Materials

All bile salts were of the highest purity available and yielded single spots upon thin-layer chromatography (butanol-acetic acid-water, 10:1:1 vol/vol/vol, application of 200 μg bile salt). Taurocholate (TC), tauroursodeoxycholate (TUDC), glycocholate (GC), taurochenodeoxycholate (TCDC), glyoursodeoxycholate (GUDC), glycochenodeoxycholate (GCDC), taurodeoxycholate (TDC),

glycodeoxycholate (GDC), tauroolithocholate (TLC) and glycolithocholate (GLC) were purchased from Sigma Chemical Co. (St. Louis, MO, USA). Methylated fatty acids (16:0, 18:0, 18:1, 18:2, 20:0, 21:0, 22:0, 23:0, 24:0, 24:1, 25:0), used as standards for gas-liquid chromatography, were purchased from Sigma. All other chemicals and solvents were of ACS or reagent grade quality. The enzymatic cholesterol assay kit was obtained from Boehringer (Mannheim, Germany). 3α -Hydroxysteroid dehydrogenase for the enzymatic measurement of bile salt concentrations (5) was purchased from Sigma. The HPLC C18 column was purchased from Supelco (Supelcosil LC-18-DB, Supelco, Bellefonte, USA) and C18 cartridges (Sep-pak[®]) for solid-phase bile salt extraction from Waters (Milford, MA, USA).

Lipid analysis

Concentrations of cholesterol were determined enzymatically in extracts of bile (6). Phospholipid concentrations were assayed by determining inorganic phosphate according to Rouser (7). The phospholipids in the extracts were separated by thin-layer chromatography (chloroform-methanol-acetic acid-water 50:25:8:2, vol/vol/vol/vol), and quantified by determining the phosphorus contents of separated phospholipid spots (7). In order to determine the fatty acid profiles of phosphatidylcholine, 1 μ mol phosphatidylcholine was hydrolyzed in 1 mL nitrogen-flushed methanol- H_2SO_4 (95:5, by weight, 2 hrs, 70°C) (8). The methylated fatty acids were extracted three times with 1 mL hexane; the pooled hexane phase was washed with 3 mL H_2O , dried over Na_2SO_4 , concentrated under nitrogen, and separated and detected by gas-liquid chromatography using a GC14-A gas-chromatograph (Shimadzu, Kyoto, Japan), equipped with a bonded FSOT capillary column (length 30m, \varnothing 0.32 mm).

Bile salt concentrations were determined with the 3α hydroxysteroid-dehydrogenase method (5). The biliary cholesterol saturation index (CSI) was calculated according to Carey's critical tables (9).

Bile salt species composition was determined by isocratic HPLC analysis with phosphate-buffered 70% methanol, pH 5.25, as the eluant (10). An external standard containing known quantities of each of the relevant major conjugated bile salts was run prior to each analysis. Bile salts were first purified from whole bile by solid-phase extraction as previously described (11). Briefly, a C18 Sep-Pak[®] cartridge was rinsed with 10 mL methanol and 10 mL water, whereupon 100 μ L of bile, dissolved in 2 mL water, was applied. Subsequently, the cartridge was rinsed with 10 mL water, 3 mL 10 % acetone, and 10 mL water, and bile salts were eluted with 3 mL methanol. After evaporation of methanol under a mild stream of nitrogen at 45°C, the residue was dissolved in 1 mL HPLC buffer, 10 μ L of which was injected for HPLC analysis. The cumulative bile salt hydrophobicity index was calculated according to Heuman (12).

Statistical analysis

Values are expressed as mean \pm SEM. Differences between groups were tested with t-tests or ANOVA using NCSS software. Statistical significance was defined as a two-tailed probability of less than 0.05.

RESULTS AND DISCUSSION

Lipid compositions of the hepatic biles are given in **Table 2**. Mol% cholesterol and phospholipid appear low compared to hepatic biles of normal subjects (13). As a result, cholesterol supersaturation is modest (although all patients display supersaturated biles) and PL/(BS+PL) ratios are low.

As expected, levels of the hydrophobic secondary bile salt deoxycholate are low, with the result that cumulative bile salt hydrophobicity index is lower than usual (0.25 ± 0.02 vs 0.32 ± 0.07 in normal subjects; **Figure 1**,

Table 2). Ratio of taurine/glycine conjugated bile salts in biles was 1.08 ± 0.09 .

As shown in Figure 2, there are considerable amounts of sphingomyelin (6.6 ± 1.9 % of total phospholipids). The presence of significant amounts of sphingomyelin in bile has been previously reported in an animal model of experimental cholestasis (14). Acyl chain composition of phosphatidylcholine appears to be similar to normal (mainly 18:2>18:1 and 20:4; **Figure 3**).

Table 2

Hepatic bile lipid compositions in 7 patients with choledocholithiasis

N	Chol mol %	PL mol %	BS Mol%	PL/(BS+PL) Ratio	TLC (g/dL)	CSI	HI
A	3.4	11.4	85.2	0.121	1.80	1.1	0.21
B	3.5	12.1	84.4	0.125	1.70	1.1	0.19
C	3.1	9.4	87.5	0.097	1.65	1.2	0.21
D	3.8	10.1	86.1	0.105	2.04	1.3	0.16
E	7.9	25.4	76.7	0.271	1.79	1.4	0.29
F	6.5	16.1	77.4	0.172	1.64	1.7	0.30
G	6.8	22.9	70.3	0.246	1.80	1.3	0.29
mean±SE	5±1	15±2	81±2	0.2±0.02	1.7±0.05	1.3±0.07	0.25±0.02

TLC: total lipid concentration; CSI: cholesterol saturation index; HI: cumulative bile salt hydrophobicity index.

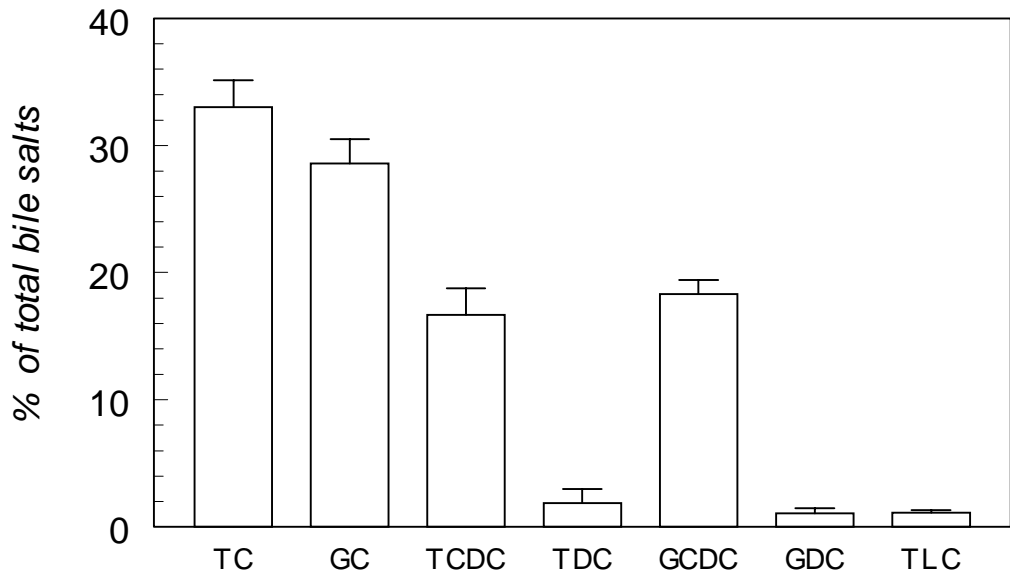


Figure 1. Bile salt composition of the hepatic biles of patients with cholesterol cholelithiasis. Biles are enriched only of the primary bile salts tauro- and glycocholate, tauro- and glycochenodeoxycholate. Bars indicate means, and vertical lines standard errors.

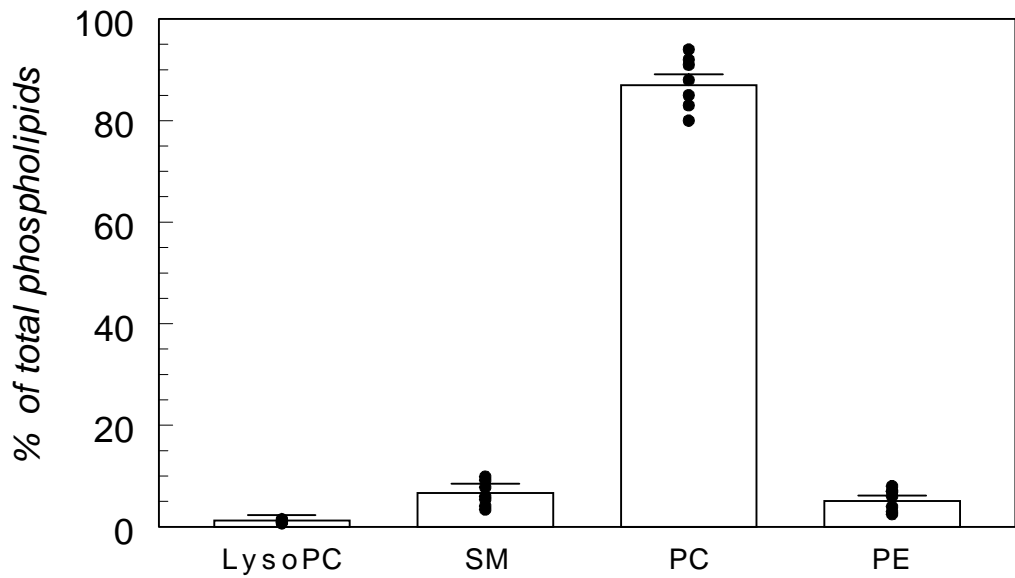


Figure 2. Phospholipid composition of the hepatic biles of patients with cholesterol cholelithiasis. Significant amounts of SM are present.

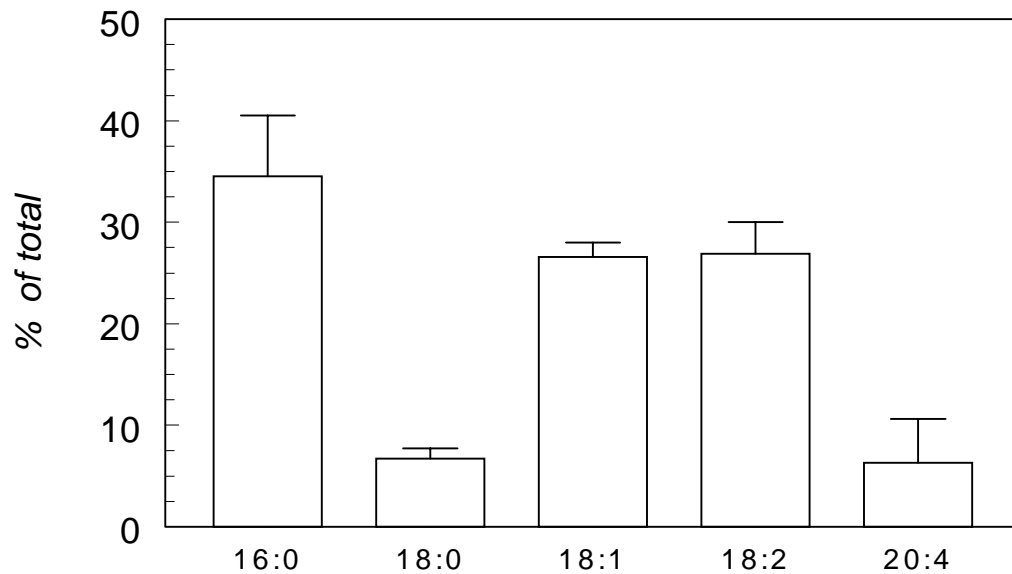


Figure 3. Phosphatidylcholine acyl chain composition in hepatic biles of patients with cholesterol choledocholithiasis.

In conclusion, significant amounts of sphingomyelin may occur in hepatic biles of patients with cholesterol choledocholithiasis. The potential consequences with regard to protection against detergent bile salts remain to be investigated.

References

1. Moschetta A, Van Berge-Henegouwen GP, Portincasa P, Palasciano G, Groen AK, Van Erpecum KJ. Sphingomyelin exhibits greatly enhanced protection compared with egg yolk phosphatidylcholine against detergent bile salts. *J Lipid Res* 2000; 41:916-924.
2. Kremmer T, Wisher MH, Evans WH. The lipid composition of plasma membrane subfractions originating from the three major functional domains of the rat hepatocyte cell surface. *Biochim Biophys Acta* 1976; 455(3):655-664.
3. Hay DW, Cahalane MJ, Timofeyeva N, Carey MC. Molecular species of lecithins in human gallbladder bile. *J Lipid Res* 1993; 34:759-768.
4. Bligh EG, Dyer WJ. A rapid method of total lipid extraction and purification. *Can J Biochem Physiol* 1959; 37:911-917.
5. Turley SD, Dietschy JM. Reevaluation of the 3 α -hydroxysteroid dehydrogenase assay for total bile acids in bile. *J Lipid Res* 1978; 19:924-928.

6. Fromm H, Hamin P, Klein H, Kupke I. Use of a simple enzymatic assay for cholesterol analysis in human bile. *J Lipid Res* 1980; 21:259-261.
7. Rouser G, Fleischer S, Yamamoto A. Two dimensional thin layer chromatographic separation of polar lipids and determination of phospholipids by phosphorus analysis of spots. *Lipids* 1970; 5(5):494-496.
8. Oldenburg V, Van Vugt F, Van Golde LM. Composition and metabolism of phospholipids of *Fasciola hepatics*, the common liver fluke. *Biochim Biophys Acta* 1975; 398(1):101-110.
9. Carey MC. Critical tables for calculating the cholesterol saturation of native bile. *J Lipid Res* 1978; 19:945-965.
10. Rossi SS, Converse JL, Hofmann AF. High pressure liquid chromatographic analysis of conjugated bile acids in human bile: simultaneous resolution of sulfated and unsulfated lithocholyl amidates and the common conjugated bile acids. *J Lipid Res* 1987; 28:589-595.
11. Eckhardt ERM, van de Heijning BJM, Van Erpecum KJ, Renooij W, VanBerge-Henegouwen GP. Quantitation of cholesterol-carrying particles in human gallbladder bile. *J Lipid Res* 1998; 39:594-603.
12. Heuman DM. Quantitative estimation of the hydrophilic-hydrophobic balance of mixed bile salt solutions. *J Lipid Res* 1989; 30:719-730.
13. Eckhardt ER, Van Erpecum KJ, de Smet MB, Go PM, Berge-Henegouwen GP, Renooij W. Lipid solubilization in human gallbladder versus hepatic biles. *J Hepatol* 1999; 31(6):1020-1025.
14. Barnwell SG, Tuchweber B, Yousef IM. Biliary lipid secretion in the rat during infusion of increasing doses of unconjugated bile acids. *Biochim Biophys Acta* 1987; 922(2):221-233.

chapter 7

**HYDROPHILIC BILE SALTS ENHANCE DIFFERENTIAL
DISTRIBUTION OF SPHINGOMYELIN AND
PHOSPHATIDYLCHOLINE
BETWEEN MICELLAR AND VESICULAR PHASES:
POTENTIAL IMPLICATIONS FOR THEIR EFFECTS *IN VIVO***

Antonio Moschetta, Gerard P. vanBerge-Henegouwen, Piero Portincasa,
Willem Renooij, Albert K. Groen, Karel J. van Erpecum.

Journal of Hepatology 2001;34:492-499.

Abstract

Background/Aims: The hepatocyte canalicular membrane outer leaflet contains both phosphatidylcholine (PC) and sphingomyelin (SM). Normally, PC is the exclusive phospholipid in bile. We examined effects of bile salt hydrophobicity on cytotoxicity and on differential SM and PC distribution between detergent-resistant aggregated vesicles (model for detergent-resistant canalicular membrane) and mixed micelles or small unilamellar vesicles (representing lipid phases in bile). *Methods:* Aggregated vesicles were obtained by ultracentrifugation of cholesterol-supersaturated model systems containing SM, PC and various bile salts, micelles by ultrafiltration and unilamellar vesicles by dialysis of the supernatant. Erythrocyte hemolysis and LDH release from CaCo-2 cells upon incubation with various micelles were quantified. *Results:* Preferential SM distribution and lipid solubilization in aggregated vesicles increased in rank order taurodeoxycholate < taurocholate < tauroursodeoxycholate < taurohyodeoxycholate, with reciprocal PC enrichment in micelles and small unilamellar vesicles. Including small amounts of PC within taurohyodeoxycholate micelles increased cytotoxicity with more erythrocyte hemolysis and LDH release from CaCo-2 cells upon incubation, but decreased cytotoxicity in case of tauroursodeoxycholate micelles. *Conclusions:* Hydrophilic but not hydrophobic bile salts preserve integrity of pathophysiologically relevant phosphatidylcholine plus sphingomyelin-containing bilayers. Enhanced biliary phospholipid secretion during taurohyodeoxycholate but not during tauroursodeoxycholate therapy (Hepatology 1997;25:1306-14) may relate to different interactions of these bile salts with phospholipids.

INTRODUCTION

Canalicular bile formation involves secretion of bile salts, phospholipids and cholesterol. *Mdr* (multi drug resistance) 2 P-glycoprotein functions as a “flippase” translocating phosphatidylcholine (PC) molecules from the inner to the outer leaflet of the hepatocyte canalicular membrane (1) and the bile salt export pump mediates bile salt transport over the membrane (2). Since unilamellar vesicles have been visualized by electron microscopy within the canalicular lumen (3), phospholipids and cholesterol may be secreted into bile by a vesicular mechanism. In addition, detergent canalicular bile salts could micellize considerable

amounts of phospholipids and cholesterol from the outer leaflet of the canalicular membrane (4,5).

Both sphingomyelin (SM) and phosphatidylcholine (PC) are the major structural phospholipids in the outer leaflet of the hepatocyte canalicular membrane (in an average ratio of 0.7)(6). In contrast, PC is the major (\approx 95%) phospholipid species secreted into bile (7), possibly due to a high lateral pressure in the membrane because of selective translocation of PC molecules by *mdr2* P-glycoprotein. The physical-chemical state of canalicular membrane phospholipids could also contribute to preferential biliary PC secretion: cholesterol has a higher affinity for SM than for PC (8-11) and may be tightly bound in laterally segregated and detergent-resistant SM domains in the membrane. Upon addition of bile salts to isolated canalicular membranes, there is considerable release of PC but not of SM from the membranes (12,13). These findings may relate to the different molecular structure of PC and SM: whereas natural PC's contain acyl chains esterified to the *sn*-1 and *sn*-2 positions of the glycerol backbone (mainly unsaturated acyl chains at the *sn*-2 position), natural SM's contain mainly saturated long acyl chains amide-linked to the sphingosine backbone, with the potential for extensive hydrogen-bonding between SM molecules (14).

In the rat model, infusion of hydrophobic bile salts causes cholestasis and a considerable increase of SM contents in bile (15). Similarly, we found in patients with benign recurrent intrahepatic cholestasis, considerable amounts of SM (10-15% of total phospholipids) in bile during cholestatic attacks, which was not the case in episodes without cholestasis (unpublished observations). On the other hand, the hydrophilic bile salt ursodeoxycholate may prevent or retard progressive liver damage in patients with cholestatic liver diseases such as primary biliary cirrhosis. A similar effect has been suggested for another hydrophilic bile salt,

hyodeoxycholate (16). Various mechanisms have been postulated for these beneficial effects, including reduction of damage of the hepatocyte canalicular membrane by more hydrophobic bile salts (17). We therefore examined in the present study effects of bile salt hydrophobicity on differential distribution of phospholipids between aggregated vesicles (that were considered because of their detergent-resistance as a model for detergent-resistant canalicular membrane (9,18)) and mixed micelles or small unilamellar vesicles (representing lipid phases in bile as visualized by electron microscopy (3,9)) in cholesterol-supersaturated model systems that contained various bile salts and both PC and SM. Although tauroursodeoxycholate and taurohyodeoxycholate have similar hydrophilicity as judged by their relative retention times at reverse phase HPLC (19), their biological effects *in vivo* are quite different: intraduodenal infusion of taurohyodeoxycholate but not tauroursodeoxycholate strongly enhances biliary phospholipid secretion (16,20). In order to examine potential mechanisms causing these differences, we also compared detergent effects of these bile salts in erythrocytes and in CaCo-2 cells.

MATERIAL AND METHODS

Materials

Taurodeoxycholate (TDC), taurocholate (TC), tauroursodeoxycholate (TUDC) and taurohyodeoxycholate (THDC) were obtained from Sigma Chemical Co. (St. Louis, MO, USA) and yielded a single spot upon thin-layer chromatography (butanol-acetic acid-water, 10:1:1 vol/vol/vol, application of 200 µg bile salt). Cholesterol (Sigma) was $\geq 98\%$ pure by reverse-phase HPLC (isopropanol - acetonitril 1:1, vol/vol, detection at 210 nm). Phosphatidylcholine from egg yolk (EYPC; Sigma) and sphingomyelin from egg yolk (EYSM; Avanti Polar-Lipids Inc.,

Alabaster, AL, USA) all yielded a single spot upon thin-layer chromatography (chloroform-methanol-water 65:25:4, vol/vol/vol, application of 200 µg lipid). Acyl-chain composition of EYSM as determined by gas-liquid chromatography (21) showed a preponderance of 16:0 acyl chains. As shown by reverse-phase HPLC, EYPC contained mainly 16:0 acyl chains at the *sn*-1 position and mainly unsaturated (18:1>18:2>20:4) acyl chains at the *sn*-2 position, similar to PC in human bile (22). All other chemicals and solvents were of ACS or reagent grade quality.

Ultrafilters with a molecular weight cut-off of 10 kDa and 300 kDa were purchased from Sartorius (Göttingen, Germany: Centrisart I), dialysis membranes with a molecular weight cut-off of 300 kDa from Spectrum Laboratories (Laguna Hills, CA, USA: SpectraPor). The enzymatic cholesterol assay kit was obtained from Boehringer (Mannheim, Germany). 3 α -Hydroxysteroid dehydrogenase for the enzymatic measurement of bile salt concentrations (23) and a colorimetric chloride-kit were purchased from Sigma. Dulbecco's modified Eagle's minimum essential medium (DMEM) was obtained from Flow Laboratories (Irvine, G.B.). The reverse-phase C18 HPLC column was from Supelco (Supelcosil LC-18-DB, Supelco, Bellefonte, PA, USA).

Preparation of lipid solutions

Lipid mixtures were vortex-mixed and dried at 45°C under a mild stream of nitrogen, and subsequently lyophilized during 24 hrs, before being dissolved in aqueous 0.15 M NaCl plus 3mM NaN₃. Tubes were sealed with Teflon-lined screw caps under a blanket of nitrogen and vortex-mixed for 5 min. followed by incubation at 37°C in the dark. The final mol percentages of cholesterol, phospholipids and bile salts did not differ more than 1% from the intended mol percentages.

Lipid analysis

Phospholipid concentrations in model systems were assayed by determining inorganic phosphate (24). Cholesterol concentrations were determined with an enzymatic assay (25), and bile salts with the 3 α -hydroxysteroid dehydrogenase method (23). In systems containing both PC and SM, the phospholipids were extracted (26), separated by thin-layer chromatography (chloroform-methanol-acetic acid-water 50:25:8:2, vol/vol/vol/vol), and quantified by determination of phosphorus contents.

IMC measurement

Apart from mixed (i.e. phospholipid-bile salt) micelles, model bile systems also contain non-phospholipid associated bile salts, either as monomers or -above their critical micellar concentration- associated in "simple" micelles. The monomeric plus simple micellar bile salt concentration is referred to as "intermixed micellar/vesicular (non phospholipid-associated) bile salt concentration", usually abbreviated as "IMC" (27). We determined IMC in various model systems, using the rapid centrifugal ultrafiltration technique with correction for Gibbs-Donnan effects (9,28,29).

Isolation of vesicular and micellar phases

After 2 weeks incubation at 37°C, various phases were isolated from cholesterol-supersaturated model systems as described (9). In brief, detergent-resistant aggregated vesicles were precipitated by ultracentrifugation during 30 min. at 50000 g and at 37°C in a TLS 55 rotor (Beckman, Palo Alto, CA, USA) (18). Micelles and small unilamellar vesicles were isolated from the supernatant by ultrafiltration with a highly selective 300 kDa ultrafilter resp. by dialysis (500 μ L sample, 16 hours, 37°C) in a SpectraPor[®] dialysis device with a

molecular weight cut-off of 300 kDa, against three times 20 volumes of aqueous 0.15 M NaCl plus 3 mM NaN₃ containing the relevant bile salt at concentrations identical to the IMC of the various original model systems in order to avoid artifactual shifts of lipids between vesicles and micelles (9,28). The ultrafilters and dialysis membranes were completely impermeable to small unilamellar or aggregated vesicles but completely permeable to simple and mixed micelles (tested with a wide range of micellar compositions (9), including TDC-, TC-, TUDC- or THDC-containing mixed micelles at 37°C, at total lipid concentration of 2.4 g/dL and at PL/(BS+PL) ratios of 0.55, 0.5, 0.4 and 0.3, either without or with small amounts (0.25 mol%) of cholesterol; with both SM and PC (SM/PC ratio 1:1) as phospholipid). Recovery of cholesterol and phospholipids in separated micellar, unilamellar and aggregated vesicular phases was 95-100 % of lipids in the original whole model system.

Preparation of small unilamellar vesicles

Small unilamellar vesicles were prepared by sonication, stored above 40°C (i.e. above the main transition temperatures of the phospholipids), and used within 12 hrs (28). Small unilamellar vesicles contained 8.4 mM EYPC, 8.4 mM EYSM and 6.9 mM cholesterol (cholesterol / phospholipid ratio 0.4).

Resistance of erythrocytes against various bile salt-phospholipid mixed micelles

Bile salt induced hemolysis was determined as described previously (28). Briefly, 0.2 mL of erythrocytes were added to 0.8 mL of TDC, TC, TUDC or THDC (bile salt conc. 2.5 to 180 mM), and incubated during 15 min. at 37°C. Thereafter, 7 mL buffer was added, in order to decrease hemolysis to negligible levels (30). After centrifugation for 1 min. at

10000 g, extent of lysis was assayed in the supernatant (absorbance at 540 nm) and compared with values after 15 min. incubation in distilled water, the latter inducing 100% hemolysis (31). Erythrocytes (0.2mL) were also added to 0.8mL TDC, TC, TUDC or THDC mixed micelles (180 mM) that contained increasing amounts of PC (PC/(BS+PC) ratios from 0 to 0.5). Experiments with THDC were also performed at a bile salt concentration of 50 mM.

Resistance of CaCo-2 cells against various bile salt-phospholipid mixed micelles

CaCo-2 cells were cultured as previously described (32) with minor modification (28). After 10 days, postconfluent cultures were washed with phosphate-buffered saline (pH 7.4) and cells were incubated with micelles containing TDC, TC, TUDC or THDC (30 mM) plus various amounts of PC (PC / (PC+BS) ratios from 0 to 0.4, pH 7.4). After 30 min. incubation at 37°C, the medium was collected and cells were treated with 0.4% Triton X-100. Lactate dehydrogenase (LDH) activity -as a sensitive parameter of cell damage- was measured according to Mitchell et al. (33) both in medium and in Triton X-100 treated cells. Enzyme activity in each single experiment was normalized as percentage of the total LDH activity (medium + Triton X-100 treated cells).

Quasielastic light scattering (QLS) spectroscopy

QLS measurements were performed on a Malvern 4700c QLS spectrometer (Malvern Ltd., Malvern, UK) equipped with an argon laser (Uniphase Corp., San Jose, CA, USA) at a wavelength of 488 nm and at an angle of 90°. All samples were maintained at a constant temperature of 37°C in a water bath, for at least 15 min. prior to measurements. In optically clear micellar solutions, the power of the laser was tuned to 50

mW. Data are given as hydrodynamic radius (Rh) and are means of at least 3 measurements.

Statistical analysis

Values are expressed as means \pm SEM. Differences between groups were tested for statistical significance by analysis of variance (ANOVA). When ANOVA detected a significant difference, results were further compared for contrasts using Fisher's least significant difference test as post-hoc test. Statistical significance was defined as a two-tailed probability of less than 0.05.

RESULTS

Effect of hydrophobic and hydrophilic bile salts on distribution of cholesterol and phospholipid between micellar and vesicular phases

Cholesterol supersaturated model systems containing both PC and SM, and TDC, TC, TUDC or THDC and plotting in the right two-phase zone of the equilibrium ternary phase diagram (inset Fig. 1 (34,35)) were all highly turbid and microscopic examination revealed large amounts of aggregated vesicles. Solid cholesterol crystals, however, were not observed. IMC values were 0.8 ± 0.1 mM, 3.7 ± 0.1 mM, 5.3 ± 0.1 mM and 4.9 ± 0.1 mM in TDC-, TC-, TUDC- and THDC-containing systems, resp. ($P < 0.05$, TDC, TC vs TUDC, THDC). As shown in Fig. 1A, cholesterol mainly distributed into the detergent-resistant aggregated vesicles. At increasing bile salt hydrophilicity, distribution of the sterol into aggregated vesicles increased, whereas distribution into small unilamellar vesicles and in mixed micelles decreased. In contrast, phospholipids distributed to a large extent into the micellar phase, particularly in case of

more hydrophobic bile salts (Fig. 1B). At increasing bile salt hydrophilicity, phospholipid solubilization in micelles decreased, and aggregated vesicles became the main phospholipid carriers. In contrast to cholesterol, phospholipid solubilization in small unilamellar vesicles increased at increasing bile salt hydrophilicity (Fig. 1B). Cholesterol/phospholipid ratios in micelles and small unilamellar vesicles decreased at increasing bile salt hydrophilicity (Table 1).

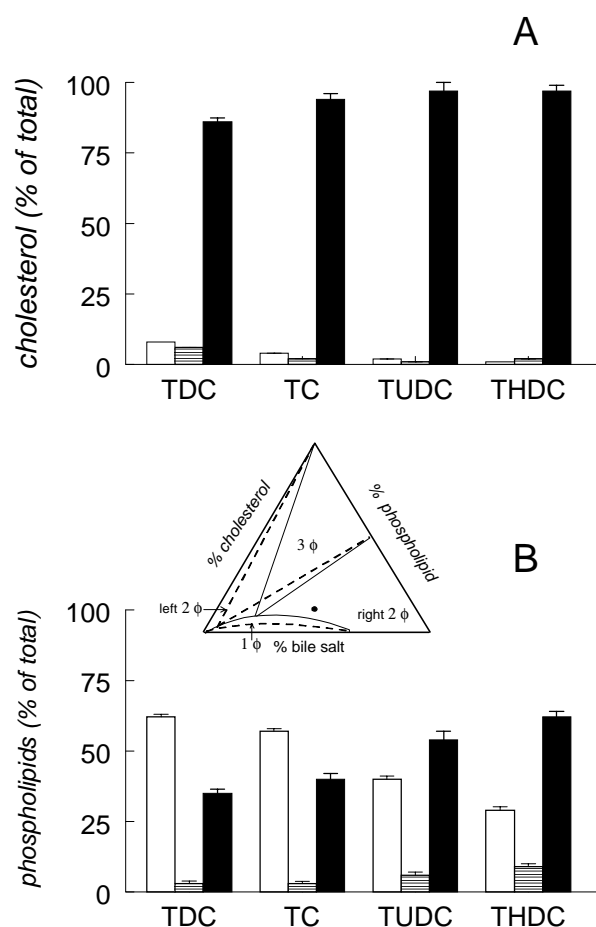


Figure 1: Solubilization of cholesterol (A) and phospholipids (B) in aggregated vesicles (solid bars), small unilamellar vesicles (hatched bars) and mixed micelles (open bars) in model systems containing 6.9 mM cholesterol, 8.4 mM PC, 8.4 mM SM, and 16.8 mM TDC, TC, TUDC or THDC after 2 weeks incubation at 37°C (total lipid concentration = 2.4 g/dL, PL/(BS+PL) ratio = 0.5, 17 mol% cholesterol; $n=4$ for each bile salt). At increasing bile salt hydrophilicity, solubilization of cholesterol and (more pronounced) phospholipids in aggregated vesicles increases significantly, with reciprocal decreases of solubilization in micelles. Whereas solubilization of cholesterol in small unilamellar vesicles decreases significantly at increasing bile salt

hydrophilicity, solubilization of phospholipids in small unilamellar vesicles increases significantly under these circumstances.

Inset: equilibrium bile salt-phospholipid-cholesterol ternary phase diagram. 1ϕ = 1-phase (micelles-containing) zone; 2ϕ = 2-phase (left: micelles+solid crystals; right: micelles+vesicles) zones; 3ϕ = 3-phase (micelles+vesicles+solid crystals-containing) zone. Dot indicates model bile plotting in right two-phase zone. Continuous line: phase diagram for EYPC and hydrophobic bile salts. Interrupted line: decreased one-phase micellar zone and extension of right two-phase zone in case of more hydrophilic bile salts or sphingomyelin as phospholipid (19,32).

Table 1. Cholesterol / Phospholipid ratios of various phases in cholesterol supersaturated model biles

	Cholesterol/Phospholipid ratio		
	AGG	SUV	MIC
TDC	0.94 ± 0.09	0.65 ± 0.05	0.05 ± 0.02
TC	1.05 ± 0.10	0.45 ± 0.05	0.04 ± 0.004
TUDC	0.98 ± 0.12	0.29 ± 0.02	0.03 ± 0.009
THDC	0.93 ± 0.09	0.35 ± 0.05	0.03 ± 0.01

AGG = aggregated vesicles. SUV = small unilamellar vesicles: Significant difference in cholesterol/phospholipid ratios for all bile salts. MIC = micelles: Significant difference in cholesterol/phospholipid ratios for TDC vs TUDC or THDC.

Effect of hydrophobic and hydrophilic bile salts on distribution of sphingomyelin and phosphatidylcholine between vesicles and micelles

Fig. 2 shows the distribution of SM and PC into micelles, small unilamellar and aggregated vesicles. Micellar enrichment with PC and enrichment of aggregated vesicles with SM was evident in all systems, but was most pronounced in the case of hydrophilic bile salts. Small unilamellar vesicles also tended to be depleted in SM. We also added TDC, TC, TUDC or THDC to sonicated PC-, SM- and cholesterol-containing vesicles, and determined SM/PC ratios in micelles (obtained

by ultrafiltration) at 15 min., 1 hr and 12 hrs. There was a progressive depletion of SM in micelles during the experiment, which was most pronounced in case of hydrophilic bile salts (Fig. 3).

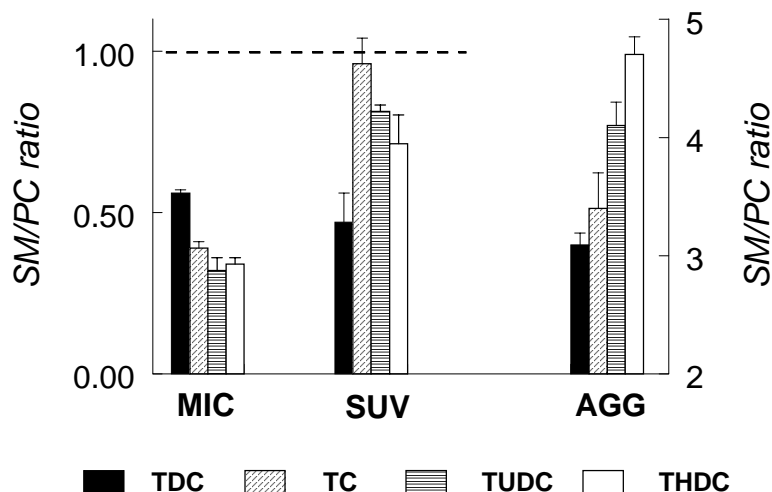


Figure 2: Distribution of SM and PC between aggregated vesicles, small unilamellar vesicles and micelles. Lipid compositions and duration of incubation of the systems were the same as in Fig. 1 ($n=4$ for each bile salt). SM preferentially distributes into aggregated vesicles with reciprocal SM depletion in micelles and small unilamellar vesicles. Asymmetric phospholipid distribution is most pronounced in case of more hydrophilic bile salts. Reciprocal results were obtained for PC solubilization. Interrupted line indicates SM / PC ratio in whole system. Left Y axis applies to micelles and small unilamellar vesicles, right Y axis to aggregated vesicles. MIC = micelles; SUV = small unilamellar vesicles; AGG = aggregated vesicles.

Effect of hydrophobic and hydrophilic bile salts on distribution of sphingomyelin and phosphatidylcholine between vesicles and micelles

Fig. 2 shows the distribution of SM and PC into micelles, small unilamellar and aggregated vesicles. Micellar enrichment with PC and enrichment of aggregated vesicles with SM was evident in all systems, but was most pronounced in the case of hydrophilic bile salts. Small unilamellar vesicles also tended to be depleted in SM. We also added TDC, TC, TUDC or THDC to sonicated PC-, SM- and cholesterol-

containing vesicles, and determined SM/PC ratios in micelles (obtained by ultrafiltration) at 15 min., 1 hr and 12 hrs. There was a progressive depletion of SM in micelles during the experiment, which was most pronounced in case of hydrophilic bile salts (Fig. 3).

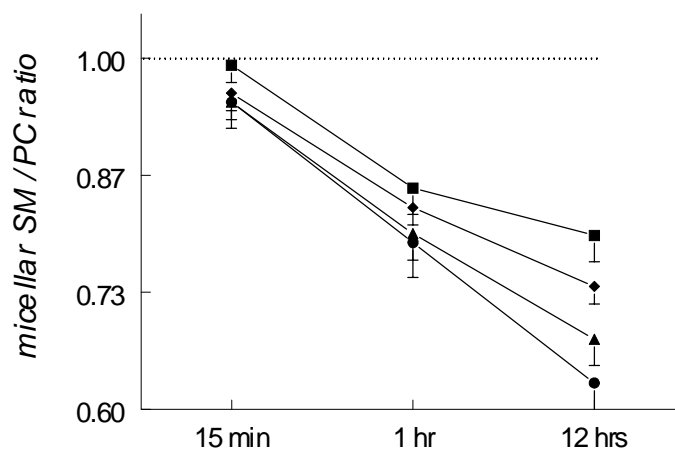


Figure 3: SM and PC distribution into the micellar phase, as determined by ultrafiltration at various time points after addition of TDC, TC, TUDC or THDC (final bile salt conc. 16.8 mM) to sonicated small unilamellar vesicles containing cholesterol (final conc. 6.9 mM) and both PC and SM (SM/PC ratio 1:1; final phospholipid conc. 16.8 mM). Temperature was maintained at 37°C throughout the experiment (n=4 for each bile salt). SM solubilization in micelles decreases during the experiment. Decreases occur at an earlier stage and are most pronounced in case of hydrophilic bile salts. Differences between each time point and between all bile salts are significant. Interrupted line indicates SM / PC ratio in whole system. (■) TDC; (◆) TC; (▲) TUDC; (●) THDC.

Effect of hydrophobic and hydrophilic bile salts on distribution of sphingomyelin and phosphatidylcholine between vesicles and micelles

Fig. 2 shows the distribution of SM and PC into micelles, small unilamellar and aggregated vesicles. Micellar enrichment with PC and enrichment of aggregated vesicles with SM was evident in all systems, but was most pronounced in the case of hydrophilic bile salts. Small

unilamellar vesicles also tended to be depleted in SM. We also added TDC, TC, TUDC or THDC to sonicated PC-, SM- and cholesterol-containing vesicles, and determined SM/PC ratios in micelles (obtained by ultrafiltration) at 15 min., 1 hr and 12 hrs. There was a progressive depletion of SM in micelles during the experiment, which was most pronounced in case of hydrophilic bile salts (Fig. 3).

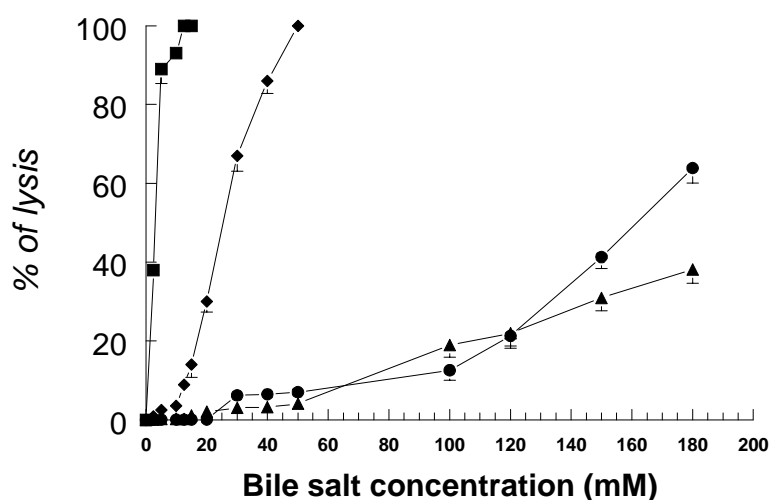


Figure 4: Effect of bile salt hydrophobicity on lysis of human erythrocytes. Red blood cells were incubated for 15 min. at 37°C with distilled water (100% lysis) or with increasing concentrations of various bile salts (see “Materials and Methods” (n=4 for each bile salt)). Whereas low concentrations of TDC or slightly higher concentrations of TC result in 100% hemolysis, this is not the case for TUDC and THDC even after incubation with extremely high concentrations.
(■) TDC; (◆) TC; (▲) TUDC; (●) THDC.

Hemolysis induced by hydrophobic and hydrophilic bile salts and protective effects of phosphatidylcholine

Although low concentrations (≥ 10 mM) of TDC and slightly higher concentrations (≥ 50 mM) of TC induced 100 % hemolysis, incubation with TUDC or THDC, up to 180 mM, induced only moderate hemolysis (Fig. 4). As displayed in Fig. 5, incorporation of PC at PC/(BS+PC)

ratios of ≥ 0.3 in TUDC micelles prevented cytolysis completely, whereas the same protective effects occurred for TC-PC and TDC-PC micelles at PC / (BS+PC) ratios of ≥ 0.4 resp. ≥ 0.5 . In contrast, incorporation of PC in THDC micelles did not prevent, but rather increased hemolysis to maximal values (Fig. 5). At 50 mM bile salt concentration, there was increased hemolysis upon incubation with THDC-PC micelles at PC/(BS+PC) ratios of 0.1 and 0.2 with a reduction at higher ratios (Fig. 5).

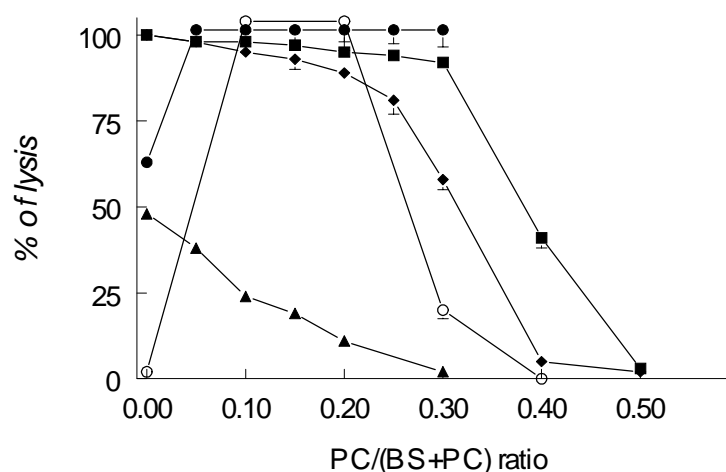


Figure 5: Protective effect of PC against lysis of human erythrocytes induced by hydrophobic or hydrophilic bile salts. Red blood cells were incubated for 15 min. at 37°C with micelles containing various bile salts (180 mM) and progressive amounts of PC ($n=5$ for each bile salt). For all bile salts except THDC, hemolysis is progressively inhibited at increasing PC contents. In contrast, in case of THDC, hemolysis increases when PC is included in these micelles. The increased detergent effects of THDC mixed micelles compared to simple micelles are even more evident at 50 mM bile salt concentration.

(■) TDC; (◆) TC; (▲) TUDC; (●) THDC (all 180 mM bile salt conc); (○) THDC 50 mM

LDH release by CaCo-2 cells induced by hydrophobic and hydrophilic bile salts and protective effects of phosphatidylcholine

As shown in Fig. 6, LDH release upon incubation of CaCo-2 cells with TUDC micelles was always negligible regardless the presence of PC. Incorporation of increasing amounts of PC in TDC- and TC-micelles progressively reduced LDH release: virtually complete protection occurred at PC/(BS+PC) ratios of 0.4 and 0.3 for TDC-PC resp. TC-PC micelles. In contrast, incorporation of PC in THDC micelles at a PC/(BS+PC) ratio of 0.1 increased rather than decreased LDH release. At higher PC/(BS+PC) ratios, LDH decreased again, with complete protection at ratios of ≥ 0.3 .

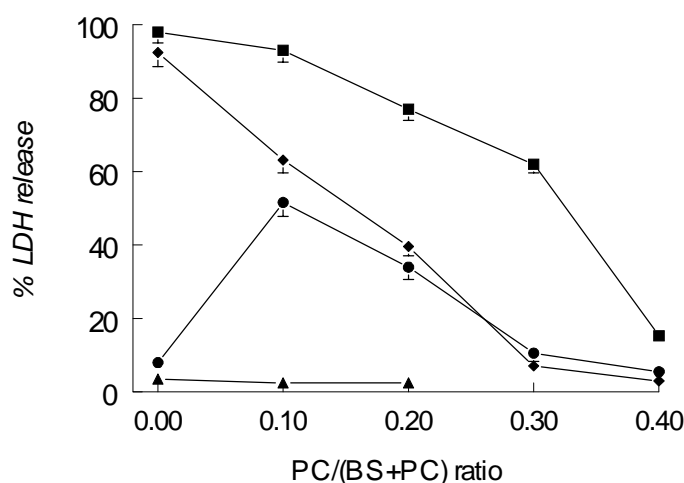


Figure 6: Effect of PC on LDH release by CaCo-2 cells induced by various bile salts. CaCo-2 cells were incubated for 30 min. at 37°C with micelles containing various bile salts (30 mM) and progressive amounts of PC ($n=4$ for each bile salt). LDH release by TUDC micelles is always negligible regardless the presence of PC. For TC and TDC, LDH release is progressively inhibited at increasing PC contents. Virtually complete prevention of LDH release occurs at PC/(BS+PC) ratios of 0.3 and 0.4 for TC and TDC respectively. The pattern is different in case of THDC: LDH release increases when PC is included in micelles at PC/(BS+PC) ratios of 0.1, with a reduction at higher ratios (complete prevention of LDH release at PC/(BS+PC) ratio ≥ 0.3). (■) TDC; (◆) TC; (▲) TUDC; (●) THDC.

Effects of phosphatidylcholine on micellar sizes

As shown in Fig. 7, TC and TUDC micellar sizes as measured by quasi-elastic light scattering spectroscopy increased progressively at increasing PC content. In case of THDC, micellar sizes were relatively high in absence of PC. There was a decrease in micellar sizes at PC/(BS+PC) ratio of 0.1, with an increase at higher ratios. For TDC-containing micelles, sizes at PC/(BS+PC) ratios of 0 and 0.1 did not differ, but sizes increased at higher PC contents.

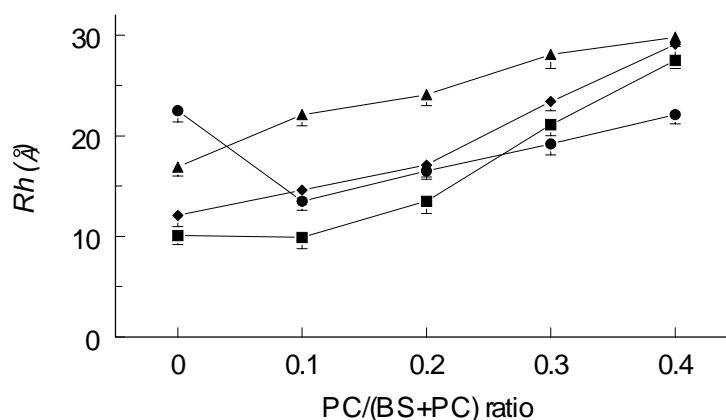


Figure 7: Micellar sizes, expressed as hydrodynamic radius (R_h), as measured by quasielastic light scattering spectroscopy, in solutions containing various bile salts (conc. 30 mM) and increasing amounts of PC ($n=4$ for each bile salt). Whereas in case of TC or TUDC solutions, micellar sizes increase progressively at increasing PC contents, in case of THDC there is a decrease of micellar size at PC/(BS+PC) ratio 0.1, with increased sizes at higher ratios. In case of TDC micelles, sizes at PC/(BS+PC) ratios 0 and 0.1 do not differ, but sizes increase at higher ratios.

(■) TDC; (◆) TC; (▲) TUDC; (●) THDC.

DISCUSSION

The main finding of the present *in vitro* study was that bile salt hydrophobicity had a strong influence on differential PC vs SM distribution: in cholesterol-supersaturated systems that contained both PC and SM, preferential SM distribution into detergent-resistant aggregated vesicles and preferential PC distribution into small unilamellar vesicles and micelles occurred in the rank order TDC < TC < TUDC < THDC. Similarly, in a time-course study, after addition of various bile salts to sonicated vesicles that contained PC, SM and cholesterol, enrichment of PC in micelles occurred earlier and to a larger extent in case of hydrophilic bile salts.

The great majority of cholesterol (84-96% of total) distributed into the aggregated vesicles, whereas micelles were a prominent (29-62% of total) phospholipid carrier. These findings are consistent with the much greater potential of micelles to solubilize phospholipids than cholesterol (36,37) The increased solubilization of lipids in aggregated vesicles and decreased solubilization in micelles in case of hydrophilic bile salts (Fig. 1) is not unexpected, given the strong reduction of the one-phase micellar zone and the marked left-ward expansion of the right two-phase (micelles + vesicles-containing) zone in the EYPC-cholesterol-bile salt equilibrium ternary phase diagram in case of hydrophilic compared to hydrophobic bile salts (see inset Fig. 1 (35)). In fact, this left-ward expansion of the right two-phase zone may relate to decreased cholesterol/phospholipid ratios and increased stability of small unilamellar vesicles at increasing bile salt hydrophilicity as found in the present study (Table 1)(38).

Although these data indicate that hydrophilic but not hydrophobic bile salts preserve integrity of pathophysiologically relevant PC+SM-containing bilayers, there were no significant differences between TUDC and THDC. In contrast to TUDC, THDC treatment induces a marked

increase in biliary phospholipid secretion *in vivo* (16,20). We therefore proceeded to the erythrocyte and CaCo-2 cell models in order to quantify detergent effects of various bile salts as well as protective effects of including PC within these micelles. In the erythrocyte model, TDC caused 100% hemolysis at low concentrations, whereas the same occurred at slightly higher concentrations for TC. In contrast, both TUDC and THDC caused only moderate hemolysis, even at very high concentrations. Nevertheless, including increasing amounts of PC within the micelles progressively decreased hemolysis in case of TUDC but increased hemolysis in case of THDC. Similar results were obtained in the CaCo-2 cell model. We have previously shown in the erythrocyte or CaCo-2 cell models that protective effects of including PC within bile salt micelles occur at the level of these micelles rather than by transfer of PC molecules from these micelles into the cell membrane (28). Our present findings suggest different bile salt-phospholipid interactions and micellar structures for TUDC and THDC. In case of THDC (but not TUDC), incorporation of PC may promote micelle formation with decreased particle sizes as a result of packing constraints. This suggestion is supported by the different patterns of micellar size variations for THDC and TUDC at progressive micellar PC contents (Fig. 7). Although these differences may be relevant for the biological effects of TUDC vs THDC *in vivo*, the exact physical-chemical explanation of our findings needs further research. One should also realize, that differential effects of TUDC vs THDC on intracellular PC transport (possibly mediated by PC transfer protein (39)) or on *mdr2* P-glycoprotein could be involved in their different effects on biliary PC secretion. In addition, results of our model bile studies (Figs 1 and 2) were obtained after two-weeks incubation, with the systems probably being near thermodynamic equilibrium.

In summary, the present study indicates that hydrophilic but not hydrophobic bile salts preserve integrity of pathophysiologically relevant phosphatidylcholine- plus sphingomyelin-containing bilayers, with enhanced differential distribution of PC vs SM between micellar and vesicular phases. Different bile salt-phospholipid interactions may account for the different *in vivo* effects of the hydrophilic bile salts tauroursodeoxycholate and taurohyodeoxycholate.

References

1. Smit JJ, Schinkel AH, Oude Elferink RPJ, Groen AK, Wagenaar E, van Deemter L et al. Homozygous disruption of the murine *mdr2* P-glycoprotein gene leads to a complete absence of phospholipid from bile and to liver disease. *Cell* 1993; 75:451-462.
2. Gerloff T, Stieger B, Hagenbuch B, Madon J, Landmann L, Roth J et al. The sister of P-glycoprotein represents the canalicular bile salt export pump of mammalian liver. *J Biol Chem* 1998; 273:10046-10050.
3. Crawford JM, Mockel GM, Crawford AR, Hagen SJ, Hatch VC, Barnes S et al. Imaging biliary lipid secretion in the rat: ultrastructural evidence for vesiculation of the hepatocyte canalicular membrane. *J Lipid Res* 1995; 36:2147-2163.
4. Oude Elferink RPJ, Tytgat GNJ, Groen AK. The role of *mdr2* P-glycoprotein in hepatobiliary lipid transport. *FASEB J* 1997; 11:19-28.
5. Smith AJ, de Vree JM, Ottenhoff R, Oude Elferink RP, Schinkel AH, Borst P. Hepatocyte-specific expression of the human MDR3 P-glycoprotein gene restores the biliary phosphatidylcholine excretion absent in *Mdr2* (-/-) mice. *Hepatology* 1998; 28:530-536.
6. Higgins JA, Evans WH. Transverse organization of phospholipids across the bilayer of plasma membrane subfractions of rat hepatocytes. *Biochem J* 1978; 174:563-567.
7. Alvaro D, Cantafora A, Attili AF, Ginanni CS, De Luca C, Minervini G et al. Relationships between bile salts hydrophilicity and phospholipid composition in bile of various animal species. *Comp Biochem Physiol [B]* 1986; 83:551-554.
8. Lund-Katz S, Laboda HM, McLean LR, Phillips MC. Influence of molecular packing and phospholipid type on rates of cholesterol exchange. *Biochemistry* 1988; 27:3416-3423.
9. Eckhardt ERM, Moschetta A, Renooij W, Goerdal SS, vanBerge-Henegouwen GP, van Erpecum KJ. Asymmetric distribution of

- phosphatidylcholine and sphingomyelin between micellar and vesicular phases: potential implication for canalicular bile formation. *J Lipid Res* 1999; 40:2022-2033.
10. Bar LK, Barenholz Y, Thompson TE. Dependence on phospholipid composition of the fraction of cholesterol undergoing spontaneous exchange between small unilamellar vesicles. *Biochemistry* 1987; 26:5460-5465.
 11. Mattjus P, Bittman R, Vilcheze C, Slotte JP. Lateral domain formation in cholesterol/phospholipid monolayers as affected by the sterol side chain conformation. *Biochim Biophys Acta* 1995; 1240:237-247.
 12. Yousef IM, Fisher MM. In vitro effect of free bile acids on the bile canalicular membrane phospholipids in the rat. *Can J Biochem* 1976; 54:1040-1046.
 13. Gerloff T, Meier PJ, Stieger B. Taurocholate induces preferential release of phosphatidylcholine from rat liver canalicular vesicles. *Liver* 1998; 18:306-312.
 14. Nibbering CP, Carey MC. Sphingomyelins of rat liver: biliary enrichment with molecular species containing 16:0 fatty acids as compared to canalicular-enriched plasma membranes. *J Membr Biol* 1999; 167:165-171.
 15. Barnwell SG, Tuchweber B, Yousef IM. Biliary lipid secretion in the rat during infusion of increasing doses of unconjugated bile acids. *Biochim Biophys Acta* 1987; 922:221-233.
 16. Loria P, Bozzoli M, Concari M, Guicciardi ME, Carubbi F, Bertolotti M et al. Effect of taurohyodeoxycholic acid on biliary lipid secretion in humans. *Hepatology* 1997; 25:1306-1314.
 17. van Erpecum KJ, Portincasa P, Eckhardt ERM, Go PMNYH, vanBerge-Henegouwen GP, Groen AK. Ursodeoxycholic acid reduces protein levels and nucleation-promoting activity in human gallbladder bile. *Gastroenterology* 1996; 110:1225-1237.
 18. Schroeder RJ, London E, Brown DA. Interactions between saturated acyl chains confer detergent resistance on lipids and glycosylphosphatidylinositol (GPI)-anchored proteins: GPI-anchored proteins in liposomes and cells show similar behavior. *Proc Natl Acad Sci U S A* 1994; 91:12130-12134.
 19. Heuman DM. Quantitative estimation of the hydrophilic-hydrophobic balance of mixed bile salt solutions. *J Lipid Res* 1989; 30:719-730.
 20. Angelico M, Baiocchi L, Nistri A, Franchitto A, Della Guardia P, Gaudio E. Effect of taurohyodeoxycholic acid, a hydrophilic bile salt, on bile salt and biliary lipid secretion in the rat. *Dig Dis Sci* 1994; 39:2389-2397.
 21. Hakomori S. Chemistry of Glycosphingolipids. In: Hanahan DJ, editor. *Handbook of Lipid Research*. New York: Plenum Press, 1983: 37-39.
 22. Hay DW, Cahalane MJ, Timofeyeva N, Carey MC. Molecular species of lecithins in human gallbladder bile. *J Lipid Res* 1993; 34:759-768.

23. Turley SD, Dietschy JM. Reevaluation of the 3 α -hydroxysteroid dehydrogenase assay for total bile acids in bile. *J Lipid Res* 1978; 19:924-928.
24. Rouser G, Fleischer S, Yamamoto A. Two dimensional thin layer chromatographic separation of polar lipids and determination of phospholipids by phosphorus analysis of spots. *Lipids* 1970; 5:494-496.
25. Fromm H, Hamin P, Klein H, Kupke I. Use of a simple enzymatic assay for cholesterol analysis in human bile. *J Lipid Res* 1980; 21:259-261.
26. Bligh EG, Dyer WJ. A rapid method of total lipid extraction and purification. *Can J Biochem Physiol* 1959; 37:911-917.
27. Donovan JM, Timofeyeva N, Carey MC. Influence of total lipid concentration, bile salt:lecithin ratio, and cholesterol content on inter-mixed micellar/vesicular (non-lecithin-associated) bile salt concentrations in model bile. *J Lipid Res* 1991; 32:1501-1512.
28. Moschetta A, van Berge-Henegouwen GP, Portincasa P, Palasciano G, Groen AK, van Erpecum KJ. Sphingomyelin exhibits greatly enhanced protection compared with egg yolk phosphatidylcholine against detergent bile salts. *J Lipid Res* 2000; 41:916-924.
29. Donovan JM, Jackson AA. Rapid determination by centrifugal ultrafiltration of inter-mixed micellar/vesicular (non-lecithin-associated) bile salt concentrations in model bile: influence of Donnan equilibrium effects. *J Lipid Res* 1993; 34:1121-1129.
30. Heuman DM, Pandak WM, Hylemon PB, Vlahcevic ZR. Conjugates of ursodeoxycholate protect against cytotoxicity of more hydrophobic bile salts: in vitro studies in rat hepatocytes and human erythrocytes. *Hepatology* 1991; 14:920-926.
31. Velardi ALM, Groen AK, Oude Elferink RP, van der Meer R, Palasciano G, Tytgat GN. Cell type-dependent effect of phospholipid and cholesterol on bile salt cytotoxicity. *Gastroenterology* 1991; 101:457-464.
32. Mohrmann I, Mohrmann M, Biber J, Urer H. Sodium-dependent transport of Pi by an established intestinal epithelial cell line (CaCo-2). *Am J Physiol* 1986; 250:G323-G330.
33. Mitchell DB, Santone KS, Acosta D. Evaluation of cytotoxicity in cultured cells by enzyme leakage. *J Tissue Cult Methods* 1980; 6:113-116.
34. van Erpecum KJ, Carey MC. Influence of bile salts on molecular interactions between sphingomyelin and cholesterol: relevance to bile formation and stability. *Biochim Biophys Acta* 1997; 1345:269-282.
35. Wang DQH, Carey MC. Complete mapping of crystallization pathways during cholesterol precipitation from model bile: influence of physical-chemical variables of pathophysiologic relevance and identification of a stable liquid

- crystalline state in cold, dilute and hydrophilic bile salt-containing systems. *J Lipid Res* 1996; 37:606-630.
36. Cohen DE, Angelico M, Carey MC. Structural alterations in lecithin-cholesterol vesicles following interactions with monomeric and micellar bile salts: physical-chemical basis for subselection of biliary lecithin species and aggregative states of biliary lipids during bile formation. *J Lipid Res* 1990; 31:55-70.
 37. Carey MC, Cohen DE. Biliary transport of cholesterol in vesicles, micelles and liquid crystals. In: Paumgartner G, Stiehl A, Gerok W, editors. *Bile acids and the liver with an update on gallstone disease*. Lancaster: MTP Press, 1987: 287-300.
 38. Halpern Z, Dudley MA, Lynn MP, Nader JM, Breuer AC, Holzbach RT. Vesicle aggregation in model systems of superaturated bile: relation to crystal nucleation and lipid composition of the vesicular phase. *J Lipid Res* 1986; 27:295-306.
 39. Cohen DE, Leonard MR, Carey MC. In vitro evidence that phospholipid secretion into bile may be coordinated intracellularly by the combined actions of bile salts and the specific phosphatidylcholine transfer protein of liver. *Biochemistry* 1994; 33:9975-9980.

chapter 8

**SPHINGOMYELIN OFFERS PROTECTION AGAINST
APOPTOSIS AND HYPERPROLIFERATION
INDUCED BY THE HYDROPHOBIC BILE SALT
DEOXYCHOLATE:
POTENTIAL IMPLICATIONS FOR COLON CANCER**

Antonio Moschetta^{*}, Piero Portincasa^{*}, Karel J. van Erpecum,
Gerard P. vanBerge-Henegouwen, Giuseppe Palasciano

preliminary data

^{*} *Authors who equally contributed to the work*

Summary

High fecal levels of hydrophobic bile salt deoxycholate are associated with increased risk of colonic adenomas and cancer. Since phospholipids protect against detergent effects and cytotoxicity of bile salt micelles, and ~30% of dietary sphingomyelin reaches the colon, we examined whether sphingomyelin influences apoptosis and hyperproliferation induced by deoxycholate in vitro. Methods: In CaCo-2 cells, apoptosis with concomitant caspase-3 activity was quantitated after 2, 4 and 16 hrs incubation with 50-500 μ M deoxycholate, with or without sphingomyelin. Hyperproliferation (by bromodeoxyuridine assay) and phosphorylation of cellular proteins were evaluated after 16 hrs incubation. In erythrocytes, phosphatidylserine exposure upon incubation with deoxycholate -with or without sphingomyelin- was determined by quantitating its binding to annexin V. Results: at 2 hrs and 4 hrs incubation, deoxycholate induced dose-dependent apoptosis, with concomitant caspase-3 activation. At 16 hrs, apoptosis had decreased markedly, but there was dose-dependent hyperproliferation (with changed phosphorylation status of cellular proteins) at this time-point. Deoxycholate also induced in the erythrocyte model (without intracellular signaling and nucleus) phosphatidylserine exposure on the membrane outer leaflet. Sphingomyelin dose-dependently reduced hyperproliferation, apoptosis and phosphatidylserine exposure at all time points. Conclusions: sphingomyelin reduced hyperproliferation and apoptosis by deoxycholate possibly by decreasing detergent activity of the bile salt in the incubation medium. These findings may be relevant for colonic cancer protection by dietary modification.

Introduction

In Western populations on high fat diet, there is a clear association between fecal bile salt excretion and risk of colon cancer (1;2). In particular, the secondary and hydrophobic bile salt deoxycholate may act as tumor promotor by inducing hyperproliferation (3-5). Deoxycholate has also been shown to increase the numbers of tumors induced by complete carcinogens (6;7). On the other hand, deoxycholate may also induce apoptosis in some adenoma and carcinoma cell lines (8-11).

Although phospholipids with unsaturated acyl chains at the *sn*-2 position such as egg yolk phosphatidylcholine or phosphatidylcholine in bile decrease detergent effects and cytotoxicity of bile salt micelles (12),

phosphatidylcholines with disaturated acyl chains such as dipalmitoyl phosphatidylcholine or sphingomyelins are considerably more effective in this respect (13). The human diet contains considerable amounts of phosphatidylcholines and sphingomyelins. Recent data indicate that disaturated phosphatidylcholines such as dipalmitoyl phosphatidylcholine are more resistant to hydrolysis by phospholipase A₂ than phosphatidylcholines with unsaturated acyl chains (14). Similarly, although alkaline sphingomyelinase in bile (15) and in the small intestine (16) may hydrolyze sphingomyelin, considerable amounts (~30% of ingested quantities) of the sphingolipid appear to reach the colon (17-19). Dietary supplementation with sphingomyelin has been shown to suppress experimental colon cancer in mice (20). We therefore examined potential effects of sphingomyelin on hyperproliferation or apoptosis induced by deoxycholate in the CaCo-2 cell model.

MATERIALS AND METHODS

Materials

Deoxycholate (DC) was obtained from Sigma Chemical Co. (St. Louis, MO, USA) and yielded a single spot upon thin-layer chromatography (butanol-acetic acid-water, 10:1:1 vol/vol/vol, application of 200 µg bile salt). Sphingomyelin from egg yolk (EYSM; Avanti Polar-Lipids Inc., Alabaster, AL, USA) yielded a single spot upon thin-layer chromatography (chloroform-methanol-water 65:25:4, vol/vol/vol, application of 200 µg lipid). Acyl chain compositions as determined by gas-liquid chromatography (21) were virtually identical to previously published data (22) and showed a preponderance of 16:0 acyl chains for EYSM, similar to sphingomyelin in human bile (23). Dulbecco's modified Eagle's minimum essential medium (DMEM) was obtained from Flow Laboratories (Irvine, G.B.). All other chemicals and solvents were of ACS or reagent grade quality.

3 α -Hydroxysteroid dehydrogenase, the Bradford reagent and the caspase-3 assay were purchased from Sigma. The cell proliferation elisa BrdU kit and the

cell death detection elisa kit were purchased from Roche Molecular Biochemicals (Mannheim, Germany). The Annexin V-fluorescein isothiocyanate (FITC) apoptosis detection kit was obtained from BD PharMingen (San Diego, USA).

Preparation of lipid solutions

Lipid mixtures containing variable proportions of deoxycholate (from stock solutions in methanol) and/or sphingomyelin (from stock solutions in chloroform) were vortex-mixed and dried at 45°C under a mild stream of nitrogen, before being dissolved in DMEM supplemented with 20% fetal calf serum (Gibco, New England, N.Y., USA). Solutions were prepared freshly for all experiments. Bile salt concentrations were assayed by the 3 α -hydroxysteroid dehydrogenase method (24) and sphingomyelin concentrations by determining inorganic phosphate according to Rouser (25).

Cell culture

CaCo-2 cells were grown in T-75 plastic flasks in DMEM supplemented with 20% fetal calf serum (Gibco, New England, N.Y., USA), 50 U/mL penicillin and 50 U/mL streptomycin (Irvine, GB). Before confluency, the cells were split (split ratio 1:8) as follows: CaCo-2 cells were rinsed twice with Hank's balanced salt solution (Gibco, New England, N.Y., USA) and incubated during 5 min. at 37°C with 1 mL of dissociation solution (Sigma, St. Louis MO, USA), after DMEM medium supplemented with 20% fetal calf serum was added to the cell suspension. Monolayers were grown in microwell plates in DMEM, which was replaced daily with fresh medium. After 10 days, the postconfluent cultures were washed with phosphate-buffered saline (pH 7.4) and the cells were incubated with DC at various concentrations (from 50 to 500 μ M) and at various incubation times (2hrs, 4hrs and 16 hrs). Experiments were also conducted with DC 400 μ M and 500 μ M plus SM at SM/(DC+SM) molar ratios ranging from 0 to 0.3 as well as with SM alone in concentrations from 50 to 200 μ M.

Apoptosis was measured based on a photometric enzyme immunoassay for the qualitative and quantitative determination of cytoplasmic DNA fragments (26).

Caspase-3 activity was assayed by the spectrophotometric detection (OD 405 nm) of the chromophore p-nitroaniline after hydrolysis of the peptide substrate acetyl-Asp-Glu-Val-Asp (Ac-DEVD-pNA) (27).

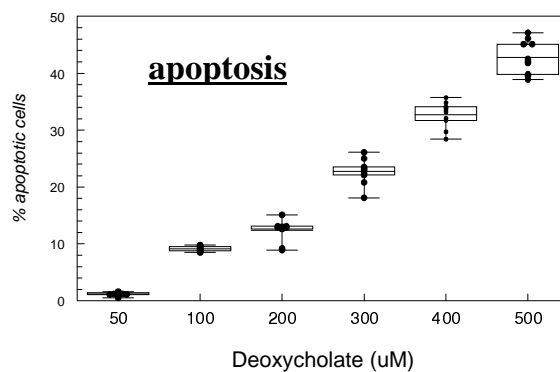
Proliferation was assayed by determining incorporation of the pyrimidine analogue bromodeoxyuridine (BrdU) during DNA synthesis (3). After incubation with the bile salt solution, BrdU was added to the cells, followed by reincubation during 4 hrs.

Phosphorylation status of proteins in cell lysates was determined with a Western blot (Mini Protean Biorad) using a specific antiphosphotyrosine antibody, after 16 hrs incubation.

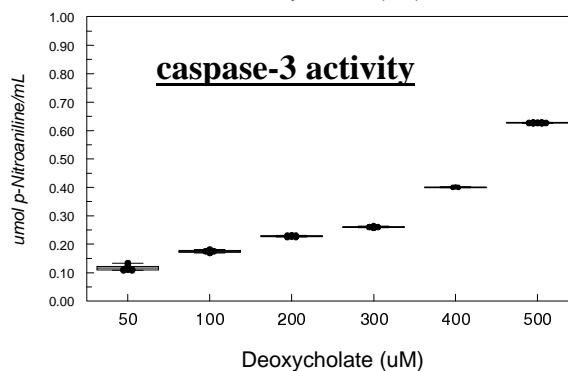
Annexin V-phosphatidylserine binding in erythrocytes. Phosphatidylserine (PS) normally localizes to the inner leaflet of cell membrane but becomes exposed to the cell surface after pro-apoptotic stimuli (28). Erythrocytes cannot undergo apoptosis because they lack a nucleus, but PS-exposure signals the removal of aged red cells from the circulation (29;30). Annexin V belongs to a family of phospholipid binding proteins and exhibits a high calcium-dependent affinity for membranes containing PS in their outer leaflets (31). First, we isolated and washed red blood cells obtained freshly from a single volunteer; then we incubated these cells for 30 min. at 37°C with DCA and/or SM. Finally, we measured cell-associated fluorescence in a Becton Dickinson FACScan, according with Kuypers *et al.* (32), after addition of FITC-labeled annexin V in the presence of calcium. During each incubation, hemolysis was also determined by measuring release of hemoglobin in supernatant (13).

Figure 1

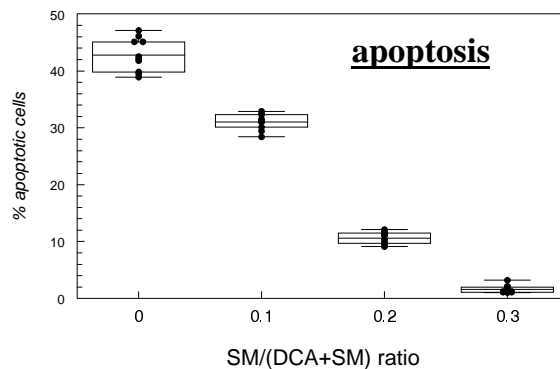
A



B



C



D

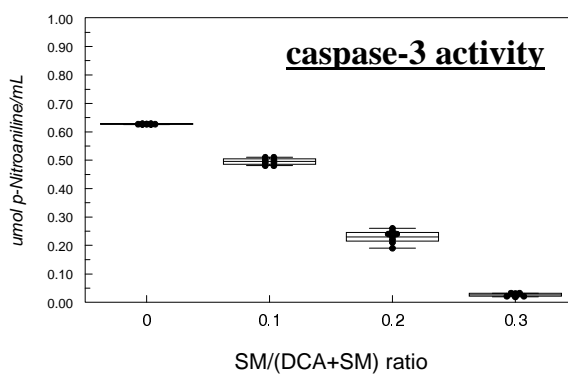


Figure 1. Apoptosis and caspase-3 activity in CaCo-2 cells after 4 hrs incubation with various deoxycholate concentrations without or with SM. There is a dose-dependent increase in DC-induced apoptosis (A) and caspase-3 activation (B) as well as a dose-dependent inhibition of 500 μ M DC-induced apoptosis (C) and caspase-3 activation (D) in presence of SM.

RESULTS

After 2 hrs (not shown) and 4 hrs (Fig 1A) incubation with various DC concentrations, there was a dose-dependent induction of apoptosis. With 500 μ M DC, there were ~35% apoptotic cells after two hrs, and ~45% apoptotic cells after 4 hrs. After 16 hrs incubation, apoptosis apparently decreased strongly, with only ~ 10% apoptotic cells at 500 μ M DC.

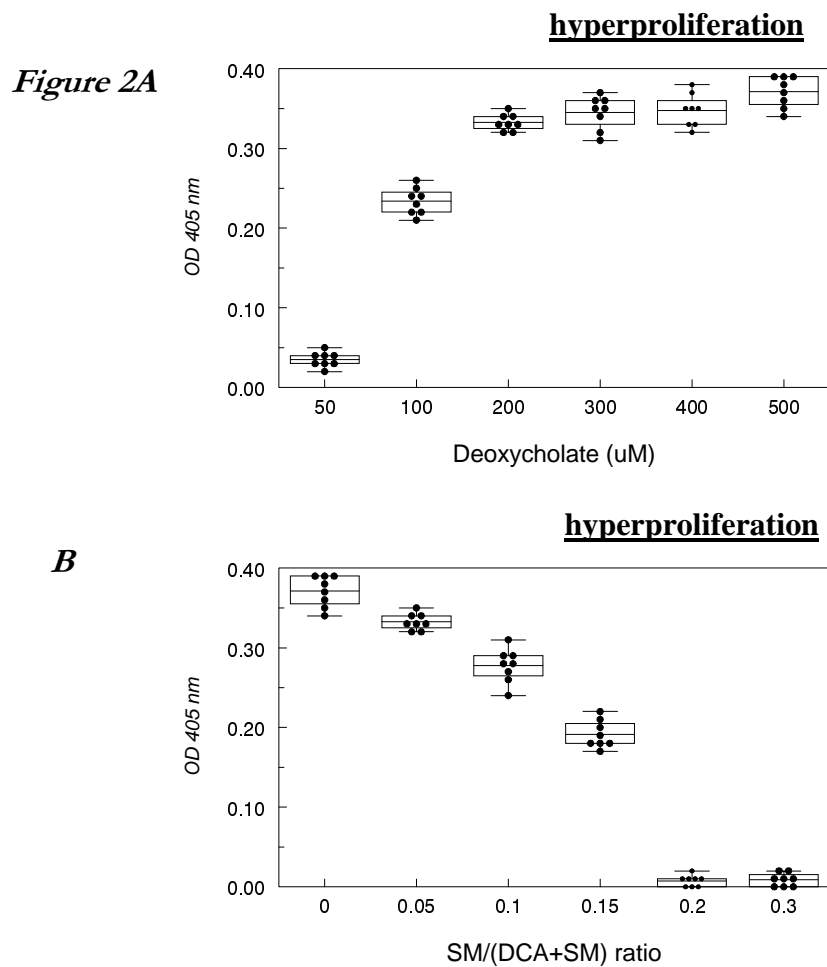


Figure 2. (A) DC induces dose-dependent hyperproliferation as measured by BrdU uptake after 16 hrs incubation and (B) there is a dose-dependent inhibition by SM of 500 μ M DC-induced hyperproliferation.

Nevertheless, dose dependency could still be observed at this time point. As shown in Figure 1B, after 4 hrs incubation, apoptosis was associated with dose-dependent caspase-3 activation. Addition of SM to the incubated bile salts dose-dependently inhibited apoptosis (Fig 1C; complete protection at SM/(DC+SM) molar ratio = 0.3 for 4 hrs incubation with 500 μ M DC) and caspase-3 activation (Fig 1D). Incubation with SM alone (50, 100, 150, 200 μ M) did not induce any apoptosis or caspase-3 activity.

Proliferation could not be studied in the earliest stages of incubation because of the time required for BrdU to be incorporated in the DNA. Nevertheless, after 16 hrs incubation, DC induced dose-dependent hyperproliferation (Fig 2A), with dose-dependent protection if SM is also included in the incubation (Fig 2B: complete protection at SM/(DC+SM) molar ratio = 0.2 for 500 μ M DC). Incubation with SM alone (50, 100, 150, 200 μ M) did not induce any hyperproliferation. These findings were confirmed by changes at inverted light microscopy (Fig 3 A-C).

Western blot with the aid of a specific antiphosphotyrosine antibody revealed a marked change in phosphorylation status of cellular proteins. After 16 hrs incubation with 300-500 μ M DC, phosphorylation of proteins < 40kDa virtually disappeared. This change was prevented by including SM in the incubation mixture. SM alone had no effects on phosphorylation status as compared with control incubation (Fig 4). It should be noted that Ponceau S. staining of the blot in Fig 4 did not reveal any differences between various lines. In particular, protein bands < 40 kDa were identical, indicating that only phosphorylation status of these proteins was affected by the incubation with DC.

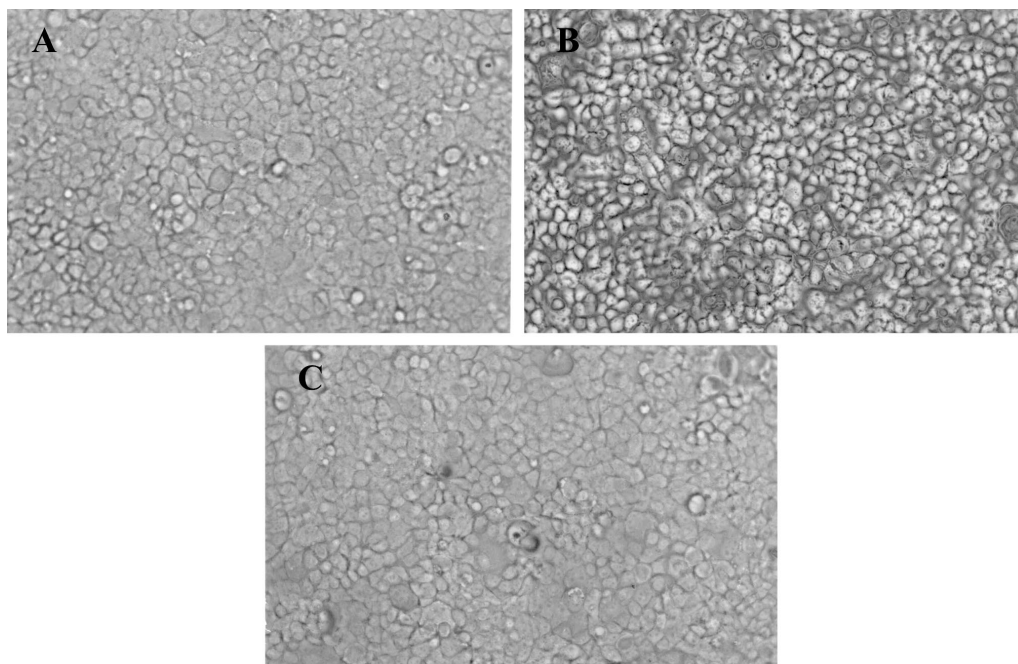
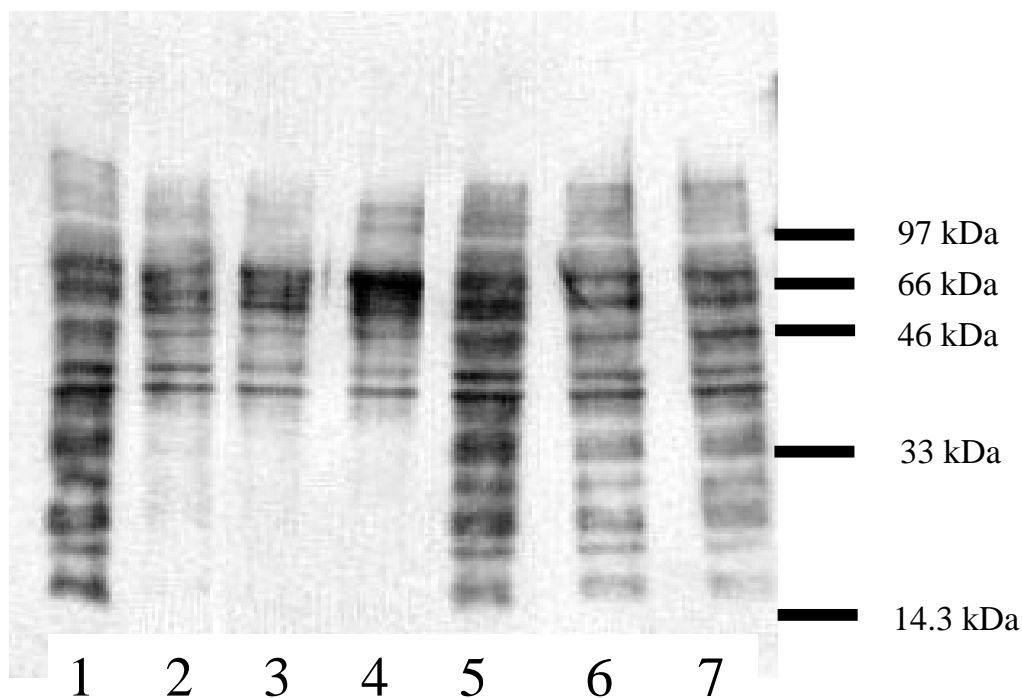


Figure 3. Morphological changes of CaCo-2 cells examined at inverted light microscopy after 16 hrs incubation with (A) control, (B) DC 500 μ M, (C) DC 500 μ M plus SM at SM/(DC+SM) ratio = 0.3.

We also examined effects of DC incubation -with or without SM- on PS-exposure to the cell surface of the erythrocyte membrane. As shown in Figs. 5A and B, during incubation with 600 μ M DC there is significant PS exposure (~ 18% of erythrocytes), without significant hemolysis. Sm dose-dependently inhibited PS exposure, with complete protection at SM/(DC+SM) molar ratio of 0.2 (Fig 5C). It is important to note that in the latter experiment, hemolysis was negligible (< 1%) with all SM/(DC+SM) ratios tested (i.e. 0, 0.05, 0.1, 0.15, 0.2).

Figure 4

Phosphorylation status of cellular proteins detected by Western blot with the aid of a specific antiphosphotyrosine antibody after 16 hrs incubation

*1. control; 2. DC 300 μ M; 3. DC 400 μ M; 4. DC 500 μ M;
5. DC 500 μ M+SM at SM/DC+SM=0.3; 6. SM 100 μ M; 7. SM 200 μ M*

DISCUSSION

Formation of colonic adenomas and cancer may occur because of a disturbed balance between (hyper)proliferation and apoptosis. High fecal levels of the secondary and hydrophobic bile salt deoxycholate (DC) are associated with increased colonic adenomas and cancer risks (1;2). Previous studies on deoxycholate have reported either apoptosis (8-11) or hyperproliferation (3-5). Different results may be explained by different methodology used in these reports. In the present study, we found evidence of dose-dependent apoptosis in the earliest stages (2 and 4 hrs) of incubation with DC. At later stages (16 hrs), apoptosis as well as caspase-3 activity were dramatically reduced. Also, DC-induced apoptosis required caspase-3 activation, as reported before (33;34).

Figure 5

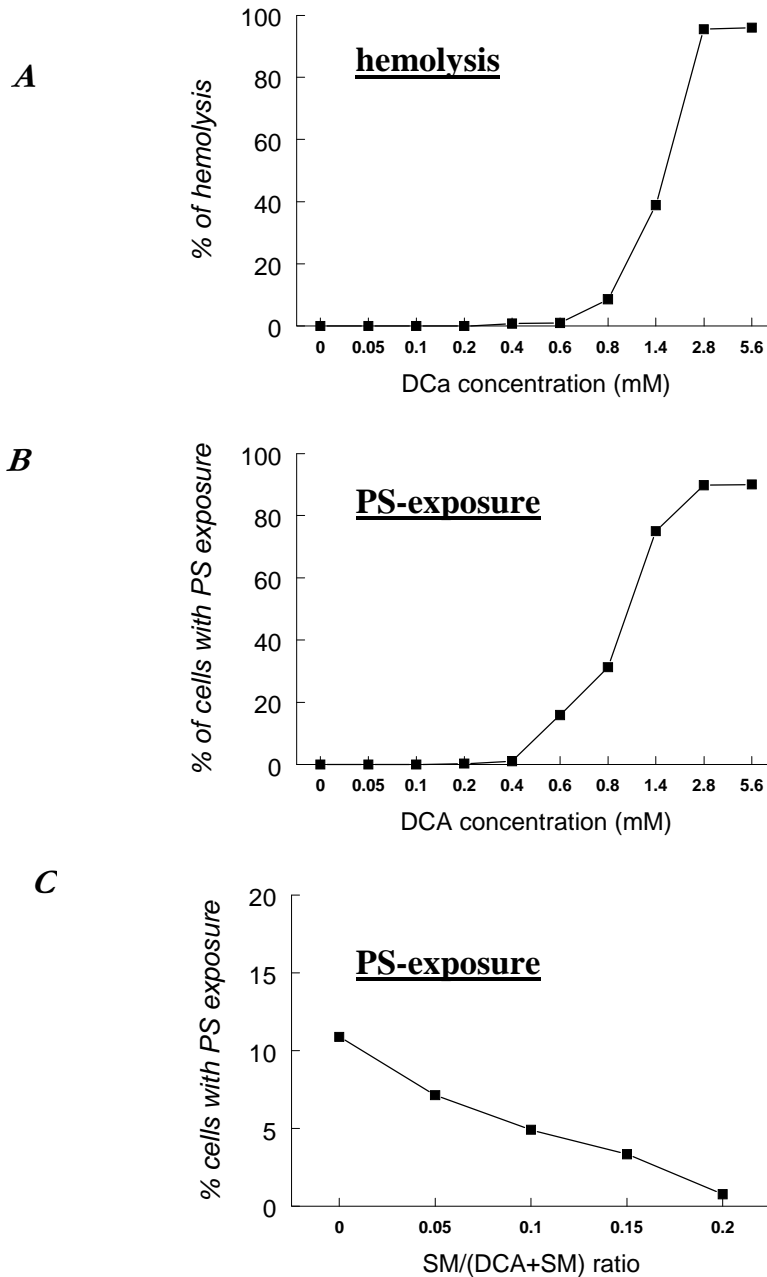


Figure 5. (A) Progressive hemolysis after 30 min. incubation with increasing concentrations of DC. (B) Progressive increase in % of cells with PS-exposure at increasing DC concentrations. (C) Dose-dependent inhibition by SM of DC-induced PS-exposure on erythrocyte surfaces. (DC conc. 600 μ M with or without SM: no significant hemolysis detected at this concentration).

Proliferation could not be evaluated in the earliest stages of incubation, because of the time required for BrdU incorporation in DNA. Nevertheless, after 16 hrs incubation, DC induced dose-dependent hyperproliferation. Western blotting with the aid of a specific antiphosphotyrosine antibody revealed marked changes of the phosphorylation status of cellular proteins at this time point. The significance of decreased phosphorylation of proteins < 40 kDa is currently being investigated.

The second major finding of this study was that sphingomyelin dose-dependently inhibited apoptosis as well as hyperproliferation. Upon hydrolysis of sphingomyelin (SM) by neutral or alkaline sphingomyelinase (35;36), resulting ceramide is currently believed to be an important pro-apoptotic molecule within the intracellular signalling pathway, and sphingomyelinase requires bile salts to express its proper enzymatic activity (37). Nevertheless, it is unlikely that in the present work, the mechanism of the SM effects was by influencing intracellular signalling, since apoptosis was inhibited rather than promoted by SM. Also, we found that SM dose-dependently inhibited DC-induced exposure of phosphatidylserine on the outer leaflet (a marker of early “apoptosis”) of the erythrocyte cell membrane; in this case the intracellular signalling pathway and nucleus are absent. An alternative explanation would be a local effect of SM on DC detergent activity in the incubation medium. In a previous study, we found evidence for such a local protective effect if SM was incorporated in bile salt micelles (13). The proposed mechanism was a decrease of intermixed micellar-vesicular bile salt concentration (i.e. non-phospholipid associated bile salts: monomers + simple micelles, thought to be responsible for detergent effects and cytotoxicity (38)), due to incorporation of the sphingolipid in the micelles. In the present study, the bile salt concentrations were much lower, far below the critical micellar

concentration. Nevertheless, one may speculate that SM inhibits activity of bile salt trimers or dimers in the solution.

In summary, we found that in the CaCo-2 cell model, pathophysiologically relevant concentrations of DC induce dose-dependent apoptosis and caspase-3 activity in the early stages of incubation, and hyperproliferation at later stages. Sphingomyelin dose-dependently inhibits apoptosis as well as hyperproliferation, presumably through a local effect on deoxycholate activity in the incubation medium. These findings may have important implications for colon cancer pathogenesis.

Acknowledgements

For this project, Antonio Moschetta was granted in the year 2000 by Società Italiana di Medicina Interna (SIMI) and “Fondazione Aventis” as “the best research project for young investigators”. Different contributions came from the following Colleagues and are warmly acknowledged: Paola De Benedictis (Internal Medicine), Ginevra Guanti, Alessandro Stella, Francesco Susca (Medical Genetic), Loreto Gesualdo, Paola Pontrelli, Michele Ursi (Nephrology), University Medical School, Bari, Italy.

References

1. Armstrong B, Doll R. Environmental factors and cancer incidence and mortality in different countries, with special reference to dietary practices. *Int J Cancer* 1975; 15:617-631.
2. Weisburger JH, Wynder EL, Horn CL. Nutritional factors and etiologic mechanisms in the causation of gastrointestinal cancers. *Cancer* 1982; 50:2541-2549.
3. Bartram HP, Scheppach W, Schmid H, Hofmann A, Dusel G, Richter F et al. Proliferation of human colonic mucosa as an intermediate biomarker of carcinogenesis: effects of butyrate, deoxycholate, calcium, ammonia, and pH. *Cancer Res* 1993; 53:3283-3288.

4. Bartram HP, Kasper K, Dusel G, Liebscher E, Gostner A, Loges C et al. Effects of calcium and deoxycholic acid on human colonic cell proliferation in vitro. *Ann Nutr Metab* 1997; 41:315-323.
5. Biasco G, Paganelli GM, Owen RW, Hill MJ. Faecal bile acids and colorectal cell proliferation. The ECP Colon Cancer Working Group. *Eur J Cancer Prev* 1991; 1 Suppl 2:63-68.
6. Reddy BS, Watanabe K, Weisburger JH, Wynder EL. Promoting effect of bile acids in colon carcinogenesis in germ-free and conventional F344 rats. *Cancer Res* 1977; 37:3238-3242.
7. Narisawa T, Magadia NE, Weisburger JH, Wynder EL. Promoting effect of bile acids on colon carcinogenesis after intrarectal instillation of N-methyl-N'-nitro-N-nitrosoguanidine in rats. *J Natl Cancer Inst* 1974; 53:1093-1097.
8. Hague A, Elder DJ, Hicks DJ, Paraskeva C. Apoptosis in colorectal tumour cells: induction by the short chain fatty acids butyrate, propionate and acetate and by the bile salt deoxycholate. *Int J Cancer* 1995; 60:400-406.
9. Marchetti MC, Migliorati G, Moraca R, Riccardi C, Nicoletti I, Fabiani R et al. Possible mechanisms involved in apoptosis of colon tumor cell lines induced by deoxycholic acid, short-chain fatty acids, and their mixtures. *Nutr Cancer* 1997; 28:74-80.
10. Martinez JD, Stratagoules ED, LaRue JM, Powell AA, Gause PR, Craven MT et al. Different bile acids exhibit distinct biological effects: the tumor promoter deoxycholic acid induces apoptosis and the chemopreventive agent ursodeoxycholic acid inhibits cell proliferation. *Nutr Cancer* 1998; 31:111-118.
11. Payne CM, Bernstein H, Bernstein C, Garewal H. Role of apoptosis in biology and pathology: resistance to apoptosis in colon carcinogenesis. *Ultrastruct Pathol* 1995; 19:221-248.
12. Velardi ALM., Groen AK, Oude Elferink RP, van der Meer R, Palasciano G, Tytgat GN. Cell type-dependent effect of phospholipid and cholesterol on bile salt cytotoxicity. *Gastroenterology* 1991; 101:457-464.
13. Moschetta A, Van Berge-Henegouwen GP, Portincasa P, Palasciano G, Groen AK, Van Erpecum KJ. Sphingomyelin exhibits greatly enhanced protection compared with egg yolk phosphatidylcholine against detergent bile salts. *J Lipid Res* 2000; 41:916-924.
14. van Ooteghem NAM, Moschetta A, Rehfeld JF, Samsom M, van Erpecum K.J., VanBerge-Henegouwen GP. Intraduodenal bile salts exert negative feedback control on gallbladder emptying in the fasting state without affecting cholecystokinin release or intestinal motility. *Gut* 2001; *in press*.
15. Duan RD, Nilsson A. Purification of a newly identified alkaline sphingomyelinase in human bile and effects of bile salts and phosphatidylcholine on enzyme activity. *Hepatology* 1997; 26:823-830.

16. Duan RD, Hertervig E, Nyberg L, Hauge T, Sternby B, Lillienau J et al. Distribution of alkaline sphingomyelinase activity in human beings and animals. Time and species differences. *Dig Dis Sci* 1996; 41:1801-1806.
17. Nilsson A. Metabolism of sphingomyelin in the intestinal tract of the rat. *Biochim Biophys Acta* 1968; 164:575-584.
18. Schmelz EM, Crall KJ, Larocque R, Dillehay DL, Merrill AH, Jr. Uptake and metabolism of sphingolipids in isolated intestinal loops of mice. *J Nutr* 1994; 124:702-712.
19. Parodi PW. Cows' milk fat components as potential anticarcinogenic agents. *J Nutr* 1997; 127:1055-1060.
20. Schmelz EM, Dillehay DL, Webb SK, Reiter A, Adams J, Merrill AH, Jr. Sphingomyelin consumption suppresses aberrant colonic crypt foci and increases the proportion of adenomas versus adenocarcinomas in CF1 mice treated with 1,2-dimethylhydrazine: implications for dietary sphingolipids and colon carcinogenesis. *Cancer Res* 1996; 56:4936-4941.
21. Hakomori S. Chemistry of Glycosphingolipids. In: Hanahan DJ, editor. *Handbook of Lipid Research*. New York: Plenum Press, 1983: 37-39.
22. Van Erpecum KJ, Carey MC. Influence of bile salts on molecular interactions between sphingomyelin and cholesterol: relevance to bile formation and stability. *Biochim Biophys Acta* 1997; 1345:269-282.
23. Nibbering CP, Carey MC. Sphingomyelins of rat liver: biliary enrichment with molecular species containing 16:0 fatty acids as compared to canalicular-enriched plasma membranes. *J Membr Biol* 1999; 167:165-171.
24. Turley SD, Dietschy JM. Reevaluation of the 3 α -hydroxysteroid dehydrogenase assay for total bile acids in bile. *J Lipid Res* 1978; 19:924-928.
25. Rouser G, Fleischer S, Yamamoto A. Two dimensional thin layer chromatographic separation of polar lipids and determination of phospholipids by phosphorus analysis of spots. *Lipids* 1970; 5:494-496.
26. Duke RC, Cohen JJ, Chervenak R. Differences in target cell DNA fragmentation induced by mouse cytotoxic T lymphocytes and natural killer cells. *J Immunol* 1986; 137:1442-1447.
27. Malina HZ, Richter C, Mehl M, Hess OM. Pathological apoptosis by xanthurenic acid, a tryptophan metabolite: activation of cell caspases but not cytoskeleton breakdown. *BMC Physiol* 2001; 1:7.
28. Fadok VA, Laszlo DJ, Noble PW, Weinstein L, Riches DW, Henson PM. Particle digestibility is required for induction of the phosphatidylserine recognition mechanism used by murine macrophages to phagocytose apoptotic cells. *J Immunol* 1993; 151:4274-4285.

29. Connor J, Pak CC, Schroit AJ. Exposure of phosphatidylserine in the outer leaflet of human red blood cells. Relationship to cell density, cell age, and clearance by mononuclear cells. *J Biol Chem* 1994; 269:2399-2404.
30. Boas FE, Forman L, Beutler E. Phosphatidylserine exposure and red cell viability in red cell aging and in hemolytic anemia. *Proc Natl Acad Sci USA* 1998; 95:3077-3081.
31. Raynal P, Pollard HB. Annexins: the problem of assessing the biological role for a gene family of multifunctional calcium- and phospholipid-binding proteins. *Biochim Biophys Acta* 1994; 1197:63-93.
32. Kuypers FA, Lewis RA, Hua M, Schott MA, Discher D, Ernst JD et al. Detection of altered membrane phospholipid asymmetry in subpopulations of human red blood cells using fluorescently labeled annexin V. *Blood* 1996; 87:1179-1187.
33. LaRue JM, Stratagoules ED, Martinez JD. Deoxycholic acid-induced apoptosis is switched to necrosis by bcl-2 and calphostin C. *Cancer Lett* 2000; 152:107-113.
34. Schlottman K, Wachs FP, Krieg RC, Kullmann F, Scholmerich J, Rogler G. Characterization of bile salt-induced apoptosis in colon cancer cell lines. *Cancer Res* 2000; 60:4270-4276.
35. Duan RD. Sphingomyelin hydrolysis in the gut and clinical implications in colorectal tumorigenesis and other gastrointestinal diseases. *Scand J Gastroenterol* 1998; 33:673-683.
36. Hannun YA, Linaudic CM. Sphingolipid breakdown products: anti-proliferative and tumor-suppressor lipids. *Biochim Biophys Acta* 1993; 1154:223-236.
37. Yedgar S, Gatt S. Enzymic hydrolysis of sphingomyelin in the presence of bile salts. *Biochem J* 1980; 185:749-754.
38. Donovan JM, Jackson AA, Carey MC. Molecular species composition of inter-mixed micellar/vesicular bile salt concentrations in model bile: dependence upon hydrophilic-hydrophobic balance. *J Lipid Res* 1993; 34:1131-1140.

SUMMARY
and
GENERAL DISCUSSION

Cholesterol is poorly soluble in an aqueous environment. In bile, the sterol is solubilized in mixed micelles by bile salts and phospholipids. In case of supersaturation, cholesterol is kept in vesicles (spherical bilayers) with phospholipid or phase-separated as crystals.

Accurate isolation of micellar and vesicular lipid carriers in model systems is important for the study of the cholesterol crystallization and gallstone formation. Gel filtration using an eluant containing bile salts in concentrations and compositions identical to the IMC (intermixed micellar-vesicular –i.e. non-phospholipid associated- bile salt concentration) of the original system is the method of choice when human biles are analyzed, since they contain most unilamellar vesicles. Separation and isolation of vesicles and mixed micelles then occurs without artifactual perturbation of the lipid distribution pseudoequilibrium. In contrast, supersaturated model biles with often large amounts of aggregated vesicles cannot generally be analyzed properly by this procedure, since aggregated vesicles are too large to enter the gel properly and may be lost during the procedure. A new method for separating lipid carriers in model biles has been proposed in **chapter 2**. First, vesicular aggregates and -if present- cholesterol crystals are precipitated by ultracentrifugation. Cholesterol crystals can be quantitated after dissolution of vesicular aggregates by adding excess deoxycholate to the pellet. Second, mixed micelles are isolated by ultrafiltration through a highly selective filter. Last, unilamellar vesicles are obtained by dialysis against a solution containing bile salts at intermixed micellar-vesicular concentrations. With this method, we investigated the effects of various bile salts and various phospholipid classes on lipid solubilization in micellar or vesicular phases as well as on cholesterol crystallization (**chapter 3**). The rationale was that the hydrophilic bile salt ursodeoxycholate is frequently used in clinical practice to dissolve cholesterol gallstones, and that dietary modulation of

biliary phospholipid composition from phosphatidylcholine with unsaturated acyl chains (the exclusive phospholipid in bile) toward phospholipids with mainly saturated acyl chains has been suggested to prevent gallstone formation. We found enhanced lipid distribution into vesicular phases, and reciprocal decreases of micellar lipid solubilization in case of more hydrophilic bile salts such as ursodeoxycholate or in case of more saturated phospholipids. Whereas disaturated phosphatidylcholines or sphingomyelins increased crystallization compared to phosphatidylcholines with unsaturated acyl chains in all crystal-containing zones, the hydrophilic bile salt tauroursodeoxycholate inhibited crystallization by formation of vesicular phases. Treatment with ursodeoxycholate appears preferable to disaturated phospholipids for the prevention of cholesterol crystallization and gallstones.

Apart from cholesterol crystallization, this thesis also focused on the process of nascent bile formation. It is uncertain why phosphatidylcholine is the predominant phospholipid in bile, although both sphingomyelin and phosphatidylcholine are the major structural phospholipids in the outer leaflet of the hepatocyte canalicular membrane. In **chapter 4**, we have determined the distribution of phosphatidylcholine from egg yolk (similar acyl chain composition as phosphatidylcholine in bile) and sphingomyelin into micelles and small unilamellar vesicles (model for canalicular bile) or detergent-resistant aggregated vesicles (model for canalicular membrane). We found at increasing cholesterol contents of the system, preferential distribution of lipids and progressive enrichment of vesicular aggregates with sphingomyelin containing long saturated acyl chains. In contrast, there was preferential distribution of phosphatidylcholine into mixed micelles and small unilamellar vesicles under these circumstances. Different physical-chemical characteristics of the two phospholipids may relate to their different distribution *in vivo*. In this respect, one should realize that

cholesterol has a high affinity for sphingomyelin and is thought to be preferentially located together with this phospholipid in detergent-resistant domains in the bilayer. In **chapter 5**, we have studied by means of spectrophotometry and by sequential state-of-the-art cryo-transmission electron microscopy, effects of including sphingomyelin within egg yolk phosphatidylcholine-containing vesicles (with and without cholesterol) on vesicle → micelle phase transitions that were induced by addition of bile salts. Incorporation of sphingomyelin destabilized egg yolk phosphatidylcholine vesicles and enhanced vesicle → micelle phase transitions, with formation of intermediate open, multilamellar and fused vesicular structures. When cholesterol was also included in the bilayer, sphingomyelin-egg yolk phosphatidylcholine vesicles appeared highly resistant against bile salt-induced micellar solubilization. Instead, intermediate disk-like micelles, and thereafter, multilamellar and large aggregated vesicles were formed. These findings point to a key role of cholesterol in formation of pathophysiologically relevant phosphatidylcholine plus sphingomyelin-containing bilayers and in modulating interactions between vesicles and detergent bile salts. These data may have implications for canalicular bile formation and intestinal lipid solubilization.

Bile salts may present as “good” or “bad” guys. The good aspect is their effect in intestinal lipid absorption, bile formation and cholesterol solubilization. The “bad” aspect is the potential cytotoxicity induced by the detergent bile salts. At the concentrations occurring in hepatic and gallbladder biles, bile salts could theoretically damage the apical membrane of the hepatocytes and of the cells lining the biliary tract. The absence of such a damaging effect *in vivo* suggests the existence of cytoprotective mechanisms. In *in vitro* studies, inclusion of egg yolk phosphatidylcholine within bile salt micelles protects against bile salt-induced cytotoxicity. In line with these findings, mice with homozygous

disruption of the *mdr2* gene (complete absence of phosphatidylcholine in bile) exhibit severe hepatocyte damage *in vivo*. In **chapter 6** we have compared protective effects of incorporating phosphatidylcholine from egg yolk (similar to phosphatidylcholine in human bile) and sphingomyelin within bile salt micelles. Sphingomyelin offered greatly enhanced protection against bile salt-induced cytotoxicity compared to egg yolk phosphatidylcholine, which may relate to lower intermixed micellar-vesicular (i.e. non-phospholipid associated) bile salt concentrations in case of sphingomyelin. Interestingly, we found that considerable amounts of sphingomyelin may occur in bile of patients with obstructive jaundice, with potential amelioration of cytotoxicity as a result (**addendum to chapter 6**).

Hydrophobic bile salts are known to exert more cytotoxic effects than hydrophilic bile salts. In fact, hydrophilic bile salts such as ursodeoxycholate or hyodeoxycholate may protect against toxicity by hydrophobic bile salts. In **chapter 7** we have examined the effects of bile salt hydrophobicity on lipid distribution between micelles and small unilamellar vesicles (model for canalicular bile) and detergent-resistant aggregated vesicles (model for canalicular membrane). Hydrophilic but not hydrophobic bile salts preserved integrity of pathophysiologically relevant phosphatidylcholine- plus sphingomyelin-containing bilayers, with enhanced differential distribution of phosphatidylcholine *vs* sphingomyelin between micellar and vesicular phases. Despite their similar hydrophilicity, the bile salts ursodeoxycholate and hyodeoxycholate exert quite different biological effects *in vivo*: intraduodenal infusion of taurohyodeoxycholate but not tauroursodeoxycholate strongly enhances biliary phospholipid secretion. We found in the erythrocyte and CaCo-2 cell models evidence for different interactions of tauroursodeoxycholate and hyodeoxycholate

with micellar phospholipids, possibly related to their different *in vivo* effects.

Epidemiological and experimental studies have indicated a consistent correlation between increased risk of colon cancer and elevated levels of fecal bile salts in Western populations that consume high-fat diets. Deoxycholate may act as a tumor promoter, inducing hyperproliferation and increasing the number of tumors elicited by complete carcinogens. Also, deoxycholate is able to induce apoptosis in some adenoma and carcinoma cell lines. High-fat diet promotes bile salt accumulation in feces, where enteric bacteria metabolize them to secondary bile salts, principally deoxycholate and lithocholate. Dietary supplementation with sphingomyelin suppresses experimental colon cancer in mice, and appreciable amounts of dietary sphingomyelin appear to reach to the colon. In **chapter 8**, we have examined in CaCo-2 cells potential effects of sphingomyelin on hyperproliferation or apoptosis induced by deoxycholate. Pathophysiologically relevant concentrations of this bile salt induced dose-dependent apoptosis and caspase-3 activity in the early stages of incubation, but hyperproliferation at later stages. Sphingomyelin dose-dependently inhibited apoptosis as well as hyperproliferation, presumably through a local effect on deoxycholate activity in the incubation medium. These findings may have important implications for colon cancer prevention.

Samenvatting en discussie

Cholesterol is slecht oplosbaar in water. In de gal wordt cholesterol daarom in oplossing gehouden door vorming van gemengde micellen samen met galzouten en fosfolipid. In geval van oververzadiging (i.e. overschrijding van de micellaire oplosbaarheid van cholesterol) vormt cholesterol samen met fosfolipid zogenaamde vesicles (“vetbolletjes”) of slaat het neer als cholesterolkristal (het begin van galsteenvorming). Een betrouwbare scheiding van micellen en vesicles is belangrijk bij de bestudering van cholesterolkristallisatie en galsteenvorming. Voor *humane* gal is gelfiltratie de beste scheidingsmethode. Er moet dan wel als eluens een buffer gebruikt worden die galzouten bevat in een concentratie en samenstelling identiek aan de zogenaamde “intermixed micellaire-vesiculaire (niet met fosfolipiden geassocieerde) concentratie” (IMC: i.e. galzout monomeren en “simpele” galzoutmicellen) in de oorspronkelijke gal. Dit is nodig om de lipiddistributie tussen de micellen en vesicles niet te verstoren. *Modelgal* bevat echter meestal veel geaggregeerde vesicles. Door hun grootte kunnen die vaak niet het gelfiltratiemateriaal passeren. In **hoofdstuk 2** wordt een nieuwe scheidingsmethode voor modelgal beschreven. Allereerst worden geaggregeerde vesicles en –indien aanwezig- cholesterolkristallen met behulp van ultracentrifugatie neergeslagen. De hoeveelheid cholesterolkristallen kan vervolgens bepaald worden, nadat eerst de geaggregeerde vesicles opgelost zijn door toevoeging van excess deoxycholaat aan de pellet. Hierna worden de gemengde micellen geïsoleerd met behulp van ultrafiltratie door een selectief filter. Ten slotte worden de unilamellaire vesicles geïsoleerd met behulp van dialyse tegen een buffer die galzouten bevat in een concentratie en een samenstelling identiek aan de IMC. Met deze nieuwe methode onderzochten wij de invloed van verschillende galzouten en fosfolipiden

op de lipiddistributie tussen micellen en vesicles en op de cholesterolkristallisatie (**hoofdstuk 3**). De reden om dit onderzoek uit te voeren was, dat door behandeling met het hydrofiele galzout ursodeoxycholaat cholesterolkristallisatie en het ontstaan van galstenen voorkomen kan worden. Bovendien heeft modificatie van de biliare fosfolipidsamenstelling (fosfatidylcholine met meer verzadigde vetzuren) door aanpassing van het dieet misschien een vergelijkbaar gunstig effect. Wij vonden minder solubilisatie van lipid in micellen en een toegenomen solubilisatie in vesicles en in geval van hydrofiele galzouten (tauroursodeoxycholaat). Fosfolipiden met verzadigde vetzuurketens hadden een zelfde effect op de verdeling van lipid tussen micellen en vesicles. Fosfolipiden met verzadigde vetzuurketens bleken echter cholesterolkristallisatie te bevorderen, terwijl kristallisatie juist geremd werd door tauroursodeoxycholaat. Behandeling met ursodeoxycholaat heeft dan ook de voorkeur boven dietaire modificatie van de biliare fosfolipidsamenstelling, als men cholesterolkristallisatie en het ontstaan van galstenen wil tegengaan.

Behalve cholesterolkristallisatie werden ook enkele aspecten van galvorming met behulp van modelsystemen bestudeerd. Fosfatidylcholine is het belangrijkste fosfolipid in de gal. Behalve fosfatidylcholine bevat de buitenlaag van de canaliculaire (i.e. aan de galgangetjes grenzende) membraan van de levercel ook een aanzienlijke hoeveelheid van het fosfolipid sfingomyeline. In **hoofdstuk 4** hebben wij daarom in modelsystemen de verdeling onderzocht van sfingomyeline en fosfatidylcholine afkomstig van eidooier (met vnl onverzadigde vetzuurketens, vergelijkbaar met fosfatidylcholine in gal) tussen enerzijds micellen en unilamellaire vesicles (beide model voor lipiden in gal) en anderszijds geaggregeerde vesicles (model voor canaliculaire membraan). Bij een toenemend cholesterolgehalte in het modelsysteem bleek er sprake van een preferentiële lipiddistributie en een toenemende

verrijking met sfingomyeline in geaggregeerde vesicles. Gemengde micellen en unilamellaire vesicles waren daarentegen verrijkt met fosfatidylcholine. Het verschil tussen beide fosfolipiden berust op hun verschillende fysisch-chemische eigenschappen. Cholesterol heeft een sterke affiniteit voor sfingomyeline en bevindt zich waarschijnlijk samen met dit fosfolipid in aparte membraandomeinen die resistent zijn tegen detergentia zoals galzouten. In **hoofdstuk 5** hebben wij met behulp van spectrofotometrie en sequentiële cryo-transmissie electronenmicroscopie de vesicle→miceltransities bestudeerd zoals die optreden na toevoeging van galzouten aan fosfatidylcholine+sfingomyeline bevattende vesicles (met of zonder cholesterol in de vesiculaire membraan). Incorporatie van sfingomyeline in fosfatidylcholine-bevattende vesicles maakte de vesicle membraan gevoeliger voor detergerende galzouten en versnelde het optreden van vesicle→miceltransities, met vorming van intermediaire open, multilamellaire en gefuseerde vesiculaire structuren. Als echter ook cholesterol in de vesiculaire membraan was geïncorporeerd, bleken fosfatidylcholine+sfingomyeline bevattende vesicles juist erg resistent tegen micellaire solubilisatie door galzouten. Met behulp van electronen microscopie werden in dit geval intermediaire schijfvormige micellen en vervolgens grote multilamellaire en geaggregeerde vesiculaire structuren gevisualiseerd. Deze gegevens wijzen op het belang van cholesterol bij de vorming van fysiologisch relevante membranen en bij de interacties tussen vesicles en detergerende galzouten. Onze bevindingen kunnen potentiële implicaties hebben voor het proces van galvorming en intestinale lipidsolubilisatie.

Galzouten hebben behalve gunstige ook potentieel ongunstige eigenschappen. Enerszijds bevorderen zij de intestinale lipidabsorptie, galvorming en cholesterol-solubilisatie. Anderszijds zouden zij door hun detergerend effect ook tot beschadiging van lever-, galweg/galblaas- en darmcellen kunnen leiden. Aangezien deze beschadiging *in vivo*

normaliter niet optreedt, bestaan er blijkbaar ook beschermende mechanismen. Zo bleek in *in vitro* studies het fosfolipid fosfatidylcholine te beschermen tegen galzouttoxiciteit. In overeenstemming met deze gegevens treedt bij *mdr2* “knockout” muizen (geen fosfatidylcholine in gal) een ernstige leverbeschadiging op. In **hoofdstuk 6** hebben wij de beschermende effecten van fosfatidylcholine afkomstig van eidooier (vergelijkbare vetzuursamenstelling als fosfatidylcholine in gal) en van sfigomyeline tegen galzouttoxiciteit vergeleken. Sfigomyeline bleek een veel betere bescherming te bieden, mogelijk doordat het de “intermixed micellaire-vesiculaire galzoutconcentratie” (IMC) sterk verlaagt. De galzouten in de IMC worden namelijk verantwoordelijk gehouden voor het optreden van cytotoxiciteit. In dit opzicht was het dan ook een interessante bevinding, dat bij patiënten met cholestase aanzienlijke hoeveelheden sfigomyeline in de gal bleken voor te komen, waardoor verdere levercelbeschadiging misschien voorkomen zou kunnen worden (**addendum hoofdstuk 6**).

Hydrofobe galzouten zijn over het algemeen meer cytotoxisch dan hydrofiele galzouten. Ursodeoxycholaat en hyodeoxycholaat –beide hydrofiele galzouten- beschermen zelfs tegen toxiciteit door meer hydrofobe galzouten. In **hoofdstuk 7** hebben wij het effect van galzouthydrofobiciteit op de verdeling van lipiden tussen micellen (model voor gal) en geaggregeerde vesicles (model voor canaliculaire membraan van de levercel) onderzocht. In tegenstelling tot hydrofobe galzouten veroorzaakten hydrofiele galzouten geen beschadiging van pathofysiologisch relevante fosfatidylcholine+sfigomyeline+cholesterol bevattende membranen. Ook was er een preferentiële distributie van fosfatidylcholine in micellen en van sfigomyeline in vesicles in het geval van hydrofiele galzouten. Hoewel ursodeoxycholaat en hyodeoxycholaat nauwelijks verschillen in mate van hydrofiliciteit, zijn hun effecten *in vivo* heel verschillend. Terwijl na intraduodenale infusie

van taurohyodeoxycholaat een sterke toename van de biliare fosfolipidsecretie optreedt, is dat niet het geval bij infusie van tauroursodeoxycholaat. Wij vonden in erythrocyten en CaCo2 cellen aanwijzingen voor een verschillende interactie van deze galzouten met micellaire fosfolipiden, wat misschien hun verschillend effect *in vivo* zou kunnen verklaren.

Op grond van epidemiologische en experimentele studies lijkt er in de westerse wereld (vetrijk dieet) een correlatie te zijn tussen het risico op dikke darm kanker en de hoeveelheid galzouten in de ontlasting. Met name het hydrofobe galzout deoxycholaat zou als een tumor promotor kunnen fungeren, waardoor hyperproliferatie van dikke darm cellen zou kunnen optreden, met verhoogd risico op tumorinductie. Aan de andere kant kan deoxycholaat ook apoptose (“geprogrammeerde celdood”) induceren in sommige kankercellijnen. Door een vetrijk dieet neemt de hoeveelheid galzouten in de faeces toe. Bacteriën in de dikke darm zetten die dan om in secundaire galzouten (voornamelijk deoxycholaat en lithocholaat). In muizen blijkt sfigomyeline in het dieet bovendien dikke darm kanker te kunnen tegengaan. Uit eerder onderzoek is gebleken, dat er aanzienlijke hoeveelheden dietair sfigomyeline in de dikke darm terecht komen. In **hoofdstuk 8** hebben wij daarom in CaCo2 cellen de invloed van sfigomyeline op de door deoxycholaat geïnduceerde apoptose en hyperproliferatie onderzocht. Deoxycholaat in pathofysiologisch relevante concentraties bleek in de eerste uren na toevoeging apoptose en daarbij behorende activatie van caspase-3 te induceren, maar in latere stadia tot hyperproliferatie te leiden. Sfigomyeline ging zowel apoptose als hyperproliferatie tegen, waarschijnlijk door een lokaal effect op het deoxycholaat in het incubatiemedium. Deze bevindingen zijn mogelijk relevant voor de preventie van dikke darm kanker.

Sommario e discussione

Il colesterolo è una molecola insolubile in acqua. Nella bile, il colesterolo è solubilizzato nelle micelle miste insieme ai sali biliari ed ai fosfolipidi. Nel caso di sovrasaturazione biliare, il colesterolo è contenuto all'interno di vescicole di fosfolipidi (*bilayer* sferici) o precipita in forma di cristalli visibili alla microscopia ottica.

Una separazione accurata dei carrier lipidici micellari e vescicolari è importante per lo studio della cristallizzazione del colesterolo e della formazione dei calcoli (colelitiasi colesterinica). Nell'analizzare la bile umana (che contiene molte vescicole piccole unilamellari), il metodo di scelta nella separazione delle micelle e vescicole è la filtrazione attraverso gel con l'utilizzo come eluenti di sali biliari in concentrazione e composizione identiche all'IMC (concentrazione di sali biliari inter micelle miste e vescicole, cioè quei sali biliari non associati ai fosfolipidi). In questo modo la separazione e l'isolamento delle vescicole e delle micelle avviene senza artefatti. Al contrario, modelli di bile sovrasaturi in colesterolo, che presentano pertanto una elevata quantità di aggregati di vescicole, non possono essere analizzati con questo metodo, poiché gli aggregati vescicolari sono troppo grandi per entrare nel gel in maniera corretta e potrebbero essere persi durante la procedura. Un nuovo metodo per separare i carrier lipidici nei modelli di bile è stato proposto nel **capitolo 2**. In primo luogo, gli aggregati di vescicole ed i cristalli di colesterolo -se presenti- sono precipitati con ultracentrifugazione. I cristalli di colesterolo possono essere quantificati dopo la dissoluzione degli aggregati di vescicole con l'aggiunta di desossicolato nel pellet. Secondo, le micelle miste sono isolate con una ultrafiltrazione del sovrantante con filtri altamente selettivi. Infine, le vescicole unilamellari sono ottenute attraverso dialisi contro una soluzione contenente sali biliari alla concentrazione inter micelle miste-

vescicole. Con questo metodo, nel successivo capitolo (**capitolo 3**), si è voluto studiare accuratamente gli effetti di varie classi di sali biliari e fosfolipidi sia sulla solubilizzazione del colesterolo nelle fasi micellare e vescicolare che sulla cristallizzazione del colesterolo stesso. Il rationale dello studio era che il sale biliare idrofilico ursodesossicolato è frequentemente usato nella pratica clinica per dissolvere i calcoli di colesterolo e che modulazioni dietetiche della composizione dei fosfolipidi biliari (dalla fosfatidilcolina con catene di acidi grassi insaturi -unico fosfolipide presente nella bile umana- a fosfolipidi principalmente con catene di acidi grassi saturi) potrebbero agire nella prevenzione della colelitiasi colesterinica. In questo studio abbiamo riscontrato una elevata distribuzione di lipidi nelle vescicole ed una reciproca diminuzione della solubilizzazione di lipidi nelle micelle miste nel caso di sali biliari più idrofilici come l'ursodesossicolato o di fosfolipidi più saturi. Mentre la sfingomieline (fosfolipide contenente catene di acidi grassi saturi) aumenta la cristallizzazione del colesterolo rispetto alla fosfatidilcolina in tutti modelli di bile con cristalli, l'idrofilico ursodesossicolato inibisce la cristallizzazione attraverso la formazione delle vescicole. Un trattamento con ursodesossicolato sembra, dunque, preferibile a modificazione dietetiche con fosfolipidi con catene di acidi grassi saturi nella prevenzione della cristallizzazione e della colelitiasi colesterinica.

In questa tesi, oltre alla cristallizzazione del colesterolo, è stato anche investigato il processo alla base della formazione della bile. Il rationale del **capitolo 4** nasce dalla considerazione che non si conosce il motivo per cui la fosfatidilcolina è il fosfolipide predominante nella bile, nonostante sia la sfingomieline che la fosfatidilcolina sono i maggiori fosfolipidi strutturali nel foglietto esterno della membrana canalicolare epatocitaria. È stata pertanto studiata la distribuzione della fosfatidilcolina isolata dal tuorlo d'uovo (con una composizione di acidi grassi simile alla fosfatidilcolina nella bile) e la sfingomieline tra micelle e

piccole vescicole unilamellari (modello per la bile canalicolare) e gli aggregati di vescicole resistenti all'attività detergente (modello per la membrana canalicolare epatocitaria). All'aumento della concentrazione di colesterolo nel sistema, si evidenziava sia una distribuzione progressiva dei lipidi che un progressivo aumento di sfingomieline negli aggregati vesicolari. Viceversa, alle stesse condizioni, la fosfatidicolina era preferenzialmente solubilizzata nelle micelle e nelle vescicole unilamellari. Questa diversa distribuzione dei due fosfolipidi tra i vari *carrier* può essere dettata dalle loro diverse caratteristiche fisico-chimiche. A tal riguardo, si deve sottolineare che il colesterolo ha una elevata affinità per la sfingomieline ed è preferenzialmente distribuito con essa all'interno di domini di membrana resistenti all'attività detergente. Nel **capitolo 5**, è descritto uno studio sull'effetto dell'inclusione di sfingomieline in vescicole di fosfatidicolina dal tuorlo d'uovo con e senza colesterolo sulla transizione dalla fase vesicolare a quella micellare indotta dall'aggiunta di sali biliari. Lo studio è stato effettuato con spettrofotometria e microscopia elettronica sequenziale con controllo della temperatura e dell'umidità. L'incorporazione della sfingomieline destabilizzava le vescicole di fosfatidilcolina ed aumentava la transizione vescicole → micelle, con la formazione di strutture intermedie quali vescicole aperte, multilamellari e fuse. In presenza di colesterolo, le vescicole contenenti anche sfingomieline risultavano altamente resistenti alla solubilizzazione micellare indotta dai sali biliari. In questo caso, strutture intermedie quali micelle a forma di disco erano visualizzate e successivamente, grandi aggregati di vescicole e vescicole multilamellari. Questi dati sottolineano il ruolo di punta del colesterolo nella formazione dei bilayer contenenti fosfatidicolina e sfingomieline e nella interazione tra vescicole e sali biliari, con potenziali implicazioni sia nel processo di formazione della bile canalicolare che nella solubilizzazione dei lipidi nel lume intestinale.

Per usare una semplificazione, i sali biliari possono essere considerati sia “buoni” che “cattivi”. L’aspetto positivo è il loro effetto sull’assorbimento intestinale di lipidi, sulla formazione della bile e sulla solubilizzazione del colesterolo. L’aspetto “cattivo” è la loro potenziale citotossicità. Alle concentrazioni riscontrate nella bile epatica e colecistica, i sali biliari potrebbero teoricamente danneggiare la membrana apicale degli epatociti e delle cellule che tappezzano le vie biliari. L’assenza di questo effetto dannoso *in vivo* suggerisce l’esistenza di meccanismi di citoprotezione. Studi *in vitro* hanno dimostrato che l’inclusione di fosfatidilcolina dal tuorlo d’uovo all’interno delle micelle di sali biliari protegge dalla tossicità indotta dai sali biliari stessi. In linea con questi dati, mice con una mutazione omozigote del gene *mdr2* (assenza completa di fosfatidilcolina nella bile) presentano un danno severo degli epatociti *in vivo*. Nel **capitolo 6** l’effetto protettivo sulla tossicità indotta dai sali biliari da parte della fosfatidilcolina dal tuorlo d’uovo è stato paragonato a quello della sfingomieline. La sfingomieline offriva una protezione significativamente maggiore rispetto alla fosfatidilcolina sull’effetto detergente dei sali biliari, probabilmente per i più bassi valori della concentrazione inter micellare-vescicolare dei sali biliari nel caso della sfingomieline. È interessante notare che una significativa concentrazione di sfingomieline si può riscontrare nella bile dei pazienti con colestasi da ostruzione della vie biliari, con un potenziale miglioramento della tossicità (**addendum capitolo 6**).

I sali biliari idrofobici hanno un effetto citotossico superiore a quello dei sali biliari idrofilici. Infatti, sali biliari idrofilici come l’urodesossicolato o l’iodesossicolato possono proteggere dalla tossicità indotta da sali biliari più idrofobici. Nel **capitolo 7**, è stato studiato l’effetto dell’idrofobicità dei sali biliari sulla distribuzione dei lipidi tra le micelle e le vescicole unilamellari (modello per la bile canalicolare) e gli aggregati di vescicole resistenti all’attività detergente (modello per la

membrana canalicolare epatocitaria). I sali biliari idrofilici sono in grado di preservare l'integrità dei bilayer contenenti sfingomieline e fosfatidicolina, con un aumento della distribuzione della fosfatidicolina vs sfingomieline tra le fasi micellari e vescicolari. Nonostante la simile idrofilicità, i sali biliari ursodesossicolato e iodesossicolato hanno effetti *in vivo* molto diversi: l'infusione intraduodenale di tauroiodesossicolato, al contrario del tauroursodeossicolato, aumenta significativamente la secrezione dei fosfolipidi nella bile. In questo studio su vari modelli cellulari (eritrociti e cellule in coltura di carcinoma di colon), sono state riscontrate evidenze per interazioni fisico-chimiche differenti tra tauroursodesossicolato e tauroiodesossicolato con i fosfolipidi all'interno delle micelle.

Studi epidemiologici e sperimentali hanno indicato una correlazione consistente tra un aumentato rischio di carcinoma del colon ed elevati livelli di sali biliari nelle feci tra la popolazione del mondo occidentale che consuma una dieta ricca in grassi. Il desossicolato può agire sia come promotore di tumori (inducendo iperproliferazione cellulare) che aumentando il numero di tumori indotti da agenti carcinogeni. Inoltre, è stato precedentemente dimostrato che il desossicolato è in grado di indurre l'apoptosi in alcune linee cellulari di adenoma ed adenocarcinoma. Una dieta ricca in grassi induce l'accumulo dei sali biliari nelle feci, dove vengono metabolizzati dalla flora batterica intestinale in sali biliari secondari, principalmente desossicolato e litocolato. L'aumentato introito di sfingomieline con la dieta sopprime la formazione di carcinoma di colon indotto in maniera sperimentale e una quantità apprezzabile di sfingomieline ingerita giunge al colon. Nel **capitolo 8**, sono stati studiati gli effetti della sfingomieline sull'apoptosi e l'iperproliferazione cellulare indotta dai sali biliari. Concentrazioni patofisiologicamente rilevanti di desossicolato inducevano apoptosi ed attivazione della caspasi-3 in maniera dose dipendente negli stadi iniziali

dell'incubazione, con iperproliferazione cellulare successivamente. La sfingomieline era in grado di inibire in maniera dose-dipendente sia l'apoptosi che l'iperproliferazione, presumibilmente attraverso un effetto diretto sull'attività del desossicolato in soluzione. Questi dati potrebbero avere implicazioni importanti nella prevenzione del carcinoma del colon.

Many Thanks

Beste Promotor, prof. Gerard vanBerge-Henegouwen: You have been a stimulating chief, a successful manager and a gentleman. I hope I did learn something from You. Many Thanks!

Beste Promotor, prof. Giuseppe Palasciano: Many thanks for all the possibilities that you give me. You were the first on pushing me in the research field. I will never forget!

Karel van Erpecum: days, nights, week-ends I used so much of Your time. I will say thanks to You, forever!

Piero Portincasa: without You, this stage would have never been possible. I hope I did continue the Bari-Utrecht connection in the right way. Many thanks for the daily support.

Lab friends in Utrecht: Erik, Karin, Martin & Willem. Also, Anneke, Bas, Nancy, Niels & Silvano. Well, it is difficult to write some words. It has been an honor for me to work with You. Thanks!

Many thanks: Bert, Michel and all the lab people in Amsterdam (Exp. Hepatology), Peter and Paul in Maastricht (Electron Microscopy).

Gastroenterologie Afdeling: many thanks to secretaries, nurses and colleagues: I really hope to meet all of You again.

Italy: All colleagues and friends in Bari, You also made this possible. A special thanks to the historical semeiotica group with Andrea, Francesco, Massimo, Ornella, Sandra, Teo and more Loredana, Marella, Michele, Mirco, Paola, Rosa, Vito.

Finally my family, the most important point for an italian. Marco, the young one, *il futuro che vale più del presente!*, Giuseppe, the second, *il braccio non medico della famiglia: la prossima PhD tesi è la tua!*, Mamma, *mi sei mancata davvero, con il tuo modo "sottile" di consigliarmi: hai sempre avuto ragione!* Papà, *non capita a tutti di avere un padre del genere (collega ed amico), grazie per la libertà e la stima.*

Francesca. *La tesi è dedicata a te che hai scelto di sopportarmi! E non è poco.....*

Curriculum vitae et studiorum



Antonio Moschetta was born in Bitonto, Bari-Italy, June 8, 1973 and obtained his diploma at Liceo Classico -Gymnasium- "C. Sylos" of Bitonto in 1991.

As medical student (Erasmus program), in 1993 he spent

3 months at the Department of Immunology, Maastricht University, NL and attended his 4th yr at the University of La Laguna (Spain) within the European Credit Transfer System. In July 1997 he qualified *cum laude* and passed the national board examination as MD at the University of Bari Medical School. In November 1997 he started his training in Internal Medicine at the University of Bari Medical School (Head Prof. G. Palasciano). In June 1998 he joined a combined project between Utrecht (supervisor K.J. van Erpecum, MD, PhD) and Bari (supervisor P. Portincasa, MD, PhD) in gastrointestinal pathophysiology and carried out several projects as research fellow at the Department of Gastroenterology and Internal Medicine, University Medical Center Utrecht NL (Head Prof. G.P. vanBerge Henegouwen). In 2000 he was awarded from the Società Italiana di Medicina Interna for the best research project of young investigators. He is currently completing his Internal Medicine training (ending in October 2002) and he is actively involved in various research projects at the University of Bari Medical School.

Antonio Moschetta è nato a Bitonto, Bari, l'8 giugno 1973 e si è diplomato (60/60) presso il Liceo Ginnasio "C. Sylos" di Bitonto nel 1991. Come studente Erasmus della Facoltà di Medicina e Chirurgia dell'Università degli Studi di Bari, nel 1993 ha frequentato uno stage di 3 mesi presso il Dipartimento di Immunologia dell'Università di Maastricht in Olanda (1993) ed ha frequentato il quarto anno del corso di laurea presso l'Università de La Laguna in Spagna, nell'ambito di un progetto di scambio internazionale (European Credit Transfer System). A luglio 1997 si è laureato in Medicina e Chirurgia *cum laude* ed ha superato nello stesso anno l'esame di abilitazione all'esercizio della professione medica. Da novembre 1997 è Specialista in formazione presso la Scuola di Specializzazione in Medicina Interna dell'Università degli Studi di Bari (Dipartimento di Medicina Interna e Medicina Pubblica, Sezione di Medicina Interna, dir. Prof. G. Palasciano). Nel giugno 1998 ha partecipato ad un progetto di studio combinato tra Utrecht (supervisore K.J. van Erpecum, MD, PhD) e Bari (supervisore P. Portincasa, MD, PhD) come research fellow presso il Dipartimento di Gastroenterologia e Medicina Interna dell'University Medical Center di Utrecht in Olanda (Dir. Prof. G.P. vanBerge Henegoweun). Nel 2000 ha vinto il premio di miglior progetto di ricerca per giovani ricercatori bandito dalla Società Italiana di Medicina Interna. Al momento attuale sta completando la Scuola di Specializzazione in Medicina Interna (diploma atteso: ottobre 2002) ed è attivamente coinvolto in numerosi progetti di ricerca dell'Università di Bari.

Publications with impact factor (november 1999 - november 2001)

- Eckhardt ERM, **Moschetta A**, Renooij W, Goerdayal SS, vanBerge-Henegouwen GP, van Erpecum KJ. Asymmetric distribution of phosphatidylcholine and sphingomyelin between micellar and vesicular phases: potential implication for canalicular bile formation. *J Lipid Res* 1999; 40: 2022-2033.
- Portincasa P, Di Ciaula A, Vendemiale G, Palmieri V, **Moschetta A**, vanBerge-Henegouwen GP, Palasciano G. Gallbladder motility and cholesterol crystallization in bile from patients with pigment and cholesterol gallstones. *Eur J Clin Invest* 2000;30:317-324.
- Portincasa P, Minerva F, **Moschetta A**, Venneman NG, vanBerge-Henegouwen GP, Palasciano G. *In vitro* studies of gallbladder smooth muscle function. Relevance in cholesterol gallstone disease. *Alim Pharmacol Ther.* 2000; 14, 19-26.
- **Moschetta A**, vanBerge-Henegouwen GP, Portincasa P, Palasciano G, Groen AK, van Erpecum KJ. Sphingomyelin exhibits greatly enhanced protection compared with egg yolk phosphatidylcholine against detergent bile salts. *J Lipid Res* 2000; 41: 916-924.
- Portincasa P, Altomare DF, **Moschetta A**, Baldassarre G, Di Ciaula A, Venneman NG, Vendemiale G, Memeo V, Palasciano G. Effect of acute oral erythromycin on gallbladder motility and on upper gastrointestinal symptoms in gastrectomized patients with and without gallstones. A randomized placebo-controlled ultrasonographic study. *Am J Gastroenterol* 2000; 95: 3444-51.
- **Moschetta A**, Stolk MFJK, Rehfeld JF, Portincasa P, Slee PHTHJ, Koppeschaar HPF, van Erpecum KJ, vanBerge-Henegouwen GP. Severe impairment of postprandial cholecystokinin release and gallbladder emptying and high risk of gallstone formation in acromegalic patients during Sandostatin LAR. *Alim Pharmacol Ther* 2001;15: 181-5.
- **Moschetta A**, vanBerge-Henegouwen GP, Portincasa P, Renooij W, Groen AK, Van Erpecum KJ. Hydrophilic bile salts enhanced differential distribution of sphingomyelin and phosphatidylcholine between micellar and vesicular phases: potential implications for their effects *in vivo*. *J Hepatol* 2001;34:492-499.
- Portincasa P, **Moschetta A**, Di Ciaula A, Palmieri VO, Milella M, Pastore G, Palasciano G. Changes of gallbladder and gastric dynamics in patients with acute hepatitis A. *Eur J Clin Invest* 2001;31:1-7.
- **Moschetta A**, Eckhardt ERM, de Smet MBM, Renooij W, vanBerge-henegouwen GP, van Erpecum KJ. Accurate separation of vesicles, micelles and cholesterol crystals in supersaturated model bile by ultracentrifugation, ultrafiltration and dialysis. *Biochim Biophys Acta* 2001; 1532:15-27.
- **Moschetta A**, vanBerge-Henegouwen GP, Portincasa P, Palasciano G, van Erpecum KJ. Cholesterol crystallization in model bile: effects of bile salt and phospholipid species composition. *J Lipid Res* 2001; 42:1273-81.

- van Ooteghem NAM, **Moschetta A**, Rehfeld JF, Samsom M, van Erpecum KJ, vanBerge-Henegouwen GP. Intraduodenal bile salts exert negative feedback control on gallbladder emptying in the fasting state without affecting cholecystokinin release or intestinal motility. *Gut* 2001; *in press*.

Publications without *impact factor* or chapters of books

- Palasciano G, **Moschetta A**. L'insufficienza respiratoria. In: Manuale di Fisiopatologia medica e chirurgica. Corazza GR, Ziparo V, eds. Rome: Il pensiero scientifico editore. 1999; cap. 12: 243-249.
- Portincasa P, **Moschetta A**, Puglisi F, De Mundo M, Ungaro F, Baldassarre G, Palmieri V, Palasciano G. La colelitiasi colesterinica. Patogenesi e terapia alle soglie del 2000. *Giornale di Gastroenterologia* 1998;3: 8-15.
- Portincasa P, **Moschetta A**, Giampaolo M, Palasciano G. Diffuse gastrointestinal dysmotility by ultrasonography, manometry and breath tests in colonic inertia. *Eur Rev Med Pharmacol Sci* 2000; 4:81-7.
- Portincasa P, **Moschetta A**, Palasciano G. Nuovi breath test per lo studio dello svuotamento gastrico e del transito intestinale. Rilevanza in pazienti con stipsi funzionale. *UCP News* 2000; 4:62-67.
- Portincasa P, **Moschetta A**, Pugliese S, Berardino M, Baldassarre G, Palasciano G. Terapia litolitica nella colelitiasi: quando, come e perché. *Giornale di Gastroenterologia* 2001; 6:61-68.
- Portincasa P, Palmieri V, **Moschetta A**, Portoghese A, Cofano M, Palasciano G. Patologie motorie gastroenteriche. Linee guida di identificazione. *Scientific Nutrition Today* 2001; 4:18-21.
- **Moschetta A**, vanBerge-Henegouwen GP, Portincasa P, Palasciano G, van Erpecum KJ. Differential distribution of sphingomyelin and phosphatidylcholine between micellar and vesicular phases: potential implication for biliary lipid secretion. In "Biology of bile acids in health and disease". vanBerge-Henegouwen GP et al. eds, Kluwer Academic Publisher, Lancaster, UK 2001; chapter 18; 121-127.